XENOLITHS AND THE NATURE OF THE UPPER MANTLE AND LOWER CRUST

NUNIVAK ISLAND, ALASKA

by

DONALD MICHAEL FRANCIS

B.SC. MCGILL UNIVERSITY (1968)
M.SC. UNIVERSITY OF BRITISH COLUMBIA (1971)

SUBMITTED IN PARTIAL

FULFILLMENT OF THE REQUIREMENTS

FOR THE

DEGREE OF DOCTOR OF PHILOSOPHY

at the

MASSACHUSETTS INSTITUTE OF TECHNOLOGY

September, 1974

Signature of Author.....
Department of Earth and Planetary Sciences, August, 1974

Certified by.....
Thesis Supervisor

Accepted by.....
Chairman, Departmental Committee on Graduate Students

ABSTRACT

XENOLITHS AND THE NATURE OF THE UPPER MANTLE AND LOWER CRUST

NUNIVAK ISLAND, ALASKA

by

DONALD MICHAEL FRANCIS

Submitted to the Department of Earth and Planetary Sciences on August 19, 1974 in partial fulfillment of the requirements for the degree of Doctor of Philosophy.

The mafic and ultramafic xenoliths of Nunivak Island occur in maars and splatter cones of alkalic basalt. Xenoliths from the splatter cones are typically iddingsitized, while those of the maars are fresh and unaltered. Lherzolite xenoliths predominate, but dunites, harzburgites, pyroxene granulites and gabbros are locally common in the splatter cones.

The lherzolites and related harburgites and dunites are interpreted to be fragments of the upper mantle. Iddingsitized lherzolites from the splatter cones range from aluminous specimens with green, Cr-poor (6 weight percent Cr_2O_3) spinels and Na-rich, tschermakitic pyroxenes to aluminum-poor nodules with red-brown Cr-spinels (27 weight percent Cr_2O_3) and endiopsidic clinopyroxenes. This variation is believed to reflect changing bulk composition in the upper mantle with depth. Eight of the fresh lherzolites contain interstitial, Cr-bearing (1.5 to 3.5 weight percent Cr_2O_3), pargasitic amphibole. This amphibole frequently contains embayed and vesicular, Cr-rich (to 45 weight percent Cr_2O_3) spinel inclusions. Fifty percent of the fresh lherzolites contain fine-grained zones of euhedral clinopyroxene, olivine, and spinel in glass. The texture and compositions of these phases indicate that the fine-grained zones represent melted amphibole. Both the amphibole lherzolites and the lherzolites with fine-grained, glass-bearing zones are characterized by interstitial clinopyroxenes rich in jadeite, but poor in calcium tschermak component. Fresh lherzolites without amphibole or fine-grained zones are identical to the aluminum-poor, iddingsitized lherzolites with red-brown spinel. The differences between the xenolith populations of the maars and splatter cones are believed to reflect a deeper sampling by the former.

The Cr-bearing amphibole is interpreted to be secondary. Two alternative mechanisms are proposed for its origin:

i. Fluid + Cr-Garnet + Cpx → Cr-Amphibole + Spinel

ii. Fluid + Cpx + Opx + Spinel → Cr-Amphibole + Cr-Rich Spinel

The first mechanism is supported by the jadeitic nature of the amphibole lherzolite's clinopyroxene and the similarity between the compositions of re-calculated garnets and reported garnets from garnet lherzolite xenoliths. The second reaction is favored by the textural relations and chemical zoning of the amphibole and its included spinel. The Na/Na + K ratios of the Nunivak basalts closely resemble those of the amphiboles. The amphibole, however, predates the entrainment of the lherzolite xenoliths in the alkalic basalts. In addition, the low Ti and Fe, but high Mg and Cr contents of the amphiboles precludes their origin by reaction between the alkalic basalts and spinel lherzolite. The formation of the amphibole may reflect a pervasive metasomatic event in the upper mantle caused by rising temperatures and the infiltration of alkali-rich volatiles prior to the introduction of basalt.

The pyroxene granulite, gabbro and certain dunite xenoliths are believed to be fragments of the lower crust. The pyroxene granulites were originally feldspathic dunites and troctolites with cumulate textures. They formed by the reaction of primary olivine and plagioclase to coronas of orthopyroxene and spinel-clinopyroxene symplectite prior to their entrainment in the alkalic basalts. This reaction may have been a response to increasing pressure associated with crustal thickening or to isobaric cooling of the original cumulate assemblage.

Thesis Supervisor: Dr. J. S. Dickey

Title: Assistant Professor of Earth and Planetary Sciences

ACKNOWLEDGEMENTS

This thesis topic was suggested by Dr. T. R. McGetchin. Tom's enthusiasm is a constant source of encouragement and working with him has been a rewarding personal and educational experience. Dr. J. S. Dickey willingly took over supervision of this project and our cabin building sessions and return trip to Nunivak Island are lasting memories. Thanks are also due to Drs. A. J. Irving, F. A. Frey and R. Hon for critical discussions of many of the ideas that have been presented. Lastly, I want to express my appreciation to my wife, Meredith, who probably has put more into this thesis than I. This project was in part supported by National Science Foundation grant G.A.-31728.

TABLE OF CONTENTS

TABLE OF CONTENTS
(Cont'd)

TABLE OF CONTENTS
(Cont'd)

TABLE OF CONTENTS
(Cont'd)

LIST OF FIGURES, PLATES, AND TABLES

LIST OF FIGURES, PLATES, AND TABLES
(Cont'd)

LIST OF FIGURES. PLATES, AND TABLES
(Cont'd)

CHAPTER 1 INTRODUCTION

Nunivak Island is one of a number of late Tertiary to recent, basaltic eruptive centers which characterize the hinterland of the Aleutian subduction zone. The island is located just off the west coast of Alaska (60° N, 166° W) in the shallow waters covering the Bering Sea shelf (Figure 1-1). For much of the island, the horizon of broad, lonely stretches of tundra with its innumerable lakes is interrupted only by scattered, low, symmetrical hills; remnants of volcanic eruptions. A low, composite shield, Mount Roberts, is the high point on the island reaching a maximum elevation of only 1675 feet. As a national wildlife refuge, the island is a natural habitat for muskox, reindeer, fox, and a myriad of nesting, migratory birds.

This thesis presents the findings of a study of the xenoliths occurring in the youngest volcanic vents of the island, clustered around Roberts Mountain. These xenoliths are concluded to be largely accidental in origin and retain important information about their source; the upper mantle and lower crust. The most significant finding of this thesis is the evidence for Cr-bearing, pargasitic amphibole in many of the lherzolite xenoliths. Nunivak Island joins a growing list of amphibole lherzolite localities throughout the world. Although there are still several hypotheses for the origin of the amphibole, it must be concluded that amphibole lherzolite is, at least locally, a common constituent of the upper mantle. Its absence in many lherzolite suites may result from its instability in the alkalic magmas which carry these nodules.

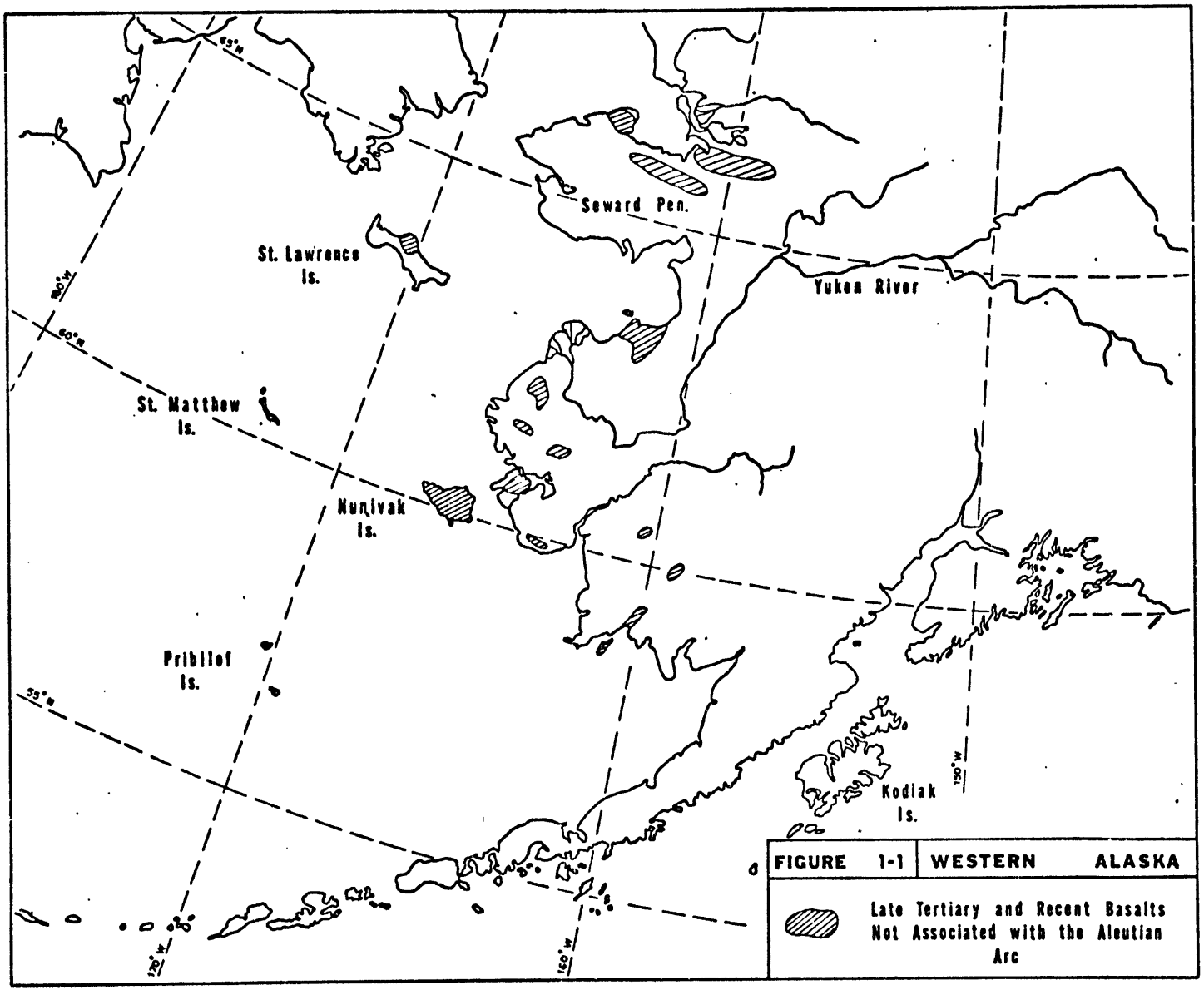
Seward Pen.
St. Lawrence Is.
Yukon River
St. Matthew Is.
Nunivak Is.
Pribilof Is.
Kodiak Is.
65°N
60°N
55°N
170°W
150°W
FIGURE 1-1 WESTERN ALASKA
Late Tertiary and Recent Basalts Not Associated with the Aleutian Arc

The similarity between the Na/K ratios of the Nunivak basalts and lherzolite amphibole is a natural enticement for theories on genetic relationships. First, however, it is essential that the nature of these amphibole lherzolites be fully understood. This thesis is a step in that direction.

CHAPTER 2 REGIONAL SETTING

The Aleutian arc is one of the major subduction zones of the Earth. The arc and the Bering Sea behind it, however, differ in many respects from other island arc systems. In Alaska, the typical elements of an oceanic island arc have been superimposed on those of a continental margin. This results in rather unique tectonics which are not fully understood. The continental margin of western Alaska is a Mesozoic feature while the Aleutian chain and trench were constructed in the Tertiary.

I Mesozoic Continental Margin

a) Alaskan West Coast

Two thirds of the rocks underlying the west coast of Alaska in the vicinity of Nunivak Island belong to the Gemuk Group (Hoare, 1961). These highly deformed rocks range in age from early Carbonaceous to early Cretaceous. They consist largely of greywacke sandstones and conglomerates; siltstones; argillites; and lesser amounts of andesitic volcanics and cherts. These rocks are cut by numerous small acidic stocks ranging in composition from gabbro to granite. The Gemuk group is believed to be part of a large eugeosynclinal belt which occupied much of Alaska during the late Paleozoic and early Mesozoic. Northwest-southeast compression beginning in the mid-Mesozoic formed large northeast trending geanticlines. Concommitant with the uplift of these positive features, the intervening geosynclines were filled with sediments. These sediments comprise the Kuskokwim Group and range from late Cretaceous to early Tertiary in age.

Though deformed, the sedimentary rocks of this group are significantly less indurated than those of the Gemuk Group.

Subparallel to the trend of regional folding is an extensive system of northeast striking faults. The Togiak-Holitna-Farewell fault zone (Figure 2-1) is the major feature of this system and is believed to be the westward extension of the Denali fault. These faults are still active, and recent movement is thought to be of a normal nature. Offsets measured in the field, however, indicate pre-Pleistocene strike-slip movements of up to 50 km. (Hoare, 1961).

The northeast trending tectonic elements of the west coast of Alaska can be traced inland where they eventually bend to the southeast, paralleling the southern coastline of Alaska.

b) Continental Shelf

Reflection seismic surveys have been conducted over most of the Bering Sea shelf. The acoustic basement under the shelf appears to be formed into broad arches and basins (Scholl, 1969). The trend of the basement arches suggests that they are extensions of the geanticlines found on the west coast of Alaska. Their high frequency, magnetic character (Pratt, 1972) is thought to be due to numerous small intrusive bodies such as characterize the Gemuk Group on the mainland. According to this interpretation, the acoustic basement would correspond to the erosional unconformity at the top of the deformed Gemuk Group (Scholl, 1968 and 1969; Pratt, 1972).

Above the acoustic basement rests 1500 meters of Cenozoic sediments which have been termed the "main layered sequence" by Scholl (1968). The

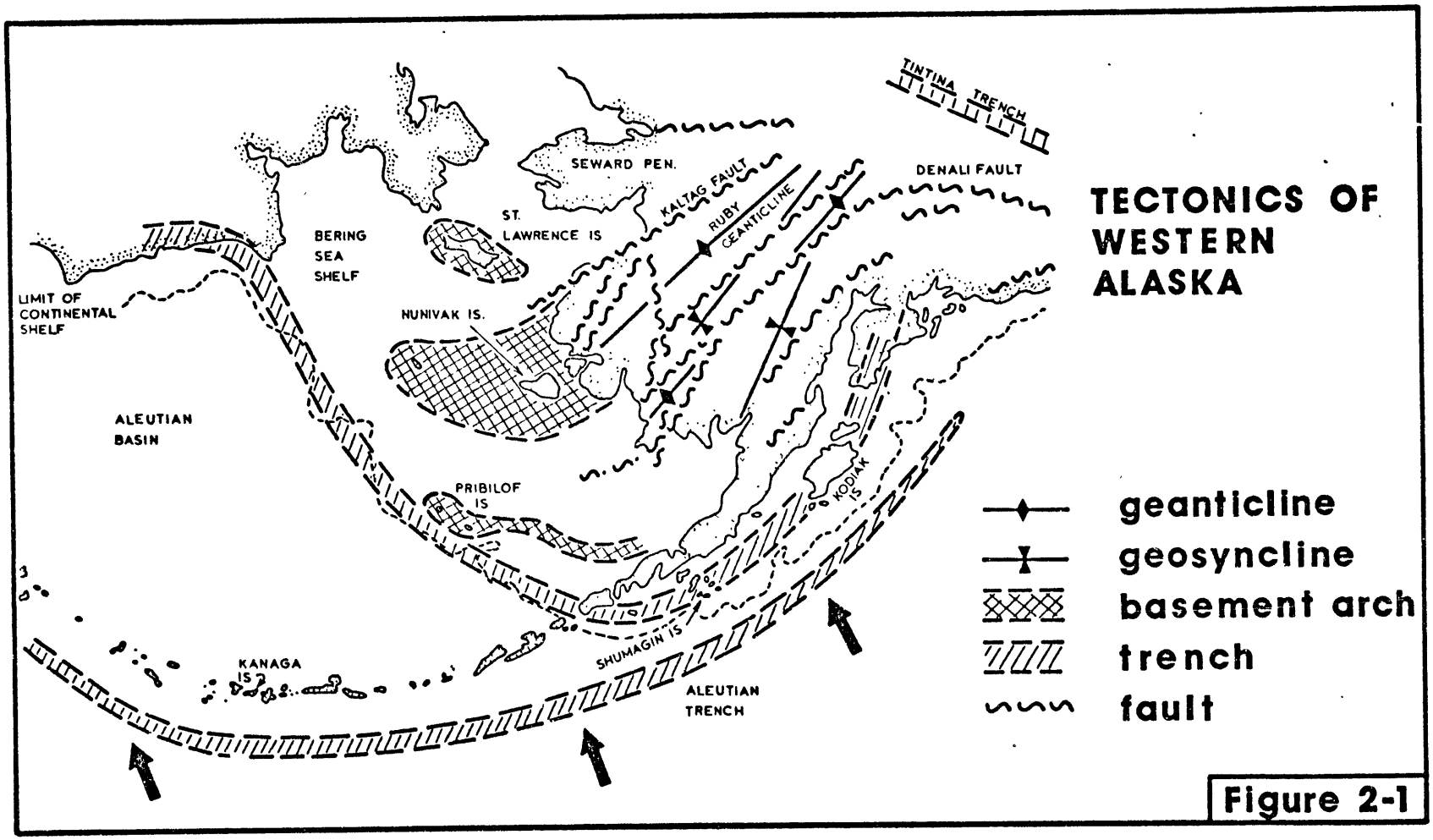
TINTINA TRENCH
SEWARD PEN.
DENALI FAULT
KALTAG FAULT
RUBY GEANTICLINE
ST. LAWRENCE IS
BERING SEA SHELF
LIMIT OF CONTINENTAL SHELF
NUNIVAK IS.
ALEUTIAN BASIN
PRIBILOF IS
KODIAK IS
KANAGA IS
SHUMAGIN IS
ALEUTIAN TRENCH
TECTONICS OF WESTERN ALASKA
geanticline
geosyncline
basement arch
trench
fault

Figure 2-1

lower part of these deposits are Paleocene in age and may correspond to the Kuskokwim Group of the mainland.

Two elongated, fault bounded, depressions parallel the margin of the continental shelf in the vicinity of the Pribilof Islands (Scholl, 1969). These have been downdropped 1 to 1.5 km. and appear to correlate with a similar depression discovered by Pratt (1972) to the Southeast (Figure 2-1). Moore (1972) believes that these depressions can be linked with a Cretaceous-Paleocene geosyncline (Burk, 1965) found on Kodiak and Shumagin Islands. He proposes that this hypothetical geosyncline can be extended to the Northeast to join similar geosynclinal sediments found in the Koryak Mountains of Siberia. According to Moore's interpretation the present continental margin of Alaska marks the site of a late Mesozoic trench system which can be traced from the Gulf of Alaska to mainland Siberia.

c) Aleutian Basin

The Aleutian basin is deduced to have been tectonically quiet since the formation of the Aleutian chain. The abyssal floor manifests no detectable stripped magnetic patterns, sea mounts, or guyots which characterize the Pacific Ocean basin to the South. Shor (1964) believes that the Bering Sea basin, which contains 3-4 km. of flat lying sediments, is a classic example of the conversion of an ocean basin to a continental shelf due to the ponding of sediments behind the Aleutian Islands. Seismic evidence indicates that the Mohoricic discontinuity is 4 km. deeper beneath the Bering Sea than it is beneath the adjacent Pacific Ocean.

Figure 2-1 is a composite interpretation of the extensions of Mesozoic tectonics defined on the Alaskan mainland beneath the Bering Sea. All the available evidence indicates that the pre-Tertiary trends of western Alaska bend northward beneath the continental shelf and eventually parallel its margin. The resultant mega "S" fold in these pre-Tertiary tectonics is striking.

II Tertiary Western Alaska

a) The Aleutian Arc

Burk (1965) interprets the Aleutian chain and trench to be a Tertiary feature. Like all present subduction zones, the Aleutians are seismically active. The hypocenters of earthquakes define a diffuse Benioff zone dipping a shallow 30° to the North beneath the Aleutian Islands. However, except on the mainland, earthquakes do not occur farther than 200 km. north of the Aleutian trench (Tobin, 1968). In addition, no earthquakes originating deeper than 180 km. are known, though quakes as deep as 300-700 km. are detected in the adjacent Kurile subduction zone. The absence of deep focus earthquakes in Alaska is puzzling!

The interpretation of magnetic and seismic data indicates that the Pacific Ocean basin is moving northwest 5-7 cm/yr (Le Pichon, 1968). The well-known magnetic "bight" of the Gulf of Alaska is thought to be the relict of a triple junction of spreading ridges that existed south of the trench in the early Tertiary (Pitman, 1968). Grow and Atwater (1970) suggest that the western arm of this junction (Kula ridge) ran nearly east-west. They calculate that the Kula ridge was engulfed in the

Aleutian subduction zone in early Miocene time. The occurrence of a major orogeny; coeval in the islands and later in the Pliocene on the Alaskan Peninsula; support this theory (Burk, 1965).

The present volcanic activity in the Aleutian chain is calc-alkaline in nature and is closely associated with the seismic activity. The character of vulcanism has evolved with time from early shield volcanoes composed largely of basalt to the present andesitic strato-volcanoes with a concomitant northward shift of the eruption centers. The presently active volcanoes are located along the northern edge of the island chain, approximately 100 km. above the top of the Benioff zone. This depth differs significantly from the 200 km. depth to the Benioff zone beneath the active Japanese volcanoes.

The seismically inactive western islands of the chain have not been the site of volcanic activity since the end of the Miocene. This may be attributed to the almost tangential motion of the Pacific plate with respect to the western islands. If Grow and Atwater's (1970) speculation about the orientation of the Kula ridge is correct, the pre-Miocene movement may have intersected the western islands at a higher angle. This would account for the evidence of pre-Miocene volcanic activity on these islands.

b) Recent Activity in the Hinterland of the Aleutian Arc

An extensive province of late Tertiary to Recent, continental, basaltic vulcanism constitutes the most important recent activity north of the Aleutian subduction zone. In addition to Nunivak Island, other eruption centers include: Pribilof Islands, St. Matthews Island, central

St. Lawrence Island, northern Seward Peninsula, plus numerous other small localities on the western mainland. All of the island centers are situated on arches in the Mesozoic basement and may be closely related to regional faulting (Hoare, 1968; Scholl, 1969). Because of the predominately alkalic nature of their basalts, Barth (1956) believed that St. Lawrence Island and the Pribilof Islands were distinct from the other eruption centers, but typical of a general occurrence of alkalic vulcanism behind circum-Pacific arcs. However, Hoare (1968) feels that the entire basaltic province consists largely of tholeiite lavas with lesser amounts of coeval alkali-olivine basalts.

Ultramafic xenoliths have been reported in the alkali basalts of the Seward Peninsula, Nunivak Island, and the Pribilof Islands, and in andesitic volcanics on Kanaga Island (Forbes, 1965) in the Aleutian chain. The latter is the only known occurrence of lherzolite nodules in andesitic volcanics. Further, Nunivak Island, the Pribilof Islands and Kanaga Island are roughly co-linear. Thus we have the unique occurrence of the "Andesite Line" being intersected by a coeval zone of ultramafic inclusion bearing volcanoes.

It is difficult to correlate the basaltic province with the current geophysical picture for western Alaska. The eruption centers are too far behind the arc to be directly associated with the present underthrusting in the Aleutians. As mentioned earlier, deep focus earthquakes do not occur farther than 200 km. behind the Aleutian trench. Shallow earthquakes are, however, common on the mainland, especially along the zone of maximum curvature of the tectonic elements. These shallow earthquakes

are believed to be associated with normal movement along faults of the Denali system.

Runcorn (1964) has computed the direction and magnitude of traction for island arc systems due to coupling between the mantle and the lithosphere using satellite gravity data. According to this analysis most areas behind island arcs experience strong traction towards the arc. The Bering Sea does not. This speculation, combined with the occurrence of normal faulting in western Alaska and the wide spread basaltic vulcanism may indicate that a tensional environment exists in the hinterland of the Aleutian arc. This might be an after-effect of the engulfing of the Kula ridge or the associated change in the spreading direction during the Miocene. This is, however, speculative and specific mechanisms are difficult to suggest.

CHAPTER 3 PREVIOUS WORK

Much of the geologic information available on Nunivak Island has come from the work of Dr. Joe Hoare of the U.S. Geological Survey. He has visited the island on several occasions, initially to study the basalts (1964, 1966) and later the xenoliths (1967). Mark (1971) has studied the strontium isotopes and major element chemistry of the Nunivak basalts. There is some confusion as to the classification of the Nunivak basalts. To avoid this problem the field occurrence of the basalts will be described first, followed by a discussion of their chemistry and an evaluation of the relative merits of the nomenclature which has been applied.

I Detailed Geology

Nunivak Island is largely covered by extensive, thin flows of what Hoare (1968) has termed "tholeiite" basalt. These flows range from 3 to 15 meters in thickness and may extend as much as 15 km. They are best observed in cliffs along the coast, stream cuts, and in felsenmeer fields in the south central portion of the island. The vents for these basalts appear to correspond to low, rounded, topographical highs. A few of these hills are capped with peculiar mesa-like outcrops of shattered basalt.

In hand specimen the basalt is medium grey and contains ubiquitous, corroded olivine phenocrysts. Less commonly augite and feldspar phenocrysts are also found. The groundmass is "subophitic to intersertal and

diktytaxitic" and consists of labradorite, clinopyroxene, olivine, iron ores, and glass (Hoare, 1968).

Two percent of the exposed volcanics on the island have a more alkaline nature. Two styles of eruption are recognized. The older and more abundant eruptions have constructed small cones 30 to 150 meters high. When fresh, they support steep exterior slopes (to 38°) which are covered in tundra vegetation and show extensive development of frost garlands due to solifluction. The youngest of these cones have sharp, outcrop defined rims and steep interior walls; the oldest cones are rounded hills with little outcrop and only faintly discernible central craters. All the cones are built of volcanic breccia or agglutinate of welded basaltic splatter, scoria, and cinders.

The second style of alkaline eruption is represented by maars. At least four of these structures occur on the island defining a linear trend bearing 092° and stretching over 13 km. (Figure 4-1). The craters involved are Nanwaksjiak (NA3-9) plus a parasite crater (NA3-6), crater 385 (NA3-7), Binalik (NA4-7), and possibly Ahkiwiksnuk (NA4-6). These maars are thought to be the most recent volcanic features on the island. They are essentially holes excavated through pre-existing tholeiite flows and rimmed by loosely consolidated ash. The interior walls are steep talus slopes of ash giving way to cliffs of tholeiite basalt. Most of these craters have central lakes.

Flows of alkaline basalt are small (1 to 3 km.) and originate at cinder cones. They are typically characterized by aa tops. One alkaline flow has been found in the interior wall of a maar (NA3-9) underlying its ash rim (Hoare, 1968).

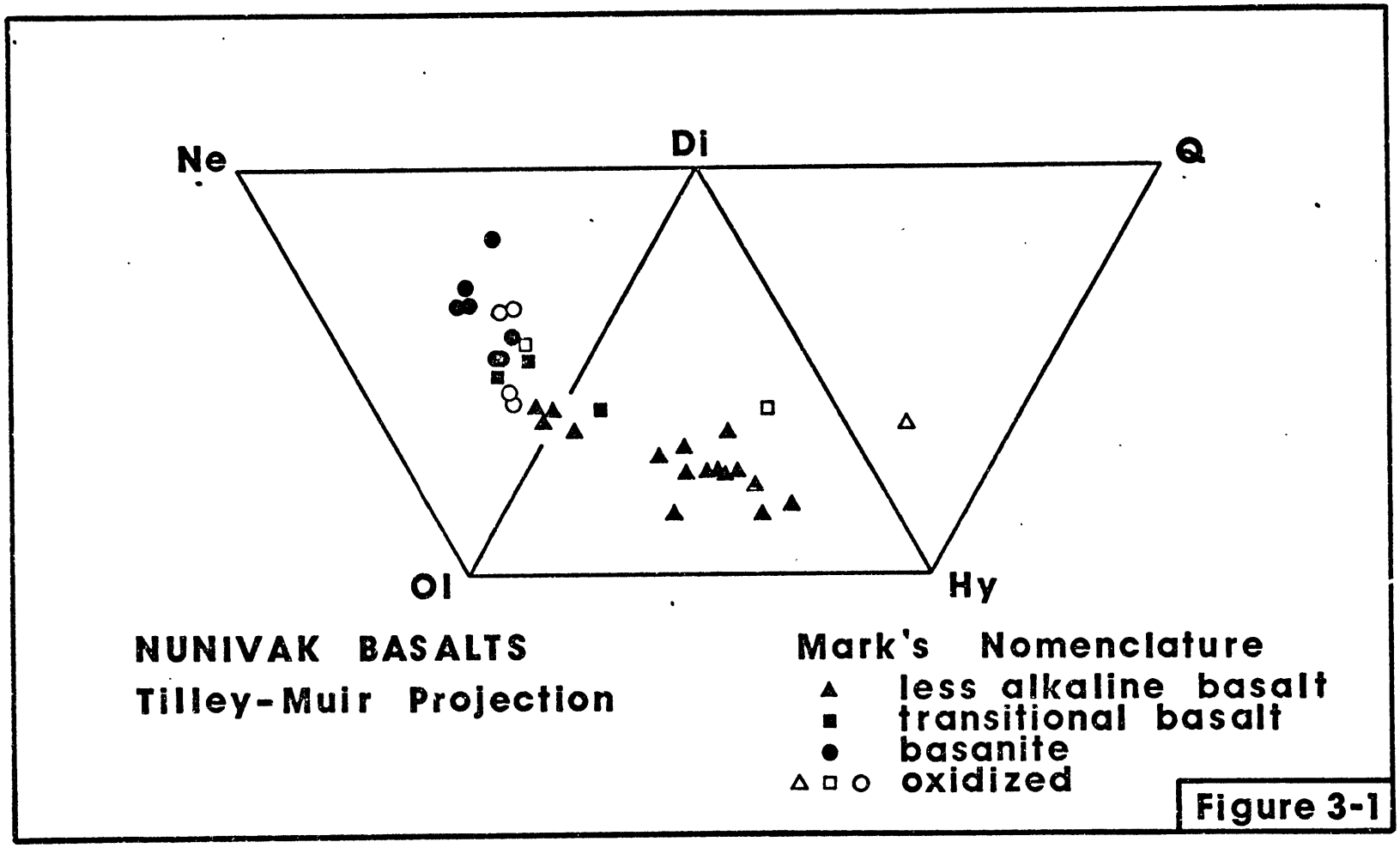
Ne
Di
Q
Ol
Hy
NUNIVAK BASALTS
Tilley-Muir Projection
Mark's Nomenclature
less alkaline basalt
transitional basalt
basanite
oxidized

Figure 3-1

In hand specimen these alkaline basalts vary in color from light grey in the older, holocrystalline specimens to black for the glass-rich, younger flows. Olivine and less commonly titanaugite are present as phenocrysts. The holocrystalline varieties often exhibit a mottled pattern thought to be caused by the hydration and crystallization of former glass (Hoare, 1968). The groundmass consists of opaques, clinopyroxene, olivine, plagioclase, nepheline, and analcime. The black color of the younger alkaline basalts is caused by the presence of finely disseminated opaques in the glass of the groundmass.

II Basalt Chemistry

Hoare's original data indicated that the two varieties of basalt observed in the field were chemically distinct: 1) voluminous olivine tholeiites containing normative olivine and orthopyroxene; and 2) less abundant basanites containing both modal and normative nepheline. On the basis of additional analyses, Mark (1971) established three basalt categories: 1) less alkaline basalts consisting of the tholeiite basalts of Hoare (1968), some of which had been found to contain normative nepheline; 2) transitional alkali-olivine basalts which are assoicated with splatter cones but contain less than about 11 weight percent normative nepheline; and 3) basanites with both modal and normative nepheline. Mark (1971) felt that the transitional basalts were chemically related to the less alkaline basalts despite the fact that their field occurrence would group them with the basanites. However, Figure 3-1, a Tilley-Muir diagram of both Mark's (1971) and Hoare's (1968) basalt analyses suggests the opposite. It appears that the basanites and transitional basalts form

a continuous series of alkali-olivine basalts while the tholeiite basalts cluster in the olivine tholeiite field (Yoder and Tilley, 1964). The three "tholeiite" basalts which Mark (1971) found to be nepheline normative come from the inside wall of Nanwaksjiak (NA3-9) crater and may have been altered during its eruption.

Considering the clustering in Figure 3-1 and the distinctive field relations, it appears that the Nunivak basalt population is bimodal as originally proposed by Hoare:

1) Olivine tholeiite basalts occurring as extensive, thin flows covering most of the island.
2) Alkali basalts ranging from basanites to olivine basalts occurring as maars, splatter cones and their associated flows.

The bimodal character of the Nunivak basalts is distinct from the quartz tholeiite/alkali-olivine duality characteristic of Cenozoic basalts in general (Chayes, 1971). The most common occurrence of olivine tholeiite is found at the mid-ocean ridges. Compared to these abyssal basalts, the Nunivak tholeiites are relatively enriched in alkalies and magnesium but depleted in calcium. This is reflected in significantly higher proportions of hypersthene in the norms of the Nunivak tholeiites.

Mark (1971) has reached the following conclusions about the chemistry of the Nunivak basalts:

1) Though the Nunivak tholeiites have relatively high potassium contents (.6 to 1.2 wt. % K_2O) characteristic of continental tholeiites, they contain less radiogenic strontium (Sr^{87}/Sr^{86} = .70313 ± .00013) than

typical oceanic tholeiites (Sr^{87}/Sr^{86} = .7035). The alkalic basalts exhibit still lower Sr^{87}/Sr^{86} ratios (.70279±0.0016). Mark argues that such low radiogenic strontium contents virtually rule out any possibility of crustal contamination of the Nunivak basalts. The Nunivak strontium ratios are so low that they indicate a prior depletion of rubidium in the upper mantle. Both the potassium and radiogenic strontium contents of the Nunivak basalts decrease with decreasing age.

2) The most significant chemical parameter is an inverse relationship between total alkalies and silica. Such a variation can not be explained by fractional crystallization of olivine, the only ubiquitous phenocryst phase. Two thirds of the parental magma must crystallize to raise the alkali level found in the tholeiites to that of the basanites. The similarity of the Mg/Mg+Fe ratios of these two magma types indicates that this degree of fractionation is unlikely. The abundance of dense xenoliths in the basanites suggests that fractional crystallization has not played a major role in their origin. The relationship between alkalies and silica in the basalts also precludes any major involvement of the anorthoclase xenocrysts, which are common in the splatter cones, in the formation of the basanites.

3) The differences between the alkalic and tholeiite basalts on Nunivak Island were generated by different degrees of partial melting in a vertically heterogenous upper mantle. The tholeiites formed by extensive partial melting of material rich in the incompatible elements, while the basanites were produced at deeper levels by small degrees of partial melting of material relatively depleted in the incompatible elements.

Mark also suggests that the strong correlation between Na_2O and K_2O (2:1) in the Nunivak basalts indicates that these elements were held in amphibole rather than in a pore fluid where Na would be buffered by clinopyroxene, independent of the potassium content of the fluid.

III Xenoliths

Xenoliths and megacrysts are abundant at most of the alkalic eruption centers. Hoare (1968) was the first to recognize the occurrence of a number of unusual xenolith types in the maars of Nunivak Island. He reported (Hoare and Condon, 1968; Hoare and Kuno, 1968) the presence of what he termed "eclogite" xenoliths which contain spinel-clinopyroxene symplectite coexisting with plagioclase and orthopyroxene mantled olivine. Because of the chemical similarity between these nodules and the garnet pyroxenites found in Salt Lake Crater, Hawaii; Hoare concluded that the symplectite formed by the breakdown of garnet. On a return trip to Nunivak Island, he claims to have found two feldspathic examples which contain relict garnet (Hoare, 1966).

McGetchin and Hoare (1968) reported the occurrence of spinel lherzolites with Cr-bearing phlogopite in the maars of Nunivak Island.

Megacrysts of anorthoclase, black clinopyroxene, and kaersutite have been found in the ejecta of both the cinder cones and maars. Mark (1971) obtained a Sr^{87}/Sr^{86} ratio of .7027 for an anorthoclase xenocryst. Since this ratio is within the range of the basaltic strontium ratios, he concludes that the anorthoclase crystals are cognate.

IV Summary of the Volcanic History of Nunivak Island

Using potassium-argon dating and paleomagnetic techniques, Hoare (1968) has recognized six episodes of volcanic activity on Nunivak Island. These active episodes were separated by periods of quiesence lasting .5 to 1.5 million years. The oldest exposed flows are found at the western end of the island and date 4 to 6.1 million years. The geographic center of each successive episode has shifted towards the East. The eruption pattern is one of voluminous tholeiite outpourings with small amounts of coeval alkalic activity. The xenolith-bearing cones and maars that were examined in this study belong to the last episode of vulcanism and are found in the south central portion of the island. This last episode began with the eruption of both tholeiite and alkalic basalts approximately one million years ago. The youngest tholeiite dated is 650,000 years old. Splatter cone NA4-6 (Figure 4-1), however, is only 30,000 years old. The state of erosion of cone NA3-1 indicates that it is significantly younger than cone NA4-6. Thus the maars which are younger still may only be a few thousand years old (Hoare, 1968). This means that alkalic eruptions have continued after cessation of the tholeiite vulcanism.

CHAPTER 4 FIELD WORK

Five weeks were spend during the summer of 1973 studying the xenolith population of Nunivak Island, Alaska. Over 3000 xenoliths were examined from 30 volcanic vents of Pleistocene to Holocene age. These host structures belong to the Oknl Formation defined by Hoare (1968) and consist of alkalic basalt. They represent the last episode of eruption on the island which commenced approximately one million years ago. Figure 4-1 is a map of the central portion of Nunivak Island showing the location of all the vents examined.

At each vent, as many xenoliths as could be found in a few hours were collected. In most cases in excess of 100 xenoliths were examined from each site. These xenoliths were hand sorted, classified and counted. A representative sample of each xenolith type from each vent was returned to the laboratory for further study. Visual modes were estimated for at least 50 of the inclusions at every site.

In addition, the relative age of each host vent was estimated and where appropriate, a sample of the associated basalt was collected. Because the splatter and cinders of the cones are usually altered and because of the inherent danger of selecting an inclusion, basalt samples were collected only from flows associated with a vent.

In the field the xenoliths were classified into 7 groups. These groups are listed below:

i. Gabbroic xenoliths: granular rocks consisting largely of plagioclase with lesser amounts of dark green clinopyroxene plus or minus olivine.

ii. Feldspathic Granulites: similar to gabbroic xenoliths but characterized by the presence of masses, blebs or bands of extremely fine grained, green-grey material (spinel-clinopyroxene symplectite under the microscope).

iii. Olivine Granulites: granular rocks consisting largely of olivine and characterized by the presence of extremely fine grained green-grey material separated from olivine by 1 mm seams of white orthopyroxene.

iv. Lherzolites: granular rocks consisting of olivine, black orthopyroxene, spinel and pale green chromian diopside.

v. Dunites: similar to lherzolites but lacking any trace of chromian diopside and containing less than 5% orthopyroxene.

vi. Harzburgites: similar to lherzolites but lacking any trace of chromian diopside.

vii. Pyroxenites: granular rocks consisting largely of greenish black clinopyroxene with lesser amounts of olivine.

In addition to the above, xenocrysts of anorthoclase and black kaersutite were frequently found. Inclusions of greywacke sandstone, conglomerate and basalt are locally common, especially in the ash rims of the maars. Notably, inclusions of gneiss or other metamorphic rocks are absent.

Each of the above groups was subdivided into two groups depending on whether the xenoliths belonging to it had been iddingsitized or not. Xenoliths were classed as "fresh" (not iddingsitized) if their olivine were green and transparent in appearance. They were termed iddingsitized

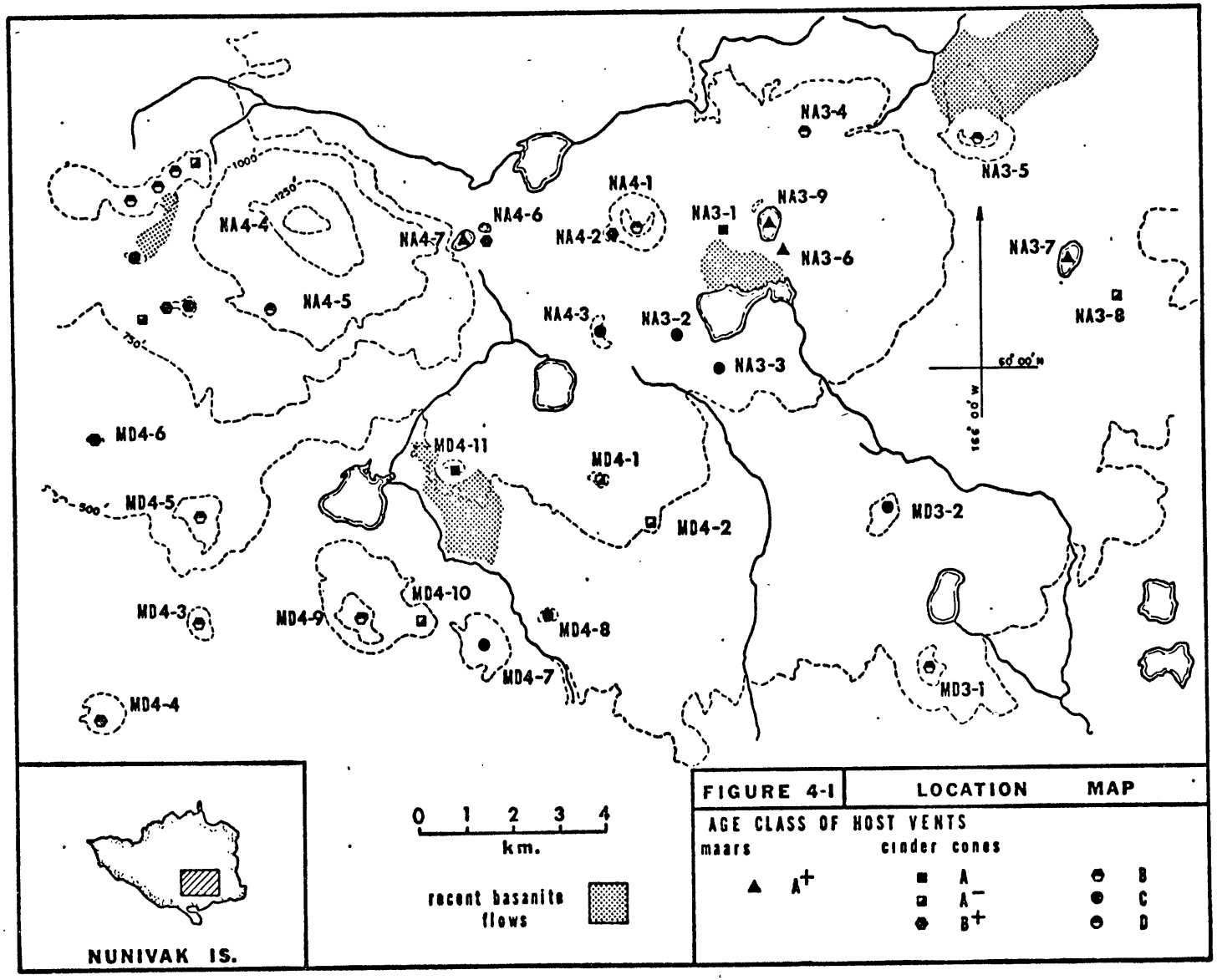
NA3-4
NA3-5
NA4-1
NA4-6
NA3-1
NA3-9
NA4-4
NA4-7
NA4-2
NA3-6
NA3-7
NA4-5
NA3-8
NA4-3
NA3-2
NA3-3
1000'
1250'
750'
500'
MD4-6
MD4-11
MD4-1
MD4-5
MD4-2
MD3-2
MD4-10
MD4-3
MD4-9
MD4-8
MD4-7
MD3-1
MD4-4
NUNIVAK IS.
0 1 2 3 4
km.
recent basanite flows
FIGURE 4-1 LOCATION MAP
AGE CLASS OF HOST VENTS
maars
cinder cones
A+
A
A−
B+
B
C
D

if their olivine were opaque and dull to bright red in appearance. Xenoliths whose olivine showed any sign of incipient red alteration were placed in the latter category. Some difficulty was encountered in distinguishing between iddingsitized harzburgites and dunites. In addition to a red discolouration, the interiors of altered olivines were often blackened. As a result the modal proportion of orthopyroxene was difficult to estimate in these xenoliths.

Table 4-1 lists the relative abundances of the various xenolith types with respect to the nature and relative age group of their host vents. The state of preservation of the geomorphic features was used as the criteria for the age grouping of these vents. The most striking feature of this table is the restriction of the iddingsitized xenoliths to the splatter cone type of host vent. With the exception of Ahkiwiksnuk crater, no iddingsitized xenoliths were found associated with the maars. However, the morphology of Ahkiwiksnuk is atypical of the other Nunivak maars. The xenolith-bearing horizons appear to be part of an older splatter cone through which the maar has cut. Fresh xenoliths are found in the splatter cones. In any particular cone, both iddingsitized and fresh xenoliths might occur, though the two types are usually spatially segregated within the cone itself. Occasionally, the fresh xenoliths found in these cones contained olivine which exhibits a darker or greyer hue of green than usual, giving the xenolith a dark gray-green appearance rather than the bright green appearance of typical lherzolites. Xenoliths found in basalt lava flows are usually not iddingsitized thougn the associated cone might contain predominately iddingsitized xenoliths.

Table 4-1

Relative Abundances of Xenoliths on Nunivak Island

Age Class	total	A^+	A	A^-	B^+	B	C	D
Number of Vents	27	3	2	4	3	8	6	1
Type of Vent		maars	← cinder cones →					
gabbro	7.4	1.2	21.9	11.3	12.6	5.8	2.8	7.5
idd. gabbro	.2	-	1.5	.5	-	-	.2	-
lherzolite	30.3	90.0	48.5	24.3	1.3	14.8	37.3	8.2
idd. lherz.	54.1	.7	9.4	50.9	80.2	73.9	54.3	73.7
dunite & harz.	2.4	6.7	17.2	1.2	.6	.1	.5	-
idd. " "	4.4	-	1.5	7.2	3.1	4.0	4.7	9.0
ol. granulite	.2	1.0	-	.7	-	.5	-	-
idd. "	.6	-	-	3.4	.3	.3	-	.8
felds. granulite	.1	.4	-	.5	-	.1	-	-
pyroxenite	.1	-	-	-	.3	.5	-	.8
idd. pyroxenite	.2	-	-	-	1.6	-	-	-
total sample	3297	720	64	415	318	1072	575	133

increasing age →

Figure 4-2 is a graphic simplification of Table 4-1. There is an apparent trend of increasing relative abundance of feldspar bearing, dunite and harzburgite xenoliths relative to lherzolite xenoliths with decreasing age of their host structure. The change in eruption style from splatter cones to maars corresponds to a discontinuity in the above trend. It is interesting that the two members of the youngest splatter cone group are characterized not only by a relative minimum in the abundance of lherzolite xenoliths, but a general paucity of xenoliths of all types. Several hours of concentrated search uncovered a combined total of only 64 xenoliths for these two cones. Usually no difficulty was incurred in collecting in excess of 100 xenoliths per cone.

Hoare's original investigation indicated that the granulite xenoliths were restricted to the maars. This study has revealed, however, that both olivine and feldspathic granulites are also to be found in small concentrations in many of the splatter cones. In particular, cone NA3-8 has the highest concentration of granulite xenoliths of any of the volcanic vents examined. Feldspathic and olivine granulites, together, comprise approximately 1% of the total xenolith population.

McGetchin and Hoare (1968) have reported the occurrence of mica-bearing lherzolites in the maars of Nunivak Island. A small number of these xenoliths were also found in this study, in the splatter cones as well as the maars. The true relative abundance of the mica-bearing xenoliths could not be estimated in the field because often the presence of mica can only be determined in thin section.

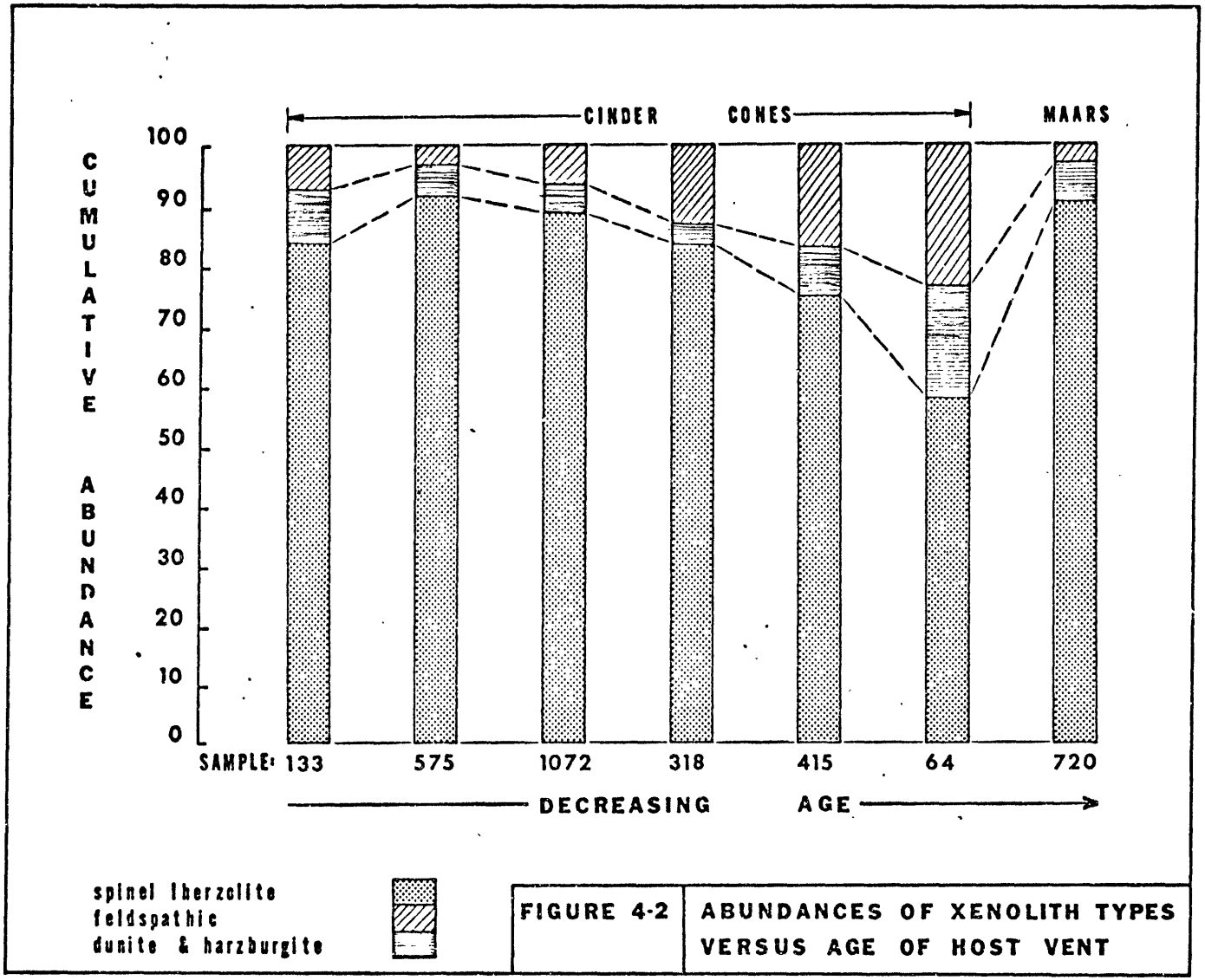

FIGURE 4-2 ABUNDANCES OF XENOLITH TYPES VERSUS AGE OF HOST VENT

CHAPTER 5 PETROGRAPHY OF ULTRAMAFIC XENOLITHS

This chapter deals with the petrography of the lherzolite xenolith suite. Xenoliths considered in this chapter contain the four essential lherzolite phases; olivine, orthopyroxene, clinopyroxene, and spinel. A few of the nodules included here are more correctly termed harzburgites or dunites. However, the criterion used to include these xenoliths was the presence of any trace of Cr-diopside. Ultramafic xenoliths which lack this phase and whose olivines have forsterite contents significantly below Fo 89 have been grouped with the feldspathic rocks and are described in Chapter 7.

The nodules of the lherzolite suite display the characteristic xenomorphic-granular texture of spinel lherzolites. Preliminary U-stage analysis of 2 specimens (10001, 10005) indicates that their olivines exhibit a moderate orthorhombic fabric. This would place these xenoliths between the "coarse-grained" and "tabular olivine and enstatite" textural types of Boullier and Nicolas (1973).

On a macroscopic scale, the most striking feature of the lherzolite nodules is their division into two groups; lherzolites with fresh olivine and lherzolites whose olivine has developed a red-brown alteration called iddingsite. The maars of Nunivak Island contain only the former group while the majority of those found in the splatter cones belong to the latter (see Table 4-1).

I Fresh Lherzolite Suite

Nodules that are assigned to this category contain fresh olivine which exhibits no sign of the development of iddingsite alteration. The characters of olivine and orthopyroxene are uniform throughout the xenoliths of this suite. Olivine occurs as 1 to 4 mm., anhedral, but slightly flattened grains. In thin section they appear tabulate and exhibit extensive development of undulatory extinction and deformational banding perpendicular to their direction of elongation. The character of orthopyroxene is essentially identical, except that it has a slightly smaller mean grain size and less commonly exhibits deformational banding. The oblate nature of the grains of these phases often defines a weak foliation in the xenoliths.

Despite the uniform nature of the two major phases of its xenoliths, the fresh lherzolite suite can be subdivided on a textural and mineralogical basis. The criteria for this subdivision are the habits of the clinopyroxene and spinel and the presence or absence of the following accessory phases; amphibole, mica, or glass. Using these criteria a sequence of xenoliths can be established in the lherzolite suite. At one end of this sequence are xenoliths which contain amphibole as an integral phase, while at the other end are xenoliths which contain only the four essential lherzolite phases. Intermediate members of the sequence contain decreasing amounts of accessory glass and mica which are interpreted to be the remnants of amphibole. Position in the sequence appears to be independent of the mode of the individual lherzolites involved.

a) Amphibole-Bearing Lherzolite

Eight lherzolites have been found containing interstitial amphibole. This amphibole is red-brown in color and is often inconspicuous in hand specimen. In transmitted light, however, it is strongly pleochroic, ranging in color from reddish brown to olive green. Two textures are observed. Typically the amphibole contains a core of black Cr-spinel. This texture ranges from single amphibole crystals with rounded spinel inclusions to large (1 to 5 mm.) oblate bodies consisting of aggregates of .3 to 1 mm., anhedral amphibole grains enclosing a highly embayed and vesicular spinel (plate 5-1). In the larger examples, anhedral masses of red-brown, pleochoic phlogopite are occasionally found between the amphibole and its core spinel. Less commonly, amphibole occurs as .3 to 3 mm., subhedral crystals without inclusions of spinel. Both of these amphibole types may be present in the same specimen. Two specimens, however, contain only the latter.

Many of the amphibole grains, especially those with core spinels, exhibit textural evidence of partial melting. This evidence is in the form of fine-grained zones replacing the amphibole adjacent to its included spinel. In reflected light, these zones are observed to consist of Cr-diopside and olivine as .05 to .1 mm. euhedral prisms with domal terminations in a homogenous matrix of low reflectivity. Spinel also occurs as .01 to .02 mm., equant, skeletal crystals in this matrix (plate 5-3). In transmitted light the matrix material is colorless and isotropic. It is assumed to be glass. Table 5-1 presents a typical mode for one of these fine-grained, glass-bearing zones.

Table 5-1

Mode of a Typical Fine-Grained, Glass-Bearing Zone

Cr-diopside	24%
olivine	11%
Cr-spinel	2%
glass	8%
voids	53%

The majority of the spinel of the amphibole-bearing lherzolites occurs as the embayed and vesicular cores found in the amphibole. Small amounts of spinel, however, are present as subhedral, .02 to .1 mm. inclusions in the other silicate phases. In olivine and Cr-diopside these inclusions tend to be isolated, equant grains; while in orthopyroxene they also occur as swarms of tiny, preferentially oriented rods. Interscitial Cr-spinel is generally absent.

The clinopyroxene of many of the amphibole-bearing lherzolites is distinctive. In hand specimen it commonly has a milky green, translucent appearance rather than the bright green, vitrious character that is typical of the Cr-diopsides in spinel lherzolites. This feature is most apparent in the clinopyroxenes of nodules whose amphibole has well developed, partial melting textures. In thin section, clinopyroxene is observed as .5 to 1^{+} mm., anhedral grains containing rounded inclusions of olivine, orthopyroxene, and occasional .01 to .2 mm vesicules. This clinopyroxene commonly has a turbid or cloudy hue in plane polarized light. Under high magnification the turbid or cloudy grains are found to

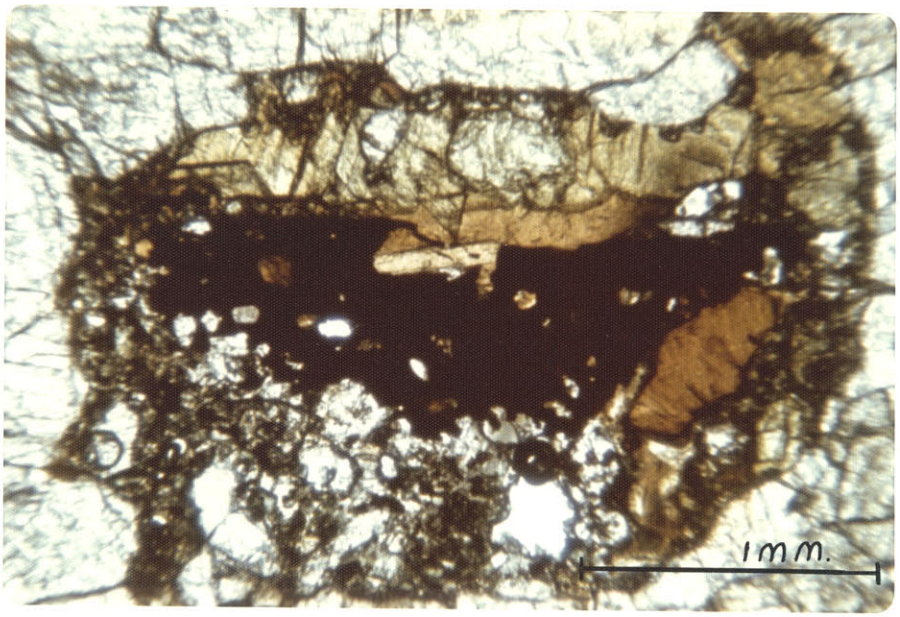

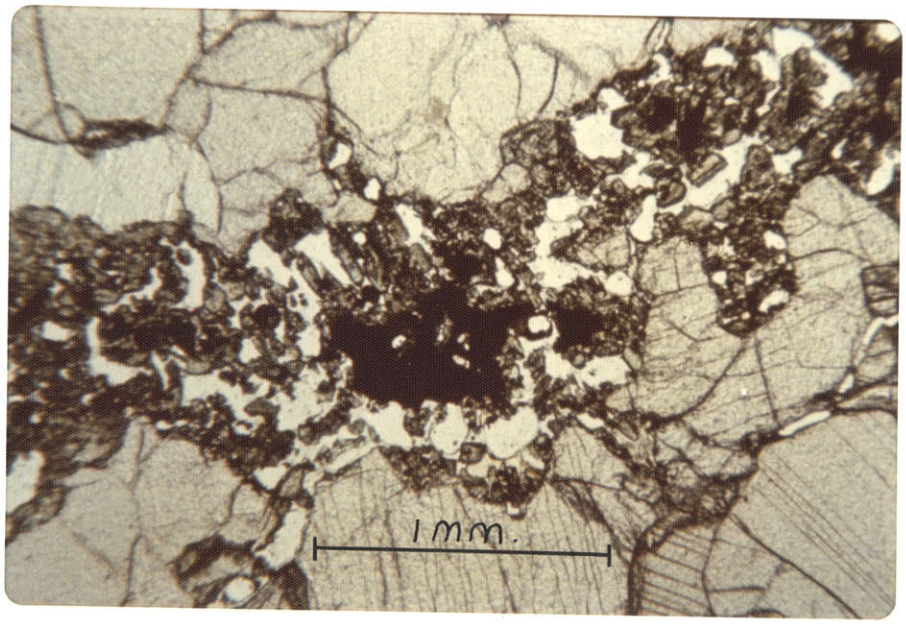

Plate 5-1 (top): Oblate body with amphibole, phlogopite, and Cr-spinel. Note development of fine-grained zone.

Plate 5-2 (bottom): Fine-grained zone containing relict spinel, euhedral crystals, and vesicular glass.

contain numerous hollow tubes 1 to 5 microns in diameter. These tubes have a common orientation, but are not arranged into planar elements. The tubes, however, do not appear to be the cause of the turbidity in the clinopyroxene. This turbidity must originate from some sub-microscopic feature.

The clinopyroxenes of lherzolites whose amphibole exhibits little or no sign of partial melting have not developed the features described above and tend to retain the bright green, vitrious character of typical Cr-diopsides.

b) Glass-Bearing Lherzolite

There is no trace of amphibole in the xenoliths in this category. The interstitial Cr-spinel of the nodules included here, however, is surrounded by fine-grained, porous zones consisting of euhedral crystals and glass (plate 5-2). The mineralogy and texture of these zones are identical to those associated with the amphibole in the foregoing section. The spinel in the center of these melt zones is highly embayed and vesicular. It commonly exhibits finely serrated edges when viewed in reflected light. Occasionally two or three irregular fragments of spinel are present which appear to be remnants of a single grain.

Less typically, fine-grained zones are observed which lack residual, core spinel. These zones are commonly characterized by an increased concentration of tiny, spinel euhedra; often localized along their boundaries. Occasionally the boundaries of such fine-grained zones are planar, suggesting monoclinic or triclinic crystal pseudomorphs (plate 5-4).

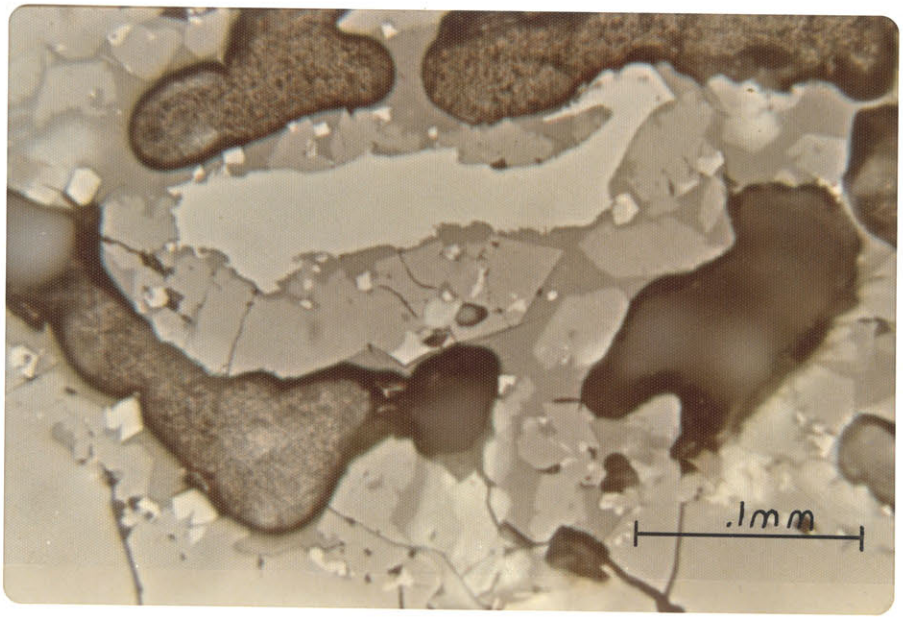

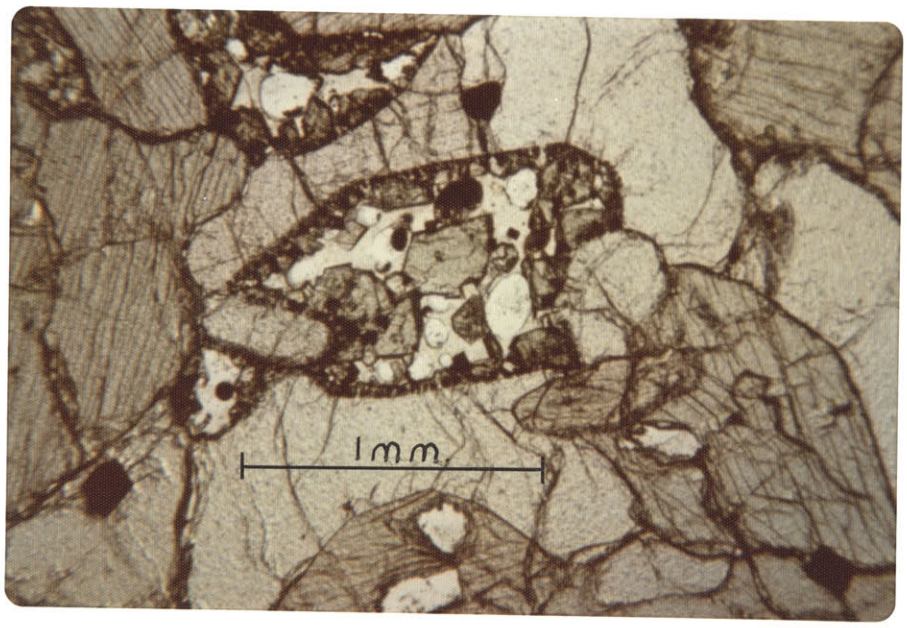

Plate 5-3 (top): Reflected light image of fine-grained zone. Note euhedral crystals, relict spinel and grey glass.

Plate 5-4 (bottom): Fine-grained, glass-bearing zone with pseudomorphic outline.

A complete spectrum of specimens exists ranging from those in which the fine-grained zones are extensively developed to those in which only traces of them can be found. Nodules in which these melting textures are best developed often contain traces of red-brown phlogopite in their fine-grained zones. This mica appears highly embayed and is usually intimately intergrown with the core spinel.

The clinopyroxene of the glass-rich lherzolites closely resembles that found in the amphibole-bearing lherzolites. It is typically a milky, translucent green in color and often contains rounded inclusions and vesicules. These clinopyroxenes have developed .02 to .05 mm altered rims (plate 5-5). The nature of these features is obscure in transmitted light because of their small scale in comparison to the thickness of a standard thin section. When viewed in reflected light, however, they are seen to consist of fragments of clinopyroxene separated from the host grain by a homogenous material of low reflectivity (plate 5-6). This material is also observed lining the grain contacts between the clinopyroxene and other silicate phases. Though these regions of darker material are too small to be observed under crossed nicols in transmitted light, they are interpreted to be glass produced by incipient melting occurring along the Cr-diopside grain boundaries.

Nodules containing only traces of fine-grained zones about their interstitial spinel are characterized by clinopyroxenes which are bright green in color, have a vitrious lustre, and lack inclusions or vesicules. They show no signs of instability along their grain boundaries.

In addition to occurring as an interstitial phase surrounded by melt zones, spinel also occurs as subhedral inclusions in all the silicate

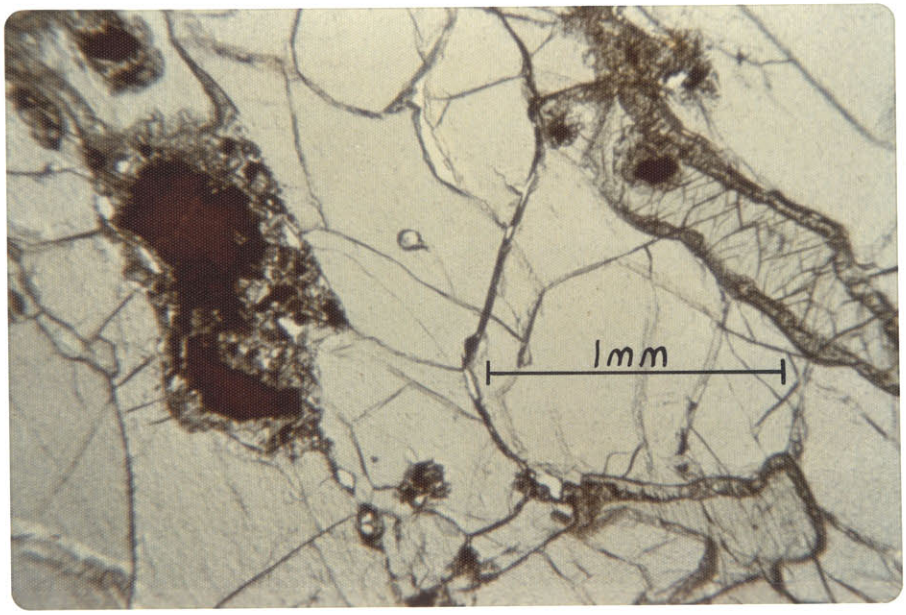

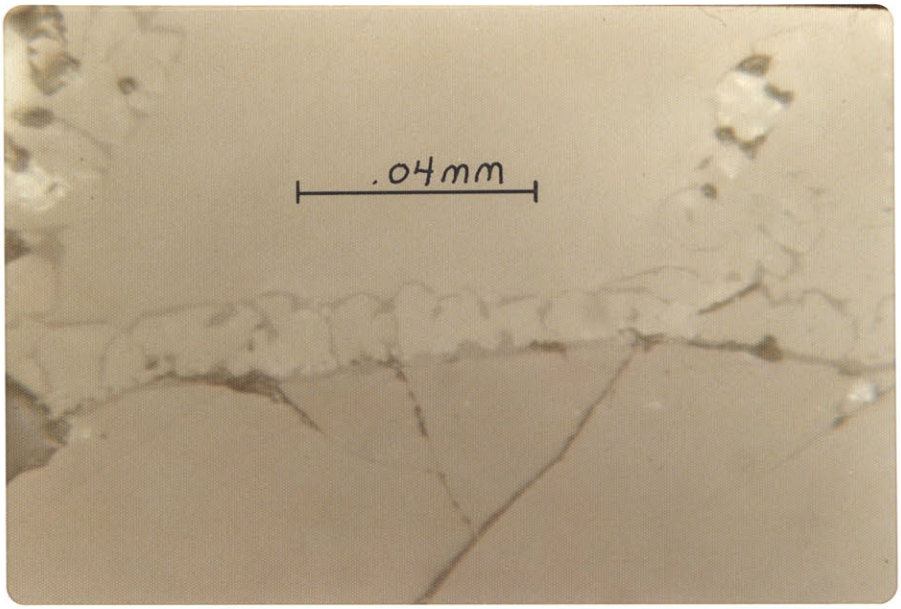

Plate 5-5 (top): Lherzolite with fine-grained zone about spinel and partially melted clinopyroxene.

Plate 5-6 (bottom): Reflected light image of the margin of a partially melted clinopyroxene.

phases of the lherzolites. This variety of spinel exhibits no sign of instability and is identical to its counterpart described in the section on amphibole-bearing lherzolites.

c) Four Phase Lherzolite

Xenoliths in this category contain no trace of either hydrous silicates or fine-grained zones. They consist only of the four essential lherzolite phases.

The Cr-diopsides of these lherzolites are bright green in color, have a vitrious lustre, and lack inclusions or vesicules. No evidence is found for partial melting along their grain boundaries. The Cr-spinel is red-brown in color and is present as both interstitial and included grains. Though the interstitial spinel continues to appear slightly embayed in some cases, it is not vesicular and shows no signs of instability.

d) Interpretation of the Petrographic Features of the Fresh Lherzolites

Of 27 nodules initially sectioned, 3 contain what appears to be primary amphibole, 12 contain fine-grained, glass-bearing zones and 11 consist only of olivine, orthopyroxene, Cr-diopside, and spinel. A few of the spinels in the remaining 2 specimens have voids about them, but it is difficult to rule out the possibility that these were created during thin sectioning.

The textural relationships of the amphibole in the first three nodules suggest that it is breaking down to an assemblage of clinopyroxene, olivine, spinel, and glass. The following criteria indicate that

the fine-grained, glass-bearing zones observed in approximately fifty percent of the fresh lherzolites represent the sites of former amphibole; identical mineralogy to the fine-grained zones observed replacing amphibole, occasional pseudomorphic outline, common presence of relict spinel similar to those found in amphibole, resemblance of associated clinopyroxene to that found with amphibole. The presence of abundant vesicules in the glass of the fine-grained zones indicates that it was molten as its xenoliths reached the surface. This implies that the melting of the original amphibole occurred as the lherzolites were entrained in their alkalic magmas.

In summary, the petrographic features of 50% of the fresh lherzolites suggest that they contained amphibole while they were in place in the upper mantle. According to this interpretation, much of the amphibole was destroyed as alkalic magmas brought the lherzolites to the surface.

Reports of interstitial, pargasitic amphibole in lherzolite xenoliths are becoming increasingly common in the literature. White (1966) recognized a number of amphibole-bearing lherzolites in his Hawaiian xenolith suite. The clinopyroxenes of such lherzolites tended to be Na-rich and exhibited partial melting textures. Varne (1970) has described an amphibole lherzolite from the Kirsh volcano, South Yemen, which lacks interstitial spinel. Partial melting of the amphibole has produced fine-grained zones of pyroxene, spinel, and glass. Wilshire (1971) has found amphibole-bearing lherzolites at Dish Hill, California. Boyd (1971) and Smith (1973) have described harzburgites containing intergrowths of Cr-

spinel and amphibole from kimberlite pipes in South Africa. Griffin (1973) reports the occurrence of amphibole, mantling embayed spinel in lherzolites from the Fen alkaline complex, Norway. Best (1974) has found six amphibole-bearing lherzolites in the western Grand Canyon. He observes, however, that half of the lherzolites from this locality contain fine-grained aggregates of pyroxene and Cr-spinel in vesicular, colorless glass. He interprets these aggregates to be remnants of amphibole. Frey (1974) describes interstitial amphibole associated with porous zones consisting of euhedral clinopyroxene, olivine, and spinel with glass in lherzolites from the Victorian basanites of Australia.

II Iddingsitized Lherzolite Suite

Xenoliths belonging to this group are characterized in hand specimen by earthy red-brown, altered olivine. In thin section the olivine is surprisingly fresh in appearance. The extent of the alteration varies from the presence of bright orange-red iddingsite along fractures and as occasional narrow wisps to a pervasive, fine feather-like network. Only olivine is affected. In some cases extensive precipitation of opaques is associated with the iddingsite alteration. The habit of these opaques ranges from parallel 5 micron plates or needles to chains and networks of 10 micron, equant grains in the same olivine crystal. Frequently, this precipitation does not extend throughout a whole slide but is localized in small patches associated with fractures or near the margins of the xenolith.

The nature of the spinel, again, appears to be a distinctive criteria for subdividing the nodules of this suite. However, unlike the relationships observed in the fresh lherzolites, fine-grained zones about spinel are rare. Instead color is the diagnostic property. The color of the spinels ranges from light olive green to dark red-brown. The green spinel has an anhedral, habit and appears embayed. In nodules with red-brown spinel, on the other hand, a significant proportion of the spinel occurs as rounded to equant inclusions in the other silicate phases. In addition, the interstitial spinel grains have a less embayed appearance than the green spinels. Intermediate colored spinels often exhibit thin, darkened margins.

The clinopyroxenes of nodules containing green spinel commonly have .1 to .3 mm altered margins. The inner edges of these margins appear to be bounded by minute crystal faces when viewed in transmitted light. The nature of the body of these margins is obscure. In reflected light, they are observed to contain irregular stringers and patches of material with a low reflectivity. Occasionally discontinuous seams of this material line the contacts of the Cr-diopside. The width of these structures rarely exceeds 10 microns. Another characteristic feature of the clinopyroxenes in nodules with green spinel is the presence of numerous planes of minute bubbles (less than one micron in size). Such structures have been interpreted to be the sites of fracture annealing (Roedder, 1965). The clinopyroxenes of nodules containing red-brown spinel do not exhibit altered margins and appear internally clear.

There is an apparent textural difference between the xenoliths with green spinel and those with red-brown spinel. The former tend to be

finer grained with an average grain size of approximately 1 mm. They also contain, however, larger grains of clinopyroxene and orthopyroxene (porphyroblasts) which often exceed 2 mm in size. These xenoliths typically exhibit a compositional foliation defined by variations in the proportion of clinopyroxene. Xenoliths with red-brown spinel tend to be very coarse-grained, the average grain size occasionally exceeding 4 mm. They commonly exhibit a strong foliation defined by the pervasive flattening of olivine and orthopyroxene grains. There appears to be a complete gradation between these two textural types.

Only one of the iddingsitized xenoliths that have been examined contains a fine-grained melt zone. It is an oval, porous patch consisting of euhedral crystals of clinopyroxene, olivine, and spinel in a colorless glass. There is, however, no relict of embayed spinel.

In summary, the most variable feature of the iddingsitized lherzolite suite is the color of its spinel. A continuous sequence of xenoliths can be organized ranging from those containing red-brown spinel to those with olive green spinel. The presence of partial melting textures in the clinopyroxenes and the general fabric of a xenolith can be correlated with its position in this sequence.

CHAPTER 6 CHEMISTRY OF THE PHASES OF THE LHERZOLITE XENOLITH SUITE

I Analytical Technique

All chemical analyses reported in this chapter were performed with a M.A.C. electron microprobe owned by the Department of Earth and Planetary Sciences of M.I.T. This probe is part of an automated system designed by Finger and Hadidiacos (1972) using a PDP 11/20 mini-computer. The instrument has a take-off angle of 38.5° and employs three spectrometers with analysing crystals of R.A.P., P.E.T. and LiF. Flow proportional counters are used with the first two crystals and a scintillation counter is used with the LiF crystal.

Analyses were reduced on-line with the "GeoLab" program of Finger and Hadidiacos (1972) which employs the correction scheme of Albee and Ray (1970). In a standard operating set-up, a filament voltage of 15 KV was used with a beam current of 300 nanoamps and counting times of 30 secs. per element.

During standardization, a minimum of 5 replicate counts were taken per element. If the ratio of the standard deviation of these counts to the error predicted by counting statistics exceeded 3, the element was re-standardized. The standards employed varied according to the nature of the material being analyzed.

Analyses whose sum concentrations were not within the range 98.5 to 101.5 were discarded. In practice, few analyses were accepted whose sums differed more than 1% from 100%. For minerals, any analysis whose cation sum (calculated on the basis of an ideal number of oxygens atoms) differed

by more than 1% of the predicted value was discarded. Again, in practice few analyses whose cation error exceeded .5% were accepted.

In the following sections, the Mg number of a phase will frequently be reported. This parameter is defined as the atomic fraction Mg/Mg + Σ Fe. This fraction is given to three significant figures with an approximate precision of $\pm$.001.

II Lherzolite Olivines

The olivines of the fresh lherzolite suite have Mg numbers ranging from .890 to .915. There is a weak correlation between the modal concentration of olivine in a lherzolite nodule and the Mg number of the olivine; i.e., the most olivine rich xenoliths tend to have the most magnesium rich olivines.

Euhedral olivine found in the fine-grained, glass-bearing zones have significantly higher Mg numbers than do their associated interstitial olivine. These higher Mg numbers range between .920 and .935. Individual euhedral olivine crystals are zoned with Mg numbers increasing towards their margins. These olivines are also characterized by relatively high CaO concentrations, averaging .10 to .24 weight percent compared to .04 to .09 weight percent for the host olivines. Though this difference is small, it is significant when compared to the standard deviation of .016 weight percent CaO for analyses of individual olivine grains. The high calcium content of the euhedral olivines supports the petrographic interpretation that they are quench crystals in a silicate glass (Simkin and Smith, 1970).

The round olivine inclusions found in the clinopyroxenes of some of the amphibole-bearing lherzolites are chemically identical to the interstitial olivine.

The olivines of the iddingsitized lherzolites have not been systematically analyzed because the iddingsite alteration and its associated opaque precipitation has altered their original compositions. In particular, heavily altered olivines in this suite exhibit anomalously high Mg numbers.

III Lherzolite Orthopyroxenes

a) Fresh Lherzolite Suite

The Mg numbers of the orthopyroxenes in the fresh lherzolite suite range between .896 and .916. Again, there is a weak correlation between the modal abundance of olivine and the Mg number of the corresponding orthopyroxene. The chemistry of the orthopyroxenes is remarkably uniform throughout the fresh lherzolite suite. The largest variation is found in their alumina contents. The weight percent Al_2O_3 in orthopyroxene varies from 2.27 to 3.43 (average standard deviation per nodule = .107 weight percent Al_2O_3).

Orthopyroxene found as rounded inclusions in the clinopyroxene of amphibole-bearing lherzolite 10006 has an Al_2O_3 content of 1.25 and a Mg number of .920 compared to 3.03 and .913 respectively for the interstitial orthopyroxene.

b) Iddingsitized Lherzolite Suite

The Mg numbers for the orthopyroxenes of this suite range from .901 to .912 and are strongly correlated to the petrographic sequence described in the preceding chapter. Orthopyroxenes from nodules with the greenest spinels have the lowest Mg numbers while those from nodules with the darkest spinels have the highest Mg numbers. The relative abundances of Al_2O_3, Cr_2O_3, and TiO_2 in the orthopyroxene of a lherzolite can also be correlated with its position in the petrographic sequence defined by the spinels. Al_2O_3 ranges from 4.58 weight percent in the nodules with green spinel to 2.74 weight percent in the nodules with red-brown spinel (average standard deviation per nodule = .082 weight percent Al_2O_3). Similarly Cr_2O_3 and TiO_2 vary from .22 and .14 weight percent to .45 and .02 weight percent respectively. Although the variations in Cr and Ti are small, they appear to be significant in light of their small average standard deviation of .01 weight percent per nodule. In addition, both these elements were analyzed using standards with correspondingly low concentrations (Di 96 CrCats 4: 0.86% Cr and Di2Ti: 1.20% Ti).

IV Cr-Spinels

Chemical data has been collected for the spinels of 21 lherzolites. These spinels are the typical Cr-bearing, magnesium-rich variety which characterize spinel lherzolites (Ross et al., 1954). Of all the phases found in the Nunivak lherzolites, however, the spinels exhibit the largest compositional variation. The chemistry of five textural spinel types will be examined:

1) interstitial spinel; ranging from the red-brown spinel of both of the iddingsitized and fresh, four phase lherzolites to the olive green spinel of the iddingsitized lherzolites.

2) relict spinel; occurring as embayed and vesicular grains in fine-grained, glass-bearing zones.

3) core spinel; occurring as central inclusions in amphibole.

4) spinel occurring as equant inclusions in silicate phases other than amphibole.

5) euhedral spinel; found as skeletal grains in the glass of fine-grained zones.

a) Chromium and Aluminum Variations

Figure 6-1 documents the variation in the trivalent cation composition of the interstitial, relict, and core spinels of both the iddingsitized and fresh lherzolites. The euhedral spinels and spinels occurring as inclusions in silicate phases other than amphibole are not represented. The relict and core spinels are highly zoned (see section IV c) and therefore each plot in Figure 6-1 represents the average of 6 to 10 analyses for a single grain. Occasionally more than one of these grains is represented per nodule. The amount of trivalent iron in the spinels was calculated by a method similar to that of Stevens (1944). After Si and Ti were removed as forsterite and illmenite respectively, sufficient Fe^{2+} was converted to Fe^{3+} to balance the equation: 2 x divalent cations = trivalent cations.

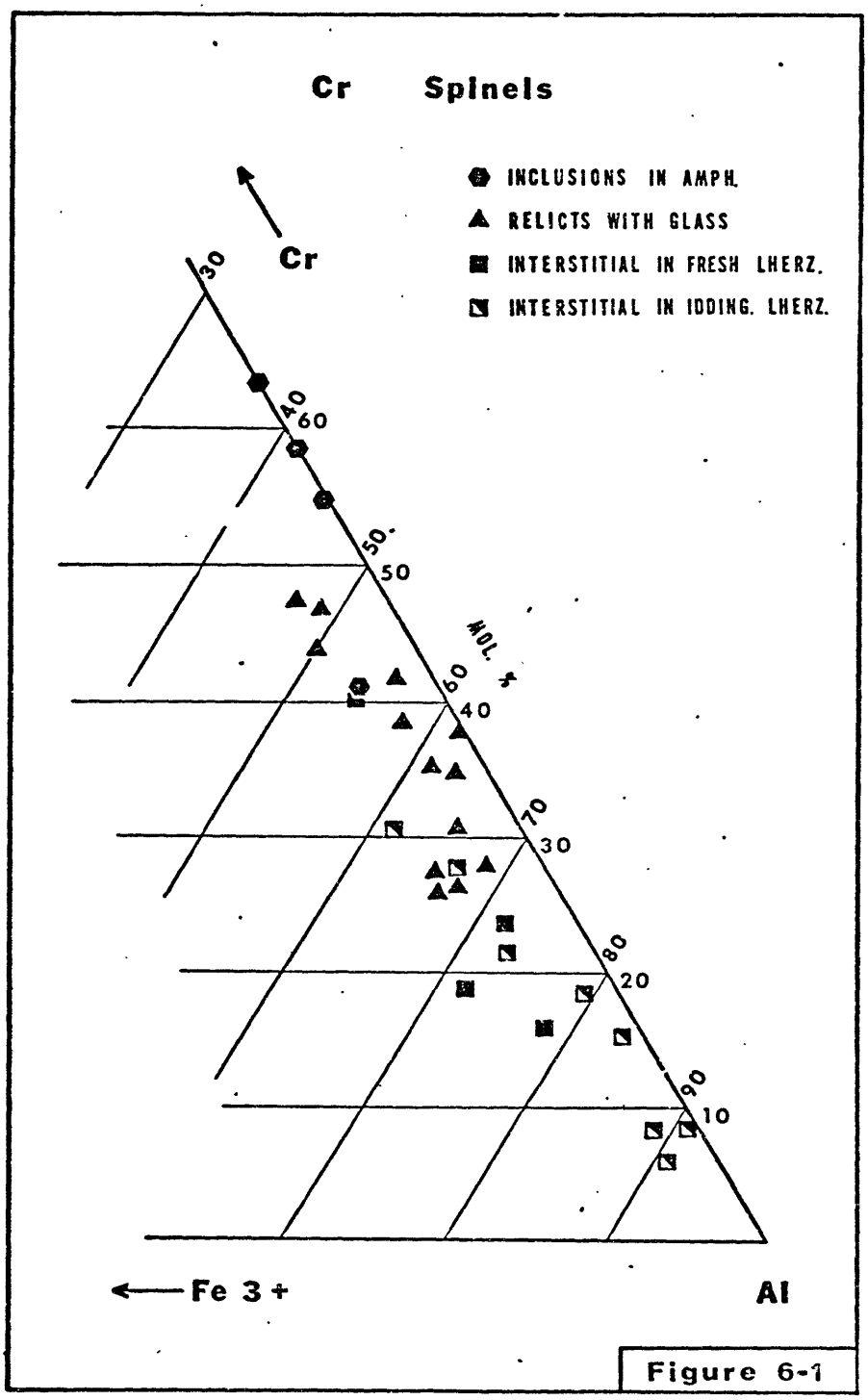
Cr Spinels
INCLUSIONS IN AMPH.
RELICTS WITH GLASS
INTERSTITIAL IN FRESH LHERZ.
INTERSTITIAL IN IDDING. LHERZ.
Cr
30
40
60
50
50
60
40
70
30
80
20
90
10
MOL. %
Fe 3+
Al

Figure 6-1

The compositional variation of the trivalent cations in the spinels (Figure 6-1) is largely restricted to Cr and Al, while the relative amount of calculated Fe^{3+} remains uniformly low (less than 10 atomic percent $Fe^{3+}/Cr + Al + Fe^{3+}$). The following spinel types are listed in order of decreasing $Cr/Cr + Al + Fe^{3+}$: core spinel in amphibole, 2) relict spinel in fine-grained zones, 3) red-brown spinel of both the fresh and iddingsitized, four phase lherzolites, 4) olive green spinels of the iddingsitized lherzolites.

The spinels of the iddingsitized lherzolite suite define a continuous compositional spectrum which can be correlated with their color variation; i.e., the red-brown spinels are the most chromian and the olive green spinels are the most aluminous. The red-brown spinel compositions of this suite coincide with those of the interstitial spinels in the four phase, fresh lherzolites.

b) Chromium and Alumium versus Magnesium and Iron

Figures 6-2 and 6-3 are log-normal plots which illustrate an excellent, inverse correlation between the Cr/Cr + Al and Mg/Mg + Fe atomic ratios for the spinels of the lherzolite suites. Figure 6-2 is the plane $MgAl_2O_4 - MgCr_2O_4 - FeCr_2O_4 - FeAl_2O_4$ of the spinel prism first used by Stevens (1944) and later by Irvine (1965), Jackson (1969) and Loney (1971). In this diagram Fe^{3+} has been neglected.

Irvine (1965) has demonstrated thermodynamically that the composition of a spinel coexisting with an olivine of a specified composition at a given temperature is constrained to what he terms an equipotential surface within the spinel prism. The trace of such a surface for olivine

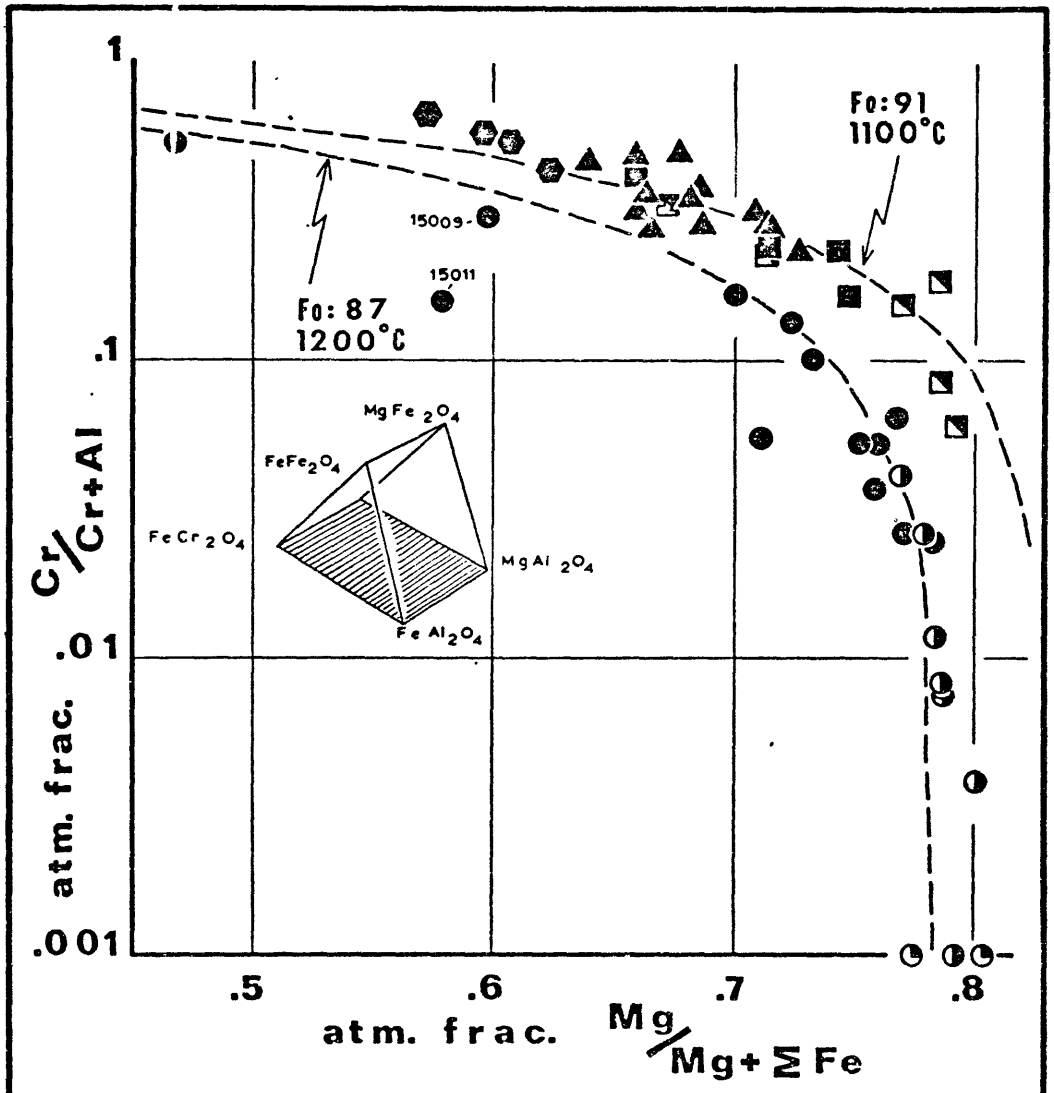

- in amph.
- in glass bearing zones
- interstitial in idd. lherz.
- interstitial in fresh lherz.
- in granulites & dunites
- in symplectites of granulites
- in felds. of granulites

SPINELS

Figure 6-2

Fo 91 (approximate mean composition of olivine in fresh lherzolites) calculated at 1100°C is shown by the dashed line in Figure 6-2. This curve was calculated according to the formula:

$$T = \{(-\Delta G^\circ_{MgSi_{0.5}O_2} - \alpha\Delta G^\circ_{FeCr_2O_4} - \beta\Delta G^\circ_{FeAl_2O_4} + \Delta G^\circ_{FeSi_{0.5}O_2} + \alpha\Delta G^\circ_{MgCr_2O_4} + \beta\Delta G^\circ_{MgAl_2O_4})/R \ln \{\frac{X_{Mg}^{OL} X_{Fe^{2+}}^{CHR}}{X_{Fe^{2+}}^{OL} X_{Mg}^{CHR}}\}\}$$

$$\alpha = Cr/Cr + Al$$

$$\beta = Al/Cr + Al$$

or

$$T = \frac{5580\alpha + 1018\beta + 2400}{.90\alpha + 2.56\beta - 1.47 + 1.987 \ln K_{DMg - Fe^{2+}}}$$

After Jackson, 1969

The curve in Figure 6-2 is not intended to represent an accurate temperature determination because the uncertainties in the ΔG° values alone yield a temperature uncertainty of ±300°C. (Jackson, 1969). However, the correspondence between the equipotential curve and the locus for the lherzolite spinels is striking; especially considering that the spinels included in amphibole and fine-grained, glass-bearing zones are not theoretically constrained by the composition of the lherzolite olivine.

The compositions of the spinels found in nodules which are thought to be crustal cumulates (Chapter 7) are also plotted in Figure 6-2. They lie at relatively lower Cr/Cr + Al and Mg/Mg + Fe atomic ratios and coincide with an equipotential curve for olivine Fo 87 (approximate mean com-

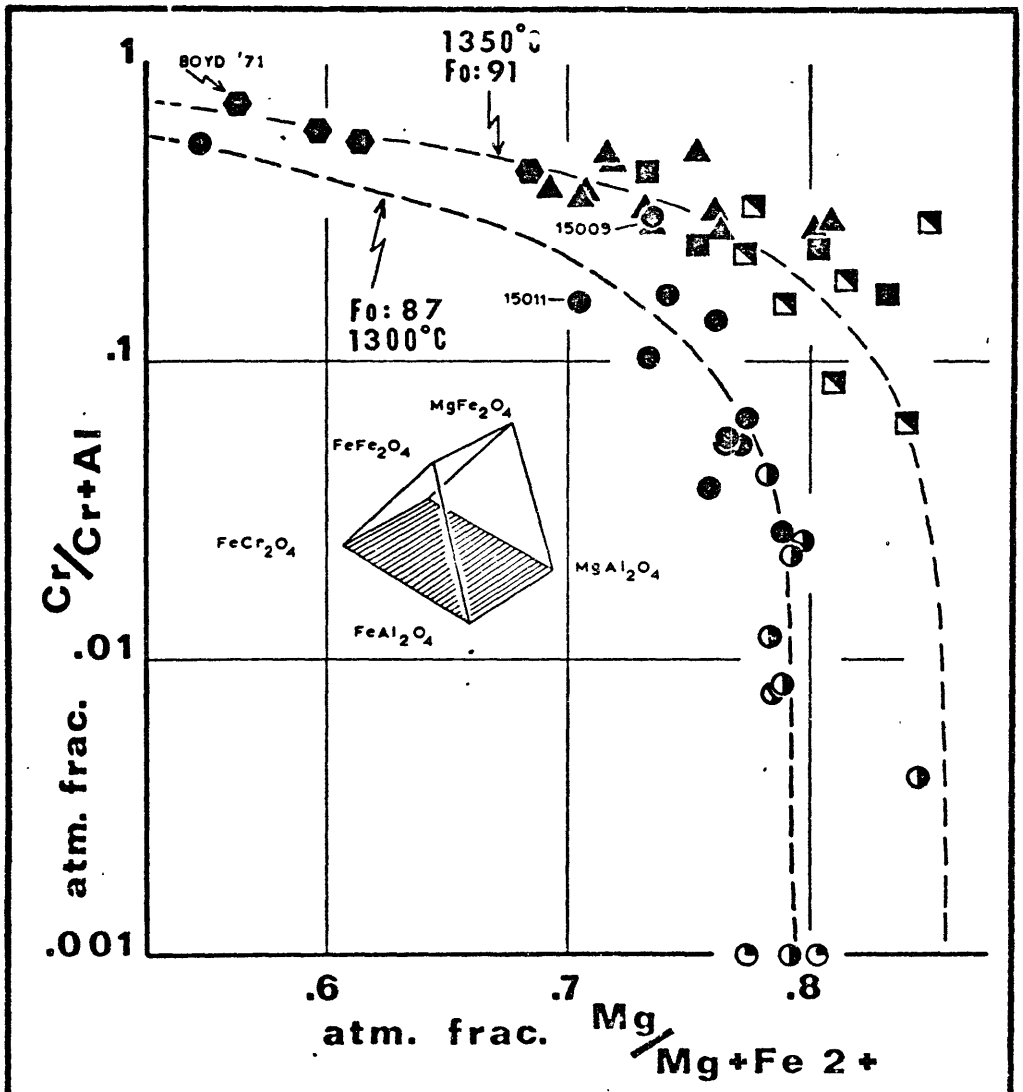

- in amph.
- in glass bearing zones
- interstitial in idd. lherz.
- interstitial in fresh lherz.
- in granulites & dunites
- in symplectites of granulites
- in felds. of granulites

SPINELS

Figure 6-3

position of cumulate olivines) determined at 1200°C.

Figure 6-3 is similar to 6-2 except that the Fe^{3+} content of the spinels has been taken into account. The diagram is constructed by projection onto the Fe^{3+} absent face of the spinel prism. Comparing Figures 6-3 and 6-2, we see that the effect of this modification is to shift corresponding points towards the right side of the diagram. Despite the resultant increased scatter in the data points, the trends observed in Figure 6-2 are preserved. The locus of the data points in Figure 6-3, however, is better modeled by an equipotential curve calculated at a temperature of 1300°C. It is interesting to note that the magnitude of the shift to the right between the two Figures is greater for the lherzolite spinels (250°C) than for the cumulate spinels (100°C).

The composition of spinel intergrown with pargasite in a harzburgite xenolith from the Wesselton mine, South Africa (Boyd, 1971) is also plotted in Figure 6-3. It plots just above the trend for the Nunivak spinels and its associated olivine has a composition of Fo 94.

To summarize Figures 6-2 and 6-3; the locus of lherzolite spinel compositions coincides with a theoretical curve calculated by assuming that the spinels are in equilibrium with their associated olivines. The position of a spinel on this locus can be correlated with its mode of occurrence. In these spinels increasing Cr/Cr + Al is accompanied by decreasing Mg/Mg + Fe.

c) Chemical Zoning

The relict spinels found at the center of fine-grained, glass-bearing zones are chemically zoned. Figure 6-4 illustrates the results

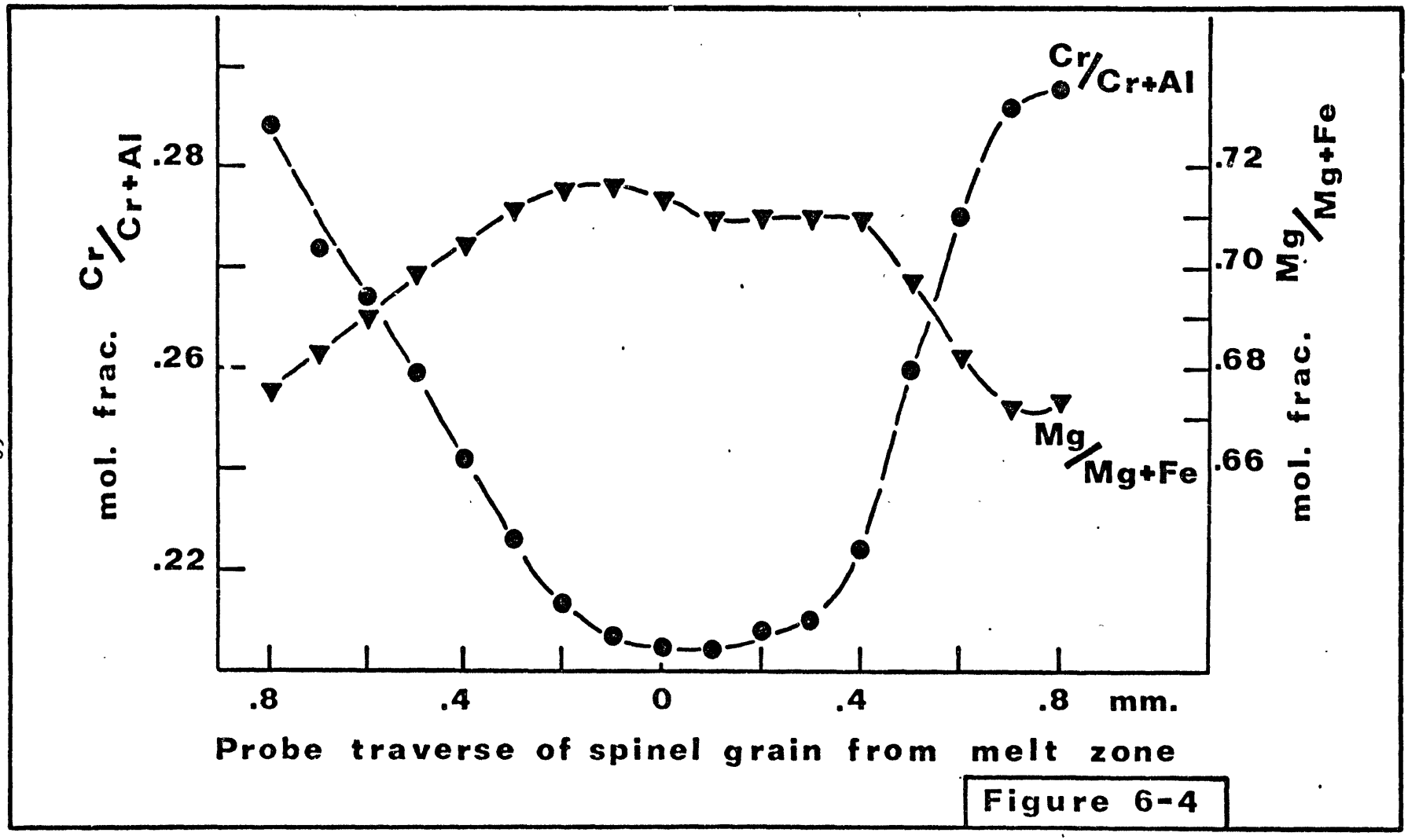
Cr/Cr+Al
mol. frac.
.28
.26
.22
Mg/Mg+Fe
mol. frac.
.72
.70
.68
.66
.8
.4
0
.4
.8 mm.
Probe traverse of spinel grain from melt zone

Figure 6-4

of a microprobe traverse across on particularly large and massive spinel grain found in specimen 10013. The zoning pattern is one of increasing iron and chromium with reciprocal decreasing magnesium and aluminum from the core to the grain margin. Because of their typical vesicular and embayed habit, the majority of the relict spinel grains exhibit zoning patterns considerably more complicated than that pictured in Figure 6-4. In these grains, all borders whether internal or external are chromium and iron rich, while the relative proportions of magnesium and aluminum increase away from these contacts.

The core spinel intergrowths in the amphiboles of specimen 10016 exhibit chemical zoning patterns similar to those of the vesicular, relict spinels. The average composition of this intergrown spinel, however, is considerably higher in chromium and iron and lower in magnesium and aluminum than those of the relict spinels. The compositional ranges of single relict spinels and core spinels in amphiboles are presented in Figure 6-5b. Though the compositional ranges of individual grains do not necessarily overlap, they parallel the locus of the average spinel compositions of the lherzolite suites (compare equipotential curve for olivine Fo 91 calculated at 1100°C in Figures 6-2 and 6-5b). The chemical zoning in the relict spinels bridges the gap between the compositions of spinels included in amphibole and the interstitial spinels of the four phase, fresh lherzolites.

d) Spinel Inclusions in Silicate Phases other than Amphibole

Spinel inclusions in the silicate phases of both the iddingsitized and fresh, four phase lherzolites have compositions identical to those of

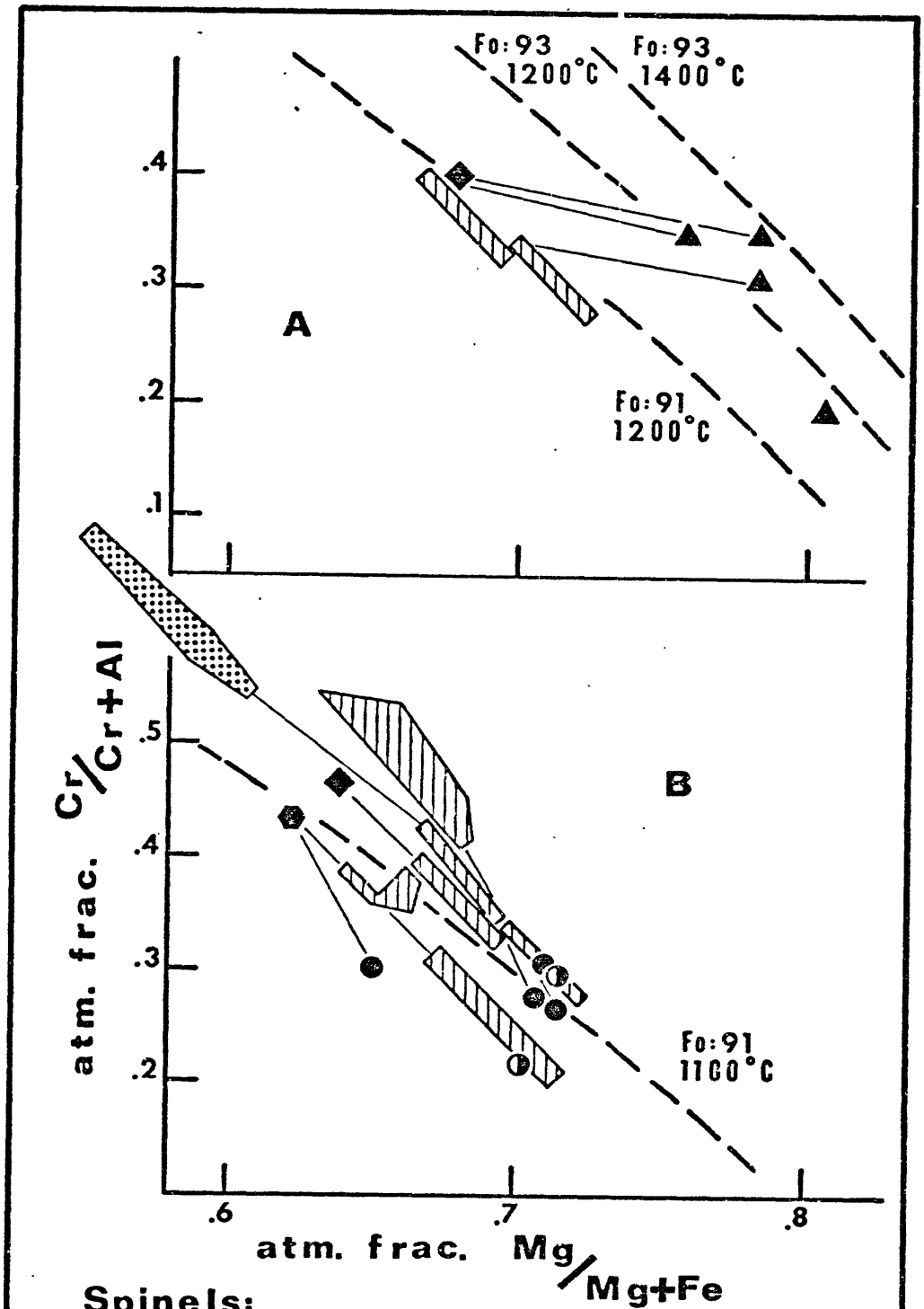
Fo:93
1200°C
Fo:93
1400°C
A
Fo:91
1200°C
.4
.3
.2
.1
B
Fo:91
1100°C
atm. frac. Cr/Cr+Al
.5
.4
.3
.2
.6
.7
.8
atm. frac. Mg/Mg+Fe
Spinels:
in amphibole
in olivine
in opx
residual: range for zoning
residual
euhedral

Figure 6-5

their associated interstitial spinel. This is not the case, however, in lherzolites which contain amphibole or fine-grained, glass-bearing zones. Here it is found that spinels included in olivine or orthopyroxene have compositions which are more magnesium-rich and chromium-poor than any of the other varieties of spinel in the same specimen. In Figure 6-5b the compositions of spinel inclusions are joined to those of associated relict spinels and, where present, core spinels in amphibole. For a given xenolith, the plots of these three varieties of spinel are approximately colinear and define trends which parallel that of the zoning in the relict and core spinels. In terms of major element chemistry, the spinel inclusions in olivine and orthopyroxene are most similar to the interiors of the relict spinels, while the spinels included in amphibole resemble the margins of the relict spinels.

e) Euhedral Spinels

The euhedral spinels in glass-bearing zones are small and difficulty was encountered in obtaining acceptable totals for microprobe analyses. Because of this problem, analyses whose oxide sum totaled as low as 97.5% were sometimes accepted and usually only one analysis was obtained per grain. Thus there are few analyses for this spinel type and conclusions about their chemistry are tenuous.

The compositions of these euhedral spinels are presented in Figure 6-5a. Tie-lines join these points to the compositions of the margins of their associated relict spinels. It is apparent that for a given Cr/Cr + Al ratio, the euhedral spinels are significantly more Mg-rich than their associated relict spinel. Equipotential curves for several temper-

atures are plotted for olivines of composition Fo 91 and 93 (interstitial olivine and euhedral olivine in fine-grained zones respectively) in Figure 6-5a. It appears that the higher Fo content of the euhedral olivine can not entirely account for the magnesium enrichment of the euhedral spinel. If these fine-grained, glass-bearing zones were equilibrium assemblages, then the euhedral spinel compositions may record higher temperatures than the relict spinels.

V Lherzolite Clinopyroxenes

a) Interstitial Clinopyroxene

The chemical variation exhibited by the interstitial, chromian diopsides is potentially the most useful petrogenetic indicator in the nodules of the two lherzolite suites. When plotted in the standard pyroxene quadrilateral (Wo-En-Fs) these clinopyroxenes appear to have a limited compositional range, falling in the upper third of the endiopside field defined by Poldervaart and Hess (1951). The compositional variations of the lherzolite clinopyroxenes, however, are largely in components which cannot be represented in the pyroxene quadrilateral.

Figure 6-6a is an unconventional projection in which the pyroxene components wollastonite, enstatite, and ferrosilite are grouped as one, endiopside, and represented by the left corner of a ternary diagram. The apex of the triangle represents the Na-bearing components jadeite and acmite, while the right corner (CaTs) represents calcium-tschermak components of both Al ($CaAlAlSiO_6$) and Cr ($CaCrAlSiO_6$) plus $CaTiAl_2O_6$. No attempt is made in this diagram to distinguish between jadeite and acmite

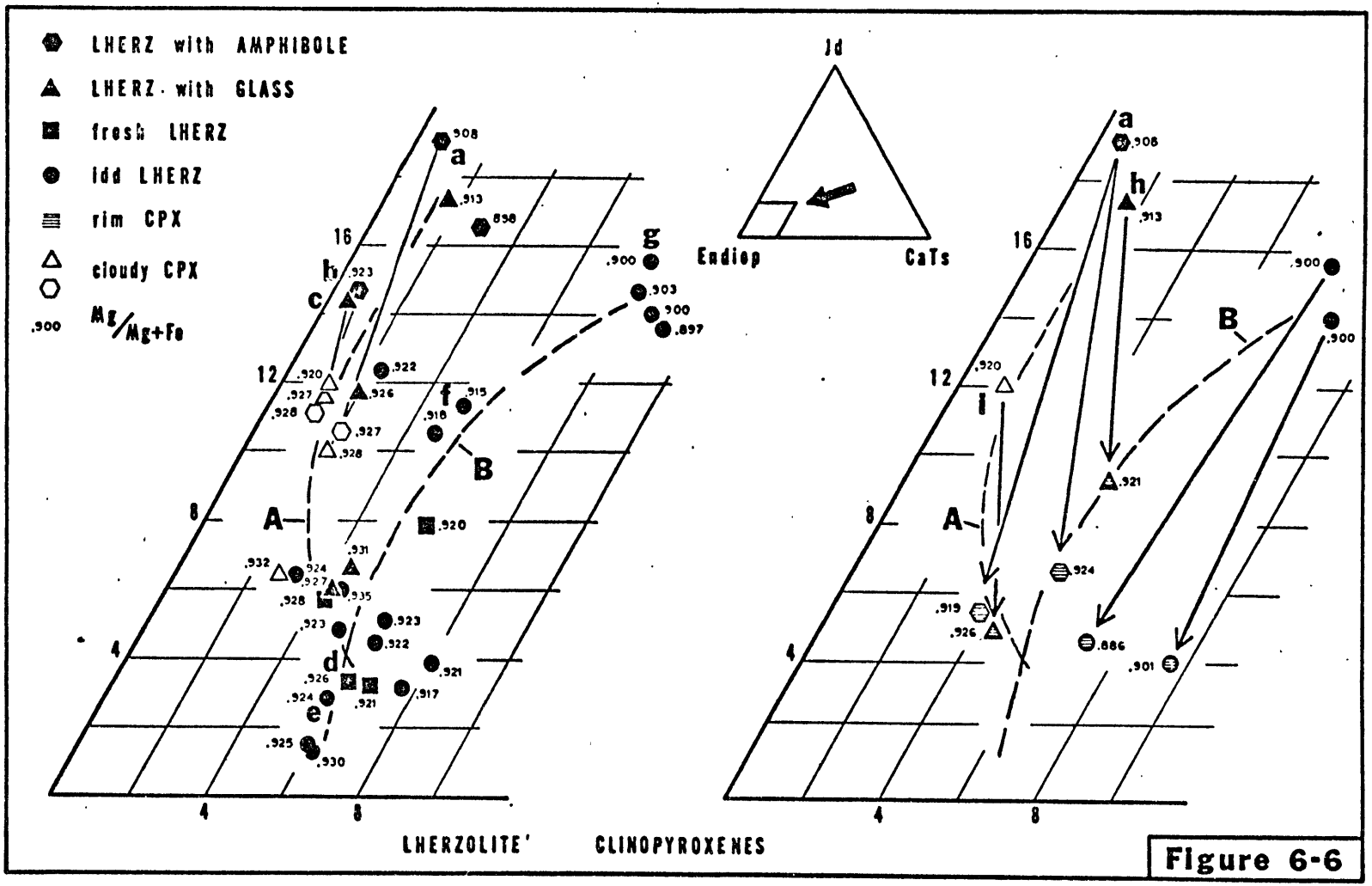
LHERZ with AMPHIBOLE
LHERZ with GLASS
fresh LHERZ
Idd LHERZ
rim CPX
cloudy CPX
.900 Mg/Mg+Fe
Jd
Endiop
CaTs
LHERZOLITE' CLINOPYROXENES

Figure 6-6

because of the large uncertainties in the calculated Fe^{3+} content of the clinopyroxenes. The majority of the analyzed clinopyroxenes gave slightly high cation totals and as a result the conversion of all the Fe^{2+} to Fe^{3+} was often insufficient to achieve ideal stoichiometry. An excess of X and Y cations appears to be a general characteristic of lherzolite clinopyroxenes (Griffin, 1973; Green, 1964; and Ross et al., 1954).

Figure 6-6a reveals the presence of two compositional trends in the lherzolite clinopyroxenes which can be correlated with the textural variations described in Chapter 5. The dashed curve labeled "A" represents a trend of Na enrichment at the expense of endiopside and tschermak components. This trend is delineated by the clinopyroxenes of lherzolites which contain either amphibole or fine-grained, glass-bearing zones. The more extensive the development of this latter texture, the more Na-rich the associated clinopyroxene. Curve "B" corresponds to a trend of increasing sodium and tschermak components at the expense of endiopside. This curve is defined by clinopyroxenes found in the iddingsitized lherzolite suite. The position of a nodule's clinopyroxene on this trend can be correlated with the color (and composition) of its spinel; i.e., the most endiopside-rich clinopyroxenes are associated with the darkest, most chromian spinels and the clinopyroxenes richest in Na and tschermak components occur with olive green, aluminous spinels. For both trends, there is a general correlation between the relative proportion of endiopside in a clinopyroxene and its Mg number (Figure 6-6a).

The relative amounts of tetrahedral and octahedral alumium in the lherzolite clinopyroxenes were calculated by assuming that there are two

tetrahedral positions for every six oxygens which are filled first by silicon and then aluminum. The results are presented in Figure 6-7. White (1964) used such data to distinguish clinopyroxenes of garnet-bearing assemblages (eclogites) from those of metamorphic granulites. Aoki (1968, 1973) has demonstrated that the clinopyroxene compositions of spinel lherzolites found in basalts all fall in the granulite field defined by White (1964) and cluster about the line $Al^{vi}/Al^{iv} = 1/1$. The clinopyroxenes of the iddingsitized lherzolites support this observation. The most aluminous clinopyroxenes in this suite are associated with the olive green, aluminous spinels, while the aluminum-poor clinopyroxenes are found with the more chromian, red-brown spinels. The majority of the clinopyroxenes from nodules which contain either amphibole or fine-grained, glass-bearing zones, however, fall in the eclogite field. This not only implies that their xenoliths equilibrated at relatively higher pressures than the other lherzolites (possibly in the presence of garnet), but that the Na enrichment trend exhibited by these clinopyroxenes in Figure 6-6a is one of increasing jadeite rather acmite. The clinopyroxenes of the four phase, fresh lherzolites fall in the granulite field of Figure 6-7, coincident with those of the iddingsitized lherzolites with red-brown spinel. Figure 6-7 also illustrates that the Mg numbers of the lherzolite clinopyroxenes are inversely proportional to their aluminum contents.

There is an interesting pattern for the distribution of Ti in the chromian diopsides of the two lherzolite suites. Figure 6-8 is an overlay of Figure 6-7 on which the Ti content of the clinopyroxenes is contoured. For clinopyroxenes whose compositions fall in the granulite

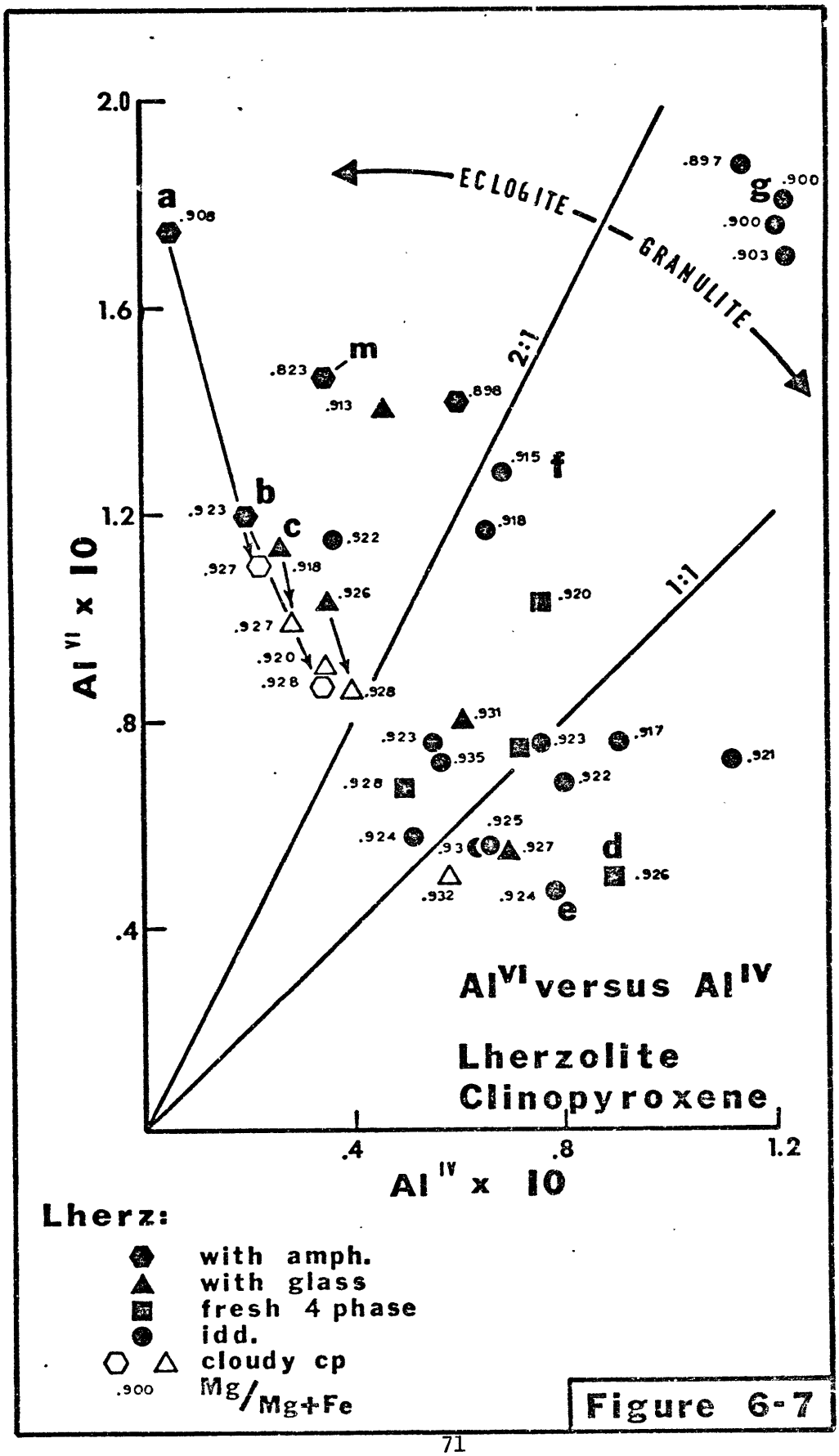
2.0
1.6
1.2
.8
.4
Al^{VI} x 10
.4
.8
1.2
Al^{IV} x 10
ECLOGITE
GRANULITE
2:1
1:1
a
.908
b
.923
c
.927
.918
.922
.926
.927
.920
.928
.928
m
.823
.913
.898
.915
f
.918
.920
.897
g
.900
.900
.903
.931
.923
.935
.923
.917
.921
.928
.922
.925
.924
.93
.927
d
.926
.932
.924
e
Al^{VI} versus Al^{IV}
Lherzolite
Clinopyroxene
Lherz:
with amph.
with glass
fresh 4 phase
idd.
cloudy cp
.900 Mg/Mg+Fe

Figure 6-7

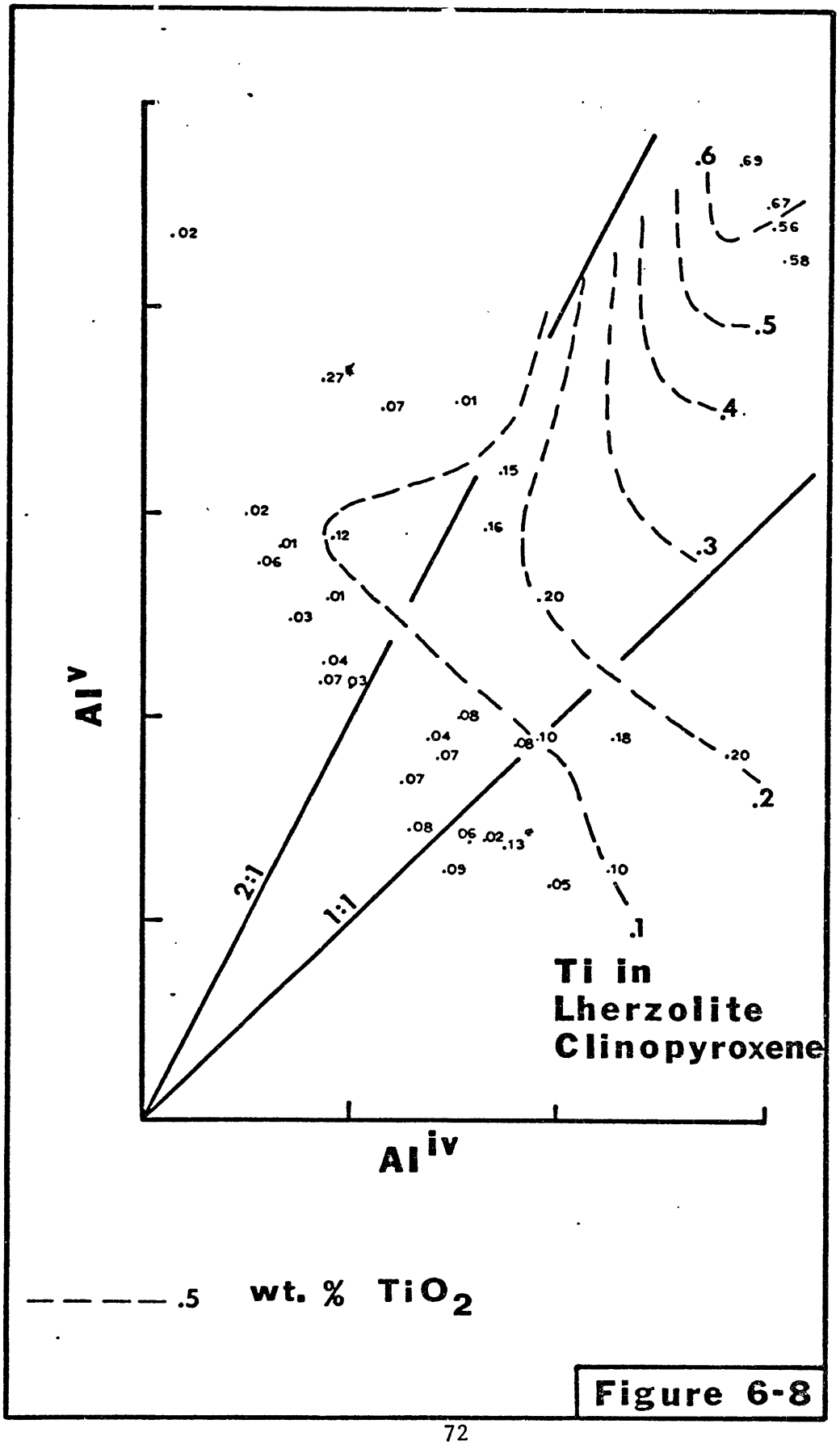
.6
.69
.67
.56
.58
.5
.4
.3
.2
.1
.02
.27
.07
.01
.15
.16
.12
.06
.03
.20
.04
.08
.10
.18
.13
.09
.05
2:1
1:1
Al^v
Al^iv
Ti in
Lherzolite
Clinopyroxene
.5 wt. % TiO2

Figure 6-8

field, there is a direct correlation between aluminum and titanium. The clinopyroxenes which plot in the eclogite field, however, have generally low Ti values over a wide range of aluminum contents.

Table 6-1 lists the compositions of a few representative clinopyroxenes which have been plotted in Figures 6-6 through 6-8. A more complete listing is available in the appendix.

b) Cloudy Alteration in Interstitial Clinopyroxene

Many of the clinopyroxenes of the fresh lherzolites with either amphibole or fine-grained, glass-bearing zones have a milky green, cloudy appearance (Chapter 5). Often one specimen or even one grain will have both clear and cloudy clinopyroxene. Table 6-2 compares the compositions of a few representative clear and cloudy clinopyroxene pairs. The cloudy clinopyroxene is relatively poorer in Na, Al, and Fe but richer in Ca and Mg. There is little difference, however, in the chromium contents of these two types of clinopyroxenes. In Figures 6-6, 6-7 and 6-9 the cloudy clinopyroxenes are represented by open symbols and are joined by tie-lines to the compositions of their coexisting clear clinopyroxenes. The development of the cloudy alteration is seen to correspond to a depletion of jadeite (Al^{vi}). The resultant compositional shift in Figure 6-6a parallels the "A" trend defined by the locus of the compositions of the fresh lherzolite clinopyroxenes.

Carswell (1973) describes a similar phenomena in the clinopyroxenes of garnet lherzolites from South Africa; "cloudy, porous outer zones around clear, pale green cores". He finds that although sodium and alumium are depleted in the cloudy zones, chromium appears to be unaffected.

TABLE 6-1

LHERZOLITE CLINOPYROXENES

	A	B	C	D	E	F	G
SPEC.	10006	10016	10045	10022	10008	10024	10211
SIO2	55.64	54.83	54.43	52.95	52.46	53.47	51.91
TIO2	0.03	0.02	0.01	0.05	0.10	0.15	0.69
AL2O3	4.28	3.27	3.27	2.94	3.25	4.63	7.14
FE2O3	0.00	0.00	0.00	0.00	0.00	0.00	0.00
CR2O3	0.87	0.78	0.63	0.74	0.68	0.75	0.49
FEO	2.80	2.42	2.59	2.58	2.47	2.72	2.90
MGO	15.94	16.22	16.26	17.54	17.40	16.35	14.85
MNO	0.13	0.13	0.08	0.06	0.05	0.11	0.11
CAO	17.61	19.89	20.12	22.91	23.01	20.10	19.16
NA2O	2.71	2.12	2.08	0.41	0.48	1.64	2.28
K2O	0.02	0.01	0.00	0.00	0.00	0.00	0.00
TOTAL	100.03	99.69	99.47	100.18	99.90	99.92	99.53

FORMULA UNITS ASSUMING 6 OXYGENS

SI	1.991	1.981	1.974	1.921	1.910	1.931	1.882
TI	0.001	0.001	0.000	0.001	0.003	0.004	0.019
AL	0.181	0.139	0.140	0.126	0.139	0.197	0.305
FE3+	0.000	0.000	0.000	0.000	0.000	0.000	0.000
CR	0.025	0.022	0.018	0.021	0.020	0.021	0.014
FE2+	0.084	0.073	0.079	0.078	0.075	0.082	0.088
MG	0.850	0.873	0.879	0.949	0.944	0.880	0.803
MN	0.004	0.004	0.002	0.002	0.002	0.003	0.003
CA	0.675	0.770	0.782	0.891	0.898	0.778	0.744
NA	0.188	0.148	0.146	0.029	0.034	0.115	0.160
K	0.001	0.000	0.000	0.000	0.000	0.000	0.000
TOTAL	4.000	4.012	4.020	4.018	4.025	4.013	4.019
MG/MG+FE	0.910	0.923	0.918	0.924	0.926	0.915	0.901

UNLESS OTHERWISE SPECIFIED; TOTAL IRON AS FEO

TABLE 6-2

CLEAR AND CLOUDY LHERZOLITE CLINOPYROXENES

	A	A	B	B	C	C
SPEC.	10006	10006	10016	10016	10045	10045
SIO2	55.64	55.05	54.83	54.99	54.43	54.52
TIO2	0.03	0.06	0.02	0.08	0.01	0.02
AL2O3	4.28	3.06	3.27	2.55	3.27	2.98
FE2O3	0.00	0.00	0.00	0.00	0.00	0.00
CR2O3	0.87	0.69	0.78	0.50	0.63	0.56
FEO	2.80	2.32	2.42	2.26	2.59	2.45
MGO	15.94	16.53	16.22	16.58	16.26	16.37
MNO	0.13	0.09	0.13	0.09	0.08	0.09
CAO	17.61	20.96	19.89	21.20	20.12	20.90
NA2O	2.71	1.51	2.12	1.67	2.08	1.77
K2O	0.02	0.00	0.01	0.00	0.00	0.00
TOTAL	100.03	100.27	99.69	99.92	99.47	99.66
FORMULA UNITS ASSUMING	6	OXYGENS				
SI	1.991	1.978	1.981	1.985	1.974	1.975
TI	0.001	0.002	0.001	0.002	0.000	0.001
AL	0.181	0.130	0.139	0.108	0.140	0.127
FE3+	0.000	0.000	0.000	0.000	0.000	0.000
CR	0.025	0.020	0.022	0.014	0.018	0.016
FE2+	0.084	0.070	0.073	0.068	0.079	0.074
MG	0.850	0.885	0.873	0.892	0.879	0.884
MN	0.004	0.003	0.004	0.003	0.002	0.003
CA	0.675	0.807	0.770	0.820	0.782	0.811
NA	0.188	0.105	0.148	0.117	0.146	0.124
K	0.001	0.000	0.000	0.000	0.000	0.000
TOTAL	4.000	3.998	4.012	4.010	4.020	4.015
MG/MG+FE	0.910	0.927	0.923	0.929	0.918	0.923
	CLEAR	CLOUDY	CLEAR	CLOUDY	CLEAR	CLOUDY

UNLESS OTHERWISE SPECIFIED; TOTAL IRON AS FEO

The absence of glass and the behavior of chromium indicates that the development of the cloudy alteration in the lherzolite clinopyroxenes is not a partial melting process. The nature of the chemical changes involved suggest that the alteration may develop in response to a pressure decrease. Aoki (1973) has proposed a similar process to account for the presence of low Na clinopyroxene in nodules that were originally garnet lherzolites. He believes that they are the product of low pressure recrystallization which has preferentially removed their jadeite components. The clear, but low-Na clinopyroxenes of speciments 10001 and 10003, (the only lherzolites with fine-grained, glass-bearing zones whose clinopyroxenes fall in the granulite field of Figure 6-7), may represent a recrystallized end-produce of such a process.

c) Rim Clinopyroxene

Figures 6-6b and 6-9 compare the compositions of the interiors and rims of the jadeite-rich clinopyroxenes of the fresh lherzolites and the jadeite and tschermak-rich clinopyroxenes of the iddingsitized lherzolites. In the fresh lherzolites, the jadeite-rich interiors of the clinopyroxenes plot in the eclogite field whereas the compositions of the rims fall in the granulite field and are strongly depleted in jadeite but enriched in tschermak and endiopside components. There are corresponding increases in the Mg numbers of the rims of these clinopyroxenes. Table 6-3 lists the compositions of some representative clinopyroxene interior-rim pairs. In addition to the chemical differences already documented in the foregoing, note the sharp increase in chromium in the clinopyroxene rims. The chemical differences between the rims and interiors of the

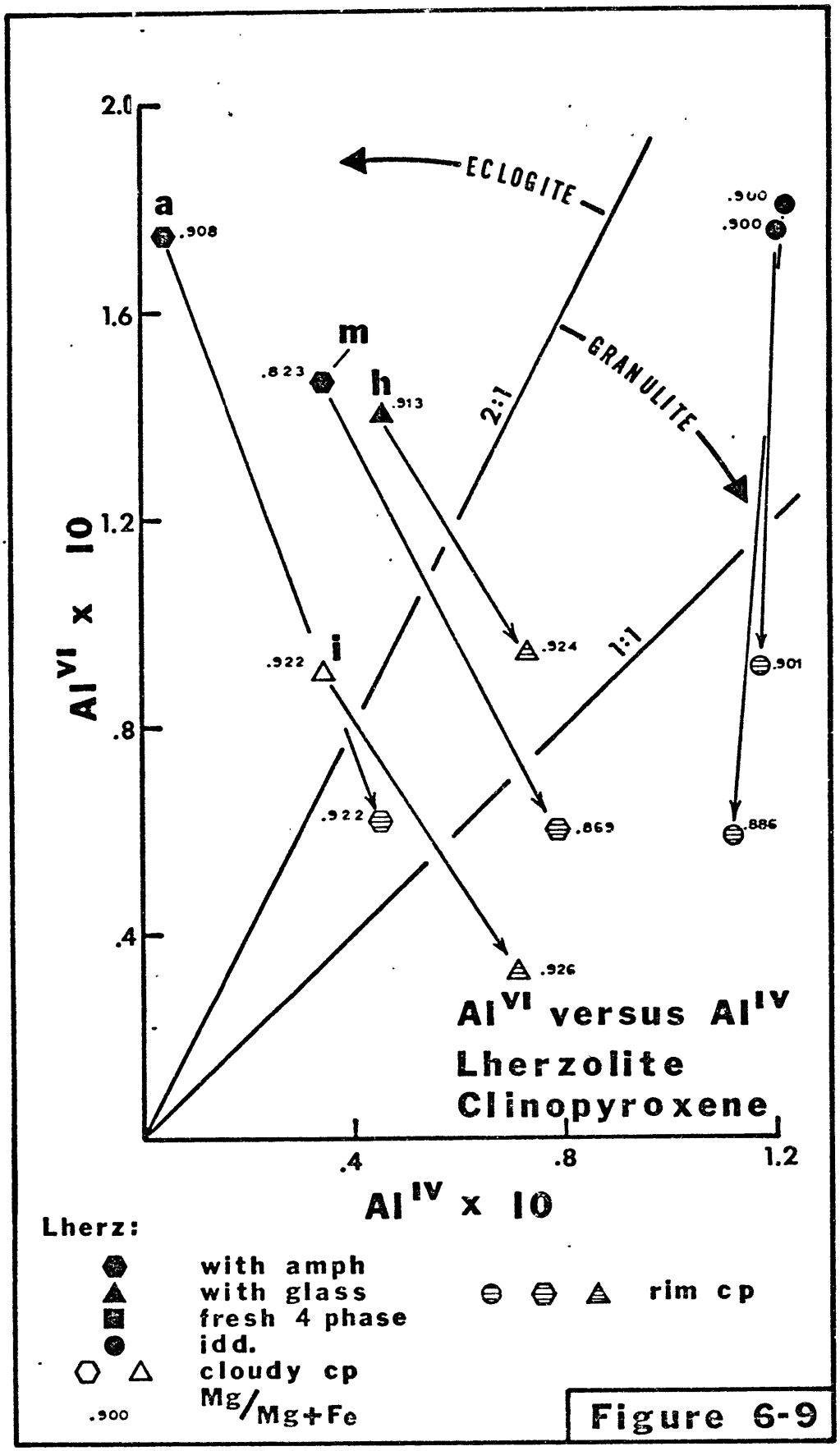
2.0
1.6
1.2
.8
.4
Al^{VI} x 10
ECLOGITE
GRANULITE
2:1
1:1
a
.908
m
.823
h
.913
i
.922
.924
.926
.922
.869
.900
.900
.901
.886
Al^{VI} versus Al^{IV}
Lherzolite
Clinopyroxene
.4
.8
1.2
Al^{IV} x 10
Lherz:
with amph
with glass
fresh 4 phase
idd.
cloudy cp
.900 Mg/Mg+Fe
rim cp

Figure 6-9

TABLE 6-3

INTERIORS AND RIMS OF LHERZOLITE CLINOPYROXENES

	H	H	I	I	A	A
SPEC.	10002	10002	10005	10005	10006	10006
SIO2	54.82	53.64	54.03	53.21	55.64	54.39
TIO2	0.07	0.04	0.04	0.04	0.03	0.03
AL2O3	4.45	3.98	2.98	2.44	4.28	2.15
FE2O3	0.00	0.00	0.00	0.00	0.00	0.00
CR2O3	0.90	1.19	0.68	1.31	0.87	1.35
FEO	2.83	2.73	2.53	2.55	2.80	2.73
MGO	16.55	17.90	16.84	18.03	15.94	17.44
MNO	0.07	0.10	0.09	0.11	0.13	0.16
CAO	18.77	19.54	20.48	21.84	17.61	20.56
NA2O	2.57	1.35	1.74	0.71	2.71	0.77
K2O	0.00	0.03	0.01	0.03	0.02	0.07
TOTAL	101.03	100.50	99.42	100.27	100.03	99.65
FORMULA UNITS ASSUMING		6	OXYGENS			
SI	1.953	1.926	1.963	1.928	1.991	1.972
TI	0.002	0.001	0.001	0.001	0.001	0.001
AL	0.187	0.168	0.128	0.104	0.181	0.092
FE3+	0.000	0.000	0.000	0.000	0.000	0.000
CR	0.025	0.034	0.020	0.038	0.025	0.039
FE2+	0.084	0.082	0.077	0.077	0.084	0.083
MG	0.879	0.958	0.912	0.974	0.850	0.943
MN	0.002	0.003	0.003	0.003	0.004	0.005
CA	0.717	0.752	0.797	0.848	0.675	0.799
NA	0.178	0.094	0.123	0.050	0.188	0.054
K	0.000	0.001	0.000	0.001	0.001	0.003
TOTAL	4.027	4.019	4.024	4.025	4.000	3.990
MG/MG+FE	0.912	0.921	0.922	0.926	0.910	0.919
	INTER	RIM	INTER	RIM	INTER	RIM

UNLESS OTHERWISE SPECIFIED; TOTAL IRON AS FEO

clinopyroxenes of the fresh lherzolites with amphibole or fine-grained, glass-bearing zones supports the conclusion based on textural arguments that these rims were produced by incongruent melting.

The origin of the rims developed on clinopyroxenes in the iddingsitized lherzolites with green spinel is less clear. They are developed only in clinopyroxenes rich in both jadeite and tschermak components. However, unlike the case in the fresh lherzolites, the clinopyroxene rims, their Mg numbers are the same or perhaps smaller than those of the clinopyroxene interiors (Figure 6-9). This last fact is difficult to reconcile with a partial melting origin. The low reflectivity material in contact with this rim clinopyroxene in one specimen (10211) has the composition of plagioclase An 54 (see section VIIa). White (1966) describes similar features developed on the margins of clinopyroxenes rich in jadeite and calcium tschermak components. He found that low reflectivity material adjacent to the clinopyroxene rims was plagioclase An 50, Or 1. He suggests the reaction; jadeite-rich clinopyroxene ⟶ jadeite-poor clinopyroxene plus feldspar and nepheline (?). Thus the apparent incongruent melting of the aluminous clinopyroxenes in the iddingsitized lherzolites may in fact be a solid state breakdown to aluminum poor clinopyroxene and feldspar.

d) Euhedral Clinopyroxene

The euhedral clinopyroxenes of the fine-grained, glass-bearing zones are very silicon deficient and characterized by a high but variable degree of calcium-tschermak substitution of both Al ($CaAlAlSiO_6$) and Cr ($CaCrAlSiO_6$). Table 6-4 lists compositions of euhedral clinopyroxenes

TABLE 6-4

EUHEDRAL LHERZOLITE CLINOPYROXENES

SPEC.	10001	10002	10045	10010	10013	10013
SIO2	49.79	49.57	49.36	51.95	49.84	50.08
TIO2	0.79	0.08	0.09	0.03	0.25	0.27
AL2O3	7.26	6.96	7.62	5.62	7.45	6.82
FE2O3	0.00	0.00	0.00	0.00	0.00	0.00
CR2O3	1.71	3.62	3.47	2.44	3.29	3.01
FEO	2.28	2.29	2.07	2.05	2.38	2.40
MGO	15.30	15.56	14.54	16.47	15.42	15.62
MNO	0.04	0.06	0.12	0.08	0.10	0.10
CAO	21.32	20.03	21.10	19.79	20.51	20.89
NA2O	1.02	1.30	1.20	1.36	1.15	0.99
K2O	0.01	0.00	0.00	0.00	0.01	0.03
TOTAL	99.52	99.47	99.57	99.79	100.40	100.21

FORMULA UNITS ASSUMING 6 OXYGENS

SI	1.819	1.816	1.809	1.882	1.809	1.822
TI	0.022	0.002	0.002	0.001	0.007	0.007
AL	0.313	0.301	0.329	0.240	0.319	0.292
FE3+	0.000	0.000	0.000	0.000	0.000	0.000
CR	0.049	0.105	0.101	0.070	0.094	0.087
FE2+	0.070	0.070	0.063	0.062	0.072	0.073
MG	0.833	0.850	0.794	0.889	0.834	0.847
MN	0.001	0.002	0.004	0.002	0.003	0.003
CA	0.835	0.786	0.829	0.768	0.798	0.814
NA	0.072	0.092	0.085	0.096	0.081	0.070
K	0.000	0.000	0.000	0.000	0.000	0.001
TOTAL	4.014	4.025	4.016	4.010	4.018	4.017
MG/MG+FE	0.923	0.924	0.926	0.935	0.920	0.921

UNLESS OTHERWISE SPECIFIED; TOTAL IRON AS FEO

from several specimens. Each composition listed in this Table is an average of a number of analyses which span a wide compositional range. The standard deviations for the oxide compcnents listed in Table 6-4 are two to five times those of the analyses of the interstitial clinopyroxenes listed in Table 6-1. This variability is in part due to chemical zoning in individual clinopyroxene crystals. The small size of these crystals makes precise characterization of the zoning difficult, but the pattern is one of decreasing chromium and aluminum towards the crystal margins. The spectrum of compositions of euhedral clinopyroxenes for a single fine-grained zone, however, appears to be wider than that found in any one crystal in that zone. As an illustration of the range of this compositional spectrum, the Cr_2O_3 and Al_2O_3 contents of euhedral clinopyroxenes in specimen 10002 range from highs of 4.89 and 8.94 to lows of 2.98 and 5.18 weight percent respectively. There is an inverse relationship between the Mg numbers for the euhedral clinopyroxenes in any one zone and the degree of tschermak substitution. In the specimen cited above, the Mg numbers range from .914 to .937. Thus, like the euhedral olivines in these fine-grained zones, the euhedral clinopyroxenes show increasing Mg numbers towards their margins.

The compositions of the euhedral clinopyroxenes from specimens which contain amphibole (10013,10006) and of the euhedral clinopyroxenes from the nodules which do not are similar.

VI Lherzolite Amphiboles

a) Nature of the Nunivak Amphiboles

Table 6-6 lists selected analyses for amphiboles found in three Nunivak lherzolites. A more complete listing is available in the appendix. The compositions of the Nunivak amphiboles are transitional between the fields of pargasitic hornblende and endenitic hornblende as defined by Leake (1968). Using Leake's prefixes, these amphiboles would be described as both chromic (Cr > .25 atoms/23 oxygens) and sodic (Na > 1 atom/23 oxygens). However, a serious problem is encountered with Leake's (1968) classification. As an example, amphibole #1 (Table 6-6) is determined, using the Si versus Ca + Na + K scale of Leake's Figure #1, to contain the end-members pargasite (Na + K) $Ca_2Mg_4(Al,Cr)Si_6Al_2O_{22}(OH)_2$ and richterite $(Na + K)_2CaMg_5Si_8O_{22}(OH)_2$ in the relative proportions 80:20. The same ratio calculated by assuming that these end-members account for all the Na, K, and Ca is 60.5:39.5. Clearly, there is a problem. The same paradox is exhibited by the Cr-bearing amphiboles found in the western Grand Canyon by Best (1974). He failed to notice the incongruity and calculated end-members by the latter method.

Figure 6-10 provides a possible solution to this classification problem. It presents the results of a microprobe traverse across an amphibole grain in specimen 10016. The significance of the chemical zoning will be discussed later, but what is germane to this discussion is that both chromium and aluminum increase together at the expense of magnesium and silicon. This indicates that chromium is substituting for magnesium and not for octahedrally coordinated aluminum. Charge balance is maintained by the concomitant replacement of silicon by aluminum.

Table 6-5

Sources for Analyses Listed in Tables 6-6 and 6-7

1 specimen 10013, Nunivak Island

2 specimen 10006, Nunivak Island

3 specimen 10016, Nunivak Island

4 harzburgite, Monastery Mine, South Africa; Smith, 1974

5 harzburgite, Wesselton Mine, South Africa; Boyd, 1971

6 hornblende lherzolite, Kirsh Volcano, Ataq; Varne, 1970

7 amphibole lherzolite, western Grand Canyon; Best, 1974

8 garnet lherzolite, Itinome-gata, Japan; Aoki, 1973

9 spinel lherzolite, Itinome-gata, Japan; Aoki, 1973

10 spinel lherzolite, Victoria, Australia; Frey and Green, 1974

11 spinel lhersolite, Dish Hill, California; Wilshire, 1971

12 spinel lherzolite, Dish Hill, California; Wilshire, 1971

13 spinel lherzolite, Fen Alkaline Complex, Norway; Griffin, 1973

14 specimen 13000, kaersutite megacryst, Nunivak Island

TABLE 6-6

CR-AMPHIBOLES I

	1	2	3	4	5	6	7
SPEC.	10013	10006	10016		7429	AT-15	S-6
SIO2	44.54	45.99	46.75	44.60	45.50	44.73	44.60
TIO2	0.38	0.08	0.11	0.01	0.01	0.29	1.20
AL2O3	13.42	12.91	11.51	11.10	11.10	12.58	13.40
FE2O3	0.00	0.00	0.00	0.00	0.00	1.10	0.00
CR2O3	2.85	3.14	2.55	2.21	1.67	2.43	2.70
FEO	4.13	3.42	3.29	2.72	3.18	2.37	3.40
MGO	17.68	18.45	19.01	20.30	20.00	19.17	18.10
MNO	0.11	0.07	0.11	0.19	0.06	0.11	0.00
CAO	9.79	9.07	9.43	11.00	10.60	10.95	10.10
NA2O	3.83	4.79	4.39	3.24	3.79	3.85	3.40
K2O	1.31	0.92	0.72	1.34	0.60	0.43	1.30
TOTAL	98.04	98.84	97.87	96.71	96.51	98.01	98.20

FORMULA UNITS ASSUMING 23 OXYGENS

SI	6.336	6.449	6.595	6.414	6.518	6.325	6.306
TI	0.041	0.008	0.012	0.001	0.001	0.031	0.128
AL	2.250	2.134	1.914	1.881	1.874	2.097	2.233
FE3+	0.000	0.000	0.000	0.000	0.000	0.117	0.000
CR	0.321	0.348	0.284	0.251	0.189	0.272	0.302
FE2+	0.491	0.401	0.388	0.327	0.381	0.280	0.402
MG	3.748	3.856	3.997	4.351	4.270	4.041	3.815
MN	0.013	0.008	0.013	0.023	0.007	0.013	0.000
CA	1.492	1.363	1.425	1.695	1.627	1.659	1.530
NA	1.056	1.302	1.201	0.903	1.053	1.056	0.932
K	0.238	0.165	0.130	0.246	0.110	0.078	0.234
TOTAL	15.986	16.035	15.959	16.093	16.030	15.968	15.882
MG/MG+FE	0.884	0.906	0.911	0.930	0.918	0.935	0.905
NA/NA+K	0.816	0.888	0.903	0.786	0.906	0.932	0.799

UNLESS OTHERWISE SPECIFIED; TOTAL IRON AS FEO

This explains why for a given silicon content, the Nunivak amphiboles are anomalously alkali rich. Their silicon contents are significantly lower than would be predicted by a combination of pargasite and richterite. Figure 6-11 illustrates how the Nunivak amphiboles deviate to the alkali-rich side of the pargasite-endenite tie-line. The shaded area is the region in which Leake's classification predicts they would plot. Because of these classification problems, the term Cr-amphibole will be used in the following discussion.

The alkali contents of the Nunivak amphiboles are remarkably uniform in any one specimen. There are, however, interesting variations in their Cr, Mg, Al, and Si contents. Amphiboles which are in contact with their core spinel intergrowths are strongly zoned. Figure 6-10 presents the results of a microprobe traverse across such a grain in specimen 10016. The pattern is one of increasing Al and Cr but decreasing Si and Mg from the grain margins to the core spinel. In another grain, with a less regular, but more extreme zoning pattern, the Cr content ranged from a low of 1.70 weight percent Cr_2O_3 at the amphibole margin to 3.85 weight percent Cr_2O_3 adjacent to spinel. Amphiboles not in contact with their core spinel are not chemically zoned and have Cr contents similar to those of the margins of the zoned amphibole grains. In specimen 10013, amphibole grains which appear stable, but contain no included spinel exhibit larger Cr contents (2.85 weight percent Cr_2O_3) than amphiboles which appear to be decomposing (2.18 weight percent Cr_2O_3). In specimen 10006, however, a partially decomposed amphibole grain with no associated relict spinel contains only 1.49 weight percent Cr_2O_3 while a nearby

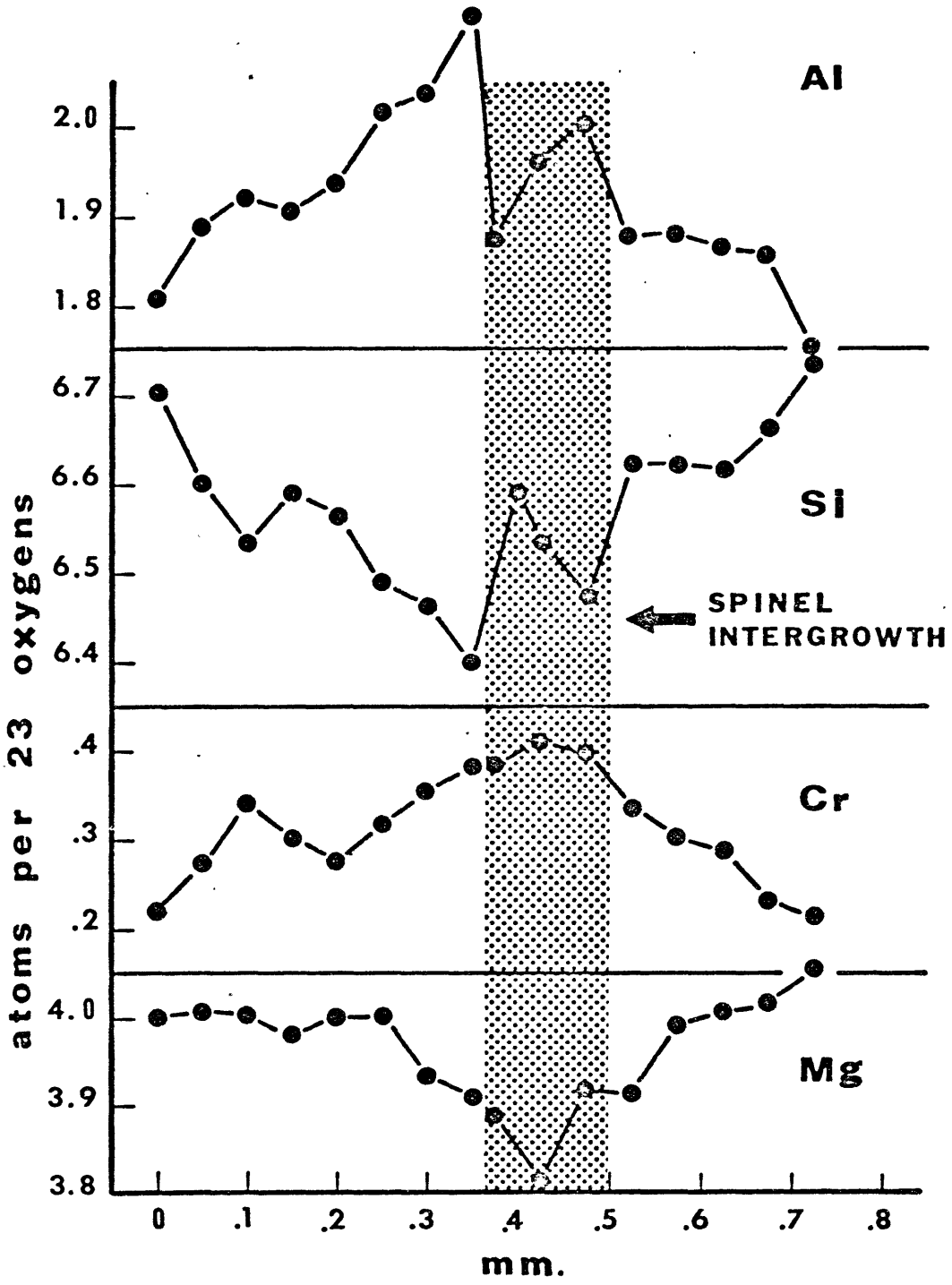

Probe Traverse of Amphibole Grain with included Spinel

Figure 6-10

amphibole remnant in a fine-grained, glass-bearing zone about an intergrowth of relict spinel and phlogopite contains 3.14 weight percent Cr_2O_3.

b) Comparison with other Lherzolite Amphiboles

Analyses #4 through #13 (Tables 6-6 and 6-7) represent selected interstitial, Cr-amphiboles reported in lherzolite nodules. In his review of possible mantle derived amphiboles, Best (1974) has noted that these interstitial amphiboles are characterized by lower K, Fe, Al, and especially Ti; but higher Cr and Mg when compared to poikilitic, vein, or megacryst amphiboles. A comparison of the above analyses with analysis #14, a kaersutite megacryst from Nunivak Island, emphasizes these differences.

Analyses in Table 6-6 are closest in composition to those of the interstitial amphiboles of Nunivak Island. They differ from those listed in Table 6-7 in having higher Na, K, and Cr contents, but lower Ca, Ti, and Al contents. Wilshire (1971) has shown that the reaction of interstitial amphibole with basanite magmas produces secondary kaersutitic amphibole enriched in K, Ti, and Al. This process cannot explain the differences between the analyses of Table 6-6 and 6-7 because of the contrary behavior of K and Ti. Figure 6-11 is a plot of tetrahedrally coordinated aluminum versus total alkalies first used by Deer et al. (1964). It illustrates the differences between the analyses of Tables 6-6 and 6-7.

An important characteristic of the amphiboles in Table 6-6 is their textural relationships to spinel. Amphiboles #4 and #5 occur as eutectic-

TABLE 6-7

CR-AMPHIBOLES II

	8	9	10	11	12	13	14
SPEC.	2313	2314	2642	BA1-52	BA1-52	1	13000
SIO2	42.40	43.10	45.19	44.20	44.50	43.51	39.89
TIO2	1.00	1.00	1.28	0.50	1.40	0.49	5.13
AL2O3	15.70	15.40	15.43	15.80	15.10	14.74	13.93
FE2O3	0.00	0.00	1.27	0.00	0.00	0.00	0.00
CR2O3	0.48	0.48	0.97	1.10	1.10	1.07	0.00
FEO	4.30	4.30	2.04	5.30	5.50	4.00	14.33
MGO	19.20	17.80	17.98	18.00	18.30	19.18	10.45
MNO	0.09	0.09	0.03	0.10	0.10	0.09	0.13
CAO	11.90	11.90	10.11	11.50	11.50	10.70	9.75
NA2O	3.10	2.60	3.47	3.00	3.10	3.93	2.81
K2O	0.07	0.07	0.04	0.50	0.30	0.19	1.95
TOTAL	98.24	96.74	97.81	100.40	100.90	97.90	98.37
FORMULA UNITS ASSUMING 23 OXYGENS							
SI	5.993	6.156	6.302	6.128	6.144	6.159	5.950
TI	0.106	0.107	0.134	0.094	0.145	0.052	0.575
AL	2.615	2.593	2.536	2.582	2.457	2.459	2.449
FE3+	0.000	0.000	0.133	0.000	0.000	0.000	0.000
CR	0.054	0.054	0.107	0.121	0.120	0.120	0.000
FE2+	0.508	0.514	0.238	0.615	0.635	0.474	1.787
MG	4.045	3.790	3.738	3.720	3.766	4.047	2.323
MN	0.011	0.011	0.004	0.012	0.012	0.011	0.016
CA	1.802	1.821	1.511	1.708	1.701	1.623	1.558
NA	0.850	0.720	0.938	0.806	0.830	1.079	0.813
K	0.013	0.013	0.007	0.008	0.053	0.034	0.371
TOTAL	15.997	15.779	15.648	15.874	15.863	16.056	15.842
MG/MG+FE	0.888	0.881	0.940	0.858	0.856	0.895	0.565
NA/NA+K	0.985	0.983	0.992	0.991	0.940	0.969	0.687

KAERSUTITE

UNLESS OTHERWISE SPECIFIED; TOTAL IRON AS FEO

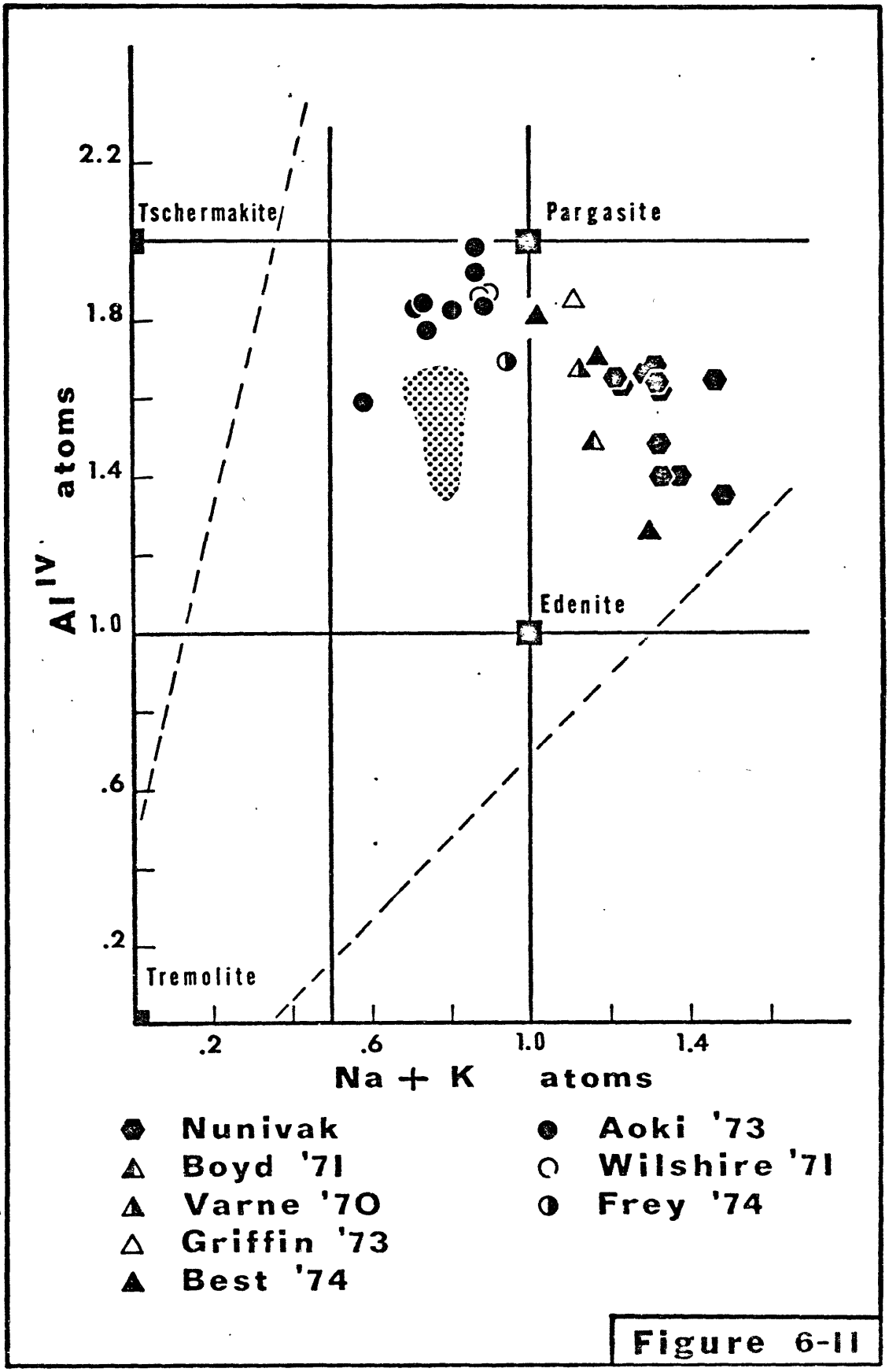
2.2
1.8
1.4
1.0
.6
.2
Tschermakite
Pargasite
Edenite
Tremolite
Al^{IV} atoms
.2
.6
1.0
1.4
Na + K atoms
Nunivak
Boyd '71
Varne '70
Griffin '73
Best '74
Aoki '73
Wilshire '71
Frey '74

Figure 6-11

like intergrowths with Cr-spinel in harzburgites from South African kimberlite pipes (Smith, 1973; Boyd, 1971). Amphiboles #6 and #7 are found in lherzolites whose only spinel is found with glass and clinopyroxene as the breakdown products of the amphibole (Varne, 1968; Best, 1974). The close relationship between the Nunivak amphiboles and spinel has been documented in Chapter 5. In all of these examples, there is an absence of interstitial spinel.[1] Amphibole #13 of Table 6-7 is texturally similar to those of Nunivak Island in that it surrounds corroded brown spinels in lherzolites from the Fen alkaline complex, Norway (Griffin, 1973). Though this amphibole is considerably lower in Cr and K than the Nunivak amphiboles, it is chemically transitional between the amphiboles of Tables 6-6 and 6-7.

In summary, the amphiboles of the Nunivak lherzolites appear to belong to a chemically distictive group of Cr-bearing, interstitial amphiboles which tend to occur in xenoliths which lack interstitial spinel. Spinel, when present, is either intimately associated with the amphibole or secondary after the breakdown of the amphibole. These amphiboles differ from other interstitial amphiboles in having relatively higher contents of Cr, K, and Na; but distictly lower values of Al and Ti.

VII Lherzolite Micas

The red-brown mica commonly found between amphibole and its core

---

[1]One lherzolite recently returned from Nunivak Island contains both interstitial spinel and amphibole without core spinel.

spinel in the amphibole lherzolites is a chromium and sodium-bearing member of the phlogopite $(K,Na)_2(Mg,Fe)_6(Si_6Al_2)O_{20}(OH)_4$ - eastonite $(K,Na)_2(Mg,Fe)_5(Cr,Al)(Si_5Al_3)O_{20}(OH)_4$ solid solution series (Table 6-8). Chromium and excess aluminum substitute for magnesium and iron in octahedral coordination. There appears to be an X cation deficiency, however, this may be accounted for by elements such as Ba, Rb, or Cs which were not analyzed. These phlogopites characteristically have Mg numbers which are slightly higher than their associated amphiboles (Table 6-8). In other respects the chemistry of a mica closely parallels that of the amphibole with which it coexists.

Occasionally a thin vein of phlogopite is found cutting a lherzolite nodule. This mica tends to be richer in titanium and poorer in chromium than the interstitial phlogopite (Table 6-8).

VIII Lherzolite Glasses

Three chemically distinct varieties of glasses can be recognized in the Nunivak lherzolites. Each has its own characteristic mode of occurrence:

1. Glasses with Na/Na + K greater than 0.90 are along the margins of Na-rich clinopyroxenes.
2. Glasses with Na/Na + K less than 0.60 are associated with phlogopite, clinopyroxene, olivine, spinel intergrowths.
3. Glasses with Na/Na + K greater than 0.69 and less than 0.86 are in the fine-grained zones.

TABLE 6-8

LHERZOLITE PHLOGOPITES

IN VEINS ** WITH AMPHIBCLE

SPEC.	MD3-1	10051	10006	10013	10013	10016
SIO2	39.24	39.38	38.31	38.53	38.68	39.91
TIO2	1.14	2.91	0.14	0.43	0.48	0.20
AL2O3	18.47	15.69	16.72	17.62	17.47	17.75
FE2O3	0.00	0.00	0.00	0.00	0.00	0.00
CR2O3	1.12	0.48	2.48	1.93	2.11	2.17
FEO	3.82	4.26	3.75	4.13	3.88	3.43
MGO	22.95	21.99	23.53	22.78	23.14	23.76
MNO	0.05	0.06	0.05	0.05	0.05	0.05
CAO	0.00	0.03	0.00	0.00	0.01	0.00
NA2O	0.47	1.08	0.82	0.92	0.99	1.47
K2O	10.21	9.00	9.19	8.60	8.49	7.30
TOTAL	97.47	94.88	94.99	94.99	95.30	96.04

FORMULA UNITS ASSUMING 22 OXYGENS

SI	5.444	5.602	5.464	5.470	5.468	5.540
TI	0.119	0.311	0.015	0.046	0.051	0.021
AL	3.020	2.631	2.811	2.948	2.911	2.904
FE3+	0.000	0.000	0.000	0.000	0.000	0.000
CR	0.123	0.054	0.280	0.217	0.236	0.238
FE2+	0.443	0.507	0.447	0.490	0.459	0.398
MG	4.745	4.663	5.003	4.820	4.876	4.916
MN	0.006	0.007	0.006	0.006	0.006	0.006
CA	0.000	0.005	0.000	0.000	0.002	0.000
NA	0.126	0.298	0.227	0.253	0.271	0.396
K	1.807	1.633	1.672	1.557	1.531	1.293
TOTAL	15.833	15.710	15.925	15.807	15.809	15.712
MG/MG+FE	0.915	0.902	0.918	0.908	0.914	0.925
NA/NA+K	0.065	0.154	0.119	0.140	0.151	0.234
MG/MG+FE AMPH:			.906	.884	.890	.911

UNLESS OTHERWISE SPECIFIED; TOTAL IRON AS FEO

a) High Sodium Glasses

High Na glasses are found lining the boundaries of, or as irregular patches within, the margins of Na-rich clinopyroxenes. In the latter case, rims of Na-poor clinopyroxene are developed with the glass on the original clinopyroxene grains. The majority of these glass patches were too small to analyse with the microprobe. The few good analyses that were obtained are listed in Table 6-9.

The analysis from specimen 10211 may be misleading. If formula units are calculated on the basis of 8 oxygens, the result closely resembles the stoichiometry of a feldspar with the cations totalling 5.04. In section Vc of this chapter it was found that the relative chemistries of the clinopyroxene interiors and rims are incompatible with a partial melting origin for the latter. Thus the low reflectivity material (in this specimen), which was interpreted to be glass, may be plagioclase with a labradorite composition (An 54.6, Ab 43.4, Or 2.0). The compositions of the low reflectivity material from the other two specimens support the petrographic interpretation that they are glasses produced by the incongruent melting of Na-rich clinopyroxene.

The compositions of the clinopyroxene interiors of specimens 10006 and 10211 were calculated from the compositions of their rims and associated glass (plagioclase? in the case of the latter) using the "mineral distribution program" of Wright and Doherty (1970). For both specimens excellent matches were obtained for all oxides except Na_2O, with the glasses representing 10.8 and 13.7 percent fractionation of the clinopyroxene interiors respectively. In each case the calculated clinopyroxenes were 1.04 weight percent low in Na_2O when compared to the

TABLE 6-9

HIGH SODIUM GLASSES AND HIGH POTASSIUM GLASSES

	HI-NA	HI-NA	HI-NA	HI-K	HI-K	HI-K	HI-K
SPEC.	10211	10025	1CCC6	1CC17	1CC17	2640	2640
SIC2	53.73	57.56	59.80	55.26	54.88	64.50	66.20
TIC2	0.05	0.53	0.01	1.94	1.33	2.00	1.50
AL2C3	28.24	23.07	29.63	18.51	19.87	18.40	18.30
FE2C3	0.CC	0.CC	C.CC	0.00	0.00	0.00	0.00
CR2C3	0.02	0.CC	C.CC	C.16	0.13	0.00	C.CC
FEC	0.53	1.10	0.27	7.12	5.41	1.40	1.20
MGC	0.15	2.19	C.30	3.15	3.18	1.60	1.50
MNC	0.01	0.02	C.CC	C.15	0.10	0.CC	0.CC
CAC	11.37	6.26	1.09	5.57	5.76	3.CC	1.50
NA2C	4.99	7.55	9.17	3.04	3.69	3.33	3.80
K2C	0.36	0.88	C.83	3.93	4.21	5.60	6.00
TOTAL	99.45	99.16	101.10	98.83	98.56	99.83	100.00
FORMULA UNITS ASSUMING 1C OXYGENS							
SI	3.063	3.280	3.263	3.279	3.251	3.621	3.691
TI	0.002	0.023	0.CCC	0.087	0.059	0.084	0.C63
AL	1.897	1.549	1.906	1.294	1.387	1.218	1.202
FE3+	0.CCC	C.CCC	0.CCC	0.CCC	0.000	0.000	0.000
CR	C.001	0.CCC	C.CCC	0.C08	0.006	0.CCC	0.CCC
FE2+	0.025	0.052	0.C12	0.353	0.268	0.066	0.056
MG	0.013	C.186	0.024	0.279	0.281	0.134	0.125
MN	0.CCC	C.C01	C.CCC	0.C08	C.C05	C.CCC	0.CCC
CA	0.695	0.382	0.064	0.354	0.366	0.180	0.090
NA	C.552	C.834	0.97C	0.350	0.424	0.363	0.411
K	C.026	C.064	0.C58	0.297	0.318	0.401	0.427
TOTAL	6.274	6.372	6.298	6.308	6.364	6.067	6.064
NA/NA+K	0.955	C.929	0.944	0.540	0.571	0.475	0.490
						FREY	FREY '74

UNLESS OTHERWISE SPECIFIED; TOTAL IRON AS FEC

analysed clinopyroxene interiors. This may indicate that some Na has been lost from the system.

The calculated K_2O contents for the clinopyroxene interiors of specimens 10006 and 10211 are 0.09 and 0.05 weight percent respectively. Analyses of the clinopyroxene interiors rarely exceeded 0.01 weight percent K_2O. The accuracy of this figure is debatable, however, because the standard used was orthoclase with 12 weight percent potassium. Erlank (1973) states that the potassium concentration in clinopyroxene ranges from less than 0.03 weight percent K_2O in chromian diopsides to 0.06 weight percent in sub-calcic diopsides from sheared garnet lherzolites. It is apparent that the potassium contents calculated for the clinopyroxene interiors are too high. If this discrepancy is significant, the glass (plagioclase? in the case of specimen of 10211) may contain more potassium than can be derived from clinopyroxene. It is unlikely that this excess potassium could be supplied by other anhydrous phases in the nodules because they typically contain less than 30 ppm potassium (Erlank, 1973). Amphibole or mica may be the source of excess potassium in specimen 10006. Alternative possibilities are that this excess potassium was preferentially leached from the interiors of the clinopyroxenes or that it was introduced from the alkalic magma which carried these xenoliths.

b) High Potassium Glasses

High K glasses are found in specimen 10017 developed around intergrowths of phlogopite, clinopyroxene, olivine, and spinel. Table 6-9 presents the compositions of two such glasses. Also in this Table are the compositions of two glasses coexisting with phlogopite in specimen

2640 of the Victorian lherzolite suite (Frey and Green, 1974). These glasses are characterized by low Na/Na + K ratios and relatively low concentrations of calcium and aluminum with respect to other glasses found in the Nunivak lherzolites. The Victorian glasses are more extreme in these characteristics, probably because they are derived from phlogopite not intimately associated with clinopyroxene.

c) Glasses in Fine-Grained Zones

Analyses of glasses from the fine-grained zones of seven lherzolites are listed in Table 6-10. Despite the ubiquitous quench textures exhibited by the fine-grain zones, these glasses are remarkably homogenous within their zones. In individual fine-grained zones, silicon analyses exhibited the greatest variability, with standard deviations in each of the seven specimens averaging 0.71 weight percent SiO_2. The highest standard deviation observed was 1.24 weight percent SiO_2 for 5 glass analyses from specimen 10002.

The compositions of the glasses from the seven different specimens are remarkably similar. The relative proportions of Ca, Na, and K for these glasses are plotted with those of other glasses in Figure 6-12. The glasses from the fine-grained zones define a distinctive group adjacent to the compositions of the Cr-bearing amphiboles. These glasses differ significantly from the high potassium glasses associated with phlogopite and are more potassium-rich than the glasses developed from clinopyroxene.

It is seen in Figure 6-12 that the glasses of the fine-grained zones can be derived (at least in terms of their Na, Ca, and K contents) by

TABLE 6-10

GLASSES IN FINE-GRAINED ZONES

WITH:	AMPH		SPINEL	SPINEL	SPINEL	SPINEL	
SPEC.	10013	10001	10046	10045	10002	10003	10010
SIO2	52.32	52.90	53.11	55.19	55.61	57.79	58.99
TIO2	0.51	1.32	0.38	0.14	0.18	0.29	0.16
AL2O3	23.44	22.29	22.53	21.25	23.84	23.94	20.87
FE2O3	0.00	0.00	0.00	0.00	0.00	0.00	0.00
CR2O3	0.11	0.05	0.09	0.15	0.15	0.13	0.09
FEO	4.01	3.78	3.06	3.37	3.37	2.72	2.77
MGO	3.98	4.30	4.69	4.46	4.00	2.84	3.60
MNO	0.09	0.06	0.07	0.09	0.03	0.06	0.07
CAO	8.02	9.11	9.95	8.50	7.46	6.44	6.58
NA2O	4.29	3.94	5.30	4.39	3.45	3.09	4.57
K2O	2.92	2.00	1.33	1.90	1.42	1.23	2.10
TOTAL	99.69	99.75	100.51	99.44	99.51	98.53	99.80

FORMULA UNITS ASSUMING 10 OXYGENS

SI	3.061	3.080	3.070	3.200	3.180	3.289	3.356
TI	0.022	0.058	0.017	0.006	0.008	0.012	0.007
AL	1.616	1.530	1.535	1.452	1.607	1.606	1.399
FE3+	0.000	0.000	0.000	0.000	0.000	0.000	0.000
CR	0.005	0.002	0.004	0.007	0.007	0.006	0.004
FE2+	0.196	0.184	0.148	0.163	0.161	0.129	0.132
MG	0.347	0.373	0.404	0.385	0.341	0.241	0.305
MN	0.004	0.003	0.003	0.004	0.001	0.003	0.003
CA	0.503	0.568	0.616	0.528	0.457	0.393	0.401
NA	0.487	0.445	0.594	0.494	0.383	0.341	0.504
K	0.218	0.149	0.098	0.141	0.104	0.089	0.152
TOTAL	6.459	6.392	6.490	6.381	6.248	6.108	6.264
MG/MG+FE	0.639	0.670	0.732	0.702	0.679	0.650	0.698
NA/NA+K	0.691	0.750	0.858	0.778	0.787	0.792	0.768

UNLESS OTHERWISE SPECIFIED; TOTAL IRON AS FEO

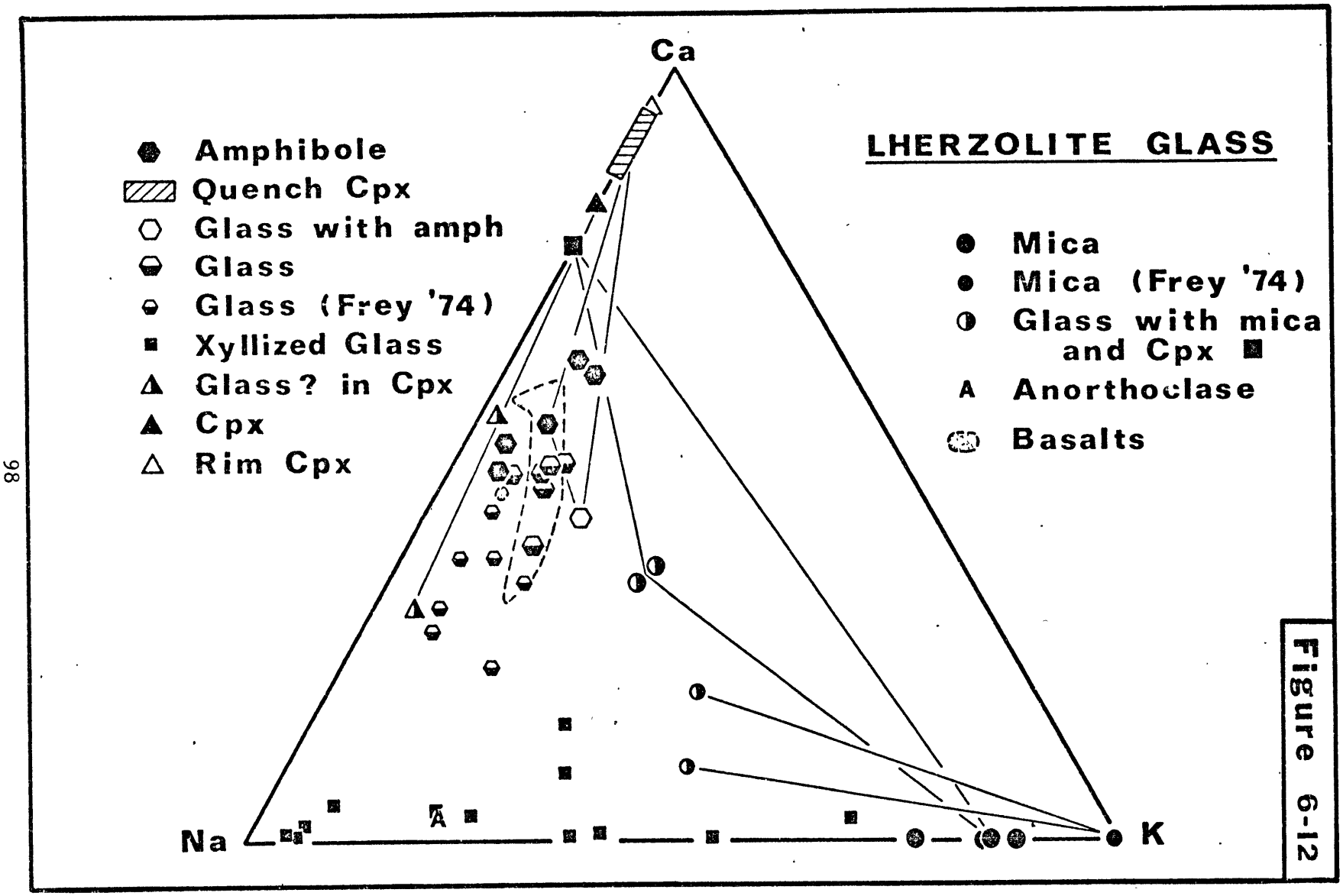
Ca
Na
K
A
LHERZOLITE GLASS
Amphibole
Quench Cpx
Glass with amph
Glass
Glass (Frey '74)
Xyllized Glass
Glass? in Cpx
Cpx
Rim Cpx
Mica
Mica (Frey '74)
Glass with mica and Cpx
Anorthoclase
Basalts

Figure 6-12

removing the euhedral clinopyroxenes from liquids similar in composition to the Cr-bearing amphiboles. On the other hand, it is impossible to reproduce the Na, Ca, K proportions of these glasses by melting either interstitial clinopyroxene or phlogopite alone. Other phases such as garnet, orthopyroxene, or olivine will not affect these conclusions because they have negligible alkali contents. The possibility remains, however, that some combination of clinopyroxene and phlogopite can produce glasses similar in composition to those of the fine-grained zones. This subject will be dealt with at length in a following section. The compositions of selected glasses from specimens 2700 and 2669 of the Victorian lherzolite suite (Frey, 1974) are also plotted in Figure 6-12. They are less Ca and K-rich than the glasses in the fine-grained zones of the Nunivak lherzolites, but significantly more K-rich than the glasses derived from interstitial clinopyroxenes. It is also possible to derive these glasses by removing a Na-poor clinopyroxene from a melt similar in composition to the Nunivak amphiboles.

The glass from specimen 10013 coexists with a partially decomposed amphibole. In Figure 6-12 this glass is joined by tie-lines to the compositions of its associated amphibole and euhedral clinopyroxene. The composition of glass 10013 is slightly more K-rich than would be predicted by simply removing the euhedral clinopyroxenes from a melt of the amphibole's composition. Some process is required which will decrease the Na/Na + K ratio of the glass. This process is not the preferential removal of K from its associated amphibole because the K content of the amphibole grains in specimen 10013 does not vary with the presence or absence of glass.

The relative proportions of Ca, Na, and K observed in the Nunivak basalts are remarkably similar to those of the glasses of the fine-grained zones and interstitial amphibole of the lherzolite xenoliths (Figure 6-12). Inferences about the significance of this correlation will be deferred until Chapter 8.

d) C.I.P.W. Norms of Glasses in Fine-Grained Zones

The normative mineralogy of the seven analysed glasses from fine-grained zones are presented in Table 6-11. Glasses from nodules 10013, 10001, and 10046 are nepheline normative while those from nodules 10010, 10002, and 10003 are quartz normative. Glass 10045 is both olivine and hyperstene normative. These relationships are illustrated in Figure 6-13. This Figure is a projection from the diopside apex of a modified basalt tetrahedron. The end-member "Feldspar" accounts for both orthoclase and plagioclase.

It is impossible to explain the spread in the normative mineralogy of these glasses in terms of the compositions of the euhedral crystals included in them. There has been some suggestion in the data presented in the preceding sections that the lherzolites have not been closed systems with respect to sodium. The occurrence of normative corundum in the norms of two of the most quartz normative glasses suggests that they are sodium deficient. To test this possibility, the norms of the non-nepheline normative glasses were recalculated after successive amounts of Na_2O had been added to them. The results of these calculations are illustrated in Figure 6-13. Except for the glass of specimen 10003, the addition of 1 to 2 weight percent Na_2O is sufficient to render all these

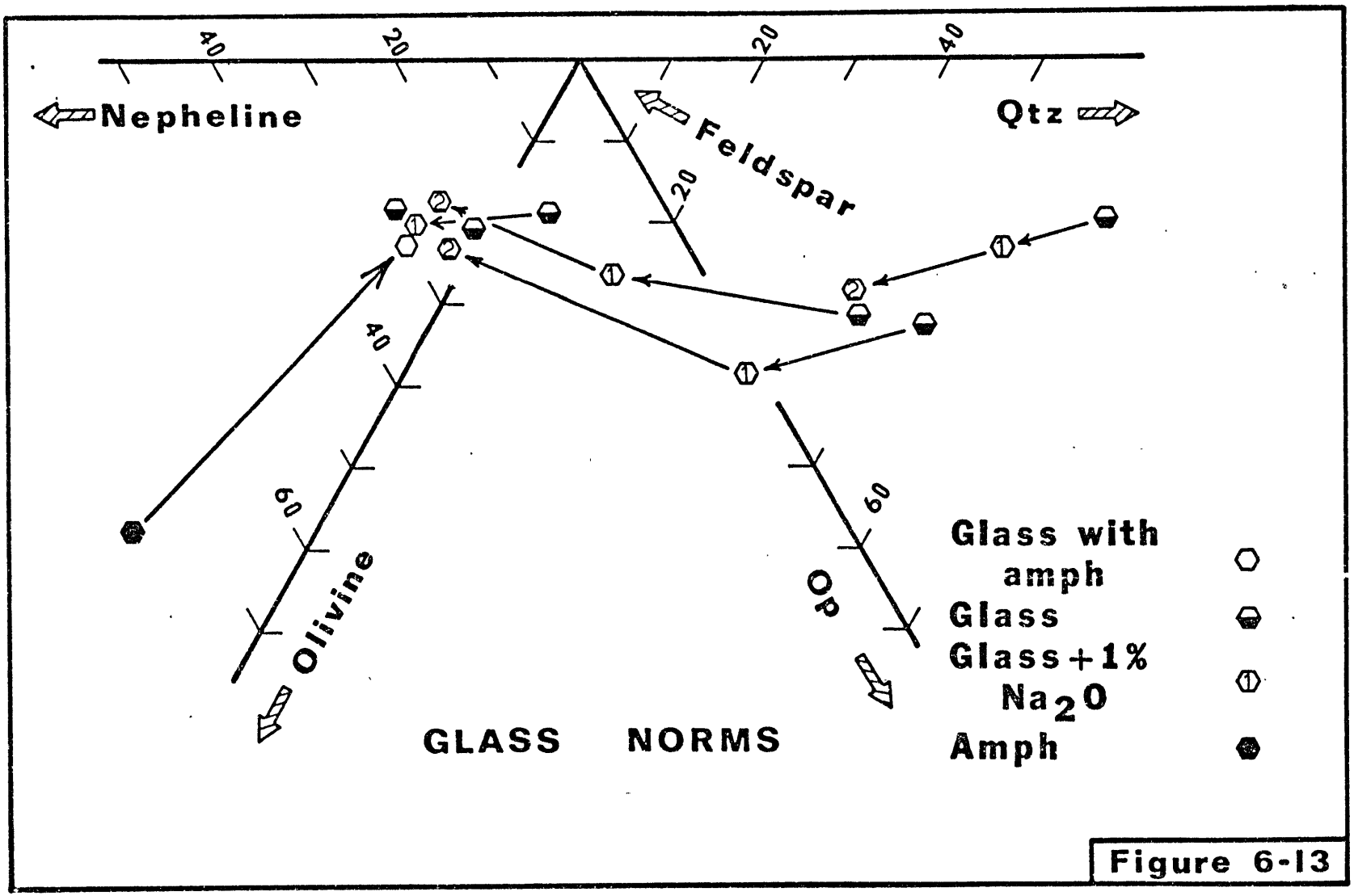
40
20
20
40
Nepheline
Feldspar
Qtz
20
40
60
60
Olivine
Qp
Glass with amph
Glass
Glass+1% Na_2O
Amph
GLASS NORMS

Figure 6-13

Table 6-11

C.I.P.W. Normative Mineralogy of Fine-Grained Zone Glasses

specimen:	10013	10001	10046	10045	10002	10003	10010
Q	-	-	-	-	5.540	15.246	3.214
C	-	-	-	-	3.080	5.904	-
Or	17.309	11.849	7.820	11.291	8.432	7.377	12.435
Ab	25.338	32.031	29.232	37.356	29.336	26.537	38.748
Ne	6.001	.755	8.336	-	-	-	-
Wo	1.554	3.335	6.483	3.991	-	-	1.010
En	.892	2.146	4.218	3.654	10.011	7.179	8.984
Fs	.593	.968	1.821	1.972	5.846	4.582	4.885
Fo	6.343	6.020	5.189	5.268	-	-	-
Fa	4.650	2.992	2.470	3.133	-	-	-
Cm	.163	.074	.132	.223	.222	.195	.133
Il	.972	2.514	.718	.268	.344	.559	.305

glasses nepheline normative. The resultant clustering of the normative compositions of all the glasses after the selective application of this "sodium fudge factor" is impressive.

e) Crystallized Glass

In a few specimens the fine-grained, glass-bearing zones are characterized by an unusually high ratio of euhedral crystals to glass (low reflectivity material). In transmitted light, under crossed nicols, the glass (?) areas appear to be microcrystalline. Compositions of this material resemble alkali feldspar, but are extremely heterogenous. Na/Na + K ratios range from more than 0.9 to 0.3 in one fine-grained zone. Table 6-12 lists some representative compositions from one such zone in contact with partially decomposed amphibole in specimen 10006. The poor quality of the analyses is due to the minute scale of the low reflectivity patches. These analyses, with others, have been plotted in Figure 6-12 along with an analysis of an anorthoclase megacryst. The similarity between the average of the analyses in Table 6-12 and the composition of the anorthoclase megacryst is striking.

The crystallized glasses are thought to have been produced by the extensive removal of clinopyroxene, olivine, and spinel from liquids produced by the melting of interstitial amphibole. The residual liquid formed by this process was essentially alkali feldspar in composition and crystallized in the sub-solvus region of anorthoclase. If residual liquids of this composition are immiscible in basaltic melts, then they may be involved in the formation of anorthoclase megacrysts.

TABLE 6-12

CRYSTALLIZED GLASSES FROM SPECIMEN 10006

SPEC.	10006	10006	10006	10006	10006	10006
SIO2	65.92	66.23	62.01	59.69	63.53	66.46
TIO2	0.34	0.40	0.10	0.10	0.05	0.21
AL2O3	20.12	23.62	25.34	25.34	30.11	23.62
FE2O3	0.00	0.00	0.00	0.00	0.00	0.00
CR2O3	0.07	0.03	0.06	0.00	0.14	0.07
FEO	0.59	0.76	0.29	0.39	0.23	0.58
MGO	0.33	0.51	0.21	0.27	0.30	0.29
MNO	0.00	0.00	0.00	0.00	0.00	0.00
CAO	0.40	0.59	0.12	2.73	0.17	1.34
NA2O	2.16	5.84	9.77	5.54	8.43	5.09
K2O	7.63	2.37	0.90	4.50	0.60	4.32
TOTAL	97.56	100.35	98.80	98.56	103.56	101.98

FORMULA UNITS ASSUMING 8 OXYGENS

SI	2.990	2.879	2.760	2.710	2.676	2.872
TI	0.012	0.013	0.003	0.003	0.002	0.007
AL	1.076	1.210	1.329	1.356	1.495	1.203
FE3+	0.000	0.000	0.000	0.000	0.000	0.000
CR	0.003	0.001	0.002	0.000	0.005	0.002
FE2+	0.022	0.028	0.011	0.015	0.008	0.021
MG	0.022	0.033	0.014	0.018	0.019	0.019
MN	0.000	0.000	0.000	0.000	0.000	0.000
CA	0.019	0.027	0.006	0.133	0.008	0.062
NA	0.190	0.492	0.843	0.488	0.689	0.426
K	0.441	0.131	0.051	0.261	0.032	0.238
TOTAL	4.775	4.815	5.019	4.983	4.933	4.851
NA/NA+K	0.301	0.789	0.943	0.652	0.955	0.642

UNLESS OTHERWISE SPECIFIED; TOTAL IRON AS FEO

f) Origin of Glass in Fine-Grained Zones

On the basis of mineralogy, textural relationships, and the relative proportions of Na, Ca, and K, the fine-grained, glass-bearing zones are inferred to have been produced by the melting of interstitial, Cr-bearing amphibole. In order to quantify this argument, the "mineral distribution program" of Wright and Doherty (1970) was used to evaluate a number of potential parent assemblages for the fine-grained zones. This program calculates, by a least squares technique, the relative proportions of the phases present in a fine-grained zone required to match the composition of a proposed parent assemblage. The most likely candidate is assumed to be the one whose composition is most closely matched by a combination of the secondary phases in proportions which are compatible with the observed mode of the fine-grained zone. Two sets of calculations were made, one for a fine-grained zone without relict spinel (10010) and one for a zone with relict spinel (10002).

The following candidates were evaluated as parental assemblages for the fine-grained zone of specimen 10010:

amphibole

amphibole + olivine

amphibole + clinopyroxene

amphibole + olivine + clinopyroxene

clinopyroxene

clinopyroxene + olivine

phlogopite + clinopyroxene

phlogopite + clinopyroxene + olivine

Table 6-13 lists the best solutions that were obtained for each of the assemblages in order of increasing sum of residuals (absolute value of the weight percent difference between an oxide's concentration in the trial and calculated assemblages). No solution could be attained for trial candidates not listed in Table 6-13a.

Of the parental candidates, assemblages of amphibole or amphibole with minor olivine yield the best solutions. Not only are these solutions characterized by the lowest residual totals, but the proportions of secondary phases required are closest to those of the estimated mode. A substantial portion of the total residuals is contributed by low values for Na_2O (residual Na_2O to 2.7 weight percent) in the calculated amphiboles. This is characteristic of all the amphibole solutions. For each of the other oxides, except silica, the difference between the calculated and trial amphibole compositions is less than one weight percent. SiO_2 usually runs 1 to 1.3 weight percent higher in the calculated amphiboles than the trial amphiboles. It should be noted that the proportion of glass required in each of the amphibole solutions is higher than its estimated modal abundance. The estimated modes, however, may not be very accurate because of the small size of the fine-grained zones. In addition, 50 percent of these zones consist of voids which may, in part, represent lost glass.

The clinopyroxene solution is not only characterized by a significantly higher residual sum, but requires relative proportions of the secondary phases which are entirely inconsistent with the observed mode. The solution for a mixture of clinopyroxene and phlogopite yields an even higher residual sum. Clinopyroxene and clinopyroxene plus phlogopite

Table 6-13

a) Trial Parent Assemblages and Solutions for Specimen 10010

Fine-Grained Assemblage	cpx	spin	oliv	glass	Total
Mode	51	4	25	20	Residuals
Trial Assemblage					
amph 10006 + oliv(9.29)	30.44	9.43	26.63	33.50	6.36
amph 10006	33.61	10.32	19.28	36.81	6.38
amph 10016 + oliv(4.40)	35.61	7.68	24.07	32.64	6.45
amph 10016	37.27	8.01	20.64	34.10	6.49
cpx	89.65	-	1.74	8.62	9.81
cpx(42.18) + phlog(57.82)	47.12	2.29	19.69	30.89	15.36

b) Trial Parent Assemblages and Solutions for Specimen 10002

Fine Grained Assemblage	cpx	spin	oliv	glass	Total
Mode	49	8	24	19	Residuals
Trial Assemblage					
amph 10006 + spin(11.09)	27.64	17.17	19.29	35.91	6.99
amph 10006 + oliv(4.50)	32.18	6.39	24.88	36.55	7.26
amph 10006	33.71	6.65	21.45	38.19	7.29
amph 10016	37.35	4.29	22.91	35.48	7.33
amph 10013	36.91	8.79	18.58	35.74	7.75
cpx	94.36	-	3.07	2.59	12.88
cpx(59.03) + phlog(40.97)	45.23	-	23.18	31.58	15.62

must therefore be rejected as parents of the fine-grained, glass-bearing zones.

The calculations for the fine-grained zone with relict spinel in specimen 10002 are summarized in Table 6-13b. Again, amphibole or amphibole with minor olivine are the most likely parents for the fine-grained zones. The solution with the lowest residual sum, amphibole plus aluminous spinel, appears less likely because of the large proportions of glass and euhedral spinel required. The solutions for clinopyroxene or clinopyroxene plus phlogopite are worse than they were for specimen 10010. The problem of sodium deficiency in the calculated amphiboles is also encountered in the solutions for specimen 10002. This deficiency accounts for almost half of the total residuals for each amphibole solution.

Despite repeated efforts, no solution could be obtained which involved the composition of the relict spinel found in the fine-grained zone of specimen 10002. This suggests that this spinel was not formed by the incongruent melting of amphibole, but was present as an inclusion in the original amphibole. If this is true, the chemical zoning in these relict spinels (section IVc) is not the result of the melting process but an artifact of the parent assemblage.

g) Conclusions on the Chemistry of Lherzolite Glasses

The glasses found in the fine-grained zones are chemically distinct from those produced by the melting of clinopyroxene and phlogopite. Except for sodium, the compositions of the glasses from these zones can be derived by the removal of their euhedral crystal assemblage from a melt similar in composition to the Nunivak Cr-bearing amphiboles. This

supports the petrographic interpretation that the fine-grained, glass-bearing zones are produced by the melting of interstitial, Cr-bearing amphibole. Mathematical models of this process indicate that the relict spinels commonly found in the fine-grained zones were not produced by incongruent melting, but were originally inclusions in the amphibole. Sodium appears to have been a mobile component during the melting process and was, in part, lost from the nodules, probably in fluids formed by the amphibole's decomposition.

IX Summary and Conclusions on the Phase Chemistry of the Lherzolite Xenoliths

a) Iddingsitized versus Fresh Xenoliths

The petrographic interpretation that the iddingsitized and fresh lherzolites are distinct xenolith populations is supported by their phase chemistry. These two suites are not mutually exclusive, however, and their distinction lies in the relative proportions of the different lherzolite textural types (Chapter 5) in each suite.

The spinels of the iddingsitized lherzolites have Cr/Cr + Al ratios which range from .062 for the olive green variety to .322 for the darkest, red-brown variety. The Cr/Cr +Al ratios of spinels of the four phase, fresh lherzolites coincide with those of the red-brown spinels of the iddingsitized suite, with a low value of .240. In the fresh lherzolite suite, however, with the development of the fine-grained, glass-bearing zones, the Cr/Cr + Al ratios of the spinels increase beyond the range of the spinels in the iddingsitized lherzolites. The most chromian spinels

(Cr/Cr + Al to .634) are those occurring as inclusions in the Cr-bearing amphiboles.

The pyroxenes of the two lherzolite suites also exhibit divergent chemical patterns. The four phase, fresh lherzolites and the iddingsitized lherzolites with red-brown spinel are both characterized by clinopyroxenes with low contents of jadeite and calcium-tschermak components. These chromian diopsides also have the highest Mg numbers exhibited by any of the lherzolite clinopyroxenes. In the iddingsitized lherzolite suite, as the chromium content of the spinels decrease, the proportions of titanium, jadeite, and calcium-tschermak component increase in the associated clinopyroxenes. There is a concomitant rise in the aluminum content of the associated orthopyroxenes and a general decrease in the Mg numbers of all phases except spinel. In contrast, as fine-grained, glass-bearing zones appear in the fresh lherzolites, the jadeite component of the interstitial clinopyroxenes increases at the expense of calcium-tschermak substitution, while the aluminum content of the associated orthopyroxenes remains the same or decreases. The Mg numbers of the phases of lherzolites containing glass or amphibole are generally lower than those of the four phase, fresh lherzolites.

In Figures 6-14 and 6-15 a number of the chemical parameters summarized in the foregoing paragraphs are plotted against the aluminum content of orthopyroxene. It is apparent from these diagrams that the four phase, fresh lherzolites are members of the spectrum of lherzolites comprising the iddingsitized lherzolite suite. The distinctions between the fresh and iddingsitized lherzolites are thus; 1) the restriction of lherzolites with fine-grained, glass-bearing zones or amphibole to the

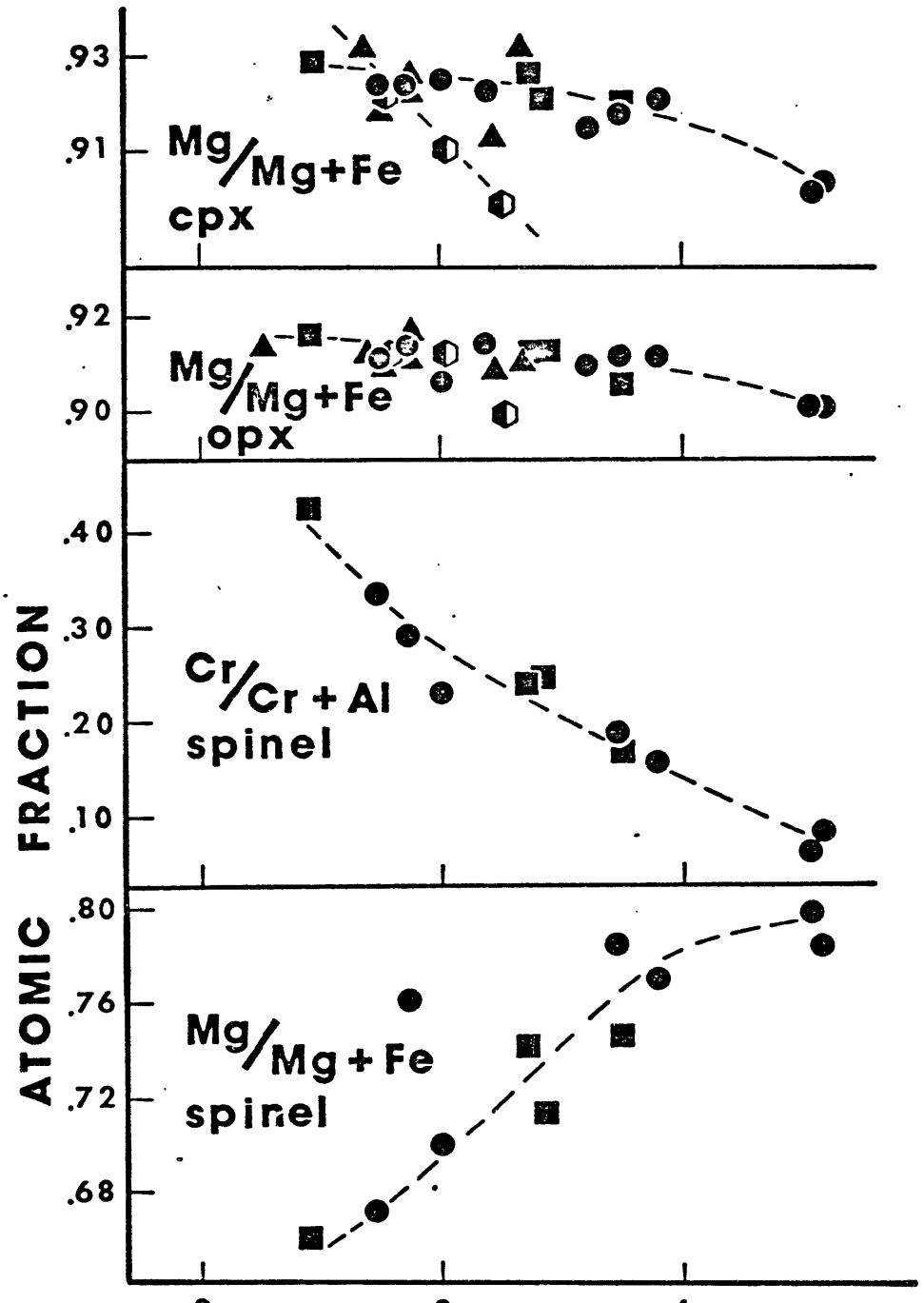
.93
.91
Mg/Mg+Fe
cpx
.92
.90
Mg/Mg+Fe
opx
.40
.30
.20
.10
Cr/Cr + Al
spinel
.80
.76
.72
.68
Mg/Mg + Fe
spinel
ATOMIC FRACTION
2
3
4
WEIGHT PERCENT Al2O3 IN OPX
lherz. with amph.
lherz. with glass
four-phase, fresh lherz.
idd. lherz.

Figure 6-14

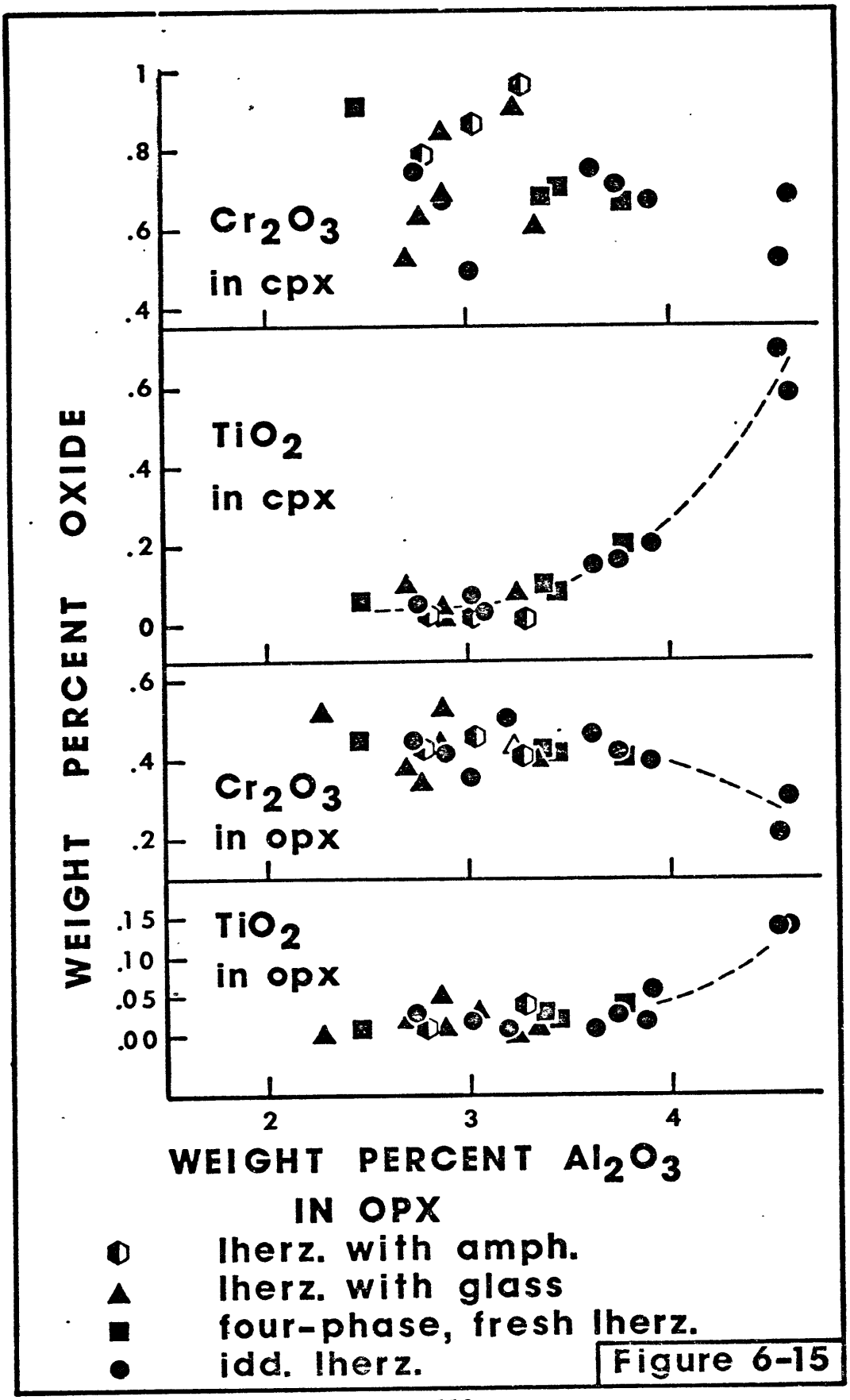
WEIGHT PERCENT OXIDE
1
.8
.6
.4
Cr_2O_3
in cpx
.6
.4
.2
0
TiO_2
in cpx
.6
.4
.2
Cr_2O_3
in opx
.15
.10
.05
.00
TiO_2
in opx
2
3
4
WEIGHT PERCENT Al_2O_3
IN OPX
lherz. with amph.
lherz. with glass
four-phase, fresh lherz.
idd. lherz.

Figure 6-15

former and 2) the high abundance of aluminous lherzolites with olive green spinel in the latter. The significance of iddingsite lies solely in its restriction to nodules from splatter cones. Baker (1967) has found iddingsite of the type present in the Nunivak xenoliths to consist of a mixture of goethite and smectite clay minerals. Using the experimental work of Tunnel and Psonjak (1931) on the stability of goethite, Baker concludes that iddingsite is formed by deuteric processes under oxidizing conditions at temperatures below 140°C. In the Nunivak case, this means that the iddingsite must have formed in the volcanic piles after eruption. This interpretation is supported by the occurrence of fresh lherzolites in alkalic flows associated with, or in localized pockets within, splatter cones. The conclusion, is therefore, that the differences between the iddingsitized and fresh lherzolite suites are correlated to the style of eruption, splatter cones or maars, which brought the xenoliths to the surface. This conclusion conflicts with the interpretation (Lorenz, 1973) that maars are simply the result of meteoric water gaining access to the magma sources of cinder cones.

b) Amphibole-Bearing Lherzolites

The clinopyroxenes and spinels of the amphibole-bearing lherzolites have been shown to be chemically distinct from those of both the iddingsitized and fresh, four phase lherzolites. The interstitial clinopyroxenes of the amphibole lherzolites are relatively rich in jadeite and plot in the eclogite field of White (1964), as opposed to those of the four phase lherzolites which fall in the granulite field. The amphibole lherzolite clinopyroxenes contain the lowest degree of calcium-tschermak

substitution of any of the Nunivak lherzolite clinopyroxenes. The spinels of the amphibole lherzolites, which occur largely as embayed inclusions in the amphibole, exhibit the highest Cr/Cr + Al and the lowest Mg numbers found in either of the lherzolite suites.

The phases of the fresh lherzolites containing fine-grained, glass-bearing zones show strong chemical affinities with those of the amphibole lherzolites. Their clinopyroxenes, when fresh, also contain high proportions of jadeite and low contents of calcium-tschermak component. The majority of these clinopyroxenes fall in the eclogite field of White (1964). Many of these clinopyroxenes, however, have developed a cloudy alteration which is associated with a depletion in jadeite and an enhancement in calcium-tschermak component. This alteration has the effect of shifting their compositions towards those of the four phase, fresh lherzolites. The interstitial spinels of these lherzolites are invariably surrounded by fine-grained, glass-bearing zones. These relict spinels are chemically zoned with margins rich in chromium, similar in composition to spinels included in amphibole, and aluminous cores, similar in composition to the spinels of the four phase, fresh lherzolites. In addition to the similarity of the clinopyroxenes and spinels between the glass and amphibole bearing lherzolites, it has also been demonstrated that the bulk composition of the fine-grained zones can be recalculated as a Cr-amphibole. All of the above characteristics support the petrographic interpretation that these glass-bearing lherzolites were originally amphibole-bearing lherzolites which have experienced partial melting after entrainment by their host basanites. If this interpretation is correct, then 50% of the fresh lherzolites were originally

amphibole lherzolites. Best (1974) has reached a remarkably similar conclusion about a suite of lherzolites found in the western Grand Canyon.

The nature and origin of the amphibole-bearing lherzolites is intriguing. Their predominance in the maars, whose xenolith population has the highest ratio of lherzolites to feldspathic xenoliths (Table 4-1), and the jadeitic nature of their clinopyroxenes suggests that they are derived from relatively deeper levels than the four phase lherzolites of both the fresh and iddingsitized suites. The chemical zoning found in the core spinels and their host amphiboles could not survive for any length of time under the pressure-temperature conditions of the upper mantle. This suggests that the amphibole-spinel intergrowths may be recent features, possibly formed during the early stages of igneous activity beneath Nunivak Island. This topic will be dealt with at length in Chapter 8.

c) Origin of the Chemical Variations in the Lherzolite Phases

The origin(s) of the variations in the lherzolite phase chemistry are intimately tied to the origin of the lherzolites themselves. Lherzolites have been generally accepted to be fragments of the upper mantle. White (1966), Wilshire and Binns (1961), and Ross et al. (1954) have reviewed the general arguments for this conclusion which apply equally well to the Nunivak lherzolites. O'Hara (1963,1968,1973) has pointed out, however, that few of these arguments are definitive and postulates that lherzolites represent a high-pressure, cummulate assemblage from alkalic basalts. With these alternatives in mind, three possible origins will be

examined for the chemical variations documented in the phases of the Nunivak lherzolites:

1. Varying degrees of fractional crystallization from a common parent liquid.
2. Varying degrees of melting of a common, upper mantle, parent solid.
3. Relicts of variations found in the upper mantle reflecting metamorphic equilibrium under varying P-T conditions and/or bulk composition.

1. The first possibility appears the least likely. For any reasonable distribution coefficients, the degree of crystallization required to produce the range of Ti values observed in the lherzolite clinopyroxenes (Figures 6-15 and 6-8) must produce an even larger variation in their Cr contents. This phenomena is not observed (Figure 6-15). In addition, studies of spinel cumulate horizons in the Stillwater Complex, Montana (Jackson, 1969), the Greak Dyke of Southern Rhodesia (Worst, 1958), and the Bushveld Complex, South Africa (Wager and Brown, 1968) reveal that Cr/Cr + Al and Mg/Mg + Fe ratios decrease in spinel as crystallization proceeds. Such a trend, however, is perpendicular to that exhibited by the spinel population of the Nunivak lherzolites (Figures 6-14, 6-2, and 6-3). These considerations virtually rule out the possibility that the Nunivak lherzolites are cumulates from their host basalts.

2. The case for the role of melting in the origin of the chemical variations in the lherzolite phases is less clear. Despite the limitations of treating Cr and Ti as trace elements, it will be qualitatively useful to use these elements to evaluate partial and fractional melting

processes. Using an equilibrium melting model, over 60% partial fusion is required to produce the Ti variation observed in the lherzolite clinopyroxenes assuming a distribution coefficient of 20 (K = conc. Ti in melt/conc. Ti in crystal). This would result, however, in more than a 100% increase in the Cr content of the residual clinopyroxene assuming a Cr distribution coefficient of 0.1. This increase is not observed (Figure 6-15). A fractional melting model (Gast, 1968) will more closely match the observed variations in the lherzolite clinopyroxenes. Assuming the same distribution coefficients, approximately 13% melting is required to produce the range of Ti values. This will be accompanied by a 13% increase in the Cr content of the clinopyroxene. If the distribution coefficient for Ti is reduced to 10, then 25% melting is required and the Cr content of the residue will increase by 30%. Such Cr increases, though not apparent in Figure 6-15, may be obscured in the scatter in the clinopyroxene Cr analyses.

The Mg/Mg + Fe and Cr/Cr + Al variations in the lherzolite spinels cannot be explained solely by partial melting. On the basis of thermodynamic (section IVb) and crystal chemical considerations, as melting proceeds the spinels must become enriched in Mg and Cr at the expense of Fe and Al. This enrichment trend is perpendicular to that observed in the lherzolite spinels (Figures 6-2, 6-3 and 6-14). Therefore the variation in the chemistry of the lherzolite spinels cannot reflect equilibration with a liquid over varying degrees of partial melting. Partial melting in the past, however, cannot be ruled out. For example, for small degrees of melting, one would expect the Mg number of lherzolite olivine to be virtually unchanged. As cooling occurs after melting, the

Mg/Mg + Fe ratio of the spinel will decrease, buffered by its associated olivine. The spinel is, however, considerably more Cr-rich than before the melting took place. Since spinel is the main storage place for Cr in lherzolite assemblages, the Cr/Cr + Al of the spinel will remain fairly constant during cooling. If the lherzolite assemblage re-equilibrates to the P-T conditions it experienced before melting took place, its spinel must become more Fe-rich than it was before melting (Figures 6-2 and 6-3). Thus, the result of partial melting followed by cooling and re-equilibration will be a spinel relatively enriched in Fe and Cr at the expense of Mg and Al. This is precisely the trend that is observed in the spinels of the Nunivak lherzolites.

The differences between the clinopyroxenes of the amphibole lherzolites and the four phase, fresh lherzolites cannot be bridged by partial melting. Although incipient (10%) melting of the jadeite-rich clinopyroxenes does produce residual rims similar in composition to the clinopyroxenes of the four phase, fresh lherzolites, this process is accompanied by a sharp rise in the clinopyroxene's Cr content (section Vd). Yet the jadeite-rich clinopyroxenes of the amphibole lherzolites often contain more Cr than the more magnesian clinopyroxenes of the four phase, fresh lherzolites. Similarly partial melting of the Cr-rich spinels of the amphibole lherzolites could not produce the more aluminous spinels of the four phase lherzolites.

3. The proceeding arguments indicate that the variations in the phase chemistry of the lherzolite xenoliths are not compatible with equilibration with a silicate liquid phase. Rather the nature of the spinels

suggests that the trends observed in the lherzolite phases reflect metamorphic equilibrium in response to varying P-T conditions and/or bulk composition. Although it is unlikely that fractional crystallization has ever played a role in the lherzolite chemistry, the occurrence of partial melting in the past cannot be ruled out. The Nunivak lherzolites are therefore concluded to be accidental fragments whose chemical variations are relicts of those existing in the upper mantle.

CHAPTER 7 FELDSPATHIC AND DUNITE XENOLITHS

This chapter deals with xenoliths which, on the basis of mineralogical and chemical criteria, have been interpreted to have had a cumulate origin. These include pyroxene granulites, dunites and harzburgites whose olivines have Mg numbers less than 0.89. Petrographic investigation has revealed that the gabbroic nodules are feldspar-rich end-members of the pyroxene granulite xenolith suite.

I Pyroxene Granulites

Nodules belonging to this suite are metamorphic rocks exhibiting corona structures developed around primary olivine and plagioclase. This texture is so pervasive that olivine and plagioclase never coexist, but are always separated by mantles of radially disposed orthopyroxene and spinel-clinopyroxene symplectite. Hoare (1968) recognized that this suite consists of a continuous spectrum of xenoliths ranging from plagioclase dominated specimens to olivine dominated specimens. Despite this fact, it will be clearer for textural and mineralogical reasons to describe the typical end-members first and then proceed to the more common intermediate examples. Many of these xenoliths contain textural evidence for partial melting. For clarity, the following general descriptions will be restricted to specimens which do not exhibit such textures and a later section will deal with the textural modifications which are introduced by partial melting.

No consistent differences have been recognized between the iddingsitized members of this suite found in splatter cones and the fresh members occurring in the maars.

a) Olivine-Rich Pyroxene Granulites

The bulk of each of these nodules consists of a xenomorphic-granular aggregate of .5 to 4 mm. olivine grains. Deformational banding and undulatory extinction are strongly developed in these olivine grains. Anhedral, 1 to 3 mm. grains of clinopyroxene are sometimes present as an accessory phase intergrown with the olivine. This pyroxene typically has a turbid appearance due to the presence of numerous preferentially oriented, colorless rods ranging from 1 to 10 microns in length and approximately 1 micron in diameter. In reflected light these inclusions have a characteristic high reflectivity and are thus probably spinel. Interstitial, green spinel is also present as a few, .4 mm. embayed grains.

This matrix contains oblate to irregular corona structures ranging from .1 to 1 cm. in size. These structures frequently have a common orientation, defining a foliation in the nodules. The outer layer of these coronas, adjacent to the olivine matrix, consists of a .1 to 1 mm. mantle of anhedral, but elongate, colorless orthopyroxene crystals disposed perpendicularly to the contact. Inside the orthopyroxene mantle is an oval body of spinel-clinopyroxene symplectite. Near the orthopyroxene contact this symplectite consists of anhedral .01 to .04 mm. clinopyroxene intergrown with .01 or smaller, equant, green spinel. The interiors of the symplectite bodies, however, consist of coarser grained (.1 to .6

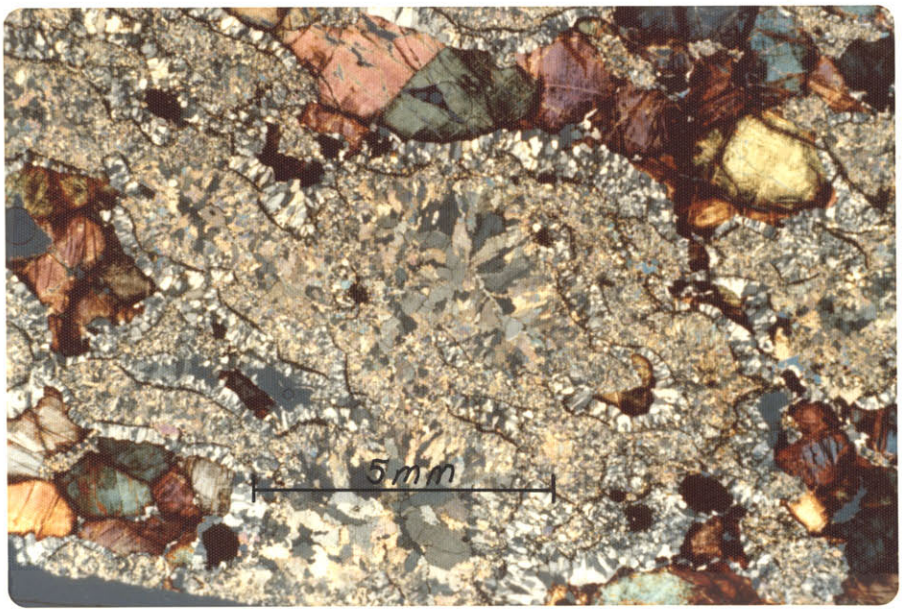

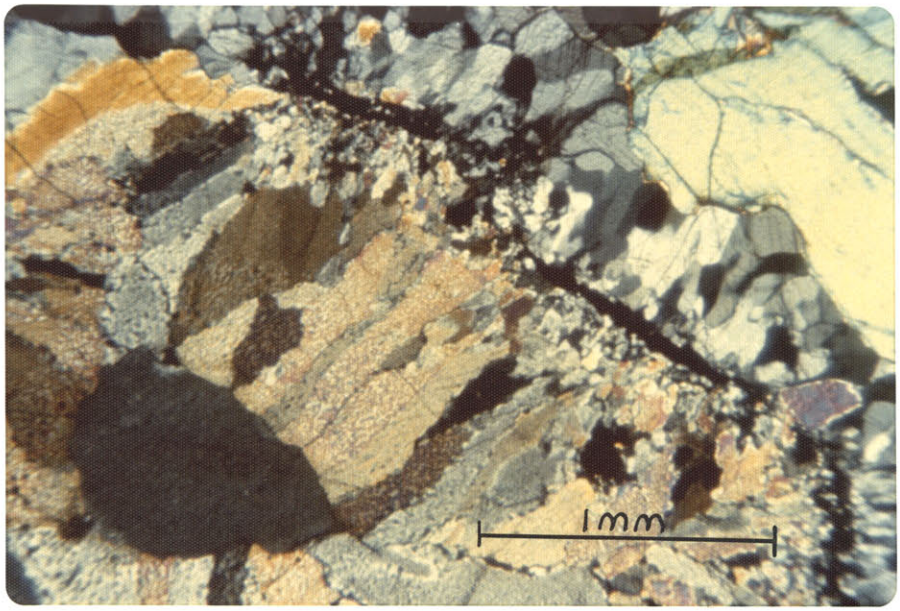

Plate 7-1 (top): Olivine-rich pyroxene granulite. Note iddingsite and fine opaques in relict olivines.

Plate 7-2 (bottom): Close up of corona structure of pyroxene granulite with remnants of both olivine and plagioclase (dark grain).

mm.), elongated and radially disposed clinopyroxene grains. Here the spinel occurs as a vermicular intergrowth in the clinopyroxene. This intergrowth is developed on such a fine scale that, though it is difficult to find clear areas large enough to obtain a clinopyroxene analysis with the microprobe, the individual spinel grains are not isotropic because they do not extend through the thickness of the thin section. Spinel also occurs as chains of single, .01 to .05 mm., equant grains lining the contact between the orthopyroxene mantle and the spinel-clinopyroxene symplectite and along the suture line of the radially disposed, core clinopyroxene (Plate 7-1 and 7-2).

Occasionally an embayed and turbid plagioclase crystal is found at the center of the spinel-clinopyroxene symplectite. The turbidity is caused by numerous, .004 to .02 mm., equant, but rounded inclusions of spinel. This texture is pervasive, but appears to be crystallographically controlled. The plagioclase commonly exhibits both albite and pericline twinning and has concentricly zoned extinction near its margin, which is free of inclusions for a depth of about .01 mm. (Figure 7-2).

b) Feldspathic Pyroxene Granulites

The feldspar-rich granulites in many respects mirror the olivine granulites. They consist largely of .2 to 3 mm., anhedral, interlocking plagioclase with lessor amounts of similar clinopyroxene. In many slides the plagioclase exhibits a hazy brown discoloration due to numerous rounded inclusions on a 1 micron scale. In two slides the feldspar contains networks of .01 to .03 mm., rounded to elongate inclusions of spinel. The arrangement of strings of these grains into a network

pattern suggests crystallographic control by their plagioclase host. Interstitial clinopyroxene is also present, but typically finer grained than the feldspar. The larger grains commonly exhibit fine orthopyroxene lamellae. The appearance of these pyroxenes varies from very turbid brown to clear, Cr-green in different slides. A couple of sections contain .4 to 2 mm., anhedral crystals of olive green to brown amphibole.

In this matrix are frequent, .5 to 1^{+} mm., oblate corona structures. The mineralogy of these bodies is the reverse of those described in the section on olivine granulites. The outer mantle consists of a hazy turbid brown (almost opaque) layer, .1 to .3 mm. in thickness. Rotation of the microscope stage under crossed nicols reveals .01 to .2 mm., ghost-like, radially disposed crystals. The turbidity appears to be caused by a crytic intergrowth of spinel and clinopyroxene, much finer grained than its counterpart in the olivine granulites. The inner margins of this spinel-clinopyroxene symplectite is markedly more opaque than that coexisting with the feldspar. This is interpreted to be due either to a finer grain size or more intense spinel exsolution. The ghost-like crystal outlines cannot be distinguished in this region.

Inside the spinel-clinopyroxene symplectite is colorless, pure orthopyroxene. Its habit varies from radially disposed, .01 to .15 mm., elongated crystals to an aggregate of anhedral crystals. Occasionally an embayed olivine crystal(s) occurs at the center of this orthopyroxene core. In addition to being present in the symplectite, green spinel again occurs as chains of .02 to .05 mm., equant crystals lining the contact between the symplectite and the orthopyroxene.

With increasing feldspar content, these feldspathic granulites grade into rocks which are better termed gabbros. A careful search under the microscope, however, usually detects a few, small, remnant corona structures.

c) Intermediate Pyroxene Granulites

As the relative amounts of olivine and plagioclase become more comparable, the extent and grain size of the mantles of orthopyroxene and spinel-clinopyroxene symplectite increase markedly. The overall granular texture of the end-members is replaced by an intricate and spectacular corona-reaction texture. In thin section these nodules consist of pods of granular aggregates of olivine or feldspar mantled by radially disposed orthopyroxene or spinel-clinopyroxene symplectite respectively. These isolated, mantled pods are connected by double chains of radial crystals of either orthopyroxene or symplectite, depending on which predominates in the slide, lending a network-like appearance to the entire specimen.

As described in the section on olivine-rich granulites, the spinel-clinopyroxene symplectite adjacent to the orthopyroxene bands is typically finer grained than usual and consists of a granular aggregate of anhedral clinopyroxene and equant spinel. Further from the contact, the clinopyroxene becomes coarser grained and elongate, while the spinel occurs largely as wormy intergrowths in the clinopyroxene. These larger clinopyroxene crystals, however, occasionally abut directly against the orthopyroxene mantles. Here an unusual texture results. The half of the clinopyroxene closest to the orthopyroxene is free of spinel inclu-

sions. In plane polarized light the boundary of the orthopyroxene grains appears to follow the edge of the spinel inclusions, which under crossed nicols is seen to be well into the clinopyroxene crystal (Figure 7-2). In other words, the apparent interface between the clinopyroxene and the orthopyroxene as defined by crystal boundaries does not correspond to that defined by the change in birefringence. Replacement of the orthopyroxene by the clinopyroxene is suggested.

d) Melting and Retrograde Textures

In many thin sections, patches of the spinel-clinopyroxene symplectite have been replaced by areas consisting of .01 to .4 mm., skeletal olivine in a matrix of laths to anhedral grains of plagioclase (Figure 7-3). This texture is most commonly developed near the contacts with the orthopyroxene mantles or adjacent to remnant plagioclase cores. In a small number of specimens the entire symplectite has been replaced. The orthopyroxene bands, themselves, do not appear to be affected. Equant (.01 to .05 mm.) grains of dark green spinel and remnants of the symplectite clinopyroxene are commonly found in these olivine-feldspar zones. In the feldspathic granulites, zones similar to those just described commonly separate primary clinopyroxene and amphibole from the coexisting plagioclase. Those surrounding the amphibole contain considerable amounts of clinopyroxene in addition to olivine and plagioclase. Strangely, this clinopyroxene has an embayed appearance and contains equant inclusions resembling the spinel found in the symplectite clinopyroxenes. These textures are interpreted to have been caused by partial melting of the granulite nodules.

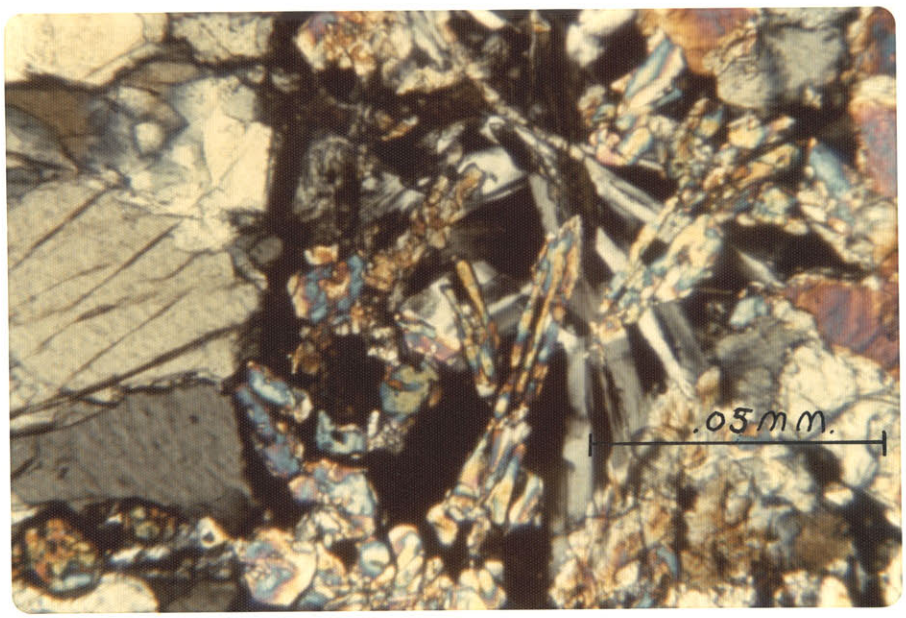

Plate 7-3: Melt zone at the contact between orthopyroxene and symplectite containing skeletal olivine with laths of plagioclase.

Occasionally chains of .02 to .04 mm., equant, olivine grains are found between the chains of equant spinel and the orthopyroxene mantles. No trace of associated secondary plagioclase is found with these olivines. This texture may be produced by the reaction of orthopyroxene + spinel to more aluminous orthopyroxene + olivine with increasing temperature.

e) Cumulate Textures

Two of the intermediate granulite members (12014 and 12024) contain unusually high concentrations of what is interpreted to be primary clinopyroxene (to 25%). This clinopyroxene occurs as turbid, intercumulous grains ranging to greater than 1 cm. in size and poikilitic ly encloses olivine. The olivine occurs as rounded to euhedral .5 to 3 mm., cumulate crystals. Plagioclase is also abundant, but tends to occur in separate aggregates of anhedral grains. Where olivine and plagioclase do coincide, reaction rims of spinel-clinopyroxene symplectite and orthopyroxene have developed. The texture exhibited by the interstitial clinopyroxenes in these specimens is textbook evidence for a cumulate origin.

II Phase Chemistry of the Pyroxene Granulites

The chemistry of the phases of four pyroxene granulite xenoliths was studied in detail:

12000 A feldspar-rich granulite with only minor, remnant olivine.

12001 A granulite with approximately equal proportions of remnant olivine and feldspar.

12004 An olivine-rich granulite with minor remnant feldspar. The

olivine in this specimen is characterized by pervasive iddingsitization and opaque precipitation.

12017 An olivine-rich granulite in which the spinel-clinopyroxene symplectite has been largely replaced by quench olivine and feldspar.

a) Olivines

The compositions of the interstitial olivines of these four nodules are presented in Table 7-1. The forsterite content of the remnant olivine from the feldspar-rich granulite (12000) is only 72% while those of the fresh olivines in the feldspar-poor nodules (12001,12017) are approximately 87%. The iddingsitized olivine of specimen 12004 is considerably more magnesium rich. This probably reflects the loss of iron during the development of its pervasive opaque inclusions. Despite efforts to detect it, no chemical zoning was found in the olivines near their contacts with the secondary orthopyroxene mantles.

The skeletal olivine developed with plagioclase in the spinel-clinopyroxene symplectites is characteristicly more magnesium-rich (Fo:90) than its associated interstitial olivine. The compositions of the skeletal olivines from specimen 12001 and 12017 are listed with those of the interstitial olivines in Table 7-1. In addition to higher Mg numbers, these skeletal olivines are also characterized by relatively higher calcium contents than the interstitial olivines. This is in accord with the conclusion based on textural arguments that these skeletal olivines are quench crystals associated with the partial melting of the spinel-clinopyroxene symplectite (Simkin and Smith, 1970).

TABLE 7-1

PYROXENE GRANULITE OLIVINES

	INTER	INTER	INTER	INTER	QUENCH	QUENCH
SPEC.	12000	12001	12004	12017	12001	12017
SIO2	35.94	40.11	40.31	40.50	40.22	40.70
TIO2	0.16	0.00	0.00	0.00	0.00	0.00
AL2O3	0.04	0.01	0.02	0.04	0.29	0.29
FE2O3	0.00	0.00	0.00	0.00	0.00	0.00
CR2O3	0.00	0.05	0.02	0.00	0.03	0.08
FEO	25.30	12.40	7.68	12.81	9.70	9.02
MGO	36.93	47.34	51.72	47.75	48.50	49.48
MNO	0.55	0.15	0.15	0.17	0.15	0.17
CAO	0.07	0.06	0.04	0.04	0.50	0.32
NA2O	0.35	0.00	0.00	0.02	0.00	0.00
K2O	0.00	0.00	0.00	0.01	0.00	0.00
TOTAL	99.34	100.12	99.94	101.34	99.39	100.06

FORMULA UNITS ASSUMING 4 OXYGENS

SI	0.963	0.994	0.981	0.993	0.993	0.994
TI	0.003	0.000	0.000	0.000	0.000	0.000
AL	0.001	0.000	0.001	0.001	0.008	0.008
FE3+	0.000	0.000	0.000	0.000	0.000	0.000
CR	0.000	0.001	0.000	0.000	0.001	0.002
FE2+	0.567	0.257	0.156	0.263	0.200	0.184
MG	1.475	1.749	1.876	1.745	1.784	1.801
MN	0.012	0.003	0.003	0.004	0.003	0.004
CA	0.002	0.002	0.001	0.001	0.013	0.008
NA	0.018	0.000	0.000	0.001	0.000	0.000
K	0.000	0.000	0.000	0.000	0.000	0.000
TOTAL	3.042	3.005	3.019	3.007	3.003	3.001
MG/MG+FE	0.722	0.872	0.923	0.869	0.899	0.907

UNLESS OTHERWISE SPECIFIED; TOTAL IRON AS FEO

b) Feldspars

Table 7-2 presents representative analyses for the interstitial or remnant feldspar of the four pyroxene granulite nodules. The interstitial plagioclase of the feldspar-rich granulite (12000) has a composition of An 73.4. However, adjacent to areas of spinel-clinopyroxene symplectite this feldspar becomes depleted in calcium. In the most extreme case in this specimen, the composition of the feldspar is reduced to An 59.8. In comparison, the remnant plagioclase of specimens 12001 and 12004 are very albite-rich (An 23 to 26). These plagioclases appear to be chemically homogenous; their inclusion free rims being essentially identical in composition to their cores. Since it is unlikely that the original feldspar of these olivine-rich nodules would have anorthite contents less than that of the feldspathic granulite (12000), it must be concluded that the formation of the two pyroxene plus spinel assemblages depleted these feldspars in calcium. In support of this conclusion, the secondary plagioclase associated with quench olivine, which is interpreted to have crystallized from liquid produced by the partial melting of symplectite, is enriched in calcium (to An 80). Individual analyses of secondary plagioclase in any one melt zone may exhibit a range of anorthite contents of up to 8%. This may reflect chemical zoning in individual crystals or lateral inhomogeneity. Because of the small grain-size of the quench plagioclase crystals this ambiguity could not be resolved.

c) Orthopyroxenes

Selected analyses of orthopyroxenes comprising the coronas developed on primary olivine are presented in Table 7-3. One of the striking

TABLE 7-2

PYROXENE GRANULITE FELDSPARS

	PRIM	RESID	RESID	RESID	RESID	QUENCH	QUENCH
SPEC.	12000	12000	12001	12004	12004	12017	12000
SIO2	47.91	52.01	61.78	61.17	61.08	48.73	46.30
TIO2	0.00	0.08	0.00	0.00	0.00	0.00	0.00
AL2O3	33.57	30.26	25.67	23.85	23.82	31.93	34.51
FE2O3	0.00	0.00	0.00	0.00	0.00	0.00	0.00
CR2O3	0.00	0.07	0.00	0.02	0.02	0.00	0.00
FEO	0.00	0.11	0.00	0.18	0.14	0.39	0.00
MGO	0.00	0.04	0.00	0.08	0.11	0.53	0.29
MNO	0.00	0.02	0.00	0.02	0.01	0.03	0.00
CAO	15.41	13.28	5.17	5.14	5.08	16.12	17.80
NA2O	3.05	4.17	7.95	8.52	8.87	2.21	1.42
K2O	0.05	0.07	0.39	0.67	0.55	0.01	0.06
TOTAL	99.99	100.11	100.96	99.65	99.68	99.95	100.38

FORMULA UNITS ASSUMING 8 OXYGENS

SI	2.194	2.361	2.709	2.734	2.730	2.234	2.122
TI	0.000	0.003	0.000	0.000	0.000	0.000	0.000
AL	1.812	1.619	1.327	1.256	1.255	1.726	1.864
FE3+	0.000	0.000	0.000	0.000	0.000	0.000	0.000
CR	0.000	0.003	0.000	0.001	0.001	0.000	0.000
FE2+	0.000	0.004	0.000	0.007	0.005	0.015	0.000
MG	0.000	0.003	0.000	0.005	0.007	0.036	0.020
MN	0.000	0.001	0.000	0.001	0.000	0.001	0.000
CA	0.756	0.646	0.243	0.246	0.243	0.792	0.874
NA	0.271	0.367	0.676	0.738	0.769	0.196	0.126
K	0.003	0.004	0.022	0.038	0.031	0.001	0.004
TOTAL	5.036	5.011	4.976	5.026	5.042	5.001	5.010
AN	73.4	63.5	25.8	24.1	23.3	80.1	87.1

UNLESS OTHERWISE SPECIFIED; TOTAL IRON AS FEO

things about these analyses is the constant value of .88 for the Mg numbers of the orthopyroxenes for the olivine-rich granulites. The magnesium number for the orthopyroxene from the feldspathic granulite, however, is significantlyllower at .77. All of these values are significantly lower than the lower bound of .90 for the Mg numbers of lherzolite orthopyroxenes. The distribution coefficients for iron and magnesium between coexisting olivine and orthopyroxene ($K = (Mg/Mg + Fe)_{ol}/(Mg/Mg + Fe)_{opx}$) are .989 and .988 for specimens 12001 and 12017 respectively. The same coefficient for the feldspar-rich granulite (12000) is only .935.

The aluminum contents of the orthopyroxenes of the three olivine-rich granulites are similar to those characteristic of lherzolite orthopyroxenes (3 to 4 weight percent Al_2O_3). The orthopyroxene developed in the feldspathic granulite (12000), however, contains considerably less aluminum.

In each specimen, detailed microprobe traverses were run across the orthopyroxene mantles in an effort to detect chemical zoning between the olivine and symplectite boundaries. In all cases the orthopyroxene mantles proved to be compositionally uniform throughout.

d) Clinopyroxenes

Table 7-4 compares the compositions of interstitial clinopyroxenes and symplectite clinopyroxenes of the pyroxene granulites. The former are characterized by higher Ti and Cr, but lower Na, Al, and Mg numbers than the latter. In Figure 7-1, the interstitial clinopyroxenes are poorer in octahedrally coordinated aluminum (jadeite) and slightly higher in tetrahedral aluminum than the symplectite clinopyroxenes. There is a direct correlation between the Al, Ti, and Cr contents of the intersti-

TABLE 7-3

PYROXENE GRANULITE ORTHOPYROXENES

SPEC.	12000	12000	12001	12001	12004	12017	12017
SIO2	53.19	54.13	54.97	55.22	55.23	54.92	55.65
TIO2	0.10	0.05	0.00	0.00	0.00	0.00	0.00
AL2O3	1.71	2.32	3.45	3.46	3.94	3.31	3.05
FE2O3	0.00	0.00	0.00	0.00	0.00	0.00	0.00
CR2O3	0.00	0.04	0.08	0.08	0.10	0.12	0.12
FEO	15.54	14.57	7.90	7.86	7.76	7.95	7.97
MGO	28.27	28.42	33.11	32.69	32.28	32.58	32.54
MNO	0.66	0.29	0.18	0.19	0.17	0.20	0.19
CAO	0.50	0.44	0.37	0.39	0.37	0.45	0.47
NA2O	0.14	0.17	0.00	0.00	0.00	0.00	0.00
K2O	0.00	0.01	0.00	0.00	0.00	0.00	0.00
TOTAL	100.11	100.44	100.06	99.89	99.85	99.53	99.99

FORMULA UNITS ASSUMING 6 OXYGENS

SI	1.923	1.934	1.910	1.920	1.919	1.919	1.934
TI	0.003	0.001	0.000	0.000	0.000	0.000	0.000
AL	0.073	0.098	0.141	0.142	0.161	0.136	0.125
FE3+	0.000	0.000	0.000	0.000	0.000	0.000	0.000
CR	0.000	0.001	0.002	0.002	0.003	0.003	0.003
FE2+	0.470	0.435	0.230	0.229	0.225	0.232	0.232
MG	1.524	1.514	1.715	1.695	1.672	1.697	1.685
MN	0.020	0.009	0.005	0.006	0.005	0.006	0.006
CA	0.019	0.017	0.014	0.015	0.014	0.017	0.017
NA	0.010	0.012	0.000	0.000	0.000	0.000	0.000
K	0.000	0.000	0.000	0.000	0.000	0.000	0.000
TOTAL	4.042	4.021	4.018	4.008	3.999	4.011	4.002
MG/MG+FE	0.764	0.777	0.882	0.881	0.881	0.880	0.879

UNLESS OTHERWISE SPECIFIED; TOTAL IRON AS FEO

TABLE 7-4

PYROXENE GRANULITE CLINOPYROXENES

	PRIMARY			**	SYMPLECTITE		
SPEC.	12000	12024	12008	12000	12001	12004	12017
SIO2	51.63	51.69	51.60	49.55	53.82	53.70	53.07
TIO2	0.56	0.64	0.85	0.18	0.02	0.00	0.00
AL2O3	2.96	3.18	4.50	5.77	5.73	6.56	4.15
FE2O3	0.00	0.00	0.00	0.00	0.00	0.00	0.00
CR2O3	0.61	0.76	1.06	0.24	0.07	0.08	0.26
FEO	5.77	3.58	3.49	6.46	2.69	2.82	2.77
MGO	14.53	15.53	15.22	15.55	14.86	13.91	15.63
MNO	0.16	0.16	0.07	0.08	0.09	0.12	0.10
CAO	22.14	22.81	21.68	22.29	20.78	20.21	21.85
NA2O	0.89	0.53	0.55	0.29	1.98	2.43	1.07
K2O	0.01	0.20	0.00	0.00	0.02	0.01	0.00
TOTAL	99.26	99.08	99.42	100.41	100.06	99.84	98.90
FORMULA UNITS ASSUMING 6 OXYGENS							
SI	1.921	1.912	1.894	1.828	1.939	1.937	1.942
TI	0.016	0.018	0.023	0.005	0.001	0.000	0.000
AL	0.130	0.139	0.195	0.251	0.243	0.279	0.179
FE3+	0.000	0.000	0.000	0.000	0.000	0.000	0.000
CR	0.018	0.022	0.031	0.007	0.002	0.002	0.008
FE2+	0.180	0.111	0.107	0.199	0.081	0.085	0.085
MG	0.806	0.856	0.832	0.855	0.798	0.748	0.853
MN	0.005	0.005	0.002	0.002	0.003	0.004	0.003
CA	0.883	0.904	0.852	0.881	0.802	0.781	0.857
NA	0.064	0.038	0.068	0.021	0.138	0.170	0.076
K	0.000	0.009	0.000	0.000	0.001	0.000	0.000
TOTAL	4.022	4.014	4.004	4.049	4.008	4.007	4.002
MG/MG+FE	0.818	0.885	0.886	0.811	0.908	0.898	0.910
MODAL OL.	1 %	25 %	59 %	1 %	29 %	27 %	45 %

UNLESS OTHERWISE SPECIFIED; TOTAL IRON AS FEO

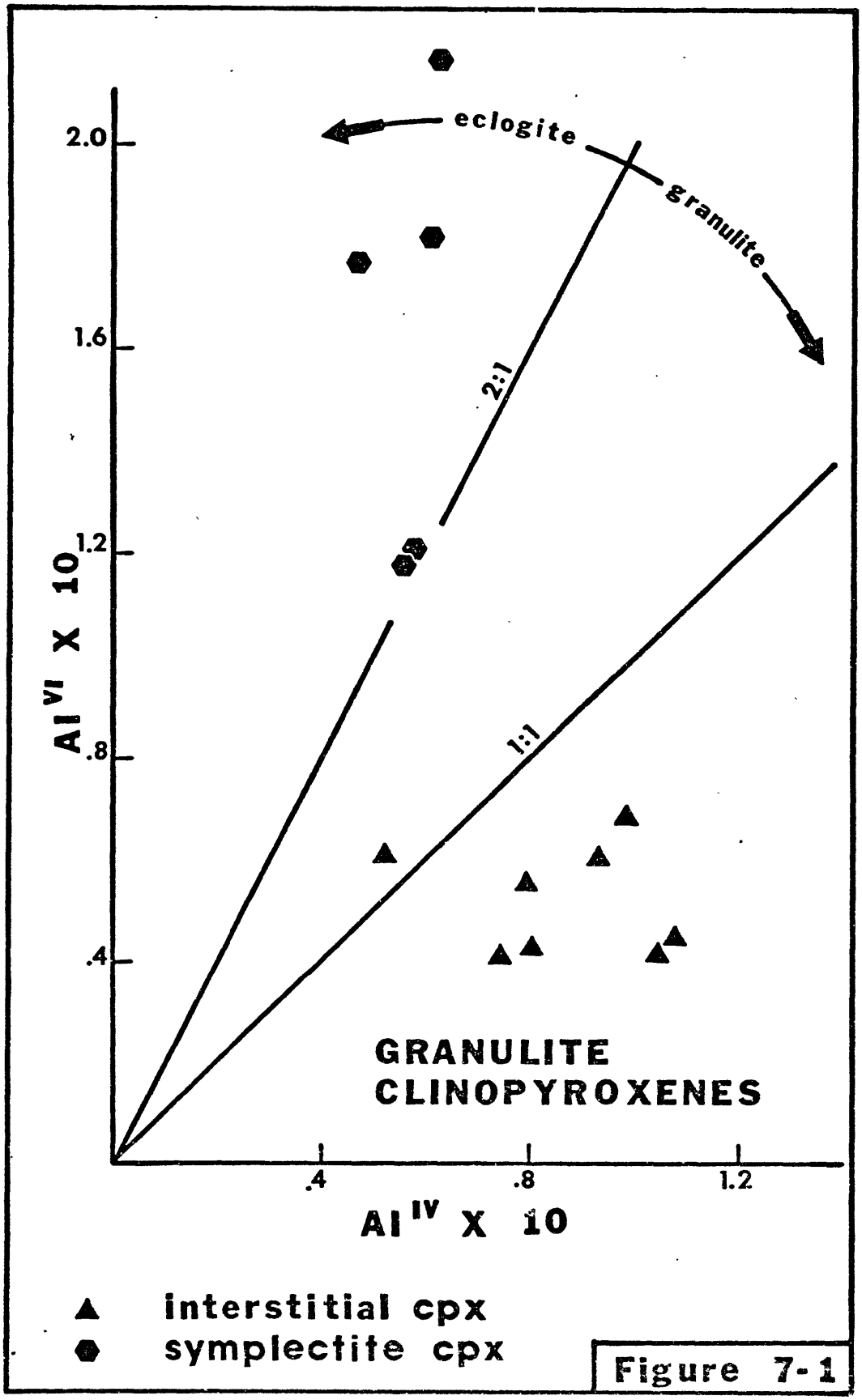
eclogite
granulite
2:1
1:1
2.0
1.6
1.2
.8
.4
Al^{VI} X 10
.4
.8
1.2
Al^{IV} X 10
GRANULITE
CLINOPYROXENES
interstitial cpx
symplectite cpx

Figure 7-1

tial clinopyroxenes and the modal olivine content of their nodules (Table 7-4).

The compositions of the symplectite clinopyroxenes are remarkably uniform in individual specimens, despite the variety of textures they exhibit. Grain-size, presence or absence of spinel inclusions, and position with respect to orthopyroxene or relict plagioclase have no influence on the symplectite clinopyroxene's composition. These clinopyroxenes have Mg numbers similar to those of the lherzolite clinopyroxenes (.900 to .910). Unlike the latter, however, the symplectite clinopyroxenes contain negligible concentrations of Cr and Ti. This reflects their origin by reaction from olivine and plagioclase, phases which do not contain these elements. The distribution coefficients for Mg and Fe between symplectite clinopyroxene and orthopyroxene ($K = (Mg/Mg + Fe)_{opx}/(Mg/Mg + Fe)_{cpx}$) are .942, .972, .982, and .967 for specimens 12000, 12001, 12004, and 12017 respectively. These distribution coefficients are characteristic of igneous assemblages (Kretz, 1963).

e) Spinels

The range of spinel compositions found in the granulite nodules is compared to those of the two lherzolite suites in Figures 6-2 and 6-3. For equivalent chromium contents, the granulite spinels are characteristically more iron-rich than the lherzolite spinels. The granulite spinel population exhibits generally lower chromium contents and Mg numbers than the lherzolite spinels.

The spinels exhibit the greatest chemical variations of any phase in the pyroxene granulites. Despite this fact, the locii of the spinel

TABLE 7-5

PYROXENE GRANULITE SPINELS

IN:	OPX	OPX	OPX	SYMPL	SYMPL	SYMPL	FELDS
SPEC.	12017	12001	12001	12001	12004	12004	12004
SIO2	0.31	0.79	0.63	1.05	0.63	1.05	1.44
TIO2	0.00	0.00	0.00	0.00	0.00	0.00	0.00
AL203	50.38	57.36	63.91	65.60	65.72	64.44	66.03
FE203	0.00	0.00	0.00	0.00	0.00	0.00	0.00
CR203	15.32	9.72	2.59	0.82	0.76	0.37	0.00
FEO	14.21	12.56	11.35	10.54	10.33	10.35	9.51
MGO	18.63	19.32	21.40	21.72	21.32	23.39	21.86
MNO	0.33	0.24	0.12	0.06	0.04	0.07	0.08
CAO	0.02	0.04	0.02	0.11	0.04	0.12	0.06
NA2O	0.00	0.00	0.00	0.00	0.00	0.00	0.00
K2O	0.00	0.00	0.00	0.00	0.00	0.00	0.00
TOTAL	99.20	100.03	100.02	99.90	98.84	99.79	98.98

FORMULA UNITS ASSUMING 4 OXYGENS

SI	0.008	0.021	0.016	0.026	0.016	0.026	0.036
TI	0.000	0.000	0.000	0.000	0.000	0.000	0.000
AL	1.607	1.755	1.897	1.928	1.951	1.897	1.942
FE3+	0.000	0.000	0.000	0.000	0.000	0.000	0.000
CR	0.328	0.200	0.052	0.016	0.015	0.007	0.000
FE2+	0.322	0.273	0.239	0.220	0.218	0.216	0.198
MG	0.751	0.748	0.803	0.807	0.800	0.871	0.813
MN	0.008	0.005	0.003	0.001	0.001	0.001	0.002
CA	0.001	0.001	0.001	0.003	0.001	0.003	0.002
NA	0.000	0.000	0.000	0.000	0.000	0.000	0.000
K	0.000	0.000	0.000	0.000	0.000	0.000	0.000
TOTAL	3.024	3.002	3.010	3.002	3.001	3.022	2.993
MG/MG+FE	0.700	0.733	0.771	0.786	0.786	0.801	0.804
CR/CR+AL	0.169	0.102	0.026	0.008	0.008	0.004	0.000

UNLESS OTHERWISE SPECIFIED; TOTAL IRON AS FEO

compositions in Figures 6-2 and 6-3 are modeled quite well by equipotential curves (Chapter 6, section IVb) for olivine of composition Fo 87 calculated at 1200°C. and 1300°C. respectively. This suggests that in spite of its variable composition, the spinels are in metamorphic equilibrium with their associated olivines. This is an interesting phenomena because most of the spinel is found in the orthopyroxene mantles or symplectite, physically removed from the olivine. The most chromian spinels occur as large blebs in the orthopyroxene mantles (Table 7-5). This spinel is similar in color and composition to the olive green spinels of the iddingsitized lherzolite suite. The chromium content of this spinel in one specimen may vary from 2 to 15 weight percent Cr_2O_3, however, each grain appears to be homogenous. Spinels occurring as chains along orthopyroxene-symplectite contacts or as intergrowths within the symplectite contain significantly less chromium. Chromium is undetectable in the spinel occurring as inclusions in relict plagioclases.

III Summary and Conclusions on the Pyroxene Granulites

The contrast between the corona texture of the orthopyroxene, spinel-clinopyroxene symplectite assemblage and the tectonic fabric of the granular aggregates of olivine and feldspar invites the conclusion that the former is a secondary feature formed by the incomplete reaction of the latter. If this interpretation is correct then the original rock was a troctolite consisting largely of varying proportions of olivine and plagioclase with lessor amounts of primary clinopyroxene. With increasing modal feldspar and clinopyroxene this rock type graded to

gabbro. The original feldspar of the olivine-rich granulites was probably similar in composition to that in the feldspar-rich granulites, where the ratio of plagioclase to olivine was such that the former was little affected by the reaction of the two. The feldspar in the olivine-rich granulites was depleted in calcium and silicon during the formation of the two pyroxene plus spinel assemblage. This, combined with the introduction of magnesium and iron, left albite-rich, relict plagioclase containing numerous spinel inclusions. There appears to have been little fractionation of iron and magnesium during the reaction of the primary olivine. The relatively chromium rich spinel found as large blebs in the orthopyroxene coronas must also be a primary phase because there is no source for its chromium in the other primary phases. The variable composition of this spinel in individual specimens indicates that it participated in the reaction of the primary olivine and plagioclase as a source for the low chromium concentrations found in the secondary spinels.

The relatively higher Mg numbers of the corona orthopyroxenes and clinopyroxenes when compared to the primary olivines is balanced by the more iron-rich nature of the symplectite spinels. The absence of chemical zoning in either the secondary or relict primary phases implies that the incompleteness of the reaction of the latter was not due to kynetic problems. According to this interpretation, the reaction terminated when the relict plagioclase became too Na-rich for it to continue under the prevailing P-T conditions. The relative enrichment of the skeletal olivine and plagioclase in magnesium and calcium, respectively, is consistent with the interpretation that they are quench crystals derived by

the partial melting of the secondary clinopyroxene and orthopyroxene. Equant spinel grains appear to remain as a refractory during this process.

To test the preceding qualitative conclusions, the "mineral distribution program" of Wright and Doherty (1970) was used to balance the equation:

Olivine + Plagioclase ± Spinel = relict Plagioclase + Cpx + Opx + Spinel

The compositions of phases from granulite 12001 were used in this calculation. The only exception was the assumption that the original composition of the plagioclase was that of the interstitial feldspar of the feldspathic granulite 12000. An excellent mass balance was attained by combining the relevant phases in the following weight proportions:

121 Plagioclase (An 72) + 100 Olivine (Fo 87) + 7 Spinel (Cr/Cr + Al) = .102) = 16 Plagioclase (An 25.8) + 87 Clinopyroxene (Mg/Mg + Fe = .908) + 75 Orthopyroxene (Mg/Mg + Fe = .882) + 49 Spinel (Cr/Cr + Al = .008).

$$\sum_{\text{oxides}} |\text{residuals}| = 1.29 \text{ weight percent}$$

The residuals for individual oxides do not exceed 0.25 weight percent and the stoichiometry closely matches the estimated mode. Thus the composition of this pyroxene granulite can be accounted for by a primary assemblage of olivine and plagioclase with minor spinel.

In conclusion, the nodules described in the foregoing sections are pyroxene granulites after the nomenclature of Ito and Kennedy (1970) and are transitional between the low and intermediate pressure granulites of Green and Ringwood (1967). Rocks similar to these nodules are commonly reported in deep seated anorthosite and gabbro bodies where the reaction

of olivine and plagioclase to form the assemblage two pyroxenes plus spinel is interpreted to reflect isobaric cooling (Gardner and Robbins, 1974; Whitney and McLelland, 1973; Griffin et al., 1973, 1971, 1969). These pyroxene granulites are, however, rare as volcanic inclusions. The only documented occurrences the author is familiar with are the Kerguelen Archipelago (McBirney and Aoki, 1973) and Iki Island, Japan (Aoki, 1968).

The occasional poikilitic character of the interstitial clinopyroxenes and the general phase chemistry suggest that the primary phase assemblages of the pyroxene granulites were cumulates. With varying proportions of the primary phases olivine, plagioclase, and clinopyroxene, the original rocks ranged from feldspathic dunites through troctolites to gabbros. The tectonic fabric of the relict, primary phases and the evidence for metamorphic equilibrium in the spinels indicate, however, that the pyroxene granulites are not cumulates from their host basanites. This conclusion is supported by the evidence for partial melting in the corona structures, which themselves postdate the deformation in the primary phases. The Nunivak pyroxene granulites are therefore concluded to be accidental xenoliths, probably derived from the lower regions of the earth's crust.

IV Dunites

This section deals with a few olivine-rich xenoliths which are interpreted to have been formed by cumulate processes. These nodules were originally selected, with others, to represent olivine-rich end-

members of the fresh lherzolite suite. Subsequent microprobe analyses of the phases of these xenoliths has revealed that they have Mg numbers which are too low to be compatible with those characteristic of the corresponding phases in spinel lherzolites. The chemistry of two of these dunites was studied in detail (specimens 15009 and 15011). They are xenomorphic-granular aggregates consisting largely of .5 to 2 mm. olivine. Deformational banding and undulatory extinction are strongly developed in these grains. Spinel is the second most abundant phase, occurring as .2 to 1.5 mm., interstitial, anhedral grains. Unlike the lherzolite spinels, those of the dunites are black in color. This spinel is typically concentrated into spinel-rich layers, defining a compositional foliation in each of the nodules. Specimen 15009 is very spinel-rich (to 20%), while specimen 15011 contains only a few percent spinel, concentrated in widely spaced bands. No fine-grained zones are observed about the spinel in either nodule. Clinopyroxene and orthopyroxene are present as minor accessories.

Specimen 15011 contains a few 1 mm., fine-grained areas of irregular shape which are not associated with interstitial spinel. These areas are filled with a porous network of closely packed, commonly oriented, .02 to .1 mm., prismatic crystals with high birefringence and inclined extinction. These crystals are believed to be clinopyroxene. The majority of these prismatic crystals have a common extinction position. However, the extinction position of the remaining crystals define bands which crosscut the network of crystals at an angle to its preferred orientation. Numerous, equant spinel inclusions (10 microns) riddle this prismatic clinopyroxene. In addition, larger, .05 mm., equant opaque grains are

common in rounded, glass lined voids which comprise up to 30% of the area of these fine-grained zones. Two of these fine-grained zones have adjacent grains of interstitial clinopyroxene which have extinction positions identical to those of the prismatic crystals within the zones. This indicates that the fine-grained zones in this specimen are produced by the melting of interstitial clinopyroxenes.

The olivine of specimen 15009 has a Mg number of .897, intermediate between those of the lherzolite and granulite olivines, while the olivine of specimen 15011 has a Mg number of .868, identical to those of granulite olivines. The Cr/Cr + Al ratios of the spinels are .308 and .160 for specimens 15009 and 15011 respectively. In both cases their respective Mg numbers (.597 and .580) are considerably lower than those of the lherzolite spinels with similar chromium contents. The compositions of these spinels are such that large amounts of calculated ferric iron are required to achieve ideal stoichiometry (15009: 10.94 weight percent Fe_2O_3; 15011: 10.51 weight percent Fe_2O_3). These values are significantly larger than those typically calculated for the lherzolite spinels (av. = 5 weight percent Fe_2O_3). After these calculations the Mg numbers of these spinels increase markedly, with that of nodule 15009 (.735) resembling those of the lherzolite spinels and that of nodule 15011 (.705) resembling those of the granulite spinels (compare Figures 6-2 and 6-3). The higher Mg number of nodule 15009's spinels probably reflects the higher Mg number of its olivine (.897). Clinopyroxene in specimen 15009 has a low Na_2O content and is similar to that of the four phase, fresh lherzolites and iddingsitized lherzolites with red-brown spinel.

The high proportions of spinel and the low Mg numbers of both the olivine and spinel indicate that these dunites are not members of the lherzolite xenolith suites. The well developed compositional banding suggests that the dunites are cumulates. The ubiquitous deformational strain exhibited by the interstitial olivines and the evidence for partial melting in specimen 15011, however, imply that they are accidental to their host basanites. These dunite xenoliths are interpreted to be olivine rich end-members of the pyroxene granulite xenolith suite.

CHAPTER 8 ORIGIN AND SIGNIFICANCE OF THE NUNIVAK XENOLITHS

I Pressure-Temperature Estimations

Figure 8-1 represents an attempt to use the available experimental data and theoretical techniques to estimate the relative and absolute P-T histories recorded in the Nunivak xenoliths. The sources of the various experimental curves are listed in Table 8-1.

The minimum equilibrium temperature of each xenolith was calculated by a direct application of the Wood and Banno (1973) pyroxene geothermometer. A direct application of MacGregor's technique (1973) of correlating pressure with Al_2O_3 content of orthopyroxenes could not be used because the majority of the lherzolite xenoliths plotted in the garnet field. MacGregor (1973) suggests that 2 weight percent Al_2O_3 must be added to the observed aluminum content of orthopyroxenes in clinopyroxene saturated assemblages. Rather than apply this arbitrary scheme, a different approach was taken. The relative pressures of the Nunivak xenoliths were determined using MacGregor's Al_2O_3 isopleths for spinel assemblages (or their metastable extensions in the garnet field). The absolute pressure recorded by granulite nodule 12001 was then estimated from the experimental data on the stability of plagioclase and olivine assemblages (Kushiro and Yoder, 1966; Emslie, 1970; and Green and Hibberson, 1970). The absolute pressures of the other nodules were assigned by comparison with that of specimen 12001. The small temperature differences calculated for these nodules (Figure 8-1) require very accurate analyses. For example, an error of 0.15 weight percent in the

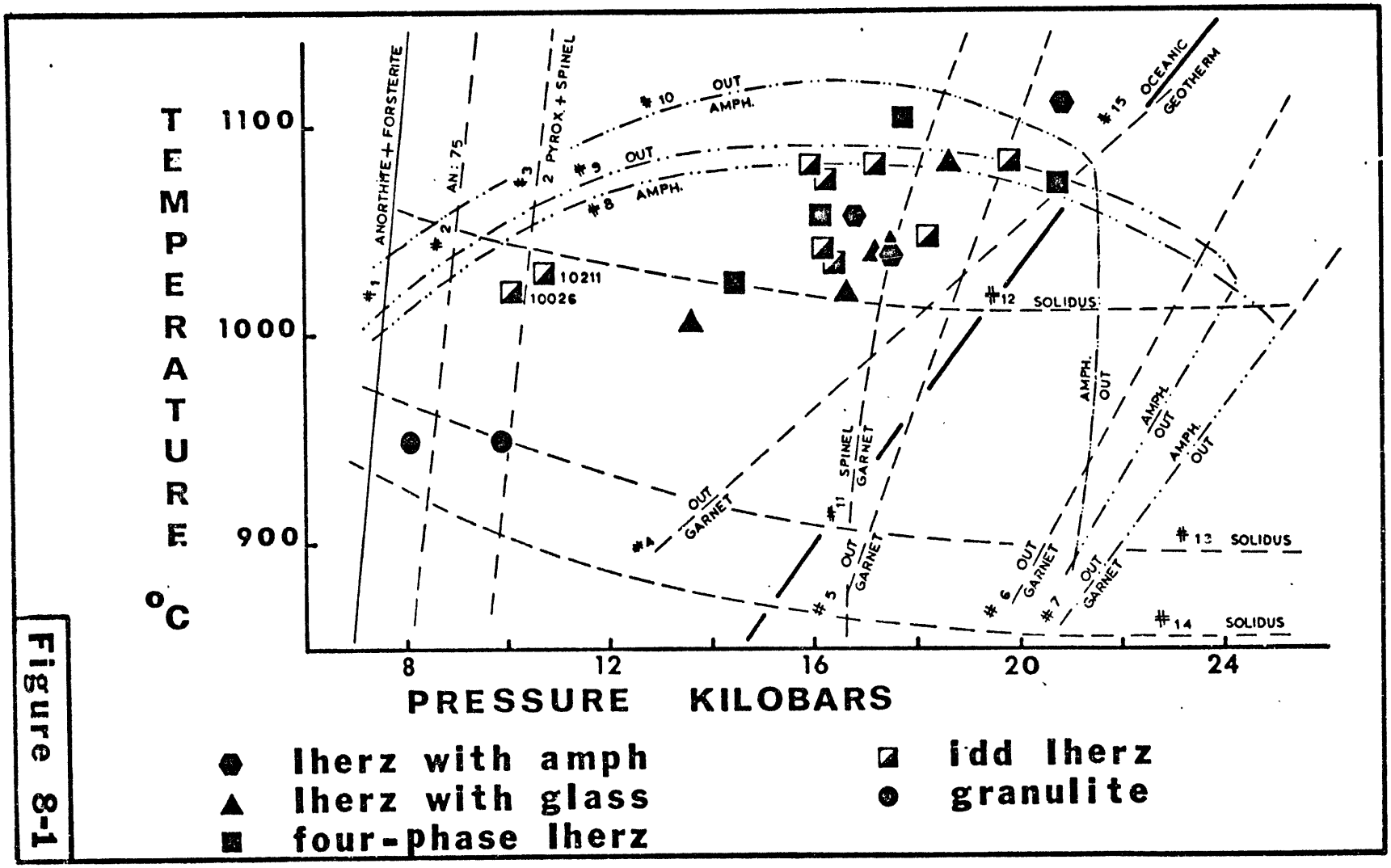
TEMPERATURE °C
1100
1000
900
8
12
16
20
24
PRESSURE KILOBARS
#1 ANORTHITE + FORSTERITE
AN: 75
#2
#3 2 PYROX + SPINEL
#10 OUT AMPH.
#9 OUT AMPH.
#8
#15 OCEANIC GEOTHERM
10211
10026
#12 SOLIDUS
#11 SPINEL OUT GARNET
#4 OUT GARNET
#5 OUT GARNET
#6 OUT GARNET
#7 OUT GARNET
AMPH. OUT
AMPH. OUT
AMPH. OUT
#13 SOLIDUS
#14 SOLIDUS
lherz with amph
lherz with glass
four-phase lherz
idd lherz
granulite

Figure 8-1

Table 8-1

Sources for Experimental and Theoretical Curves in Figure 8-1

1	Anorthite plus forsterite to 2 pyroxenes plus spinel; Kushiro and Yoder, 1966.
2	Plagioclase (An 73) plus olivine (Fo 73) to 2 pyroxenes plus spinel; Emslie, 1970.
3	Two pyroxenes plus spinel to plagioclase plus olivine; Green and Hibberson, 1970.
4 to 7	Garnet out curves for water saturated lherzolites; 66SAL-1, 66PAL-3, 618-138b.1, and Ga-p(1) respectively; Mysen, 1973.
8 to 10	Amphibole out curves for water saturated lherzolites; Ga-p(1), 618-138b.1, and 66PAL-3 respectively, Mysen, 1973.
11	Garnet lherzolite to spinel lherzolite; O'Hara, Richardson, and Wilson, 1971.
12	Wet spinel lherzolite solidus; Kushiro, Syono, and Akimoto, 1968.
13 and 14	Wet solidus curves for lherzolites Ga-p(1) and 618-138b.1 respectively; Mysen, 1973.
15	Oceanic geotherm; Ringwood, MacGregor, and Boyd, 1964.

MgO analysis of a typical orthopyroxene will result in a temperature shift of 10°C. Because of the positive P-T slope of MacGregor's Al_2O_3 isopleths, such a temperature error will in turn result in a significant error in the estimated pressure. An additional source of error is inherent in the assumption that MacGregor's experimental data can be applied to amphibole-bearing assemblages.

Despite these uncertainties, a number of important features can be recognized in Figure 8-1:

i. All xenoliths yield temperatures considerably higher than those predicted by conventional geotherms. In addition, the P-T slope defined by the lherzolite xenoliths is significantly shallower than that of any conventional geotherm.

ii. The majority of the lherzolite xenoliths fall close to the experimentally determined stability limits of both garnet and amphibole.

iii. The granulite nodules record the lowest temperatures and pressures.

iv. The iddingsitized lherzolites with aluminous spinels and tschermakitic pyroxenes record the shallowest depths in the lherzolite suite, just below those of the granulite xenoliths. There is, however, a large temperature discontinuity between the lherzolite xenoliths and the granulite xenoliths.

v. There is a slight tendency for the amphibole and glass-bearing lherzolites to record lower temperatures for a given pressure, or vice versa, than do the other lherzolites.

One feature which is not explicit in Figure 8-1, is that the iddingsitized and fresh, four phase lherzolites which overlap with the amphibole

and glass-bearing lherzolites in P-T space tend to contain more chromium-rich spinels and less aluminous orthopyroxenes than those which do not.

II Origin of the Amphibole Lherzolites

The conclusion has been reached, on the basis of chemical and textural arguments, that 50% of the fresh lherzolites contained amphibole prior to entrainment in basanitic magmas. The nature and origin of this amphibole must be understood before implications arising from the similarity of its composition to those of the Nunivak basalts can properly be evaluated.

Three alternatives for the origin of the Nunivak amphibole will be examined:

1. The amphibole is a primary, integral phase of a stable upper mantle assemblage containing olivine, orthopyroxene and clinopyroxene.
2. The amphibole is secondary, after primary spinel and clinopyroxene.
3. Both the amphibole and spinel are secondary phases produced by the decomposition of primary garnet.

a) Amphibole as a Primary Phase

The possibility that the amphibole is a primary phase in the upper mantle is an appealing concept. Not only would it provide a handy storage place for water, but the similarity of its Na/Na + K ratio to those of the Nunivak basalts could lead to a whole range of genetic speculations. There are a number of arguments which support a primary

origin for the amphibole:

i. The majority of the lherzolites plot in the experimentally determined P-T stability fields for amphibole in water saturated peridotites. In addition, the works of Holloway (1973) and Eggler (1974) indicate that these stability fields will expand to higher temperatures for water undersaturated conditions.

ii. Where amphibole is present, spinel does not occur as an interstitial phase. Rather, spinel, when present, occurs as intergrowths in the amphibole or as minor inclusions in other silicate phases.

iii. The clinopyroxenes of the amphibole lherzolites are distinct from those which characterize the spinel lherzolites (Chapter 6, sections Ia and IXb). These differences may reflect equilibrium with amphibole in one case and spinel in the other.

In a primary amphibole model, the lherzolites would originally have consisted solely of olivine, orthopyroxene, clinopyroxene, and amphibole. The spinel inclusions found in many of the amphiboles and at the center of the fine-grained, glass-bearing zones would have originated in part by exsolution from the amphibole and in part by the incongruent melting of the amphibole after it was incorporated into its host basalt. There are, however, a number of serious problems with such a model:

i. The occasional subhedral habit of some of the amphibole grains and pseudomorphic outline of a few of the fine-grained, glass-bearing zones are inconsistent with the granular, metamorphic texture exhibited by the other lherzolite phases.

ii. Calculations (Chapter 6, section VIIIf) have shown that the amphibole compositions can be accounted for by the phases of the fine-grained, glass-bearing zones without considering the relict spinels. In support of this observation, both Best (1974) and Varne (1970) have described the partial melting of chromium-bearing amphibole to produce fine-grained zones of glass with euhedral pyroxene, olivine and spinel. No relict spinel is reported. These considerations require that the relict spinels of the fine-grained, glass-bearing zones were not produced by the incongruent melting, but were present as inclusions in the original amphibole.

iii. Because of the preceding argument, one must conclude that the chemical zoning documented in the relict spinels (Chapter 6, section IVc) predates the melting of the amphibole. This conclusion is supported by the occurrence of zoning in the unmelted amphibole and its enclosed spinel in specimen 10016. This chemical zoning could not survive for any length of time under the P-T conditions of the upper mantle. Thus the spinel-amphibole intergrowths must be a relatively recent phenomena.

iv. The large modal proportions of relict spinel in a few fine-grained, glass-bearing zones are incompatible with its origin by incongruent melting or exsolution from amphibole.

b) Amphibole after Spinel

The second alternative, namely that the amphibole is secondary after spinel, is particularly attractive because it is the only one of the three hypotheses which provides an explanation for the chemical zoning observed in the amphibole and its enclosed spinel. The formation of amphibole

about spinel should selectively remove aluminum. As the process continues, the amphibole would be forced to incorporate more chromium into its structure. The end result would be that which is in fact observed; amphibole becoming increasingly chromium-rich towards its included spinel which in turn would exhibit chromium-rich borders and aluminous cores. The more complete the replacement process, the more chromium-rich the spinel.

A replacement model is consistent with:

i. The presence of spinel inclusions in anhydrous silicates of the amphibole lherzolites which are significantly more aluminous than the spinel associated with the amphibole (Chapter 6, section IVd).

ii. The subhedral morphology of some of the amphibole grains and the embayed and vesicular appearance of the spinel inclusions in amphibole and the relict spinels in the fine-grained, glass-bearing zones.

iii. The large modal proportions of relict spinel found in a few of the fine-grained, glass-bearing zones.

iv. The lack of distinction between the P-T conditions determined for the amphibole lherzolites and the chromium-rich, four phase lherzolites. Conquéré (1971) has described spinel lherzolite near Ariège, France which contains local pockets of secondary(?) amphibole lherzolite. The development of the amphibole apparently depends on access to volatiles.

Griffin (1973) has described a suite of lherzolites from the Fen alkaline complex, Norway, in which amphibole is found surrounding embayed grains of spinel. The spinel is chemically zoned with chromium-rich margins and, according to Griffin's interpretation, is being replaced by

the amphibole. Though the textural relationships of this occurrence sound remarkably similar to those observed in the Nunivak lherzolites, there are some differences. The phases of the Norwegian lherzolites are considerably more aluminous than those of their Nunivak equivalents. The spinels are olive green in color and run only 8 to 14 weight percent Cr_2O_3. The associated pyroxenes exhibit high degrees of tschermakitic substitution. In total, the Norwegian lherzolites resemble those at the aluminous-end of the iddingsitized lherzolite suite of Nunivak Island. As we shall see in a later section, aluminous lherzolites of this type are probably derived from considerably shallower depths than the Nunivak amphibole lherzolites.

Best (1974) interprets Cr-pargasites in xenoliths from the western Grand Canyon to be secondary after spinel. He proposes the reaction; chromian spinel + diopside + fluid → amphibole. The "mineral distribution program" of Wright and Doherty (1970) was used to evaluate this reaction as a mechanism for the formation of the Nunivak amphiboles. The initial assumption required concerns the composition of the elusive fluid phase. For simplicity, the model fluid was assumed to consist solely of Na, K, and water. Trial solutions for Best's reaction yielded unacceptibly large total residuals (> 9 weight percent), with the calculated amphiboles typically containing more than 5 weight percent excess CaO. A more complex fluid composition might, of course, produce a better fit. The inclusion of orthopyroxene as one of the reactants, however, improves the results significantly. The following two reactions represent the best solutions obtained:

i. Specimen 10016

Fluid (Na/Na + K = .863) + 71 Spinel (Cr/Cr + Al = .376) + 28 Orthopyroxene + 54 Cliropyroxene → 57 Spinel (Cr/Cr + Al + .465) + 100 Amphibole (Cr_2O_3 = 2.19 weight percent)

$$\sum_{\text{oxides}} |\text{residuals}| = 4.58 \text{ weight percent}$$

ii Specimen 10013

Fluid (Na/Na + K = .721) + 39 Spinel (Cr/Cr + Al = .288) + 19 Orthopyroxene + 61 Clinopyroxene → 23 Spinel (Cr/Cr + Al = .435) + 100 Amphibole (Cr_2O_3 = 2.85 weight percent)

$$\sum_{\text{oxides}} |\text{residuals}| = 7.24 \text{ weight percent}$$

In both solutions excess MgO and CaO in the calculated amphiboles contribute approximately 3 percent of the total residuals. Individual residuals for the other oxides do not exceed 1 weight percent.

If the hypothesis that the Nunivak amphibole is secondary, replacing spinel, is correct, then one is forced to conclude that a recent, pervasive amphibolization event has occurred in the upper mantle. Such an event might resemble the light element metasomatism model proposed by Loyd and Bailey (1973), the upward migration of aqueous, alkalic magmas from the low velocity zone proposed by Wilshire (1971), or the introduction of a migratory, highly undersaturated liquid, enriched in the incompatible elements, proposed by Frey and Green (1974). The amphiboles usually attributed to such processes, however, are characteristically

titanium and iron-rich: Dish Hill, California (Wilshire, 1971); St. Peter and St. Paul Rocks (Melson et al., 1967); and possibly Ariège, France (Conquéré, 1971). The interstitial amphibole of the Victorian lherzolites (Frey and Green, 1974) does, however, resemble the composition of the Nunivak amphibole (compare Tables 6-6 and 6-7). Because of their low titianium and iron contents, the Nunivak amphiboles are unlikely to have been produced by the direct action of a basanitic fluid. Wilshire (1971) has documented the conversion of interstitial pargasite to titianiferrous kaersutite by reaction with basanite.

The preceding discussion has emphasized the textural and chemical arguments supporting a secondary origin for the Nunivak amphibole. There are, however, problems with this hypothesis:

i. The reactions which best model the replacement of spinel by amphibole consume large quantities of clinopyroxene and orthopyroxene, yet there is no apparent deficiency of these phases in the amphibole lherzolites.

ii. The distinctive jadeite-rich character of many of the amphibole lherzolite clinopyroxenes cannot be explained by a replacement model.

iii. An amphibole lherzolite collected on a return trip to Nunivak Island contains both amphibole and interstitial spinel which are not texturally related.

c) Amphibole after Garnet

The third alternative for the origin of the Nunivak amphibole lherzolites involves the recrystallization of primary garnet lherzolites in a hydrous environment. One of the main advantages of this model is

that the clinopyroxenes of garnet lherzolites, like those of the Nunivak amphibole lherzolites, are characterized by high ratios of octahedral aluminum to tetrahedral aluminum. Boyd (1971) has attributed intergrowths of spinel and Cr-pargasite in harzburgites from the Wesselton and Monastery (Smith, 1973) kimberlite pipes of South Africa to the reaction of garnet and clinopyroxene. The amphibole and spinel in these xenoliths and their counterparts in the Nunivak suite are nearly identical in composition (Table 6-6, Figures 6-3 and 6-11). In addition to the absence of clinopyroxene in the harzburgites, however, there are a number of differences between the spinel-amphibole assemblages of the kimberlite and Nunivak nodules. In the harzburgites, the intergrowths are described as "finger print" symplectites (Smith, 1973), while in the Nunivak examples the spinel is present as embayed and vesicular, core inclusions in amphibole. No chemical zoning has been reported in the amphibole or spinel of the kimberlite xenoliths.

The Nunivak amphibole occurrence may more closely resemble the amphibole-spinel assemblages which are commonly found in the kelyphite reaction rims developed about garnets in eclogites and kimberlites (Holmes, 1936; Kushiro and Aoki, 1968). Haggerty (1973) has made obscure reference to skeletal grains of Cr-spinel in these kelyphite rims which commonly exhibit complex zoning patterns. The significance of these kimberlite features to the Nunivak amphibole-spinel occurrence is difficult to evaluate because of the lack of detailed studies on the former.

The "mineral distribution program" of Wright and Doherty (1970) was used to evaluate the reaction proposed by Boyd (1971) for the formation of spinel and amphibole from garnet, clinopyroxene, and fluid. The

parent garnet was specified in terms of the end-members; pyrope, almandine, grossularite, spessartite, and knorringite; whose relative proportions were to be determined by the computer program. The fluid involved in the reaction was assumed to consist solely of Na, K, and water. Probe analyses were used for the compositions of the clinopyroxene, amphibole and spinel. Excellent solutions were obtained using the above model for three of the amphibole lherzolites:

i. Specimen 10016

Fluid (Na/Na + K = .864) + 67 Garnet + 35 Clinopyroxene → 7 Spinel (Cr/Cr + Al = .585) + 100 Amphibole (Cr_2O_3 = 2.55 weight percent)

$$\sum_{\text{oxides}} |\text{residuals}| = 2.17 \text{ weight percent}$$

ii. Specimen 10013

Fluid (Na/Na + K = .763) + 66 Garnet + 32 Clinopyroxene → 3 Spinel (Cr/Cr + Al = .435) + 100 Amphibole (Cr_2O_3 = 2.85 weight percent)

$$\sum_{\text{oxides}} |\text{residuals}| = 2.77 \text{ weight percent}$$

iii. Specimen 10006

Fluid (Na/Na + K = .880) + 79 Garnet + 26 Clinopyroxene → 10 Spinel (Cr/Cr + Al = .585) + 100 Amphibole (Cr_2O_3 = 3.24 weight percent)

$$\sum_{\text{oxides}} |\text{residuals}| = 1.44 \text{ weight percent}$$

No oxide has a residual greater than 0.4 weight percent and the majority

of the individual oxide residuals are less than 0.2 weight percent. The garnet compositions calculated in these solutions are listed in Table 8-2 with selected compositions of chromium-bearing garnets from garnet lherzolites described in the literature. The CaO contents of the calculated garnets fall within the range (4 to 7 weight percent) of those characteristic of chromium-bearing garnets in lherzolite assemblages (Sobolev, 1973). The similarity between the calculated and observed garnet compositions is striking.

At this point it is of interest to speculate on the possible mechanisms of the proposed transition from garnet lherzolite to spinel lherzolite. The estimated equilibrium conditions for the amphibole lherzolites lie close to the experimentally determined upper stability limits of garnet lherzolite in water saturated systems (Figure 8-1). The general positive slopes of the garnet-out curves suggest a thermal mechanism for the breakdown of garnet lherzolite. If the upper mantle originally supported a geothermal gradient similar to that predicted by conventional geotherms, then, for their estimated depths, the amphibole lherzolites would lie within the stability field of garnet lherzolite. Accordingly much of the upper mantle would have been garnet lherzolite. The initiation of igneous activity in the upper mantle beneath Nunivak Island would be proceeded by rising temperatures and the introduction of volatiles. The result of this isobaric temperature increase would be the formation of amphibole at the expense of garnet and clinopyroxene. Eventually fragments of this amphibolized upper mantle material would be entrained in the basanitic magmas and reach the surface as partially melted, lherzolite xenoliths. According to this model the source of the

TABLE 8-2

CHROMIUM-BEARING GARNETS

	CALCULATED GARNETS **			SELECTED GARNET ANALYSES			
SPEC.	10006	10016	10013	1573	LBM 11	UD-5	UD-3
SIO2	41.41	41.79	41.85	41.20	41.95	41.68	41.75
TIO2	0.00	0.00	0.00	0.05	0.13	0.80	0.16
AL203	17.04	18.08	19.76	17.60	19.71	16.58	19.66
FE203	0.00	0.00	0.00	0.00	0.00	2.30	1.99
CR203	9.50	8.28	5.82	8.30	5.38	7.15	5.07
FEO	5.69	5.65	5.82	6.50	7.26	5.39	5.82
MGO	20.31	21.72	20.11	17.90	20.47	20.40	19.24
MNO	0.39	0.51	0.51	0.50	0.35	0.27	0.38
CAO	5.66	3.97	6.14	7.70	5.24	5.90	5.68
NA20	0.00	0.00	0.00	0.05	0.00	0.00	0.00
K20	0.00	0.00	0.00	0.00	0.00	0.00	0.00
TOTAL	100.00	100.00	100.01	99.80	100.49	100.47	99.75
FORMULA UNITS ASSUMING 12 OXYGENS							
SI	3.000	3.000	3.000	3.010	3.000	3.006	3.005
TI	0.000	0.000	0.000	0.003	0.007	0.043	0.009
AL	1.455	1.530	1.670	1.515	1.661	1.409	1.668
FE3+	0.000	0.000	0.000	0.000	0.000	0.125	0.108
CR	0.544	0.470	0.330	0.479	0.304	0.408	0.289
FE2+	0.345	0.339	0.349	0.397	0.434	0.325	0.350
MG	2.193	2.324	2.149	1.949	2.182	2.193	2.064
MN	0.024	0.031	0.031	0.031	0.021	0.016	0.023
CA	0.439	0.305	0.472	0.603	0.401	0.456	0.438
NA	0.000	0.000	0.000	0.007	0.000	0.000	0.000
K	0.000	0.000	0.000	0.000	0.000	0.000	0.000
TOTAL	8.000	8.000	8.000	7.994	8.011	7.980	7.954
MG/MG+FE	0.864	0.873	0.860	0.831	0.834	0.871	0.855
CR/CR+AL	0.272	0.235	0.165	0.240	0.155	0.224	0.147
				BOYD	GURNEY	SOBOLEV	

UNLESS OTHERWISE SPECIFIED; TOTAL IRON AS FEO

basanites and the volatiles which preceded them would be significantly deeper than the source of the xenoliths, probably the low velocity layer.

There are, however, a number of difficulties with a garnet parent model for the Nunivak amphiboles:

i. There appears to be little significant difference between the P-T conditions estimated for the amphibole lherzolites and the chromium-rich, four phase lherzolites (both iddingsitized and fresh). This may be in part due to the inability of the geothermometer used, or the analytical precision, to differentiate the small temperature differences involved. In addition, Mysen (1973) has demonstrated that the transition from garnet to spinel lherzolite is very sensitive to bulk composition. Compositional layering in the upper mantle may have supported intercalated layers of garnet and spinel lherzolite.

ii. The chemical zoning exhibited by the amphibole and its included spinel is contrary to what one might predict. The experimental work of MacGregor (1971) indicates that the first spinel to be produced by the breakdown of garnet should be relatively enriched in chromium. This would result in spinels zoned from chromium-rich cores to aluminous rims; opposite to what is observed.

In summary, of the three proposed origins for the Nunivak amphiboles, the first seems the least likely. The choice between the last two hypotheses; i.e., whether the amphibole is secondary after spinel or garnet; is difficult. The strongest arguments for the former are the textural relationships and chemical zoning of the relict spinels, while the latter is supported by the jadeitic nature of the amphibole lherzolite clinopyroxenes and the fact that the proposed conversion reaction

better accounts for the chemistry of the phases while consuming significantly less clinopyroxene.

III Nature of the Source Regions

a) Lherzolites and the Upper Mantle

One prime interest of ultramafic xenoliths is the possibility that they retain information about the upper mantle. At the end of Chapter 6, the lherzolite xenoliths were concluded to be metamorphic assemblages derived from the upper mantle. The slope of the P-T curve defined by the locus of the lherzolite nodules is considerably less, however, than that of conventional, calculated geotherms (Figure 8-1) and is, in fact, less than that of MacGregor's (1973) Al_2O_3 isopleths for orthopyroxene coexisting with spinel and olivine. The validity of this observation is supported by the close approximation of the lherzolite spinel compositions to that predicted by a theoretical isotherm (Chapter 6, section IVb). This leads to the remarkable conclusion that the Al_2O_3 content of orthopyroxene is inversely proportional to depth of origin. The conclusion is the reverse of what would be predicted for lherzolite assemblages constrained to a conventional geotherm (Ringwood et al., 1964) whose P-T slope is greater than that of MacGregor's Al_2O_3 isopleths. If the lherzolites in Figure 8-1 were labeled with the Al_2O_3 content of their orthopyroxenes, one would see that the foregoing conclusion would be upheld in general, but that the decrease of Al_2O_3 with estimated depth would not be monotonic. Because of the sensitivity of pressure estimates to small errors in the calculated temperatures, however, the alumina

content of orthopyroxene by itself may be a more reliable measure of the relative depths of the Nunivak lherzolites.

If the preceding observations are correct, then the chemical variations in the lherzolite phase chemistry illustrated in Figures 6-14 and 6-15 may represent vertical zoning in the upper mantle in response to increasing pressure and changing bulk composition with depth. This proposed gradient in bulk composition may reflect the accumulated effects of past episodes of partial melting and light element metasomatism. On a more speculative level, the correlation between the lherzolite phase chemistry and the alumina content of their orthopyroxenes can be used to construct a model for the upper mantle beneath Nunivak Island immediately prior to the eruption of the alkalic magmas. Figure 8-2 is a cartoon which illustrates such a model. At the base of the crust (≃ 30 km.) the mantle would consist of lherzolite material characterized by aluminous spinels and Na-rich, tschermakitic pyroxenes. With increasing depth, the spinels become more chromic while the pyroxenes become less tschermakitic. The Na, Al, and Ti contents of the clinopyroxenes decrease as they approach an endiopside composition. There is a concomitant increase in the Mg numbers of all the lherzolite phases except spinel.

At some depth (40 to 50 km.) horizons of amphibole-bearing lherzolite appear. The clinopyroxenes of this assemblage are relatively enriched in jadeite, but poor in calcium tschermak component. Intercalated with the amphibole lherzolite are horizons of spinel lherzolite. This assemblage would be continuous with its counterpart above the amphibole-bearing horizons, with its spinel becoming even more chromium-rich with depth. The clinopyroxene of the spinel lherzolite would contain slightly

more calcium tschermak component than adjacent amphibole lherzolite clinopyroxene, but little or no jadeite. The reason for the persistence of spinel lherzolite horizons after the appearance of amphibole would depend on the origin of the amphibole. If the amphibole formed by the replacement of spinel, then the problem may simply be one of access to volatiles. On the other hand, the amphibole lherzolites may represent former garnet lherzolite. The works of Mysen (1973) and MacGregor (1970) indicate that the transition from spinel lherzolite to garnet lherzolite is very sensitive to bulk composition. The amphibole-bearing horizons may represent material whose composition was such that garnet was stable and vice versa for the adjacent spinel lherzolite horizons. In either case the amphibole is a relatively recent phenomena and reflects the wide scale introduction of fluids in the upper mantle.

b) Dunites and Pyroxene Granulites and the Lower Crust

The dunite and pyroxene granulite nodules of Chapter 7 were concluded to be cumulates which are accidental to their alkalic basalts. The primary mineralogy of the granulites is interpreted to consist of feldspar and olivine with lesser amounts of clinopyroxene and spinel. The original rock types range from feldspathic dunite through troctolite to gabbro, depending on the relative proportions of these primary phases. The P-T relationships of these primary rock types cannot be determined because of the absence of quantitative petrogenetic indicators in their primary mineralogy. There is a striking similarity, however, between the primary rock types of this xenolith suite and those which characterize the transition zone of alpine ophiolite complexes (Church, 1972; Dewey and

Bird, 1971). In particular, the interbanded dunites, feldspathic dunites, troctolites, and gabbros of the "Critical Zone" in the Bay of Islands complex (Smith, 1958) are all represented in the Nunivak xenolith suite. Malpas (1974) has placed his "Petrological Moho" at the gradation between the basal, 350 foot, dunite layer of this "Critical Zone" and the interbedded harzburgites and dunites below. Although the crust beneath the Bering Sea shelf is not oceanic, it appears reasonable to conclude that the dunite-granulite xenolith suite may represent an analogous transition zone beneath Nunivak Island. The mineralogy of the corona structures indicates that this zone is located at an approximate depth of 30 km.

According to the foregoing interpretation, the Mohorovicic discontinuity beneath Nunivak Island would correspond to a transition from aluminous spinel lherzolite to a cumulate, chromite-rich dunite. With decreasing depth, interbedded layers of what were originally feldspathic dunite and troctolite would appear and become increasingly abundant. These rock types would eventually grade into overlying gabbros (Figure 8-2). The thickness of this hypothetical transition zone is uncertain, but its counterpart in the Bay of Islands has an approximate thickness of 1 mile (Smith, 1958).

The development of the corona structures between olivine and plagioclase may reflect increasing pressure or isobaric cooling. There has been some debate as to whether the P-T slope of the olivine-plagioclase reaction curve is small enough to permit the later mechanism in a geologic setting (Gardner and Robbins, 1974). Students of corona structures in deep seated anorthosite bodies, however, argue that the field

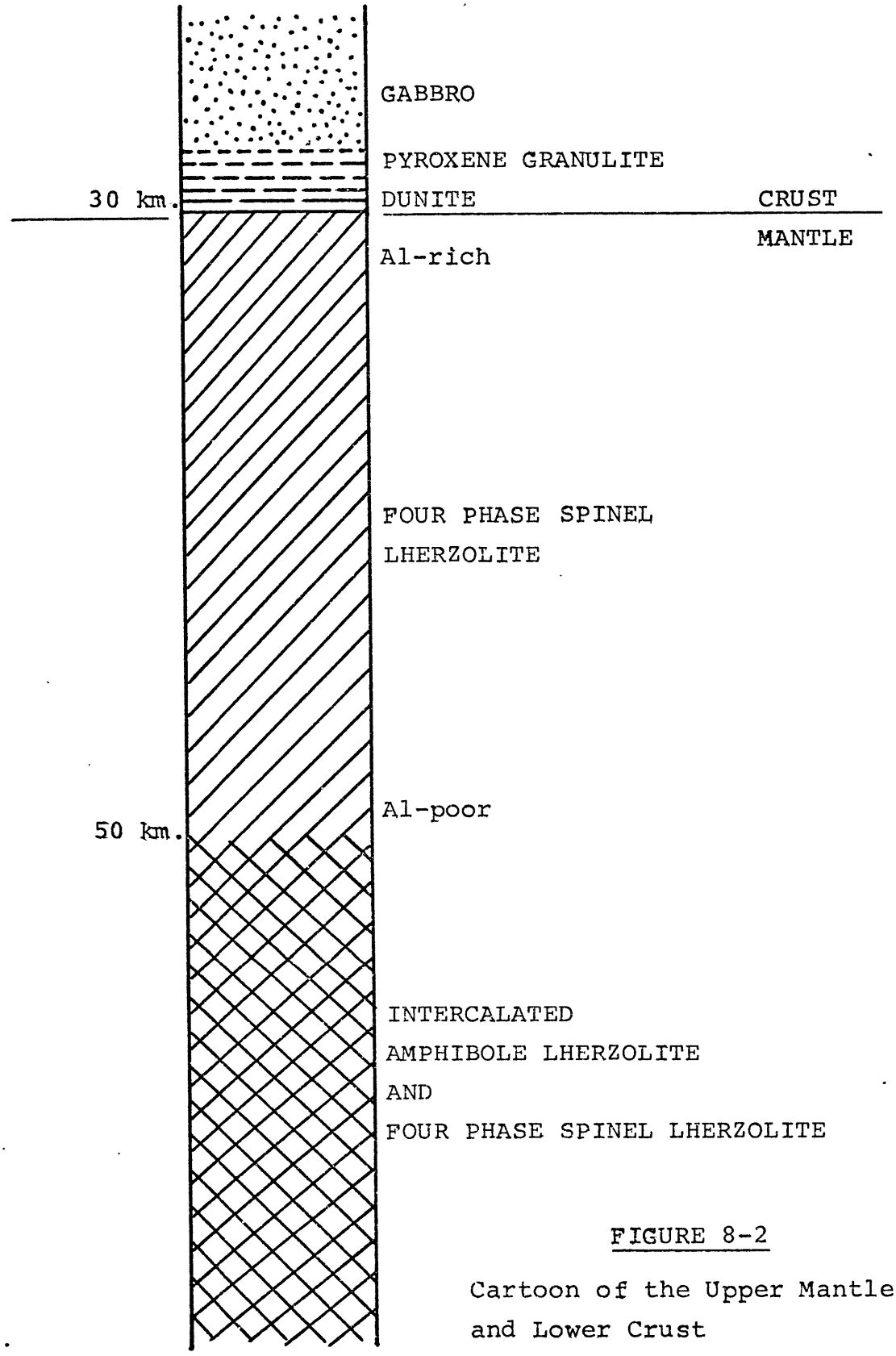

FIGURE 8-2

Cartoon of the Upper Mantle and Lower Crust

relations usually support the isobaric cooling mechanism (Griffin, 1973, 1971, 1969; Gardner and Robbins, 1974; Whitney and McLelland, 1973). The absence of deformation in the Nunivak coronas and the large differences between the estimated temperatures of the pyroxene granulites and the aluminous lherzolites 10025 and 10211 (Figure 8-1) support an isobaric cooling model. However, a gradual thickening of the crust accompanying the accumulation of sediments on the Bering Sea shelf could be proposed as a mechanism for a pressure increase. In the absence of field relations, neither of these models can be eliminated.

IV Concluding Statement

The most significant finding of this thesis is the evidence for Cr-bearing, interstitial amphibole in 50% of the fresh lherzolite xenoliths. This amphibole is believed to be secondary, the product of a pervasive metasomatic event in the upper mantle. The remarkable similarity of the Na/Na + K ratios of the basalts and amphiboles implies that the fluids which formed the latter are genetically related to the basalts. However, the textural relations require that the amphibole predates the alkalic basalts and the composition of the amphiboles precludes its formation by the direct interaction of alkalic basalt and lherzolite. The metasomatic fluids and basalts may have a common source in the low velocity zone. According to this interpretation the upward migration of basalts was preceded by the infiltration of alkali-rich fluids and the development of interstitial amphibole in the upper mantle. The comments about the

nature of the upper mantle and the lower crust in the preceding section are intended as a speculative interpretation of the available data rather than a rigid model. They are presented in the belief that a report of observations without speculation is an insult to the scientific curiosity of both the reader and the author.

BIBLIOGRAPHY

Albee A.L. and Ray L. (1970) "Correction Factors for Electron Probe Microanalysis of Silicates, Oxides, Carbonates, Phosphates, and Sulphates", Anal. Chem. 42:1408-1414.

Allen J.C., et al. (1972) "The Role of Water in the Mantle of the Earth: The Stability of Amphiboles and Micas", 24th Inter. Geol. Congress, Section 2, Petrology, 231-240.

Aoki K. (1968) "Petrogenesis of Ultrabasic and Basic Inclusions in Alkali Basalts, Iki Island, Japan", Amer. Min. 53:241-256.

_____ (1971) "Petrology of Mafic Inclusions from Itinome-gata, Japan", Contr. Min. Petrol. 30:314-331.

Aoki K. and Kushiro I. (1968) "Some Clinopyroxenes from Ultramafic Inclusions in Dreiser Weiher, Eifel", Contr. Min. Petrol. 18:326-337.

Aoki K. and Shiba I. (1973) "Pargasites in Lherzolite and Websterite Inclusions from Itinome-gata, Japan", J. Japan Assoc. Min. Pet. Econ. Geol. 68:303-310.

_____ (1973) "Pyroxenes from Lherzolite Inclusions of Itinome-gata, Japan", Lithos 6:41-51.

Baker I. and Haggerty S.E. (1967) "The Alteration of Olivine in Basalts and Associated Lavas", Contr. Min. Petrol. 16:233-273.

Barth T.F.W. (1956) "Geology and Petrology of the Pribilof Islands, Alaska", USGS Bull. 1028-F:160.

Best M.G. (1974) "Mantle-Derived Amphibole Within Inclusions in Alkalic-Basaltic Lavas", J. Geophys. Res. 79:2107-2113.

Birks L.S. (1971) Electron Probe Microanalysis, p. 190.

Borley G.D., et al. (1971) "Some Xenoliths from the Alkalic Rocks of Tenriffe, Canary Islands", Contr. Min. Petrol. 31:102-114.

Boullier A.M. and Nicolas A. (1973) "Textures and Fabrics of Peridotite Nodules from Kimberlite at Mothae, Thaba Putsoa and Kimberley", Int. Conf. Kimberlites, 43-49.

Boyd F.R. (1971) "Pargasite-Spinel Peridotite Xenolith from the Wesselton Mine", Carnegie Inst. Wash. Yearb. 70:138-142.

Boyd F.R. and Nixon P. (1972) "Ultramafic Nodules from the Thaba Putsoa Kimberlite Pipe", Ann. Report Director Geophys Lab 1971-72, 362-373.

Boyd F.R. and Nixon P.H. (1973) "Structure of the Upper Mantle Beneath Lesotho", Carnegie Inst. Wash. Yearb. 72:431-445.

Burk C.A. (1965) "The Geology of the Alaska Peninsula-Island Arc and Continental Margin", G.S.A. Mem. 99:245.

Carswell D.A. (1973) "Primary and Secondary Phlogopites and Clinopyroxenes in Garnet Lherzolite Xenoliths", Int. Conf. Kimberlites, 59-62.

Carter J.L. (1970) "Mineralogy and Chemistry of the Earth's Upper Mantle Based on Partial Fusion-Partial Crystallization Model", G.S.A. Bull. 81:2021-2034.

Chayes F. (1972) "Silica Saturation in Cenozoic Basalts", Phil. Trans. Roy. Soc. Lond. series A 271, 285-296.

Church W.R. (1972) "Ophiolite: its Definition, Origin as Oceanic Crust, and Mode of Emplacement in Orogenic Belts, with Special References to the Applachians", The Ancient Oceanic Lithosphere, Publns. Earth Phys. Br., Can. 42:71-85.

Coats R.R. (1962) "Magma Type and Crustal Structure in the Aleutian Arc", The Crust of the Pacific Basin, Amer. Geophys. Union Mono. 6:92-109.

Conquéré F. (1971) "La Lherzolite a Amphibole du Gisement de Cassou (Ariège, France)", Contr. Min. Petrol. 30:296-313.

Davis B.T.C. and Boyd F.R. (1966) "The join $Mg_2Si_2O_6$-$CaMgSi_2O_6$ at 30 kb. Pressure and its Application to Pyroxenes from Kimberlites", J. Geophys. Res. 71:3567-3576.

Dawson J.B. and Smith J.V. (1973) "Alkaline Pyroxenite Xenoliths from the Lashaine Volcano, Northern Tanzania", J. Petrol. 14:113-133.

Deer W.A., Howie R.A. and Zussman J. (1964) Rock Forming Minerals, Longmans.

Dewey J.F. and Bird J.M. (1971) "Origin and Emplacement of the Ophiolite Suite: Applachian Ophiolites in Newfoundland", J. Geophysics Res. 76: 3179-3206.

Dickey J.S. (1970) "Partial Fusion Products in Alpine-Type Peridotites: Serrania de la Ronda and other Examples", Min. Soc. Amer. Spec. Paper 3.

Dickey J.S. and Yoder H.S. (1972) "Partitioning of Chromium and Aluminum between Clinopyroxene and Spinel", Carnegie Inst. Wash. Yearb. 71:384-392.

Eggler D.H. (1972b) "Amphibole Stability in H_2O-Undersaturated Calc-Alkaline Melts", Earth Planet. Sci. Lett. 15:28-34.

_____ (1973) "Principles of Melting of Hydrous Phases in Silicate Melt", Carnegie Inst. Wash. Yearb. 72:491-495.

Emslie R.F. (1970) "Upper P-T Stability of a Natural Olivine-Plagioclase Assemblage", Carnegie Inst. Wash. Yearb. 69:154-155.

Erlank A.J. (1973) "Kimberlite Potassic Richterite and the Distribution of Potassium in the Upper Mantle", Int. Conf. Kimberlites, 103-106.

Ewing M. et al. (1965) "Oceanic Structural History of the Bering Sea", J. Geophys. Res. 70:4593-4600.

Finger L.W. and Hadidiacos C.G. "Electron Microprobe Automation", Carnegie Inst. Wash. Yearb. 71:578-600.

Forbes R.B. and Kuno H. (1965) "The Regional Petrology of Peridotite Inclusions and Basaltic Host Rocks", The Upper Mantle Symposium, New Delhi, 1964, Internat. Union Geol. Sci. (Copenhagen), 161-179.

Forbes W.C. and Starmer R.J. (1974) "Kaersutite is a Possible Source of Alkali Olivine Basalt", Nature 250:209-210.

Frey F.A. and Green D.H. (1974) "The Mineraolgy and Origin of Lherzolite Inclusions in Victorian Basanites", Geochimica Cosmochimica Acta 38, in press.

Green D.H. and Hibberson W. (1970) "The Instability of Plagioclase in Peridotite at High Pressure", Lithos 3:209-231.

Green D.H. and Ringwood A.E. (1967) "The Genesis of Basaltic Magmas", Contr. Min. Petrol. 15:103-190.

_____ (1967) "An Experimental Investigation of the Gabbro to Eclogite Transformation and its Petrologic Applications", Geochim. Cosmochim. Acta. 31:767-833.

_____ (1970) "Mineralogy of Peridotitic Compositions under Upper Mantle Conditions", Phys. Earth Planet. Int. 3:151-160.

Griffin W.L. (1971) "Genesis of Coronas in Anorthosite of the Upper Jatun Nappe, Indre Sogn, Norway", J. Petrol. 12:219-243.

_____ (1973) "Lherzolite Nodules from the Fen Alkaline Complex, Norway", Contr. Min. Petrol. 38:135-146.

Griffin W.L. and Heier K.S. (1973) "Petrologic Implications of some Corona Structures", Lithos 6:315-335.

Grow J.A. and Atwater T. (1970) "Mid-Tertiary Tectonic Transition in the Aleutian Arc", G.S.A. Bull. 81:3715-3722.

Gurney J.J. and Switzer G.S. (1973) "The Discovery of Garnets Closely Related to Diamonds in Finsch Pipe, South Africa", Contr. Min. Petrol. 39:103-116.

Haggerty S.E. (1973) "The Chemistry and Genesis of Opaque Minerals in Kimberlites", Int. Conf. Kimberlites, 147-149.

Henson B.J. (1973) "Pyroxenes and Garnets as Geothermometers and Barometers", Ann. Report Director Geophys. Lab., 527,534.

Hoare J.M. (1961) "Geology and Tectonic Setting of the Lower Kuskokwim-Bristol Bay Region, Alaska", Amer. Assoc. Petrol. Geol. 45:594-611.

Hoare J.M. and Condon W.H. (1966) "Nanwaksjiak Explosion Crater, Nunivak Island, Alaska", unpublished talk, G.S.A. Cord. Sec. meeting, Tuscon, Arizona.

_____ (1968) "Occurrence and Origin of Eclogite and Peridotite Inclusions in Volcanic Rocks of Nunivak Island, Alaska", G.S.A. Spec. Paper 101, 311, abst.

Hoare J.M., et al. (1968) "Geology, Paleomegnetism and Potassium-Argon Ages of Basalts from Nunivak Island, Alaska", G.S.A. Mem. 116:377-412.

Hoare J.M. and Kuno H. (1968) "Occurrence of Olivine Eclogite in Volcanic Ash of Nanwaksjiak Crater, Nunivak Island, Alaska", G.S.A. Spec. Paper 101, 94, abst.

Holloway J.R. (1973) "The System Pargasite-H_2O-CO_2: A Model for Melting of a Hydrous Mineral with a Mixed-Volatile Fluid, Experimental Results to 8 kb.", Geochim. Cosmochim. Acta 37:651-666.

Holmes A. (1937) "A Contribution to the Petrology of Kimberlite and its Inclusions", Trans. Geol. Soc. S. Africa 39:379-428.

Hopkins D.M. (1963) "Geology of the Imeruk Lake Area, Seward Pen., Alaska", U.S.G.S. Bull. 1141-C, C1-C101.

Irvine T.N. (1965) "Chromian Spinel as a Petrogenetic Indicator: Part 1, Theory", Can. J. Earth Sci. 2:648-672.

_____ (1967) "Chromian Spinel as a Petrogenetic Indicator: Part 2, Petrologic Implications", Can. J. Earth Sci 4:71-103.

Irvine T.N. and Smith C.H. (1969) "Primary Oxide Minerals in the Layered Series of the Muskox Intrusion", Magmatic Ore Deposits, Econ. Geol. Mono. 4:76-95.

Irving A.J. (1974) "Pyroxene-Rich Ultramafic Xenoliths in the Newer Basalts of Victoria, Australia", Neues. Jb. Miner. Abs. 120:147-167.

Ito K. and Kennedy G.C. (1967) "Melting and Phase Relations in a Natural Peridotite to 40 kb", Amer. Jour. Sci. 265:519-538.

_____ (1970) "Melting and Phase Relations in the Plane Tholeiite-Lherzolite-Nepheline Basanite to 40 kb. with Geologic Implications", Contr. Min. Petrol. 19:177-211.

_____ (1970) "The Fine Structure of the Basalt-Eclogite Transition", Min. Soc. Amer. Spec. Paper 3:77-83.

Jackson E.D. (1969) "Chemical Variation in Coexisting Chromite and Olivine in Chromitite Zones of the Stillwater Complex", Magmatic Ore Deposits, Econ. Geol. Mono. 4:41-71.

Jackson E.D. and Wright J.A. (1970) "Xenoliths in the Honolulu Volcanic Series, Hawaii", J. Petrol. 11:405-432.

Kretz R. (1963) "Distribution of Mg and Fe between Orthopyroxene and Calcium Pyroxene in Natural Mineral Assemblages", J. Geol. 71:773-785.

Kuno H. (1967) "Mafic and Ultramafic Nodules from Itinome-gata, Japan", Ultramafic and Related Rocks, 337-342; P.J. Wyllie, editor.

_____ (1969) "Mafic and Ultramafic Nodules in Basaltic Rocks of Hawaii", G.S.A. Mem. 115:189-234.

Kuno H. and Aoki K. (1970) "Chemistry of Ultramafic Nodules and their Bearing on the Origin of Basaltic Magmas", Phys. Earth Planet. Int. 3:273-301.

Kushiro I. (1962) "Clinopyroxene Solid Solutions, Part I: The $CaAl_2SiO_6$ Component", Jap. J. Geol. Geog. Trans. 33-34, 213-220.

_____ (1969) "Clinopyroxene Solid Solution Formed by Reactions Between Diopside and Plagioclase at High Pressures", Pyroxenes and Amphiboles: Crystal Chemistry and Phase Petrology, Min. Soc. Amer. Spec. Paper 2:179-191.

_____ (1970) "Stability of Amphibole and Phlogopite in the Upper Mantle", Ann. Report Geophys. Lab. 68:245-247.

Kushiro I. and Aoki K. (1968) "Origin of some Eclogite Inclusions in Kimberlite", Amer. Min. 53:1347-1367.

Kushiro I., et al. (1968) "Stability of Phlogopite at High Pressures and Possible Presence of Phlogopite in the Earth's Upper Mantle", Earth Planet. Sci. Lett. 3:197-203.

Kushiro I., et al. (1968) "Melting of a Peridotite Nodule at High Pressures and High Water Pressures", J. Geophys. Res. 73:6023-6029.

_____ (1972) "Compositions of Coexisting Liquid and Solid Phases formed upon Melting of Natural Garnet and Spinel Lherzolites at High Pressures: a preliminary report", Earth Planet. Sci. Lett. 14:19-25.

Kushiro I. and Yoder H.S. (1966) "Anorthite-Forsterite and Anorthite-Enstatite Relations and their Bearing on the Basalt-Eclogite Transformation", J. Petrol. 7:337-362.

Leake B.E. (1968) "A Catalog of Analyzed Calciferous and Sub-calciferous Amphiboles Together with their Nomenclature and Associated Minerals", Geol. Soc. Amer. Spec. Paper, 98:1-210.

LeBas (1962) "The Role of Aluminum in Igneous Clinopyroxenes with Relation to their Parentage", Amer. J. Sci. 260:267-288.

LePichon X. (1968) "Sea Floor Spreading and Continental Drift", J. Geophys. Res. 73:3661-3697.

Loney, et al. (1971) "Structure and Petrology of the Alpine-Type Peridotite at Burro Mountain, California, USA", J. Petrol. 12:245-309.

Lorenz V. (1973) "On the Origin of Maars", Bull. Volcan. XXXVII-2, 183-204.

Loyd F.E. and Bailey D.K. (1973) "Light Element Metasomatism of the Continental Mantle: The Evidence and the Consequences", Int. Conf. Kimberlites, 199-202.

McBirney A.R. and Aoki K. (1973) "Factors Governing the Stability of Plagioclase at High Pressures as Shown by Spinel-Gabbro Xenoliths from the Kerguelen Archipelago", Amer. Min. 58:271-276.

MacDonald G.A. (1972) Volcanoes, Prentice-Hall, p. 510.

McGetchin T.R. and Hoare J.M. (1968) "Mica-Spinel-Lherzolite Fragment from Nanwaksjiak Crater, Nunivak Island, Alaska", Amer. Geophys. Union Trans. 49:760, abst.

MacGregor I.D. (1970) "The Effect of CaO, Cr_2O_3, Fe_2O_3, and Al_2O_3 on the Stability of Spinel and Garnet Peridotites", Phys. Earth Planet. Int. 3:372-377.

_____ (1972) "The System $MgO-Al_2O_3-SiO_2$: Solubility of Al_2O_3 in Enstatite for Spinel and Garnet Peridotite Compositions", Amer. Min. 59:110-119.

Malpas J. (1974) "The 'Petrological Moho' as identified in the Bay of Islands Igneous Complex, Western Newfoundland", in press.

Mark R.K. (1971) "Strontium Isotopic Study of Basalts from Nunivak Island, Alaska", unpublished Ph.D. Thesis, Stanford Un. p. 50.

Melson W.G., et al. (1967) "St. Peter and St. Paul Rocks: A High Temperature Mantle-Derived Intrusion", Science 155:1532-1535.

_____ (1973) "St. Paul's Rocks, Equatorial Atlantic: Petrogenesis, Radiometric Ages and Implications", G.S.A. Mem. 132:241-272.

Modreski P.J. and Boettcher A.L. (1972) "The Stability of Phlogopite Enstatite at High Pressures: a Model for Micas in the Interior of the Earth", Amer. J. Sci. 272:852-869.

Moore (1972) "Uplifted Trench Sediments: Southwestern Alaska-Bering Sea Shelf Edge", Science 175:1103-1104.

Mysen B. (1973) "Melting in a Hydrous Mantle: Phase Relations of Mantle Peridotite with Controlled Water and Oxygen Fugacities", Carnegie Inst. Wash. Yearb. 72:467-478.

Nixon P.H. and Hornung G. (1968) "A New Chromium Garnet End-Member, Knorringite from Kimberlites", Amer. Min. 53:1833-1840.

O'Hara M.J. and Mercy E.L.P. (1963) "Petrology and Petrogenesis of some Garnetiferous Peridotites", Trans. Roy. Soc. Edin. 65:251-314, #12.

O'Hara M.J. (1967) "Mineral Paragenesis in Ultrabasic Rocks", Ultrabasic and Related Rocks, ed. P.J. Wyllie, 393-403.

O'Hara M.J (1968) "The Bearing of Phase Equilibria Studies in Synthetic and Natural Systems on the Origin and Evolution of Basic and Ultrabasic Rocks", Earth Sci Rev. 4:69-133.

O'Hara M.J., et al. (1971) "Garnet-Peridotite Stability and Occurrence in Crust and Mantle", Contr. Min. Petrol. 32:48-68.

O'Hara M.J. (1973) "Paragenesis of Ultramafic Nodules in Basalts Contrasted with those of Nodules in Kimberlites, Int. Conf. Kimberlites, 255-257.

Oxburgh E.R. (1964) "Petrological Evidence for the Presence of Amphibole in the Upper Mantle and its Petrogenetic and Geophysical Implications", Geol. Mag. 101:1-19.

Pitman W.C. and Hayes D.E. (1968) "Sea-Floor Spreading in the Gulf of Alaska", J. Geophys. Res. 73:6571-6580.

Pratt R.M., et al. (1972) "Extension of Alaskan Structural Trends Beneath Bristol Bay, Bering Sea Shelf, Alaska", J. Geophys. Res. 77:4994-4999.

Ringwood A.E., et al. (1964) "Petrological Constitution of the Upper Mantle", Carnegie Inst. Wash. Yearb. 63:147-157.

Roeder P.L. and Emslie R.F. (1970) "Olivine Liquid Equilibrium", Contr. Min. Petrol. 29:275-289.

Ross C.S., et al. (1954) "Origin of Dunites and of Olivine-Rich Inclusions in Basaltic Rocks", Amer. Min. 39:693-737.

Runcorn S.K. (1964) "Satellite Gravity Measurements and a Laminar Viscous Flow Model of the Earth's Mantle", J. Geophys. Res. 69:4389-4394.

Scholl D.W., et al. (1968) "Geologic History of the Continental Margin of North America in the Bering Sea", Mar. Geol. 6:297-330.

Scholl D.W. and Hopkins D.M. (1969) "Newly Discovered Cenozoic Basins, Bering Sea Shelf", Amer. Assoc. Petrol. Geol. Bull. 53:2067-2078.

Shor G.G. (1964) "Structure of the Bering Sea and the Aleutian Ridge", Mar. Geol. 1:213-219.

Simkin T. and Smith (1970) "Minor Element Distribution in Olivine", J. Geol. 78:304-325.

Smith C.H. (1958) "Bay of Islands Igneous Complex, Western Newfoundland", Geol. Survey Can. Mem. 290:132 p.

Smith J.V., et al. (1973) "Sulphide-Oxide and Silicate-Oxide Intergrowths in Xenoliths of Upper Mantle Peridotite", Int.Conf. Kimberlites, 291-293.

Sobolev N.V. (1970) "Eclogites and Pyrope Peridotites from the Kimberlites of Yakutia", Phys. Earth Planet. Int. 3:398-404.

Sobolev N.V, et al. (1973) "Chrome-Rich Garnets from the Kimberlites of Yakutia and their Paragenesis", Contr. Min. Petrol. 40:39-52.

Stevens R.E. (1944) "Compositions of some Chromites of the Western Hemisphere", Amer. Min. 29:1-34.

Stone B.B. (1968) "Geophysics in the Bering Sea and Surrounding Areas: A Review", Tectonophysics 6:433-460.

Talbot J.L, et al. (1963) "Xenoliths and Xenocrysts from Lavas of the Kerguelen Archipelago", Amer. Min. 48:159-179.

Tobin D.G. and Sykes L.R. (1966) "Relationship of the Hypocenters of Earthquakes to the Geology of Alaska", J. Geophys. Res. 71:1659-1667.

Varne R. (1970) "Horneblende Lherzolite and the Upper Mantle", Contr. Min. Petrol. 27:45-51.

Varne R. and Graham A.L. (1971) "Rare Earth Abundance in Horneblende and Clinopyroxene of a Horneblende Lherzolite Xenolith: Implications for Upper Mantle Fractionation Processes", Earth Planet. Sci. Lett. 13:11-18.

Wager L.R. and Brown G.M. (1968) Layered Igneous Rocks, Oliver and Boyd, p.588.

White A.J.R. (1964) "Clinopyroxenes from Eclogites and Basic Granulites", Amer. Min. 49:883-888.

White R.W. (1966) "Ultramafic Inclusions in Basaltic Rocks from Hawaii", Contr. Min. Petrol. 12:245-314.

Whitney P.R. and McLelland J.M. (1973) "Origin of Coronas in Meta-Gabbros of Adirondak Mountains, New York", Contr. Min. Petrol. 39:81-98.

Wilshire H.G. and Binns R.A. (1961) "Basic and Ultrabasic Xenoliths from Volcanic Rocks of New South Wales", J. Petrol. 2:185-208.

Wilshire H.G. and Trask N.J. (1971) "Structural and Textural Relationships of Amphibole and Phlogopite in Peridotite Inclusions, Dish Hill, California", Amer. Min. 56:240-255.

Wilshire H.G., et al. (1971a) "Kaersutite-A Product of Reaction between Pargasite and Basanites at Dish Hill, California", Earth Planet. Sci. Lett. 10:281-284.

Wilshire H.G. and Shervais J.W. (1974) "Al-Augite and Cr-Diopside Ultramafic Xenoliths in Basaltic Rocks from Western United States; Structural and Textural Relationships", Phys. Chem. Earth, in press.

Wood J. and Banno S. (1973) "Garnet-Orthopyroxene and Orthopyroxene-Clinopyroxene Relationships in Simple and Complex Systems", Contr. Min. Petrol. 42:109-124.

Worst B.G. (1958) "The Great Kyke of Southern Rhodesia", Trans. Geol. Soc. S. Africa 61:283-365.

Wright T.L. and Doherty P.C. (1970) "A Linear Programming and Least Squares Computer Method for Solving Petrographic Mixing Problems", G.S.A. Bull. 81:1995-2008.

Wyllie P.J. (1970) "Ultramafic Rocks and the Upper Mantle", Min. Soc. Amer. Spec. Paper 3:3-32.

Wyllie P.J. (1971) "Role of Water in Magma Generation and the Initiation of Diapiric Uprise in the Mantle", J. Geophys. Res. 76:1328-1338.

Appendix 1

Sources for Xenoliths

Appendix 1

Sources for Xenoliths

	Host Vent	Comments
1) Fresh Lherzolites		
10001	NA3-9	glass bearing
10002	NA4-7	glass bearing
10003	NA4-7	glass bearing
10004	NA3-7	four phase
10005	MD3-1	glass bearing
10006	MD3-1	amphibole bearing
10007	NA3-7	four phase
10008	NA4-7	four phase
10009	NA4-7	glass bearing
10010	NA4-7	glass bearing
10012	NA3-7	four phase
10013	NA4-7	amphibole bearing
10016	NA4-6	amphibole bearing
10017	NA4-6	mica bearing
10041	NA4-7	mica bearing
10043	NA3-9	four phase
10045	maar	glass bearing
10046	maar	glass bearing
10050	MD3-1	amphibole bearing
10051	MD3-1	amphibole bearing
10052	MD3-1	amphibole bearing
2) Iddingsitized Lherzolite		
10022	MD4-4	
10023	MD4-3	
10024	MD4-3	
10025	NA4-2	
10026	NA4-1	
10027	MD4-9	glass bearing
10029	NA3-5	
10211	MD4-6	
10212	MD3-1	
10213	NA4-6	
10214	NA3-4	
10215	MD4-1	

Iddingsitized Lherzolite (cont'd)

10216	NA3-2	
10217	MD4-4	
10218	NA3-5	
10219	MD4-5	
10220	NA4-6	
10221	NA4-5	

3) Granulites

12000	NA3-9	
12001	NA3-4	iddingsitized
12004	NA3-4	iddingsitized
12008	MD4-4	iddingsitized
12017	MD4-1	
12024	MD4-3	iddingsitized

4) Dunites and Harzburgites

15005	maar	
15009	NA3-7	
15011	maar	

5) Megacrysts

13000	NA4-7	kaersutite
13020	NA4-12	clinopyroxene

APPENDIX 2-1

CLIVINE

FRESH LHERZOLITE SUITE

SPEC.	1C001	1CC02	1CC03	1CC04	1CC05	1CCC6	1CC07
SIC2	40.39	4C.75	41.03	4C.63	41.35	40.90	40.88
TIC2	0.01	C.01	C.01	C.01	C.C1	C.C2	C.C2
AL2C3	C.CC	0.00	C.CO	0.00	0.00	0.00	C.CO
FE2C3	C.CC	C.CO	C.CC	C.CO	0.00	0.00	0.00
CR2C3	0.CC	C.CO	C.CC	C.CO	0.CC	C.CO	C.CO
FEC	9.C8	9.14	9.40	9.46	8.95	8.72	8.44
MGC	49.74	49.12	49.45	49.35	50.24	50.02	5C.27
MNC	0.13	0.10	C.14	C.12	0.13	C.12	C.10
CAC	0.C5	C.05	C.06	0.08	0.05	0.04	C.04
NA2C	0.CC	0.CO	C.CO	C.00	0.00	0.00	0.CO
K2C	0.CO	C.CO	C.CC	C.00	0.CO	0.CO	0.CO
TCTAL	99.4C	99.17	10C.09	99.65	100.73	99.82	99.75

FCRMULA UNITS ASSUMING 4 OXYGENS

SI	0.993	1.CC3	1.CC2	0.997	1.CC1	0.999	0.998
TI	C.CCC	C.CCC	C.CCC	C.CCC	C.CCC	C.CCC	C.CCC
AL	C.CCC	C.CCC	C.CCC	C.CCC	C.CCC	C.CCC	C.CCC
FE3+	C.CCC	C.CCC	C.CCC	C.CCC	C.CCC	C.CCC	C.CCC
CR	C.CCC	C.CCC	C.CCC	C.CCC	C.CCC	C.CCC	C.CCC
FE2+	C.187	C.188	C.192	C.194	C.181	C.178	C.172
MG	1.823	1.802	1.8CC	1.806	1.813	1.820	1.829
MN	C.CC3	C.CC2	C.CC3	C.CC2	C.CC3	C.CC2	C.CC2
CA	C.CC1	C.CC1	C.CC2	C.CC2	C.CC1	C.CC1	C.CC1
NA	C.CCC	C.CCC	C.CCC	C.CCC	C.CCC	C.CCC	C.CCC
K	C.CCC	C.CCC	C.CCC	C.CCC	C.CCC	C.CCC	C.CCC
TCTAL	3.CC7	2.997	2.998	3.CC2	2.999	3.CC1	3.CC2
MG/MG+FE	C.9C7	C.905	C.904	C.903	C.909	C.911	C.914

UNLESS OTHERWISE SPECIFIEC; TCTAL IRON AS FEC

APPENDIX 2-1

OLIVINE

FRESH LHERZOLITE SUITE

SPEC.	1CC08	1CC09	1CC10	1CC13	1C013	1C013	1CC16
SIO2	40.48	4C.53	4C.55	4C.28	4C.14	39.82	40.83
TIC2	0.02	C.02	C.01	C.CO	0.CC	C.CO	C.CO
AL2C3	0.CO	0.00	0.00	0.03	0.01	0.02	0.04
FE2C3	0.CC	0.CO	C.CO	C.00	0.CO	0.CO	0.00
CR2C3	0.CO	0.CO	C.CC	C.03	C.02	C.C4	C.02
FEC	8.84	8.66	8.74	10.99	10.97	1C.77	9.35
MGC	49.69	49.88	49.73	48.98	49.53	49.59	49.96
MNC	0.14	0.12	C.12	C.20	C.15	C.16	C.16
CAC	0.06	0.04	0.05	0.07	C.07	C.C7	C.C5
NA2C	0.CC	C.CO	C.CO	0.00	0.00	0.00	C.01
K2C	0.CC	C.CO	C.CO	0.00	0.00	0.00	0.00
TCTAL	99.23	99.25	99.20	100.58	100.89	1C0.47	1CC.42

FCRMULA UNITS ASSUMING 4 OXYGENS

SI	0.996	C.996	0.997	C.988	0.982	C.978	0.994
TI	C.CCO	C.CCO	C.CCC	C.CCO	C.CCO	C.CCO	0.CCO
AL	C.CCO	0.CCO	0.CCO	0.C01	0.CCO	0.CC1	0.C01
FE3+	C.CCC	C.CCO	C.CCO	0.C00	0.CCO	0.CCO	0.C00
CR	0.CCO	0.CCO	C.CCC	0.C01	0.CCO	C.CC1	0.CCC
FE2+	0.182	0.178	0.180	0.225	0.224	C.221	0.19C
MG	1.822	1.826	1.822	1.791	1.806	1.815	1.814
MN	0.003	C.CC2	C.CC2	C.C04	C.CC3	C.CC3	C.CC3
CA	C.002	0.001	0.C01	0.C02	0.002	C.CC2	0.CC1
NA	C.CCC	C.CCO	0.CCO	0.C00	0.000	0.000	0.CCO
K	0.CCO	C.CCO	0.CCC	C.C00	C.CCO	C.CCO	C.CCC
TCTAL	3.CC4	3.CC4	3.CC3	3.011	3.018	3.021	3.C05
MG/MG+FE	C.909	C.911	0.91C	0.888	C.889	0.891	0.9C5

UNLESS OTHERWISE SPECIFIEC; TCTAL IRCN AS FEC

APPENDIX 2-1

OLIVINE

FRESH LHERZOLITE SUITE

SPEC.	1C017	1CC17	1CC17	1CC17	1C042	1C043
SIC2	39.48	39.17	38.86	38.39	40.48	41.07
TIC2	0.CC	0.C0	C.CC	C.C0	C.C1	C.C1
AL2C3	0.CC	0.03	C.03	C.02	0.00	0.C0
FE2C3	0.CC	0.C0	C.CC	C.C0	0.C0	0.C0
CR2C3	0.01	C.C8	C.C5	C.C6	C.CC	C.CC
FEC	17.67	19.20	16.25	20.67	8.67	9.C7
MGC	42.73	41.92	44.37	40.86	49.52	49.10
MNC	0.31	0.35	C.30	0.37	0.14	C.15
CAC	0.06	0.08	0.04	0.09	0.07	0.04
NA2C	0.CC	C.C0	C.CC	0.00	0.00	0.00
K2C	0.CC	0.C0	C.CC	C.C0	0.00	0.00
TCTAL	1C0.26	100.83	99.9C	100.46	98.89	99.44

FCRMULA UNITS ASSUMING 4 CXYGENS

SI	1.CC1	C.995	C.985	0.988	0.998	1.C07
TI	0.CCC	C.CC0	C.CC0	0.CCC	C.CCC	C.CC0
AL	C.CCC	0.C01	0.C01	0.C01	0.CC0	0.CC0
FE3+	C.CCC	C.CC0	0.CCC	0.C00	0.000	C.000
CR	C.CCC	C.C02	C.CC1	0.C01	C.CCC	C.CCC
FE2+	0.375	0.408	0.344	0.445	0.179	0.186
MG	1.615	1.588	1.676	1.567	1.820	1.795
MN	C.C07	C.C08	C.CC6	C.C08	0.003	0.C03
CA	C.002	C.CC2	C.CC1	C.C02	C.CC2	C.CC1
NA	C.CCC	0.000	0.CC0	0.C00	0.CC0	C.CC0
K	C.CCC	C.CC0	C.CCC	0.C00	0.CC0	C.CC0
TCTAL	2.999	3.003	3.014	3.011	3.002	2.993
MG/MG+FE	C.812	C.796	0.83C	0.77S	0.911	0.906

UNLESS OTHERWISE SPECIFIEC; TCTAL IRON AS FEC

APPENDIX 2-2

EUHEDRAL OLIVINE

FRESH LHERZCLITE SUITE

SPEC.	1CCC2	1CCC6	1CC10	1C017	1C017	10045
SIC2	41.C1	38.65	4C.99	39.27	39.90	40.84
TIC2	0.C2	0.CO	C.C1	C.CO	0.00	0.CO
AL2C3	0.24	C.28	C.12	C.08	C.07	C.C7
FE2C3	0.CC	C.CO	C.CO	C.00	0.00	0.CO
CR2O3	0.21	C.82	C.18	0.22	0.11	0.20
FEC	7.22	7.46	6.55	14.04	11.14	6.93
MGC	50.1C	51.63	51.03	45.31	48.17	5C.73
MNC	0.12	C.09	C.C8	C.24	0.20	0.11
CAC	0.24	0.C6	C.2C	C.25	0.19	C.14
NA2C	0.14	0.03	C.1C	0.00	0.00	0.03
K2C	0.CC	0.CO	C.C1	0.00	0.00	0.00
TCTAL	99.30	99.C2	99.27	99.41	99.78	99.05

FCRMULA UNITS ASSLMING 4 CXYGENS

SI	1.001	C.954	C.998	0.990	0.988	0.998
TI	C.CCC	C.CCO	C.CCC	0.CCO	0.CCO	0.CCO
AL	C.007	C.CC8	C.C03	C.C02	C.CC2	C.CC2
FE3+	C.CCO	0.CCO	C.CCO	0.CCO	C.CCO	C.CCO
CR	C.CC4	C.016	C.CC3	0.C04	0.C02	0.C04
FE2+	C.147	C.154	C.133	0.296	0.231	C.142
MG	1.822	1.899	1.851	1.702	1.778	1.847
MN	C.CC2	C.CC2	C.C02	0.C05	0.004	0.002
CA	C.006	C.CC2	C.C05	0.C07	C.005	0.004
NA	C.007	C.CC1	C.C05	0.CCO	C.CCC	C.CC1
K	C.CCO	C.CCO	C.CCO	C.CCO	0.CCO	C.CCO
TCTAL	2.997	3.C35	3.CC1	3.C07	3.01C	3.CCC
MG/MG+FE	C.925	0.925	0.933	0.852	0.885	0.929

UNLESS OTHERWISE SPECIFIED; TCTAL IRON AS FEC

APPENDIX 2-3

OLIVINE INCLUDED IN CLINOPYROXENE

FRESH LHERZOLITE SUITE

SPEC. 1C006

SIO2	40.83
TIO2	0.01
AL2O3	0.05
FE2O3	0.00
CR2O3	0.00
FEO	8.81
MGO	50.07
MNO	0.14
CAO	0.09
NA2O	0.00
K2O	0.00
TOTAL	100.00

FORMULA UNITS ASSUMING 4 OXYGENS

SI	0.996
TI	0.000
AL	0.001
FE3+	0.000
CR	0.000
FE2+	0.180
MG	1.821
MN	0.003
CA	0.002
NA	0.000
K	0.000
TOTAL	3.003

MG/MG+FE 0.910

UNLESS OTHERWISE SPECIFIED; TOTAL IRON AS FEO

APPENDIX 2-4

INTERSTITIAL AND RELICT CR-SPINEL

FRESH LHERZOLITE SUITE

SPEC.	10002	10002	10003	10003	10004	10005	10006
SIO2	0.00	1.21	0.00	0.00	0.00	0.00	0.00
TIO2	0.01	0.02	0.07	0.00	0.13	0.06	0.05
AL2O3	29.02	36.46	45.05	39.70	50.52	41.17	41.77
FE2O3	0.00	0.00	0.00	0.00	0.00	0.00	0.00
CR2O3	37.60	29.77	20.83	27.69	15.29	25.41	24.18
FEO	16.48	14.32	13.28	13.37	12.83	14.35	13.96
MGO	16.42	17.19	19.81	18.20	21.32	20.01	19.65
MNO	0.69	0.57	0.43	0.33	0.35	0.54	0.54
CAO	0.00	0.05	0.00	0.00	0.00	0.00	0.00
NA2O	0.00	0.02	0.00	0.00	0.00	0.00	0.00
K2O	0.00	0.00	0.00	0.00	0.00	0.00	0.00
TOTAL	100.22	99.61	99.47	99.29	100.44	101.54	100.15

FORMULA UNITS ASSUMING 4 OXYGENS

SI	0.000	0.034	0.000	0.000	0.000	0.000	0.000
TI	0.000	0.000	0.001	0.000	0.003	0.001	0.001
AL	1.015	1.225	1.460	1.322	1.583	1.336	1.367
FE3+	0.000	0.000	0.000	0.000	0.000	0.000	0.000
CR	0.882	0.671	0.453	0.618	0.321	0.553	0.531
FE2+	0.409	0.341	0.305	0.316	0.285	0.330	0.324
MG	0.727	0.730	0.812	0.766	0.845	0.821	0.813
MN	0.017	0.014	0.010	0.008	0.008	0.013	0.013
CA	0.000	0.002	0.000	0.000	0.000	0.000	0.000
NA	0.000	0.001	0.000	0.000	0.000	0.000	0.000
K	0.000	0.000	0.000	0.000	0.000	0.000	0.000
TOTAL	3.051	3.018	3.042	3.030	3.045	3.054	3.050
MG/MG+FE	0.640	0.681	0.727	0.708	0.748	0.713	0.715
CR/CR+AL	0.465	0.354	0.237	0.319	0.169	0.293	0.280

UNLESS OTHERWISE SPECIFIED; TOTAL IRON AS FEO

APPENDIX 2-4

INTERSTITIAL AND RELICT CR-SPINEL

FRESH LHERZOLITE SUITE

SPEC.	1CCC6	1CCC7	1CCC8	1CCC9	10009	10010	10043
SIC2	0.CC	0.CO	C.CO	0.00	0.00	0.CO	0.06
TIC2	0.CO	C.C9	C.03	0.06	0.01	0.00	0.05
AL2C3	27.75	31.67	45.68	41.52	38.30	27.05	45.77
FE2C3	0.CC	0.CO	C.CO	C.00	0.00	0.00	0.CO
CR2C3	39.84	35.CO	21.49	23.80	27.53	40.29	22.39
FEC	14.86	15.63	12.32	16.74	15.98	14.54	13.34
MGC	16.15	17.00	19.99	18.75	17.41	17.13	18.77
MNC	0.46	0.C6	C.35	C.44	0.38	0.73	0.30
CAC	0.CO	0.CO	C.CC	C.CO	0.CO	0.CO	C.C1
NA2C	0.CO	0.00	0.CO	0.00	0.00	0.CO	C.C1
K2C	0.CC	C.CO	C.CO	0.00	0.00	0.00	0.01
TCTAL	99.06	99.45	99.86	101.31	99.61	99.74	10C.71

FORMULA UNITS ASSUMING 4 CXYGENS

SI	C.CCO	C.CCO	C.CCO	0.C00	0.000	0.0C0	0.C02
TI	0.0C0	C.C02	C.CC1	0.C01	0.C00	C.CCO	0.CC1
AL	0.982	1.097	1.468	1.359	1.290	0.952	1.467
FE3+	C.CCC	C.CCO	0.CCO	0.C00	0.000	0.000	0.CCO
CR	0.946	C.813	C.463	0.523	0.622	0.952	0.481
FE2+	0.373	0.384	0.281	0.389	C.382	C.363	C.3C3
MG	0.723	0.745	0.813	0.776	0.741	0.763	0.761
MN	C.012	C.C01	0.C08	0.C10	C.009	C.018	0.C07
CA	C.0CC	C.CCO	C.CCC	0.CCO	C.CCC	C.CCC	0.CCC
NA	C.CCC	0.C00	0.CCO	0.C00	0.CCO	C.0CC	0.CC1
K	C.0CC	0.CCO	0.CCO	0.C00	0.000	0.CCO	0.C00
TCTAL	3.036	3.043	3.034	3.058	3.044	3.048	3.C24
MG/MG+FE	C.66C	C.660	C.743	0.66o	0.660	0.67/	0.715
CR/CR+AL	C.491	C.426	0.24C	0.278	C.325	0.5CC	0.247

UNLESS CTHERWISE SPECIFIED; TCTAL IRON AS FEC

APPENDIX 2-4

INTERSTITIAL AND RELICT CR-SPINEL

FRESH LHERZOLITE SUITE

SPEC.	1C013	1C013	1CC16	1CC17	1CC17
SIC2	0.14	0.60	1.CC	C.78	0.62
TIC2	0.05	C.06	C.C1	1.42	C.35
AL2C3	41.96	36.C2	35.87	15.62	20.84
FE2C3	0.CC	C.CC	C.CC	C.CC	0.CC
CR2C3	25.35	3C.63	32.17	41.52	41.32
FEC	14.62	15.31	13.75	3C.83	24.22
MGC	17.95	16.96	16.79	8.89	11.03
MNC	0.41	C.48	C.61	C.97	0.66
CAC	0.02	C.C3	C.C2	C.C7	C.C2
NA2C	0.CC	0.00	C.CC	0.00	0.00
K2C	0.CC	0.CC	C.CC	0.00	0.00
TCTAL	1CC.5C	1CC.C9	1CC.22	1CC.1C	99.C6

FCRMULA UNITS ASSUMING 4 CXYGENS

SI	C.CC4	C.C17	C.C28	0.C26	0.C20
TI	C.CC1	C.CC1	C.CCC	0.C35	0.C08
AL	1.374	1.215	1.2C2	C.611	C.787
FE3+	C.CCC	0.CCC	0.CC0	0.C00	0.CC0
CR	C.557	C.693	C.723	1.C90	1.046
FE2+	C.34C	C.366	C.327	0.856	0.649
MG	C.743	C.723	C.712	C.440	C.527
MN	C.C1C	C.C12	C.C15	C.C27	C.C18
CA	C.CC1	C.CC1	C.C01	C.C02	C.C01
NA	C.CCC	C.CCC	C.CCC	C.CCC	C.CCC
K	C.CCC	C.CCC	C.CCC	C.CCC	C.CCC
TCTAL	3.C3C	3.C28	3.C08	3.C88	3.C55
MG/MG+FE	C.686	C.664	C.685	C.339	C.448
CR/CR+AL	C.288	C.363	C.376	C.641	C.571

UNLESS CTHERWISE SPECIFIED; TCTAL IRCN AS FEC

APPENDIX 2-5

EUHEDRAL CR-SPINEL

FRESH LHERZOLITE SUITE

SPEC.	10001	10002	10010	10017	10017
SIO2	0.39	1.54	0.90	1.41	0.92
TIO2	0.22	0.07	0.08	2.41	1.07
AL2O3	47.16	36.30	37.43	17.45	21.44
FE2O3	0.00	0.00	0.00	0.00	0.00
CR2O3	19.19	29.00	30.04	37.36	40.78
FEO	9.31	11.31	10.16	26.35	19.92
MGO	21.53	20.07	20.45	12.72	14.20
MNO	0.22	0.52	0.58	0.81	0.88
CAO	0.06	0.23	0.14	0.07	0.01
NA2O	0.02	0.10	0.04	0.00	0.00
K2O	0.00	0.00	0.01	0.00	0.00
TOTAL	98.10	99.14	99.83	98.58	99.22

FORMULA UNITS ASSUMING 4 OXYGENS

SI	0.011	0.043	0.025	0.046	0.029
TI	0.004	0.001	0.002	0.059	0.025
AL	1.508	1.206	1.231	0.667	0.788
FE3+	0.000	0.000	0.000	0.000	0.000
CR	0.412	0.646	0.663	0.958	1.005
FE2+	0.211	0.267	0.237	0.715	0.519
MG	0.871	0.843	0.850	0.615	0.660
MN	0.005	0.012	0.014	0.022	0.023
CA	0.002	0.001	0.004	0.002	0.000
NA	0.001	0.005	0.002	0.000	0.000
K	0.000	0.000	0.000	0.000	0.000
TOTAL	3.025	3.032	3.028	3.083	3.050
MG/MG+FE	0.805	0.760	0.782	0.462	0.560
CR/CR+AL	0.214	0.349	0.350	0.590	0.561

UNLESS OTHERWISE SPECIFIED; TOTAL IRON AS FEO

APPENDIX 2-6

CR-SPINEL INCLUDED IN AMPHIBOLE

FRESH LHERZOLITE SUITE

SPEC.	1CC13	1C016	1CC16
SIC2	0.CC	1.91	1.47
TIC2	0.06	C.04	C.C5
AL2C3	30.9C	21.61	23.95
FE2C3	0.CC	0.00	C.CC
CR2C3	35.47	45.32	43.08
FEC	16.74	16.59	16.30
MGC	15.61	13.77	14.14
MNC	0.45	0.94	C.87
CAC	0.CC	0.19	C.11
NA2C	0.CC	C.CC	C.05
K2C	0.CC	0.C1	C.01
TCTAL	99.23	1CC.38	10C.03

FCRMULA UNITS ASSUMING 4 CXYGENS

SI	C.CCC	C.C58	0.C45
TI	0.001	C.001	0.C01
AL	1.C84	C.776	0.855
FE3+	0.CCC	C.CCC	C.CCC
CR	0.834	1.092	1.C32
FE2+	C.417	0.423	0.413
MG	C.692	C.626	0.638
MN	C.011	C.024	0.C22
CA	C.CC0	C.C06	0.C04
NA	C.CC0	0.CCC	0.C03
K	C.CCC	C.CC0	0.CC0
TCTAL	3.04C	3.CC7	3.C13
MG/MG+FE	C.624	0.597	0.607
CR/CR+AL	C.435	C.585	0.547

UNLESS CTHERWISE SPECIFIEC; TCTAL IRCN AS FEC

APPENDIX 2-7

CR-SPINEL INCLUDED IN ORTHOPYROXENE

FRESH LHERZOLITE SUITE

SPEC.	1C0C3	1CC13
SIO2	0.CC	0.CO
TIO2	0.CC	0.CO
AL2O3	41.33	47.24
FE2O3	0.CC	0.CO
CR2O3	26.04	19.85
FEO	13.09	14.08
MGO	18.51	18.71
MNO	C.3C	0.23
CAO	0.CC	0.CO
NA2O	0.CC	0.CO
K2O	0.CO	0.CO
TOTAL	99.27	1CC.11

FORMULA UNITS ASSUMING 4 OXYGENS

SI	C.CCC	C.CCO
TI	C.CCC	C.CCO
AL	1.365	1.516
FE3+	C.CCC	C.CCO
CR	C.577	C.427
FE2+	C.307	C.321
MG	C.773	C.759
MN	C.CC7	C.CC5
CA	C.CCC	C.CCO
NA	C.CCC	C.CCC
K	C.CCC	C.CCO
TOTAL	3.029	3.028
MG/MG+FE	C.716	C.703
CR/CR+AL	C.297	C.220

UNLESS OTHERWISE SPECIFIED; TOTAL IRON AS FEO

APPENDIX 2-8

CR-SPINEL INCLUDED IN OLIVINE

FRESH LHERZOLITE SUITE

SPEC.	1C003	1CC06	1CC13	1CC16
SIC2	0.CC	C.CC	C.CC	C.CC
TIC2	0.CC	0.CC	C.03	C.03
AL2C3	40.3C	42.81	39.77	42.88
FE2C3	0.CC	C.CC	C.CC	C.CC
CR2C3	26.72	23.52	25.96	24.85
FEC	13.38	13.40	16.09	13.13
MGC	18.49	18.83	16.89	17.85
MNC	0.31	0.25	C.32	C.35
CAC	0.CC	0.CC	C.CC	C.CC
NA2C	0.CC	0.CC	C.CC	C.CC
K2C	0.CC	C.CC	C.CC	C.CC
TCTAL	99.20	98.81	99.C6	99.09

FORMULA UNITS ASSUMING 4 OXYGENS

SI	C.CCC	0.CCC	C.CCC	0.CCC
TI	C.CCC	C.CCC	0.CC1	0.CC1
AL	1.338	1.411	1.339	1.412
FE3+	C.CCC	0.CCC	0.CCC	0.CCC
CR	C.595	C.520	0.586	0.549
FE2+	0.315	C.313	0.384	0.307
MG	C.777	0.785	C.719	C.743
MN	C.007	0.CC6	0.CC8	0.CC8
CA	C.CCC	C.CCC	0.CCC	0.CCC
NA	0.CCC	0.CCC	C.CCC	0.CCC
K	C.CCC	C.CCC	C.CCC	0.CCC
TCTAL	3.033	3.035	3.C37	3.019
MG/MG+FE	C.711	C.715	C.652	0.708
CR/CR+AL	C.3C8	0.269	0.305	0.280

UNLESS OTHERWISE SPECIFIED; TCTAL IRON AS FEC

APPENDIX 2-9

ORTHOPYROXENE

FRESH LHERZOLITE SUITE

SPEC.	1C002	1C003	1CC04	1CC05	1CC06	1CC07	1CC08
SIC2	56.44	55.21	55.53	56.95	56.32	57.13	56.49
TIC2	0.CC	0.01	C.C4	0.05	0.03	0.01	0.03
AL2C3	3.23	3.34	3.76	2.86	3.C3	2.46	3.37
FE2C3	0.CC	C.CO	C.CC	C.CO	0.CC	C.CO	C.CC
CR2C3	0.43	0.40	C.41	0.44	0.46	0.45	0.43
FEC	5.98	6.C5	6.11	5.85	5.77	5.60	5.81
MGC	33.22	34.49	33.C3	33.68	33.79	34.29	33.91
MNC	0.11	0.14	C.14	0.12	0.12	0.15	C.13
CAC	0.58	0.60	C.61	0.55	0.53	0.59	0.59
NA2C	0.26	C.C6	C.2C	C.04	C.03	0.07	C.04
K2C	0.CC	C.CO	C.CO	C.01	C.CC	0.CO	C.CC
TCTAL	1C0.25	1CC.30	99.83	1CC.55	1CC.08	1C0.75	100.80

FCRMLLA UNITS ASSUMING 6 CXYGENS

SI	1.94C	1.9C3	1.92C	1.948	1.937	1.950	1.929
TI	C.CCC	C.CCO	0.001	0.C01	0.C01	C.CCO	0.C01
AL	C.131	C.136	C.153	0.115	0.123	C.099	0.136
FE3+	C.CCC	C.CCO	C.CCC	0.CCO	C.CCC	C.CCC	0.CCC
CR	C.012	C.011	0.C11	0.C12	0.013	C.012	0.C12
FE2+	C.172	C.174	0.177	0.167	0.166	0.160	0.166
MG	1.7C2	1.772	1.7C2	1.717	1.732	1.745	1.726
MN	C.003	C.004	0.C04	0.003	0.003	C.C04	0.C04
CA	C.C21	C.022	C.C23	0.020	0.020	0.022	0.C22
NA	C.017	C.CC4	0.C13	C.C03	0.002	0.005	0.003
K	0.CCC	C.CCO	0.CCC	0.CCO	C.CCO	C.CCO	0.CCC
TCTAL	3.998	4.026	4.CC4	3.988	3.996	3.996	3.998
MG/MG+FE	C.9C8	C.910	C.9C6	0.911	0.913	0.91C	0.912

UNLESS CTHERWISE SPECIFIED; TCTAL IRON AS FEC

APPENDIX 2-9

ORTHOPYROXENE

FRESH LHERZOLITE SUITE

SPEC.	10009	10010	10013	10013	10016	10043	10045
SIO2	55.82	56.69	55.70	55.87	57.07	56.36	56.18
TIO2	0.02	0.00	0.04	0.04	0.01	0.02	0.01
AL2O3	2.69	2.27	3.34	3.21	2.78	3.43	2.76
FE2O3	0.00	0.00	0.00	0.00	0.00	0.00	0.00
CR2O3	0.38	0.52	0.45	0.38	0.43	0.42	0.34
FEO	5.97	5.79	6.77	6.80	5.82	5.69	6.07
MGO	34.85	34.29	32.82	33.01	34.01	33.48	34.29
MNO	0.13	0.07	0.18	0.16	0.15	0.17	0.16
CAO	0.44	0.54	0.56	0.65	0.41	0.58	0.46
NA2O	0.16	0.20	0.20	0.34	0.08	0.00	0.16
K2O	0.00	0.00	0.00	0.00	0.00	0.00	0.00
TOTAL	100.46	100.37	100.06	100.46	100.76	100.15	100.43

FORMULA UNITS ASSUMING 6 OXYGENS

SI	1.919	1.946	1.927	1.927	1.948	1.935	1.930
TI	0.001	0.000	0.001	0.001	0.000	0.001	0.000
AL	0.109	0.092	0.136	0.130	0.112	0.139	0.112
FE3+	0.000	0.000	0.000	0.000	0.000	0.000	0.000
CR	0.010	0.014	0.012	0.010	0.012	0.011	0.009
FE2+	0.172	0.166	0.196	0.196	0.166	0.163	0.174
MG	1.786	1.754	1.692	1.697	1.730	1.714	1.756
MN	0.004	0.002	0.005	0.005	0.004	0.005	0.005
CA	0.016	0.020	0.021	0.024	0.015	0.021	0.017
NA	0.011	0.013	0.013	0.023	0.005	0.000	0.011
K	0.000	0.000	0.000	0.000	0.000	0.000	0.000
TOTAL	4.026	4.008	4.004	4.013	3.993	3.989	4.014
MG/MG+FE	0.912	0.913	0.896	0.896	0.912	0.913	0.910

UNLESS OTHERWISE SPECIFIED; TOTAL IRON AS FEO

APPENDIX 2-9

ORTHOPYRCXENE

FRESH LHERZOLITE SUITE

SPEC.	10046
SIC2	56.38
TIC2	0.01
AL2O3	2.87
FE2C3	0.CC
CR2C3	0.53
FEC	5.54
MGC	34.36
MNC	0.12
CAC	0.53
NA2C	0.14
K2C	0.CC
TCTAL	1C0.48

FORMULA UNITS ASSUMING 6 OXYGENS

SI	1.932
TI	C.0CC
AL	C.116
FE3+	C.CCC
CR	C.014
FE2+	C.159
MG	1.755
MN	C.CC3
CA	C.019
NA	0.009
K	C.CCC
TCTAL	4.008
MG/MG+FE	C.917

UNLESS OTHERWISE SPECIFIED; TCTAL IRCN AS FEC

APPENDIX 2-10

ORTHOPYROXENE INCLUDED IN CLINOPYROXENE

FRESH LHERZOLITE SUITE

SPEC.	10006
SIO2	57.43
TIO2	0.00
AL2O3	1.25
FE2O3	0.00
CR2O3	0.22
FEO	5.42
MGO	34.83
MNO	0.15
CAO	0.60
NA2O	0.14
K2O	0.00
TOTAL	100.04

FORMULA UNITS ASSUMING 6 OXYGENS

SI	1.973
TI	0.000
AL	0.051
FE3+	0.000
CR	0.006
FE2+	0.156
MG	1.783
MN	0.004
CA	0.022
NA	0.009
K	0.000
TOTAL	4.004
MG/MG+FE	0.920

UNLESS OTHERWISE SPECIFIED; TOTAL IRON AS FEO

APPENDIX 2-11

CLINOPYROXENE

FRESH LHERZOLITE SUITE

SPEC.	10001	10002	10003	10004	10005	10006	10006
SIO2	53.35	54.82	53.20	53.56	54.03	55.58	56.46
TIO2	0.13	0.07	0.08	0.20	0.04	0.00	0.00
AL2O3	2.92	4.45	3.27	4.22	2.98	4.00	3.82
FE2O3	0.00	0.00	0.00	0.00	0.00	0.00	0.00
CR2O3	0.87	0.90	0.60	0.66	0.68	0.85	0.69
FEO	2.45	2.83	2.20	2.66	2.53	2.81	2.96
MGO	17.52	16.55	16.72	17.14	16.84	16.22	15.85
MNO	0.08	0.07	0.11	0.07	0.09	0.07	0.11
CAO	22.08	18.77	22.25	20.90	20.48	17.46	17.80
NA2O	0.87	2.57	0.94	1.14	1.74	2.97	2.67
K2O	0.01	0.00	0.01	0.00	0.01	0.00	0.02
TOTAL	100.28	101.03	99.38	100.55	99.42	99.96	100.38

FORMULA UNITS ASSUMING 6 OXYGENS

SI	1.930	1.953	1.939	1.924	1.963	1.992	2.012
TI	0.004	0.002	0.002	0.005	0.001	0.000	0.000
AL	0.125	0.187	0.140	0.179	0.128	0.169	0.160
FE3+	0.000	0.000	0.000	0.000	0.000	0.000	0.000
CR	0.025	0.025	0.017	0.019	0.020	0.024	0.019
FE2+	0.074	0.084	0.067	0.080	0.077	0.084	0.088
MG	0.945	0.879	0.908	0.918	0.912	0.866	0.842
MN	0.002	0.002	0.003	0.002	0.003	0.002	0.003
CA	0.856	0.717	0.869	0.805	0.797	0.670	0.680
NA	0.061	0.178	0.066	0.079	0.123	0.206	0.184
K	0.000	0.000	0.000	0.000	0.000	0.000	0.001
TOTAL	4.022	4.027	4.013	4.011	4.024	4.015	3.991
MG/MG+FE	0.927	0.912	0.931	0.920	0.922	0.911	0.905

UNLESS OTHERWISE SPECIFIED; TOTAL IRON AS FEO

APPENDIX 2-11

CLINOPYROXENE

FRESH LHERZOLITE SUITE

SPEC.	10006	10006	10007	10008	10009	10013	10016
SIO2	55.64	55.20	53.40	52.46	53.26	53.81	54.83
TIO2	0.03	0.03	0.06	0.10	0.09	0.01	0.02
AL2O3	4.28	4.66	2.71	3.25	2.51	4.77	3.27
FE2O3	0.00	0.00	0.00	0.00	0.00	0.00	0.00
CR2O3	0.87	0.86	0.91	0.68	0.52	0.96	0.78
FEO	2.80	2.93	2.35	2.47	2.27	3.24	2.42
MGO	15.94	15.49	17.07	17.40	17.34	16.04	16.22
MNO	0.13	0.11	0.10	0.05	0.09	0.10	0.13
CAO	17.61	17.72	21.70	23.01	22.52	18.82	19.89
NA2O	2.71	2.84	0.81	0.48	0.94	2.44	2.12
K2O	0.02	0.01	0.01	0.00	0.01	0.00	0.01
TOTAL	100.03	99.85	99.12	99.90	99.55	100.19	99.69

FORMULA UNITS ASSUMING 6 OXYGENS

SI	1.991	1.982	1.950	1.910	1.942	1.940	1.981
TI	0.001	0.001	0.002	0.003	0.002	0.000	0.001
AL	0.181	0.197	0.117	0.139	0.108	0.203	0.139
FE3+	0.000	0.000	0.000	0.000	0.000	0.000	0.000
CR	0.025	0.024	0.026	0.020	0.015	0.027	0.022
FE2+	0.084	0.088	0.072	0.075	0.069	0.098	0.073
MG	0.850	0.829	0.929	0.944	0.942	0.862	0.873
MN	0.004	0.003	0.003	0.002	0.003	0.003	0.004
CA	0.675	0.682	0.849	0.898	0.880	0.727	0.770
NA	0.188	0.198	0.057	0.034	0.066	0.171	0.148
K	0.001	0.000	0.000	0.000	0.000	0.000	0.000
TOTAL	4.000	4.005	4.006	4.025	4.028	4.030	4.012
MG/MG+FE	0.910	0.904	0.928	0.926	0.932	0.898	0.923

UNLESS OTHERWISE SPECIFIED; TOTAL IRON AS FEO

APPENDIX 2-11

CLINOPYROXENE

FRESH LHERZOLITE SUITE

SPEC.	10017	1CC17	1CC43	1CC45	1CC46
SIC2	53.88	54.53	52.86	54.43	54.39
TIC2	0.27	C.11	C.C8	C.01	C.01
AL2C3	4.36	4.15	3.40	3.27	3.24
FE2C3	0.CC	0.00	C.CC	C.00	0.00
CR2C3	2.39	1.08	C.7C	C.63	0.84
FEC	5.64	5.85	2.56	2.59	2.37
MGC	14.43	15.49	16.74	16.26	16.49
MNC	0.24	C.22	C.13	C.08	0.06
CAC	16.53	15.69	22.5C	20.12	20.83
NA2C	2.76	2.75	0.45	2.08	1.68
K2C	0.C2	C.00	C.01	0.00	0.00
TCTAL	1CC.52	99.87	99.43	99.47	99.91

FCRMULA UNITS ASSUMING 6 CXYGENS

SI	1.953	1.977	1.929	1.974	1.965
TI	C.CC7	C.CC3	0.CC2	0.CC0	0.CC0
AL	C.186	C.177	0.146	0.140	C.138
FE3+	C.CCC	0.CCC	0.CCC	0.CC0	0.CCC
CR	C.068	C.C31	0.C2C	0.018	0.024
FE2+	C.171	C.177	C.C78	C.C79	0.072
MG	C.780	C.837	0.91C	0.879	C.888
MN	C.CC7	0.CC7	0.CC4	0.CC2	0.CC2
CA	C.642	C.610	0.880	0.782	0.806
NA	C.194	C.193	0.C32	0.146	0.118
K	0.CC1	C.CC0	C.CCC	0.CC0	C.CCC
TCTAL	4.01C	4.012	4.C02	4.020	4.013
MG/MG+FE	C.820	C.825	0.921	0.91E	0.925

UNLESS CTHERWISE SPECIFIEC; TCTAL IRCN AS FEC

APPENDIX 2-12

CLOUDY CLINOPYROXENE

FRESH LHERZOLITE SUITE

SPEC.	10006	10016	10016	10016	10045	10045	10046
SIO2	55.05	54.99	54.96	53.68	54.52	54.46	54.29
TIO2	0.06	0.08	0.06	0.08	0.02	0.05	0.03
AL2O3	3.06	2.55	2.87	3.15	2.98	2.98	2.96
FE2O3	0.00	0.00	0.00	0.00	0.00	0.00	0.00
CR2O3	0.69	0.50	0.65	0.66	0.56	0.63	0.70
FEO	2.32	2.26	2.12	2.26	2.45	2.28	2.33
MGO	16.53	16.58	16.64	17.11	16.37	16.15	16.78
MNO	0.09	0.09	0.10	0.06	0.09	0.10	0.06
CAO	20.96	21.20	21.96	21.29	20.90	21.78	21.53
NA2O	1.51	1.67	1.51	1.64	1.77	1.57	1.45
K2O	0.00	0.00	0.00	0.01	0.00	0.00	0.00
TOTAL	100.27	99.92	100.87	99.94	99.66	100.00	100.13

FORMULA UNITS ASSUMING 6 OXYGENS

SI	1.978	1.985	1.969	1.944	1.975	1.969	1.960
TI	0.002	0.002	0.002	0.002	0.001	0.001	0.001
AL	0.130	0.108	0.121	0.134	0.127	0.127	0.126
FE3+	0.000	0.000	0.000	0.000	0.000	0.000	0.000
CR	0.020	0.014	0.018	0.019	0.016	0.018	0.020
FE2+	0.070	0.068	0.064	0.068	0.074	0.069	0.070
MG	0.885	0.892	0.888	0.924	0.884	0.870	0.903
MN	0.003	0.003	0.003	0.002	0.003	0.003	0.002
CA	0.807	0.820	0.843	0.826	0.811	0.844	0.833
NA	0.105	0.117	0.105	0.115	0.124	0.110	0.102
K	0.000	0.000	0.000	0.000	0.000	0.000	0.000
TOTAL	3.998	4.010	4.012	4.035	4.015	4.012	4.017
MG/MG+FE	0.927	0.929	0.933	0.931	0.923	0.927	0.928

UNLESS OTHERWISE SPECIFIED; TOTAL IRON AS FEO

APPENDIX 2-13

RIM CLINCPYROXENE

FRESH LHERZOLITE SUITE

SPEC.	1CCC2	1CCC5	1CCC6	1CC06	1CC17	1CC17
SIC2	53.64	53.21	54.39	53.03	52.50	53.18
TIC2	0.04	C.04	C.03	C.04	0.46	C.2C
AL2C3	3.98	2.44	2.15	2.87	3.38	3.13
FE2C3	0.CC	C.CO	C.CC	C.00	0.CC	0.00
CR2C3	1.19	1.31	1.35	1.77	2.C1	1.97
FEC	2.73	2.55	2.73	2.42	4.98	4.06
MGC	17.9C	18.C3	17.44	16.63	16.54	17.05
MNC	0.1C	C.11	C.16	C.09	0.2C	C.19
CAC	19.54	21.84	2C.56	21.72	18.80	19.74
NA2C	1.35	0.71	C.77	0.95	1.15	1.10
K2C	0.C3	C.C3	C.C7	C.03	C.04	0.03
TCTAL	1C0.50	1CC.27	99.65	99.55	1CC.06	1CC.65

FCRMULA UNITS ASSUMING 6 CXYGENS

SI	1.926	1.928	1.972	1.936	1.917	1.925
TI	C.001	C.CC1	C.CC1	0.C01	C.C13	C.CC5
AL	C.168	0.104	0.C92	0.123	C.145	0.134
FE3+	C.CCC	C.CCO	C.CCO	0.CCO	0.000	0.CCO
CR	C.034	C.038	C.C39	0.C51	C.058	C.056
FE2+	0.082	0.077	0.C83	0.074	0.152	0.123
MG	C.958	C.974	0.943	0.905	0.900	0.920
MN	C.003	C.C03	C.CC5	0.C03	C.006	0.CC6
CA	0.752	C.848	C.799	0.849	C.735	C.766
NA	C.094	0.050	0.054	0.067	0.081	0.077
K	C.CC1	C.C01	C.C03	0.C01	C.C02	0.C01
TCTAL	4.019	4.025	3.990	4.010	4.010	4.014
MG/MG+FE	C.921	C.926	0.919	0.925	0.855	0.882

UNLESS OTHERWISE SPECIFIED; TCTAL IRON AS FEC

APPENDIX 2-14

EUHEDRAL CLINOPYROXENE

FRESH LHERZOLITE SUITE

SPEC.	1CCC1	1CCC2	1CCC6	1CC06	10013	10013	10010
SIC2	49.79	49.57	51.33	51.30	49.84	50.08	51.95
TIC2	0.79	C.C8	C.15	C.09	0.25	C.27	0.03
AL2C3	7.26	6.96	6.41	4.64	7.45	6.82	5.62
FE2C3	0.CC	0.C0	C.C0	C.00	0.00	0.00	0.00
CR2C3	1.71	3.62	2.66	2.59	3.29	3.01	2.44
FEC	2.28	2.29	2.43	2.20	2.38	2.40	2.C5
MGC	15.3C	15.56	16.06	16.97	15.42	15.62	16.47
MNC	C.C4	C.C6	C.C7	C.09	0.10	0.10	0.08
CAC	21.32	20.C3	2C.63	2C.61	2C.51	2C.89	19.79
NA2C	1.C2	1.30	1.13	0.85	1.15	0.99	1.36
K2C	0.C1	0.C0	C.C0	0.03	0.01	0.03	0.C0
TCTAL	99.52	99.47	1CC.87	99.37	1CC.4C	1CC.21	99.79

FCRMULA UNITS ASSUMING 6 CXYGENS

SI	1.819	1.816	1.849	1.875	1.809	1.822	1.882
TI	C.022	C.CC2	C.C04	0.C02	C.C07	0.C07	0.C01
AL	0.313	C.3C1	0.272	0.2C0	C.31S	0.292	0.24C
FE3+	C.0CC	0.000	0.C00	0.C00	0.000	0.C00	0.C00
CR	C.049	C.1C5	0.C76	0.C75	0.094	C.087	0.C70
FE2+	C.07C	C.C70	0.C73	0.C67	C.C72	C.C73	C.C62
MG	0.833	0.850	0.862	0.925	0.834	0.847	0.889
MN	C.CC1	C.CC2	0.CC2	0.C03	0.C03	0.C03	0.C02
CA	0.835	C.786	C.796	0.807	0.798	0.814	0.768
NA	C.072	0.092	0.079	0.060	0.081	C.070	0.C96
K	C.CCC	C.C00	0.CC0	0.001	0.000	0.001	0.CC0
TCTAL	4.014	4.025	4.C13	4.C16	4.C18	4.017	4.C10
MG/MG+FE	C.923	0.924	0.922	0.932	0.920	0.921	0.935

UNLESS OTHERWISE SPECIFIED; TCTAL IRCN AS FEC

APPENDIX 2-14

EUHEDRAL CLINOPYROXENE

FRESH LHERZOLITE SUITE

SPEC. 10045

SIO2	49.36
TIO2	0.09
AL2O3	7.62
FE2O3	0.00
CR2O3	3.47
FEO	2.07
MGO	14.54
MNO	0.12
CAO	21.10
NA2O	1.20
K2O	0.00
TOTAL	99.57

FORMULA UNITS ASSUMING 6 OXYGENS

SI	1.809
TI	0.002
AL	0.329
FE3+	0.000
CR	0.101
FE2+	0.063
MG	0.794
MN	0.004
CA	0.829
NA	0.085
K	0.000
TOTAL	4.016
FE/MG+FE	0.926

UNLESS OTHERWISE SPECIFIED; TOTAL IRON AS FEO

APPENDIX 2-15

CR-BEARING AMPHIBOLE

FRESH LHERZOLITE SUITE

SPEC.	10006	10006	10013	10013	10013	10013	10013
SIO2	47.60	45.99	44.88	44.26	44.54	44.67	44.27
TIO2	0.11	0.08	0.24	0.27	0.38	0.32	0.33
AL2O3	12.06	12.91	13.73	13.52	13.42	13.53	13.78
FE2O3	0.00	0.00	0.00	0.00	0.00	0.00	0.00
CR2O3	1.45	1.14	2.11	2.19	2.85	2.23	2.48
FEO	3.43	3.42	4.23	3.99	4.13	3.91	3.94
MGO	19.35	18.45	18.16	18.19	17.68	17.94	17.71
MNO	0.06	0.07	0.05	0.06	0.11	0.11	0.15
CAO	8.73	9.07	9.64	9.63	9.79	9.75	9.84
NA2O	4.87	4.79	3.64	3.55	3.83	3.98	3.93
K2O	0.94	0.92	1.28	1.28	1.31	1.24	1.24
TOTAL	98.60	98.84	97.96	96.94	98.04	97.68	97.67

FORMULA UNITS ASSUMING 23 OXYGENS

SI	6.642	6.449	6.363	6.343	6.336	6.358	6.312
TI	0.012	0.008	0.026	0.029	0.041	0.034	0.035
AL	1.983	2.134	2.294	2.283	2.250	2.270	2.316
FE3+	0.000	0.000	0.000	0.000	0.000	0.000	0.000
CR	0.160	0.348	0.237	0.248	0.321	0.251	0.280
FE2+	0.400	0.401	0.502	0.478	0.491	0.465	0.470
MG	4.024	3.856	3.838	3.885	3.748	3.806	3.764
MN	0.007	0.008	0.006	0.007	0.013	0.013	0.018
CA	1.305	1.363	1.464	1.479	1.492	1.487	1.503
NA	1.317	1.302	1.001	0.986	1.056	1.098	1.087
K	0.167	0.165	0.232	0.234	0.238	0.225	0.226
TOTAL	16.018	16.035	15.962	15.973	15.986	16.009	16.010
MG/MG+FE	0.910	0.906	0.884	0.890	0.884	0.891	0.889
NA/NA+K	0.887	0.888	0.812	0.808	0.816	0.830	0.828

UNLESS OTHERWISE SPECIFIED; TOTAL IRON AS FEO

APPENDIX 2-15

CR-BEARING AMPHIBOLE

FRESH LHERZOLITE SUITE

SPEC.	1C016	1C016	1CC16
SIC2	46.69	46.43	46.75
TIC2	0.07	C.09	C.11
AL2C3	11.64	12.09	11.51
FE2C3	0.CC	C.C0	C.00
CR2C3	2.19	3.24	2.55
FEC	3.33	3.38	3.29
MGC	19.C4	18.73	19.01
MNC	C.1C	0.11	C.11
CAC	9.38	9.42	9.43
NA2C	4.55	4.38	4.39
K2C	0.72	0.72	C.72
TCTAL	97.71	98.59	97.87

FCRMULA UNITS ASSUMING 23 CXYGENS

SI	6.595	6.518	6.595
TI	C.CC7	C.C10	0.C12
AL	1.938	2.CC0	1.914
FE3+	C.0C0	C.CCC	0.CCC
CR	0.245	0.360	0.284
FE2+	C.393	C.397	C.388
MG	4.009	3.919	3.997
MN	C.012	C.013	0.C13
CA	1.42C	1.417	1.425
NA	1.246	1.192	1.2C1
K	C.13C	C.129	C.13C
TCTAL	15.994	15.954	15.959
MG/MG+FE	C.911	C.9C8	C.911
NA/NA+K	0.9C6	C.902	C.9C3

LNLESS CTHERWISE SPECIFIEC; TCTAL IRCN AS FEC

APPENDIX 2-16

CR-BEARING PHLOGOPITE

FRESH LHERZOLITE SUITE

SPEC.	1C0C6	1CC13	1CC13	1CC16	1CC17	1C017	1CC17
SIC2	38.31	38.53	38.68	39.91	37.58	38.80	39.55
TIC2	0.14	0.43	0.48	0.20	2.91	1.69	2.02
AL2C3	16.72	17.62	17.47	17.75	14.84	15.61	15.11
FE2C3	0.CC	C.CO	C.CC	C.CO	0.CO	C.CC	C.CC
CR2C3	2.48	1.93	2.11	2.17	1.85	2.08	1.34
FEC	3.75	4.13	3.88	3.43	7.92	6.11	6.59
MGC	23.53	22.78	23.14	23.76	20.24	21.43	21.32
MNC	0.C5	C.C5	C.C5	C.05	0.11	C.C9	C.C7
CAC	0.CO	0.CO	C.01	0.00	0.00	0.00	C.CO
NA2O	0.82	0.92	C.99	1.47	0.98	1.19	1.05
K2C	9.19	8.60	8.49	7.30	8.66	8.65	8.74
TCTAL	94.99	94.99	95.3C	96.04	95.09	95.65	95.79

FCRMULA UNITS ASSUMING 22 CXYGENS

SI	5.464	5.470	5.468	5.540	5.464	5.543	5.636
TI	C.015	C.046	0.C51	0.C21	0.318	0.182	0.216
AL	2.811	2.948	2.911	2.904	2.543	2.628	2.538
FE3+	C.CCC	C.CCO	C.CCC	0.CCO	C.COO	0.COO	0.COO
CR	C.280	C.217	C.236	0.238	0.213	C.235	0.151
FE2+	C.447	C.490	0.459	0.398	0.963	0.730	0.785
MG	5.CC3	4.820	4.876	4.916	4.386	4.563	4.529
MN	C.CC6	C.C06	C.CC6	0.CC6	C.014	C.011	C.CC8
CA	C.CCC	0.CCO	0.C02	0.COO	0.COO	C.CCO	0.CCO
NA	C.227	C.253	C.271	0.396	0.276	0.330	0.290
K	1.672	1.557	1.531	1.293	1.6C6	1.576	1.589
TCTAL	15.925	15.807	15.8C9	15.712	15.782	15.797	15.743
FG/MG+FE	C.918	C.9C8	C.914	0.925	C.82C	C.862	C.852
NA/NA+K	C.119	0.140	0.151	0.234	0.147	0.173	0.154

UNLESS CTHERWISE SPECIFIED; TCTAL IRON AS FEC

APPENDIX 2-17

GLASS FROM FINE-GRAINED ZONES

FRESH LHERZOLITE SUITE

SPEC.	1CCC1	1CCC2	1CCC3	1CC10	1CC13	1CC13	1CC13
SIC2	52.9C	55.61	57.79	58.99	51.15	51.35	52.32
TIC2	1.32	C.18	C.29	0.16	0.52	0.56	0.51
AL2C3	22.29	23.84	23.94	2C.87	21.52	23.07	23.44
FE2C3	0.CC	C.CO	C.CC	C.CC	0.CC	C.CO	C.CC
CR2C3	0.C5	0.15	C.13	C.09	0.58	0.68	0.11
FEC	3.78	3.37	2.72	2.77	3.94	3.60	4.01
MGC	4.3C	4.CC	2.84	3.6C	5.C1	4.34	3.98
MNC	0.C6	0.C3	C.C6	C.07	0.09	C.C9	0.09
CAC	9.11	7.46	6.44	6.58	8.80	8.05	8.02
NA2C	3.94	3.45	3.09	4.57	4.22	4.66	4.29
K2C	2.CC	1.42	1.23	2.10	3.07	3.71	2.92
TCTAL	99.75	99.51	98.53	99.80	98.9C	1CC.11	99.69

FCRMLLA UNITS ASSUMING 1C CXYGENS

SI	3.08C	3.18C	3.289	3.356	3.042	3.017	3.C61
TI	C.058	C.CC8	C.C12	C.C07	C.023	C.025	C.C22
AL	1.53C	1.6C7	1.6C6	1.399	1.509	1.598	1.616
FE3+	C.CCC	C.CCC	C.CCC	C.CCC	C.CCC	C.CCC	C.CCC
CR	C.CC2	C.C07	C.C06	C.C04	C.027	C.032	C.C05
FE2+	C.184	C.161	C.129	C.132	C.196	C.177	C.196
MG	C.373	C.341	C.241	C.3C5	C.444	C.38C	C.347
MN	C.CC3	C.CC1	C.CC3	C.CC3	C.CC5	C.CC4	C.CC4
CA	C.568	C.457	C.393	C.401	C.561	C.507	C.503
NA	C.445	C.383	C.341	C.5C4	C.487	C.531	C.487
K	C.149	C.104	C.C89	C.152	C.233	C.278	C.218
TCTAL	6.392	6.248	6.108	6.264	6.526	6.548	6.459
MG/MG+FE	C.67C	C.679	C.65C	C.698	C.694	C.682	C.639
NA/NA+K	C.75C	C.787	C.792	C.768	C.676	C.656	C.691

UNLESS OTHERWISE SPECIFIED; TCTAL IRON AS FEC

APPENDIX 2-17

GLASS FROM FINE-GRAINED ZONES

FRESH LHERZOLITE SUITE

SPEC.	1CC45	1CC45	1CC46	1C017	1C017
SIC2	55.19	53.49	53.11	54.88	55.26
TIC2	0.14	C.17	C.38	1.33	1.94
AL2C3	21.25	21.04	22.53	19.87	18.51
FE2C3	0.CC	0.00	C.CO	0.00	0.00
CR2C3	0.15	0.63	C.09	0.13	0.16
FEC	3.37	3.63	3.C6	5.41	7.12
MGC	4.46	5.63	4.69	3.18	3.15
MNC	0.09	0.09	C.07	0.10	0.15
CAC	8.5C	9.49	9.95	5.76	5.57
NA2C	4.39	4.84	5.3C	3.69	3.04
K2C	1.9C	1.73	1.33	4.21	3.93
TCTAL	99.44	1CC.74	1CC.51	98.56	98.83

FORMULA UNITS ASSUMING 1C CXYGENS

SI	3.2CC	3.098	3.C7C	3.251	3.279
TI	C.CC6	C.007	0.C17	0.059	C.087
AL	1.452	1.436	1.535	1.387	1.294
FE3+	C.CCC	C.CCO	C.CCC	0.CCO	0.CCO
CR	C.007	C.C29	C.CC4	C.C06	0.CC8
FE2+	C.163	C.176	0.148	0.268	0.353
MG	C.385	C.486	C.4C4	0.281	0.279
MN	C.004	C.C04	C.CC3	C.C05	0.CC8
CA	0.528	C.589	C.616	0.366	C.354
NA	C.494	0.544	0.594	0.424	0.350
K	C.141	C.128	0.C98	0.318	0.297
TCTAL	6.381	6.497	6.49C	6.364	6.308
MG/MG+FE	C.7C2	0.734	0.732	0.512	0.441
NA/NA+K	C.778	C.810	0.858	C.571	0.540

UNLESS CTHERWISE SPECIFIED; TCTAL IRCN AS FEC

APPENDIX 2-18

CRYSTALLIZED GLASS

FRESH LHERZOLITE SUITE

SPEC.	1CCC6	1CCC6	1CCC6	1CC06	1CC06
SIC2	63.97	57.29	55.07	63.95	59.11
TIC2	0.18	C.14	C.12	C.22	C.C6
AL2C3	25.37	24.44	24.64	23.87	28.72
FE2C3	C.CC	C.CC	C.CC	0.00	0.00
CR2C3	0.C6	0.69	C.92	C.CC	0.00
FEC	0.47	0.80	1.C4	C.C8	0.12
MGC	0.32	2.77	3.59	C.32	0.18
MNC	C.CC	C.C2	C.C3	C.00	0.00
CAC	0.8S	3.74	4.91	C.21	1.03
NA2C	6.14	7.07	7.46	5.91	1C.C4
K2C	3.39	2.29	C.99	6.19	1.40
TCTAL	1CC.79	99.25	98.77	1CC.75	1CC.66

FCRMULA UNITS ASSUMING 8 CXYGENS

SI	2.795	2.605	2.527	2.828	2.610
TI	C.CC6	C.CC5	C.C04	0.C07	0.002
AL	1.307	1.310	1.333	1.244	1.495
FE3+	C.CCC	C.CC0	C.CCC	0.CC0	C.CCC
CR	C.002	C.025	C.C33	0.C00	0.C00
FE2+	C.017	C.C30	C.C40	0.C03	0.004
MG	C.021	C.188	C.246	0.C21	C.012
MN	C.CCC	C.C01	C.C01	0.CC0	C.CCC
CA	C.042	0.182	0.241	0.010	0.049
NA	C.52C	C.623	0.664	0.507	0.860
K	C.18S	C.133	C.C58	0.349	C.079
TCTAL	4.8S9	5.101	5.147	4.970	5.110
NA/NA+K	C.734	C.824	0.92C	0.592	0.916

UNLESS OTHERWISE SPECIFIEC; TCTAL IRON AS FEC

APPENDIX 2-19

GLASS WITH CLINOPYROXENE

FRESH LHERZOLITE SUITE

SPEC.	1CCC6	1CCC6
SIC2	62.83	59.80
TIC2	0.C1	C.C1
AL2C3	28.C7	29.63
FE2C3	0.CC	0.00
CR2C3	0.CC	C.CC
FEC	0.43	C.27
MGC	0.29	0.30
MNC	0.CC	C.CC
CAC	0.66	1.C9
NA2C	6.87	9.17
K2C	1.18	0.83
TCTAL	1CC.34	1C1.10

FCRMULA UNITS ASSUMING 1C CXYGENS

SI	3.411	3.263
TI	C.CCC	C.CCC
AL	1.796	1.9C6
FE3+	C.CCC	C.CCC
CR	C.CCC	C.CCC
FE2+	C.C2C	C.C12
MG	C.C23	C.C24
MN	C.CCC	C.CCC
CA	C.C38	C.C64
NA	C.723	C.970
K	C.C82	C.C58
TCTAL	6.093	6.298
NA/NA+K	C.898	C.944

UNLESS CTHERWISE SPECIFIEC; TCTAL IRON AS FEC

APPENDIX 2-20

CR-SPINEL

ICDINGSITIZED LHERZCLITE SUITE

SPEC.	1CC22	1C023	1CC25	1CC26	1CC26	1CC27	1CC27
SIC2	0.C8	1.01	C.95	0.26	0.87	1.09	0.66
TIC2	0.C9	C.11	C.11	0.13	0.13	0.04	0.03
AL2C3	37.CC	52.30	49.6C	58.37	59.21	44.73	44.91
FE2C3	0.CC	C.CO	C.CO	0.00	0.00	0.CO	C.CO
CR2C3	27.44	14.46	17.29	8.11	8.26	19.61	20.27
FEC	16.22	11.C4	1C.36	1C.62	10.51	13.61	15.13
MGC	18.61	20.79	21.26	21.93	21.49	20.67	19.28
MNC	0.48	0.29	C.36	C.20	0.19	0.45	0.48
CAC	0.CC	C.CO	C.CC	C.CO	C.CC	C.CC	C.CC
NA2C	0.CC	0.00	0.CO	0.00	0.00	0.CO	C.CO
K2C	C.CC	C.CO	C.CC	0.00	0.00	0.CO	0.CO
TCTAL	99.92	1CC.CO	99.93	99.62	1CC.66	1CC.20	1CC.76

FORMULA UNITS ASSUMING 4 CXYGENS

SI	C.CC2	C.C27	0.C25	0.C07	0.022	0.030	0.018
TI	C.CC2	C.CC2	C.CC2	0.C03	C.CC2	0.CC1	C.CC1
AL	1.246	1.619	1.549	1.772	1.774	1.433	1.444
FE3+	C.CCC	C.CCO	C.CCC	0.C00	0.000	0.000	0.CCO
CR	C.62C	C.3CO	C.362	C.165	C.166	0.421	0.437
FE2+	C.388	C.243	C.23C	0.229	C.223	C.3C9	C.345
MG	C.793	C.814	0.84C	0.842	0.814	0.838	0.784
MN	C.C12	C.CC6	C.CC8	0.C04	0.C04	C.010	0.C11
CA	C.CCC	C.CCO	C.CCC	C.CCO	C.CCC	C.CCC	C.CCC
NA	C.CCC	0.C00	0.CCO	0.C00	0.C00	C.CCO	0.CCO
K	C.CCC	C.CCO	0.CCC	0.C00	0.000	C.CCO	0.CCO
TCTAL	3.063	3.011	3.017	3.022	3.006	3.042	3.C41
MG/MG+FE	C.672	C.770	0.785	0.786	0.785	0.730	0.694
CR/CR+AL	C.332	C.156	C.190	0.C85	0.C86	C.227	C.232

UNLESS CTHERWISE SPECIFIED; TCTAL IRCN AS FEC

APPENDIX 2-20

CR-SPINEL

ICDINGSITIZED LHERZOLITE SUITE

SPEC.	1C027	1CC29	1C211
SIC2	0.53	C.C4	C.21
TIC2	C.C2	C.C2	C.14
AL2C3	44.68	41.35	6C.36
FE203	0.CC	C.C0	C.CC
CR203	19.96	25.19	5.94
FEC	13.87	11.67	1C.44
MGC	19.58	20.86	22.41
MNC	0.47	0.48	C.20
CAC	0.CC	C.C0	C.CC
NA2C	0.CC	0.C0	C.C0
K2C	0.CC	0.C0	C.C0
TCTAL	99.11	99.61	99.70

FORMULA UNITS ASSUMING 4 CXYGENS

SI	C.015	C.CC1	C.CC5
TI	C.CCC	C.CC0	C.CC3
AL	1.453	1.351	1.816
FE3+	C.0CC	0.CC0	0.CC0
CR	C.436	C.552	C.120
FE2+	0.320	C.270	C.223
MG	C.8C5	C.862	0.853
MN	C.011	0.011	0.C04
CA	C.CCC	C.CC0	0.CC0
NA	C.0CC	C.CC0	C.CC0
K	C.0C0	C.CC0	C.CCC
TCTAL	3.041	3.047	3.C24
MG/MG+FE	C.716	C.761	C.793
CR/CR+AL	0.231	0.290	0.062

UNLESS CTHERWISE SPECIFIEC; TCTAL IRON AS FEC

APPENDIX 2-21

ORTHOPYROXENE

ICCINGSITIZED LHERZOLITE SUITE

SPEC.	10022	10023	10024	10025	10026	10027	10C27
SIO2	56.60	55.26	56.60	55.86	55.16	56.24	55.48
TIO2	0.03	0.06	0.01	0.03	0.14	0.02	0.03
AL2O3	2.74	3.90	3.61	3.74	4.58	3.06	2.96
FE2O3	0.00	0.00	0.00	0.00	0.00	0.00	0.00
CR2O3	0.45	0.40	0.47	0.42	0.31	0.38	0.34
FEO	5.94	5.86	5.80	5.86	6.52	6.15	6.35
MGO	34.36	34.03	32.75	34.03	33.52	33.97	34.27
MNO	0.15	0.14	0.16	0.15	0.18	0.18	0.19
CAO	0.57	0.62	0.69	0.61	0.60	0.46	0.47
NA2O	0.16	0.02	0.09	0.10	0.14	0.14	0.02
K2O	0.00	0.00	0.00	0.00	0.00	0.00	0.00
TOTAL	101.00	100.29	100.18	100.80	101.15	100.60	100.11

FORMULA UNITS ASSUMING 6 OXYGENS

SI	1.933	1.901	1.943	1.911	1.888	1.929	1.916
TI	0.001	0.002	0.000	0.001	0.004	0.001	0.001
AL	0.110	0.158	0.146	0.151	0.185	0.124	0.120
FE3+	0.000	0.000	0.000	0.000	0.000	0.000	0.000
CR	0.012	0.011	0.013	0.011	0.008	0.010	0.009
FE2+	0.170	0.169	0.167	0.168	0.187	0.176	0.183
MG	1.749	1.745	1.676	1.735	1.710	1.737	1.764
MN	0.004	0.004	0.005	0.004	0.005	0.005	0.006
CA	0.021	0.023	0.025	0.022	0.022	0.017	0.017
NA	0.011	0.001	0.006	0.007	0.009	0.009	0.001
K	0.000	0.000	0.000	0.000	0.000	0.000	0.000
TOTAL	4.010	4.014	3.980	4.010	4.017	4.008	4.019
MG/MG+FE	0.912	0.912	0.910	0.912	0.902	0.908	0.906

UNLESS OTHERWISE SPECIFIED: TOTAL IRON AS FEO

APPENDIX 2-21

ORTHOPYROXENE

KOOINGSITIZED LHERZOLITE SUITE

SPEC.	10029	10211	10218
SIO2	56.43	55.15	56.46
TIO2	0.02	0.14	0.01
AL2O3	2.87	4.53	3.19
FE2O3	0.00	0.00	0.00
CR2O3	0.42	0.22	0.51
FEO	5.70	6.41	5.57
MGO	33.90	32.87	33.54
MNO	0.09	0.13	0.10
CAO	0.51	0.65	0.55
NA2O	0.02	0.12	0.04
K2O	0.00	0.00	0.00
TOTAL	99.96	100.22	99.97

FORMULA UNITS ASSUMING 6 OXYGENS

SI	1.941	1.901	1.941
TI	0.001	0.004	0.000
AL	0.116	0.184	0.129
FE3+	0.000	0.000	0.000
CR	0.011	0.006	0.014
FE2+	0.164	0.185	0.160
MG	1.738	1.689	1.719
MN	0.003	0.004	0.003
CA	0.019	0.024	0.020
NA	0.001	0.008	0.003
K	0.000	0.000	0.000
TOTAL	3.995	4.004	3.989
MG/MG+FE	0.914	0.901	0.915

UNLESS OTHERWISE SPECIFIED; TOTAL IRON AS FEO

APPENDIX 2-22

CLINOPYROXENE

IDDINGSITIZED LHERZOLITE SUITE

SPEC.	10022	10023	10024	10025	10026	10027	10C27
SIO2	52.95	52.51	53.47	53.19	51.66	53.20	53.46
TIO2	0.05	0.20	0.15	0.16	0.58	0.03	0.04
AL2O3	2.94	4.37	4.63	4.26	6.87	2.76	2.73
FE2O3	0.00	0.00	0.00	0.00	0.00	0.00	0.00
CR2O3	0.74	0.67	0.75	0.71	0.68	0.46	0.49
FEO	2.58	2.70	2.72	2.62	2.87	2.55	2.44
MGO	17.54	17.63	16.35	16.38	15.06	17.55	17.18
MNO	0.06	0.14	0.11	0.08	0.05	0.07	0.06
CAO	22.91	22.27	20.10	20.38	19.66	23.27	23.35
NA2O	0.41	0.57	1.64	1.51	2.13	0.30	0.19
K2O	0.00	0.00	0.00	0.01	0.00	0.00	0.00
TOTAL	100.18	101.06	99.92	99.30	99.56	100.19	99.94

FORMULA UNITS ASSUMING 6 OXYGENS

SI	1.921	1.888	1.931	1.934	1.877	1.929	1.941
TI	0.001	0.005	0.004	0.004	0.016	0.001	0.001
AL	0.126	0.185	0.197	0.183	0.294	0.118	0.117
FE3+	0.000	0.000	0.000	0.000	0.000	0.000	0.000
CR	0.021	0.019	0.021	0.020	0.020	0.013	0.014
FE2+	0.078	0.081	0.082	0.080	0.087	0.077	0.074
MG	0.949	0.945	0.880	0.888	0.815	0.949	0.930
MN	0.002	0.004	0.003	0.002	0.002	0.002	0.002
CA	0.891	0.858	0.778	0.794	0.765	0.904	0.908
NA	0.029	0.040	0.115	0.106	0.150	0.021	0.013
K	0.000	0.000	0.000	0.000	0.000	0.000	0.000
TOTAL	4.018	4.025	4.013	4.013	4.026	4.015	4.000
MG/MG+FE	0.924	0.921	0.915	0.918	0.903	0.925	0.926

UNLESS OTHERWISE SPECIFIED; TOTAL IRON AS FEO

APPENDIX 2-22

CLINOPYROXENE

ICCINGSITIZED LHERZOLITE SUITE

SPEC.	10027	1C029	1C029	1C029	10211	1C211	1C211
SIC2	53.5C	53.77	53.22	53.04	51.91	51.97	51.45
TIC2	0.1C	0.CO	C.04	C.05	0.69	0.68	0.65
AL2O3	3.C3	2.92	3.08	3.13	7.14	6.99	7.25
FE2O3	0.CC	C.CO	C.CC	C.CO	C.CC	C.CO	C.CO
CR2C3	0.54	0.62	0.69	0.72	0.49	0.54	0.53
FEC	2.66	2.54	2.68	2.52	2.90	3.05	2.91
MGC	16.99	17.23	16.94	17.00	14.85	14.96	14.80
MNC	0.12	0.03	C.07	C.08	0.11	0.C7	C.09
CAC	23.54	21.68	21.70	21.99	19.16	19.79	19.31
NA2C	0.16	C.82	C.66	C.57	2.28	2.16	2.35
K2C	0.CC	C.CO	C.CO	C.CO	C.CC	0.CO	0.CO
TCTAL	1CO.64	99.61	99.C8	99.10	99.53	1CO.21	99.34

FCRMLLA UNITS ASSUMING 6 CXYGENS

SI	1.932	1.952	1.945	1.938	1.882	1.877	1.872
TI	C.CC3	C.CCO	C.C01	C.C01	C.019	C.018	0.018
AL	C.129	C.125	C.133	C.135	C.305	0.297	0.311
FE3+	C.CCC	C.CCO	C.CCC	C.CCO	C.CCC	C.CCO	C.CCO
CR	C.015	0.018	0.C20	0.021	0.014	0.015	C.C15
FE2+	C.C8C	C.C77	0.C82	0.C77	0.088	0.092	0.C89
MG	C.914	C.932	C.923	C.926	C.8C3	0.8C5	0.8C3
MN	C.CC4	C.C01	C.C02	C.C02	C.C03	C.CC2	C.CC3
CA	C.911	C.843	0.850	0.861	0.744	0.766	0.753
NA	C.011	C.C58	C.C47	C.C40	0.160	0.151	0.166
K	C.CCC	C.CCO	C.CCC	C.CCO	C.CCC	C.CCO	C.CCO
TCTAL	3.999	4.CC6	4.C01	4.C03	4.019	4.024	4.030
MG/MG+FE	C.919	0.924	0.918	0.92C	0.9C1	C.897	C.9C1

UNLESS CTHERWISE SPECIFIEC; TCTAL IRCN AS FEC

APPENDIX 2-22

CLINCPYRCXENE

iCCINGSITIZED LHERZCLITE SUITE

SPEC.	10213	10214	10215	10216	10217	10218	10219
SIC2	51.86	52.13	52.82	52.09	52.7C	54.40	53.64
TIC2	0.69	0.56	C.10	C.18	C.07	0.12	C.C2
AL2C3	7.C3	7.CC	3.53	3.85	3.45	3.55	2.79
FE2C3	0.CC	0.CC	C.CC	C.CC	C.CC	C.CC	C.CC
CR2C3	0.64	0.75	0.86	0.65	0.82	0.80	0.63
FEC	2.96	3.CC	2.49	2.72	2.54	2.44	2.36
MGC	14.51	15.18	16.80	16.88	16.86	16.19	17.48
MNC	C.07	C.C8	C.C6	C.11	0.05	0.08	C.C8
CAC	19.58	19.51	22.19	22.11	22.61	20.55	23.25
NA2C	1.95	2.04	C.73	C.44	0.64	1.78	0.20
K2C	0.01	C.01	C.CC	C.CC	0.CC	C.CC	C.CC
TCTAL	99.3C	1CC.26	99.58	99.03	99.74	99.91	100.45

FCRMULA UNITS ASSUMING 6 CXYGENS

SI	1.886	1.879	1.924	1.910	1.92C	1.964	1.937
TI	C.019	0.015	0.003	0.C05	0.C02	0.CC3	0.C01
AL	C.3C1	C.297	C.152	C.166	C.148	0.151	0.119
FE3+	C.0CC	C.CC0	0.CC0	C.CC0	C.CC0	C.CCC	C.CC0
CR	C.018	0.021	0.025	0.019	0.024	C.023	C.C18
FE2+	C.09C	C.090	0.C76	0.083	0.077	0.074	C.C71
MG	C.787	C.816	C.912	0.922	0.915	C.871	C.941
MN	C.0C2	C.002	0.002	0.C03	0.002	C.C02	C.C02
CA	C.763	C.753	0.866	0.868	0.882	0.795	0.899
NA	C.137	C.143	0.C52	0.C31	0.045	0.125	0.C14
K	C.0CC	C.CC0	0.CC0	0.CC0	C.CC0	C.CC0	0.CC0
TCTAL	4.004	4.018	4.C11	4.C09	4.015	4.008	4.002
MG/MG+FE	C.897	C.9C0	0.923	C.917	0.922	C.922	0.93C

UNLESS OTHERWISE SPECIFIED; TCTAL IRCN AS FEC

APPENDIX 2-22

CLINCPYRCXENE

ICDINGSITIZED LHERZOLITE SUITE

SPEC.	10220	10221
SIC2	53.55	53.38
TIC2	0.07	0.08
AL2C3	3.C3	2.54
FE2C3	0.CC	0.C0
CR2C3	0.82	0.68
FEC	2.C5	2.43
MGC	16.66	16.71
MNC	0.10	C.C5
CAC	22.78	22.70
NA2C	0.86	0.92
K2C	0.CC	C.C0
TCTAL	99.92	99.49

FCRMULA UNITS ASSUMING 6 CXYGENS

SI	1.942	1.949
TI	C.0C2	C.C02
AL	0.13C	0.109
FE3+	C.CCC	C.CC0
CR	C.024	C.C20
FE2+	C.062	C.C74
MG	C.9C1	C.909
MN	C.0C3	C.CC2
CA	C.885	C.888
NA	C.C60	C.C65
K	C.CC0	0.CC0
TCTAL	4.009	4.017
MG/MG+FE	0.935	C.925

UNLESS CTHERWISE SPECIFIED; TCTAL IRCN AS FEC

APPENDIX 2-23

RIM CLINOPYROXENE

ICCINGSITIZED LHERZOLITE SLITE

SPEC.	10211	10214	10218
SIC2	50.74	51.51	54.21
TIC2	0.86	0.58	C.10
AL2C3	3.91	4.85	1.87
FE2C3	0.CC	C.C0	C.CC
CR2C3	0.65	0.84	C.70
FEC	3.69	3.18	2.05
MGC	16.15	16.20	17.97
MNC	0.11	C.C6	C.08
CAC	21.41	21.74	22.54
NA2C	0.65	C.57	C.68
K2C	0.CC	C.C1	C.CC
TCTAL	98.17	99.54	100.20

FCRMULA UNITS ASSUMING 6 CXYGENS

SI	1.888	1.883	1.958
TI	C.024	C.016	C.CC3
AL	C.171	0.209	0.080
FE3+	C.CCC	0.CC0	0.CC0
CR	C.019	C.024	0.C20
FE2+	C.115	C.097	C.C62
MG	C.896	0.882	0.968
MN	C.CC3	C.CC2	C.CC2
CA	C.853	C.851	0.872
NA	C.047	C.040	C.C48
K	C.CCC	0.CC0	0.CC0
TCTAL	4.016	4.CC5	4.C13
MG/MG+FE	C.886	C.9C1	C.940

UNLESS CTHERWISE SPECIFIEC; TCTAL IRCN AS FEC

APPENDIX 2-24

EUHEDRAL CLINOPYROXENE

ICCINGSITIZED LHERZOLITE SUITE

SPEC. 10027

SIO2	48.25
TIO2	0.39
AL2O3	8.25
FE2O3	0.00
CR2O3	1.86
FEO	2.84
MGO	15.06
MNO	0.03
CAO	22.08
NA2O	0.50
K2O	0.00
TOTAL	99.26

FORMULA UNITS ASSUMING 6 OXYGENS

SI	1.778
TI	0.011
AL	0.358
FE3+	0.000
CR	0.054
FE2+	0.087
MG	0.827
MN	0.001
CA	0.872
NA	0.036
K	0.000
TOTAL	4.023

MG/MG+FE 0.904

UNLESS OTHERWISE SPECIFIED; TOTAL IRON AS FEO

APPENDIX 2-25

GLASS WITH INTERSTITIAL CLINOPYROXENE

IDDINGSITIZED LHERZOLITE SUITE

SPEC.	10025	10211
SIO2	57.56	53.73
TIO2	0.53	0.05
AL2O3	23.07	28.24
FE2O3	0.00	0.00
CR2O3	0.00	0.02
FEO	1.10	0.53
MGO	2.19	0.15
MNO	0.02	0.01
CAO	6.26	11.37
NA2O	7.55	4.99
K2O	0.88	0.36
TOTAL	99.16	99.45

FORMULA UNITS ASSUMING 10 OXYGENS

SI	3.280	3.063
TI	0.023	0.002
AL	1.549	1.897
FE3+	0.000	0.000
CR	0.000	0.001
FE2+	0.052	0.025
MG	0.186	0.013
MN	0.001	0.000
CA	0.382	0.695
NA	0.834	0.552
K	0.064	0.026
TOTAL	6.372	6.274
MG/MG+FE	0.780	0.335
NA/NA+K	0.929	0.955

UNLESS OTHERWISE SPECIFIED; TOTAL IRON AS FEO

APPENDIX 2-26

PRIMARY CLIVINE

PYROXENE GRANULITE SUITE

SPEC.	12CCC	12CC0	12C01	12C01	12004	12017	12C17
SIC2	37.63	35.94	4C.37	40.11	40.31	40.50	40.84
TIC2	0.15	C.16	C.CC	C.00	C.C0	C.C0	0.00
AL2C3	0.11	C.04	C.C0	C.01	C.C2	C.C4	C.C2
FE2C3	0.C0	0.00	C.C0	0.00	0.00	0.C0	0.C0
CR2O3	C.CC	0.C0	C.C2	C.05	0.02	0.C0	0.03
FEC	25.48	25.30	12.49	12.40	7.68	12.81	12.69
MGC	36.30	36.93	47.88	47.34	51.72	47.75	47.23
MNC	0.53	C.55	C.18	C.15	0.15	0.17	0.19
CAC	0.C2	C.07	C.C5	C.06	C.04	C.C4	C.C4
NA2C	0.2C	C.35	C.C0	0.00	0.00	C.02	C.C0
K2C	C.CC	C.C0	C.C0	C.00	0.00	0.01	0.C0
TCTAL	1C0.42	99.34	1CC.99	1CC.12	99.94	1C1.34	101.C4

FCRMULA UNITS ASSUMING 4 CXYGENS

SI	C.992	0.963	C.992	0.994	0.981	0.993	1.C02
TI	C.CC3	C.CC3	C.CCC	C.CC0	0.CC0	C.CC0	0.C00
AL	C.CC3	C.C01	C.CCC	C.CC0	C.CC1	C.CC1	0.CC1
FE3+	C.CCC	0.C00	0.CC0	0.C00	0.CC0	0.CC0	0.CC0
CR	C.CCC	C.CC0	C.CC0	0.C01	0.C00	0.CC0	0.C01
FE2+	C.562	C.567	C.257	C.257	C.156	C.263	0.260
MG	1.426	1.475	1.754	1.749	1.876	1.745	1.728
MN	C.012	C.012	C.C04	0.C03	0.003	0.C04	0.C04
CA	C.CC1	C.CC2	C.CC1	0.C02	C.C01	C.CC1	C.CC1
NA	C.01C	C.018	0.CC0	0.C00	0.C00	C.CC1	0.CC0
K	C.CCC	C.CC0	C.CC0	0.C00	0.000	0.000	0.C00
TCTAL	3.009	3.042	3.CC8	3.CC5	3.C19	3.CC7	2.997
MG/MG+FE	C.717	0.722	C.872	0.872	0.923	0.869	0.869

UNLESS CTHERWISE SPECIFIEC; TCTAL IRON AS FEC

APPENDIX 2-27

QUENCH OLIVINE

PYROXENE GRANULITE SUITE

SPEC.	12001	12017
SIO2	40.22	40.70
TIO2	0.00	0.00
AL2O3	0.29	0.29
FE2O3	0.00	0.00
CR2O3	0.03	0.08
FEO	9.70	9.02
MGO	48.50	49.48
MNO	0.15	0.17
CAO	0.50	0.32
NA2O	0.00	0.00
K2O	0.00	0.00
TOTAL	99.39	100.06

FORMULA UNITS ASSUMING 4 OXYGENS

SI	0.993	0.994
TI	0.000	0.000
AL	0.008	0.008
FE3+	0.000	0.000
CR	0.001	0.002
FE2+	0.200	0.184
MG	1.784	1.801
MN	0.003	0.004
CA	0.013	0.008
NA	0.000	0.000
K	0.000	0.000
TOTAL	3.003	3.001
MG/MG+FE	0.899	0.907

UNLESS OTHERWISE SPECIFIED; TOTAL IRON AS FEO

APPENDIX 2-28

PRIMARY SPINEL

PYROXENE GRANULITE SUITE

SPEC.	12CC1	12001	12C01	12004	12017	12017	12C17
SIC2	0.63	C.52	0.79	0.69	0.48	0.57	0.42
TIC2	0.CC	C.CO	C.CO	0.00	0.00	0.00	0.CO
AL2C3	63.91	61.99	57.36	60.81	62.14	64.34	53.59
FE2C3	0.CC	0.CO	C.CO	0.00	0.00	0.CO	C.CO
CR2C3	2.59	5.19	9.72	6.28	5.23	3.72	12.76
FEC	11.35	11.76	12.56	11.23	12.02	11.64	13.32
MGC	21.40	2C.7C	19.32	2C.71	2C.49	2C.46	19.62
MNC	0.12	0.18	C.24	0.18	0.13	0.11	C.26
CAC	C.C2	C.C5	C.C4	C.03	C.03	0.02	0.04
NA2C	0.CC	C.CO	C.CC	C.CO	C.CO	C.CC	C.CC
K2C	0.CC	0.00	C.CO	0.00	0.CO	0.CO	C.CO
TCTAL	1C0.C2	1CC.39	1CC.C3	99.93	1C0.52	1C0.86	1CC.C1

FORMULA UNITS ASSUMING 4 CXYGENS

SI	C.016	C.013	0.C21	0.018	0.012	C.014	C.C11
TI	C.CCC	C.CCO	C.CCC	0.C00	0.C00	0.CCO	0.CCO
AL	1.897	1.853	1.755	1.829	1.857	1.9C0	1.669
FE3+	0.CC0	C.CCO	C.CCC	0.CC0	C.CCC	C.CC0	0.CCC
CR	C.C52	0.104	C.2CC	0.127	0.105	0.074	0.267
FE2+	C.239	C.249	C.273	C.240	0.255	0.244	0.294
MG	0.803	C.783	C.748	C.788	C.774	C.764	0.773
MN	C.CC3	C.C04	0.C05	0.C04	C.003	C.CC2	0.CC6
CA	C.CC1	C.C01	C.CC1	0.C01	0.C01	0.C01	0.C01
NA	C.CCC	C.CCO	C.CCC	C.CC0	C.CCC	C.CCC	C.CCC
K	C.CCC	0.C00	0.CC0	0.C00	0.C00	C.CC0	0.CC0
TCTAL	3.010	3.CC8	3.CC2	3.C05	3.C07	2.999	3.C21
MG/MG+FE	C.771	C.758	0.733	0.767	0.752	0.758	0.724
CR/CR+AL	C.026	C.C53	C.102	0.065	0.053	0.037	0.138

UNLESS OTHERWISE SPECIFIED; TCTAL IRON AS FEC

APPENDIX 2-28

PRIMARY SPINEL

PYROXENE GRANULITE SUITE

SPEC. 12017

SIO2	0.31
TIO2	0.00
AL2O3	50.38
FE2O3	0.00
CR2O3	15.32
FEO	14.21
MGO	18.63
MNO	0.33
CAO	0.02
NA2O	0.00
K2O	0.00
TOTAL	99.20

FORMULA UNITS ASSUMING 4 OXYGENS

SI	0.008
TI	0.000
AL	1.607
FE3+	0.000
CR	0.328
FE2+	0.322
MG	0.751
MN	0.008
CA	0.001
NA	0.000
K	0.000
TOTAL	3.024
MG/MG+FE	0.700
CR/CR+AL	0.169

UNLESS OTHERWISE SPECIFIED; TOTAL IRON AS FEO

APPENDIX 2-28

SECONDARY SPINEL

PYROXENE GRANULITE SUITE

SPEC.	12CC1	12CC1	12CC4	12C04	12C04	12017	12C17
SIC2	1.C5	1.21	1.C5	C.99	0.63	0.63	0.59
TIC2	0.CC	C.CO	C.CC	C.CO	0.CO	0.CO	C.00
AL2C3	65.6C	65.65	64.44	65.15	65.72	63.40	65.13
FE2C3	0.CC	C.CO	C.CC	0.00	0.00	0.CO	0.CO
CR2O3	0.82	C.CO	C.37	1.17	0.76	2.20	2.50
FEC	10.54	1C.C8	1C.35	1C.47	1C.33	1C.15	10.86
MGC	21.72	21.55	23.39	21.29	21.32	22.91	21.86
MNC	0.C6	C.C7	C.C7	0.08	0.04	0.10	0.07
CAC	0.11	0.27	C.12	C.23	0.C4	C.10	C.11
NA2C	0.CC	0.CO	C.CO	0.00	0.CO	0.CO	C.CO
K2C	0.CC	C.CO	C.CC	0.00	0.00	0.00	0.00
TCTAL	99.9C	98.83	99.79	99.38	98.84	99.49	101.12

FORMULA UNITS ASSUMING 4 OXYGENS

SI	C.026	C.C30	C.C26	0.025	0.016	0.016	0.C15
TI	C.0CC	C.CCO	C.CCO	0.CCO	0.CCO	C.CCO	0.C00
AL	1.928	1.942	1.897	1.927	1.951	1.882	1.9C6
FE3+	C.0CC	0.000	0.CCO	0.C00	0.0CC	0.000	0.CCO
CR	C.016	C.CCO	C.CC7	0.C23	C.015	C.044	0.C49
FE2+	C.22C	C.212	C.216	C.220	C.218	C.214	C.225
MG	C.807	0.806	0.871	0.797	0.800	0.860	0.8C9
MN	C.001	C.CC1	C.CC1	0.C02	0.001	0.CC2	0.C01
CA	C.003	C.CC7	C.CC3	0.C06	C.CC1	C.CC3	C.CC3
NA	C.CCC	0.CCO	0.CCO	0.C00	0.CCO	C.CCO	0.CCO
K	C.CCC	C.CCO	C.CCC	0.C00	0.000	0.C00	0.CCO
TCTAL	3.0C2	2.999	3.C22	3.CCO	3.CC1	3.021	3.CC8
MG/MG+FE	C.786	0.792	C.801	0.784	0.786	0.801	0.782
CR/CR+AL	C.0C8	C.CCO	C.C04	0.C12	C.C08	C.023	0.025

UNLESS OTHERWISE SPECIFIED; TOTAL IRON AS FEC

APPENDIX 2-28

SECONDARY SPINEL

PYROXENE GRANULITE SUITE

SPEC.	12017	12C17	12CC4	12C01
SIO2	1.06	1.02	1.44	1.38
TIO2	0.00	0.00	0.00	0.00
AL2O3	63.72	62.07	66.03	65.80
FE2O3	0.00	0.00	0.00	0.00
CR2O3	2.59	3.97	0.00	0.00
FEO	11.04	11.36	9.51	10.33
MGO	21.79	21.21	21.86	19.89
MNO	0.07	0.11	0.08	0.11
CAO	0.08	0.13	0.06	0.42
NA2O	0.00	0.00	0.00	0.00
K2O	0.00	0.00	0.00	0.00
TOTAL	100.35	99.87	98.98	97.93

FORMULA UNITS ASSUMING 4 OXYGENS

SI	0.027	0.026	0.036	0.035
TI	0.000	0.000	0.000	0.000
AL	1.881	1.854	1.942	1.964
FE3+	0.000	0.000	0.000	0.000
CR	0.051	0.080	0.000	0.000
FE2+	0.231	0.241	0.198	0.219
MG	0.814	0.801	0.813	0.751
MN	0.001	0.002	0.002	0.002
CA	0.002	0.004	0.002	0.011
NA	0.000	0.000	0.000	0.000
K	0.000	0.000	0.000	0.000
TOTAL	3.007	3.007	2.993	2.983
MG/MG+FE	0.779	0.769	0.804	0.774
CR/CR+AL	0.027	0.041	0.000	0.000

UNLESS OTHERWISE SPECIFIED; TOTAL IRON AS FEO

APPENDIX 2-29

PRIMARY AND RESIDUAL FELDSPAR

PYROXENE GRANULITE SUITE

SPEC.	12CCC	12CCO	12CCC	12CCO	12CC1	12CC4	12C04
SIC2	47.91	52.75	51.8C	52.01	61.78	61.17	61.08
TIC2	0.CC	0.00	C.07	C.08	0.CO	0.CO	C.CC
AL2C3	33.57	29.37	3C.57	30.26	25.67	23.85	23.82
FE2C3	0.CC	0.CO	C.CC	0.CO	0.CO	0.00	0.00
CR2C3	0.CC	0.CO	C.C5	C.07	0.CO	0.C2	0.C2
FEC	0.CO	0.CO	C.24	C.11	0.00	0.18	0.14
MGC	0.CC	0.CO	C.13	C.04	0.CO	0.08	0.11
MNC	0.CO	0.CO	C.C2	C.02	C.CC	C.C2	C.C1
CAC	15.41	13.21	13.31	13.28	5.17	5.14	5.08
NA2O	3.C5	4.85	4.09	4.17	7.95	8.52	8.87
K2C	0.C5	C.09	C.C8	C.07	0.39	C.67	C.55
TCTAL	99.99	1C0.27	1CC.36	1CC.11	100.96	99.65	99.68

FCRMULA UNITS ASSUMING 8 OXYGENS

SI	2.194	2.393	2.348	2.361	2.7C9	2.734	2.73C
TI	C.CCC	0.000	0.C02	0.C03	0.CC0	C.CC0	0.CC0
AL	1.812	1.570	1.633	1.619	1.327	1.256	1.255
FE3+	C.CCC	C.CC0	C.CC0	0.C00	0.000	C.CC0	0.C00
CR	C.CCC	C.CC0	0.C02	0.C03	0.CC0	C.C01	0.C01
FE2+	C.CCC	C.CC0	0.C09	0.C04	0.000	0.C07	0.C05
MG	C.CCC	C.CC0	C.C09	0.C03	0.CC0	C.C05	0.C07
MN	C.CCC	C.CC0	0.CC1	C.C01	C.CCC	C.CC1	0.CCC
CA	C.756	0.642	0.646	0.646	C.243	0.246	0.243
NA	C.271	C.427	0.359	0.367	0.676	C.738	0.769
K	C.0C3	C.CC5	C.CC5	C.C04	C.C22	C.C38	C.C31
TCTAL	5.036	5.038	5.C14	5.011	4.976	5.026	5.042
AN	73.4	59.8	64.0	63.5	25.8	24.1	23.3

UNLESS OTHERWISE SPECIFIED; TCTAL IRON AS FEC

APPENDIX 2-3C

QUENCH FELDSPAR

PYROXENE GRANULITE SUITE

SPEC.	12CCC	12C17	12C17
SIC2	46.30	48.73	48.76
TIC2	0.CC	C.CC	C.CC
AL2C3	34.51	31.93	33.07
FE2C3	0.CC	C.CC	C.CC
CR2C3	0.CC	C.CC	C.CC
FEC	0.CC	0.39	C.37
MGC	0.29	0.53	C.54
MNC	0.CC	C.C3	C.03
CAC	17.80	16.12	16.32
NA2C	1.42	2.21	2.41
K2C	C.C6	0.01	C.CC
TCTAL	1CC.38	99.95	101.5C

FORMULA UNITS ASSUMING 4 OXYGENS

SI	1.061	1.117	1.102
TI	C.CCC	C.CCC	C.CCC
AL	0.932	C.863	C.881
FE3+	C.CCC	0.CCC	0.CCC
CR	C.CCC	C.CCC	0.CCC
FE2+	C.CCC	C.C07	0.C07
MG	C.01C	C.C18	0.C18
MN	C.CCC	C.C01	0.C01
CA	C.437	C.396	0.395
NA	C.063	C.098	0.106
K	C.002	C.CCC	C.CCC
TCTAL	2.5C5	2.501	2.510
AN	87.1	80.1	78.9

UNLESS OTHERWISE SPECIFIED; TOTAL IRON AS FEC

APPENDIX 2-31

SECONDARY ORTHOPYROXENE

PYROXENE GRANULITE SUITE

SPEC.	12000	12000	12001	12001	12004	12017	12017
SIO2	53.19	54.13	54.97	55.22	55.23	54.92	55.65
TIO2	0.10	0.05	0.00	0.00	0.00	0.00	0.00
AL2O3	1.71	2.32	3.45	3.46	3.94	3.31	3.05
FE2O3	0.00	0.00	0.00	0.00	0.00	0.00	0.00
CR2O3	0.00	0.04	0.08	0.08	0.10	0.12	0.12
FEO	15.54	14.57	7.90	7.86	7.76	7.95	7.97
MGO	28.27	28.42	33.11	32.69	32.28	32.58	32.54
MNO	0.66	0.29	0.18	0.19	0.17	0.20	0.19
CAO	0.50	0.44	0.37	0.39	0.37	0.45	0.47
NA2O	0.14	0.17	0.00	0.00	0.00	0.00	0.00
K2O	0.00	0.01	0.00	0.00	0.00	0.00	0.00
TOTAL	100.11	100.44	100.06	99.89	99.85	99.53	99.99

FORMULA UNITS ASSUMING 6 OXYGENS

SI	1.923	1.934	1.910	1.920	1.919	1.919	1.934
TI	0.003	0.001	0.000	0.000	0.000	0.000	0.000
AL	0.073	0.098	0.141	0.142	0.161	0.136	0.125
FE3+	0.000	0.000	0.000	0.000	0.000	0.000	0.000
CR	0.000	0.001	0.002	0.002	0.003	0.003	0.003
FE2+	0.470	0.435	0.230	0.229	0.225	0.232	0.232
MG	1.524	1.514	1.715	1.695	1.672	1.697	1.685
MN	0.020	0.009	0.005	0.006	0.005	0.006	0.006
CA	0.019	0.017	0.014	0.015	0.014	0.017	0.017
NA	0.010	0.012	0.000	0.000	0.000	0.000	0.000
K	0.000	0.000	0.000	0.000	0.000	0.000	0.000
TOTAL	4.042	4.021	4.018	4.008	3.999	4.011	4.002
MG/MG+FE	0.764	0.777	0.882	0.881	0.881	0.880	0.879

UNLESS OTHERWISE SPECIFIED; TOTAL IRON AS FEO

APPENDIX 2-32

PRIMARY CLINOPYROXENE

IDDINGSITIZED LHERZOLITE SUITE

SPEC.	12000	12024	12008
SIO2	51.63	51.69	51.60
TIO2	0.56	0.64	0.85
AL2O3	2.96	3.18	4.50
FE2O3	0.00	0.00	0.00
CR2O3	0.61	0.76	1.06
FEO	5.77	3.58	3.49
MGO	14.53	15.53	15.22
MNO	0.16	0.16	0.07
CAO	22.14	22.81	21.68
NA2O	0.89	0.53	0.95
K2O	0.01	0.20	0.00
TOTAL	99.26	99.08	99.42

FORMULA UNITS ASSUMING 6 OXYGENS

SI	1.921	1.912	1.894
TI	0.016	0.018	0.023
AL	0.130	0.139	0.195
FE3+	0.000	0.000	0.000
CR	0.018	0.022	0.031
FE2+	0.180	0.111	0.107
MG	0.806	0.856	0.832
MN	0.005	0.005	0.002
CA	0.883	0.904	0.852
NA	0.064	0.038	0.068
K	0.000	0.009	0.000
TOTAL	4.022	4.014	4.004
MG/MG+FE	0.818	0.885	0.886

UNLESS OTHERWISE SPECIFIED; TOTAL IRON AS FEO

APPENDIX 2-33

SECONDARY CLINOPYROXENE

PYROXENE GRANULITE SUITE

SPEC.	12000	12001	12001	12001	12004	12017	12017
SIO2	49.55	53.82	54.03	53.06	53.70	53.07	52.93
TIO2	0.18	0.02	0.00	0.32	0.00	0.00	0.00
AL2O3	5.77	5.73	5.27	5.54	6.56	4.15	4.02
FE2O3	0.00	0.00	0.00	0.00	0.00	0.00	0.00
CR2O3	0.24	0.07	0.12	0.65	0.08	0.26	0.25
FEO	6.46	2.69	2.64	2.54	2.82	2.77	2.79
MGO	15.55	14.86	14.93	14.95	13.91	15.63	15.73
MNO	0.08	0.09	0.10	0.08	0.12	0.10	0.11
CAO	22.29	20.78	20.69	20.47	20.21	21.85	21.73
NA2O	0.29	1.98	1.85	1.96	2.43	1.07	0.97
K2O	0.00	0.02	0.01	0.02	0.01	0.00	0.00
TOTAL	100.41	100.06	99.64	99.59	99.84	98.90	98.53

FORMULA UNITS ASSUMING 6 OXYGENS

SI	1.828	1.939	1.953	1.924	1.937	1.942	1.944
TI	0.005	0.001	0.000	0.009	0.000	0.000	0.000
AL	0.251	0.243	0.224	0.237	0.279	0.179	0.174
FE3+	0.000	0.000	0.000	0.000	0.000	0.000	0.000
CR	0.007	0.002	0.003	0.019	0.002	0.008	0.007
FE2+	0.199	0.081	0.080	0.077	0.085	0.085	0.086
MG	0.855	0.798	0.804	0.808	0.748	0.853	0.861
MN	0.002	0.003	0.003	0.002	0.004	0.003	0.003
CA	0.881	0.802	0.801	0.795	0.781	0.857	0.855
NA	0.021	0.138	0.130	0.138	0.170	0.076	0.069
K	0.000	0.001	0.000	0.001	0.000	0.000	0.000
TOTAL	4.049	4.008	3.999	4.009	4.007	4.002	4.000
MG/MG+FE	0.811	0.908	0.910	0.913	0.898	0.910	0.909

UNLESS OTHERWISE SPECIFIED; TOTAL IRON AS FEO

APPENDIX 2-33

SECONDARY CLINCPYROXENE

PYRCXENE GRANULITE SUITE

SPEC. 12C17

SIC2	51.81
TIC2	0.CC
AL2C3	4.64
FE2C3	0.CC
CR2C3	0.56
FEC	2.89
MGC	15.89
MNC	C.11
CAC	21.85
NA2C	0.96
K2C	0.CC
TCTAL	98.71

FCRMULA UNITS ASSUMING 6 CXYGENS

SI	1.907
TI	C.CCC
AL	C.2C1
FE3+	C.CCC
CR	C.016
FE2+	C.C89
MG	C.872
MN	C.CC3
CA	C.862
NA	C.C69
K	C.CCC
TCTAL	4.019
MG/MG+FE	C.9C7

UNLESS CTHERWISE SPECIFIEC; TCTAL IRON AS FEC

APPENDIX 2-34

OLIVINE

DUNITES, HARZBURGITES, AND PYROXENITES

SPEC.	15CC3	15C05	15CC9	15C11	15C13	15013
SIC2	38.9C	39.88	4C.86	4C.18	39.82	39.82
TIC2	0.C1	C.C1	C.C2	C.03	C.03	0.03
AL2C3	C.02	C.CO	C.CC	C.CO	0.CO	0.CO
FE2C3	0.CC	0.CO	C.CO	C.00	0.00	0.00
CR2C3	0.C1	C.CO	C.CC	0.CO	0.CO	0.CO
FEC	15.5C	12.45	S.86	12.65	12.27	12.27
MGC	45.33	47.45	48.32	46.50	46.90	46.90
MNC	0.24	C.19	C.14	0.17	0.17	0.17
CAC	0.C5	C.C3	C.C6	C.04	C.C5	C.C5
NA2C	0.C4	0.CO	C.CO	C.00	0.CO	0.CO
K2C	0.CC	C.CO	C.CC	C.00	0.00	0.CO
TCTAL	1CC.1C	1CC.01	99.26	99.57	99.24	99.24

FCRMULA UNITS ASSUMING 4 CXYGENS

SI	C.981	C.990	1.CC8	1.CC1	0.995	0.995
TI	C.CCC	C.CCO	C.CCC	0.C01	C.C01	C.C01
AL	C.CC1	C.CCO	C.CCC	0.CCC	C.CCC	C.CCC
FE3+	C.CCO	0.000	0.CCO	0.C00	0.000	C.CCO
CR	C.CCC	C.CCO	C.CCC	0.C00	0.C00	C.CCO
FE2+	C.327	0.259	C.2C3	0.264	C.256	C.256
MG	1.703	1.756	1.776	1.728	1.747	1.747
MN	C.CC5	C.CC4	0.C03	0.C04	0.004	0.004
CA	C.CC1	C.CC1	0.CC2	0.C01	C.C01	C.C01
NA	C.CC2	C.CCO	C.CCC	C.CCO	0.C00	C.CCO
K	C.CCC	C.CCO	0.CCC	0.C00	0.000	C.CCO
TCTAL	3.020	3.C10	2.992	2.998	3.CC4	3.CC4
MG/MG+FE	C.839	C.872	0.897	0.866	0.872	0.872

UNLESS CTHERWISE SPECIFIED; TCTAL IRCN AS FEC

APPENDIX 2-35

CR-SPINEL

DUNITES,HARZBURGITES, AND PYROXENITES

SPEC.	15002	15003	15005	15009	15011
SIO2	0.32	2.10	0.00	0.00	0.00
TIO2	0.18	0.94	0.06	0.27	0.02
AL2O3	58.86	24.83	23.00	36.51	46.44
FE2O3	0.00	0.00	0.00	0.00	0.00
CR2O3	5.17	20.58	40.37	24.28	13.15
FEO	14.66	38.06	24.09	21.12	22.36
MGO	20.16	11.93	11.87	17.59	17.29
MNO	0.17	0.51	0.86	0.50	0.32
CAO	0.00	0.68	0.00	0.00	0.00
NA2O	0.00	0.01	0.00	0.00	0.00
K2O	0.00	0.00	0.00	0.00	0.00
TOTAL	99.52	99.64	100.25	100.27	99.58

FORMULA UNITS ASSUMING 4 OXYGENS

SI	0.008	0.067	0.000	0.000	0.000
TI	0.004	0.023	0.001	0.006	0.000
AL	1.807	0.939	0.852	1.247	1.537
FE3+	0.000	0.000	0.000	0.000	0.000
CR	0.106	0.522	1.004	0.556	0.292
FE2+	0.319	1.021	0.634	0.512	0.525
MG	0.783	0.570	0.556	0.760	0.724
MN	0.004	0.014	0.023	0.012	0.008
CA	0.000	0.023	0.000	0.000	0.000
NA	0.000	0.001	0.000	0.000	0.000
K	0.000	0.000	0.000	0.000	0.000
TOTAL	3.031	3.180	3.070	3.093	3.085
MG/MG+FE	0.710	0.358	0.468	0.597	0.580
CR/CR+AL	0.056	0.357	0.541	0.308	0.160

UNLESS OTHERWISE SPECIFIED; TOTAL IRON AS FEO

APPENDIX 2-35

ORTHOPYROXENE

DUNITES, HARZBURGITES, AND PYROXENITES

SPEC.	15001	15001	15005
SIO2	54.97	54.97	54.18
TIO2	0.07	0.07	0.02
AL2O3	2.24	2.24	3.72
FE2O3	0.00	0.00	0.00
CR2O3	0.19	0.19	0.23
FEO	8.92	8.92	8.50
MGO	32.78	32.78	32.09
MNO	0.25	0.25	0.16
CAO	0.45	0.45	0.28
NA2O	0.04	0.04	0.05
K2O	0.00	0.00	0.01
TOTAL	99.91	99.91	99.24

FORMULA UNITS ASSUMING 6 OXYGENS

SI	1.926	1.926	1.905
TI	0.002	0.002	0.001
AL	0.092	0.092	0.154
FE3+	0.000	0.000	0.000
CR	0.005	0.005	0.006
FE2+	0.261	0.261	0.250
MG	1.712	1.712	1.682
MN	0.007	0.007	0.005
CA	0.017	0.017	0.011
NA	0.003	0.003	0.003
K	0.000	0.000	0.000
TOTAL	4.025	4.025	4.016
MG/MG+FE	0.868	0.868	0.871

UNLESS OTHERWISE SPECIFIED; TOTAL IRON AS FEO

APPENDIX 2-36

CLINOPYROXENE

DUNITES, HARZBURGITES, AND PYROXENITES

SPEC.	15001	15001	15003	15009	15013	15013
SIO2	53.52	53.52	52.86	53.77	51.37	51.37
TIO2	0.22	0.22	0.16	0.24	0.14	0.14
AL2O3	2.13	2.13	2.13	3.11	3.07	3.07
FE2O3	0.00	0.00	0.00	0.00	0.00	0.00
CR2O3	0.32	0.32	0.26	0.53	0.87	0.87
FEO	3.26	3.26	3.63	2.60	3.45	3.45
MGO	17.20	17.20	16.76	16.78	17.36	17.36
MNO	0.11	0.11	0.13	0.08	0.15	0.15
CAO	23.67	23.67	23.46	23.21	23.17	23.17
NA2O	0.11	0.11	0.35	0.60	0.19	0.19
K2O	0.00	0.00	0.00	0.00	0.00	0.00
TOTAL	100.54	100.54	99.74	100.92	99.77	99.77

FORMULA UNITS ASSUMING 6 OXYGENS

SI	1.941	1.941	1.938	1.935	1.887	1.887
TI	0.006	0.006	0.004	0.006	0.004	0.004
AL	0.091	0.091	0.092	0.132	0.133	0.133
FE3+	0.000	0.000	0.000	0.000	0.000	0.000
CR	0.009	0.009	0.008	0.015	0.025	0.025
FE2+	0.099	0.099	0.111	0.078	0.106	0.106
MG	0.930	0.930	0.916	0.900	0.951	0.951
MN	0.003	0.003	0.004	0.002	0.005	0.005
CA	0.920	0.920	0.922	0.895	0.912	0.912
NA	0.008	0.008	0.025	0.042	0.014	0.014
K	0.000	0.000	0.000	0.000	0.000	0.000
TOTAL	4.007	4.007	4.020	4.006	4.036	4.036
MG/MG+FE	0.904	0.904	0.892	0.920	0.900	0.900

UNLESS OTHERWISE SPECIFIED; TOTAL IRON AS FEO